UNIVERSITAT DE BARCELONA

Biotechnological approaches to cardiac differentiation of human induced pluripotent stem cells

Claudia Di Guglielmo

University of Barcelona (UB)

Biomedicine PhD Program

Institute for Bioengineering of Catalonia (IBEC)

Control of Stem Cell Potency Group

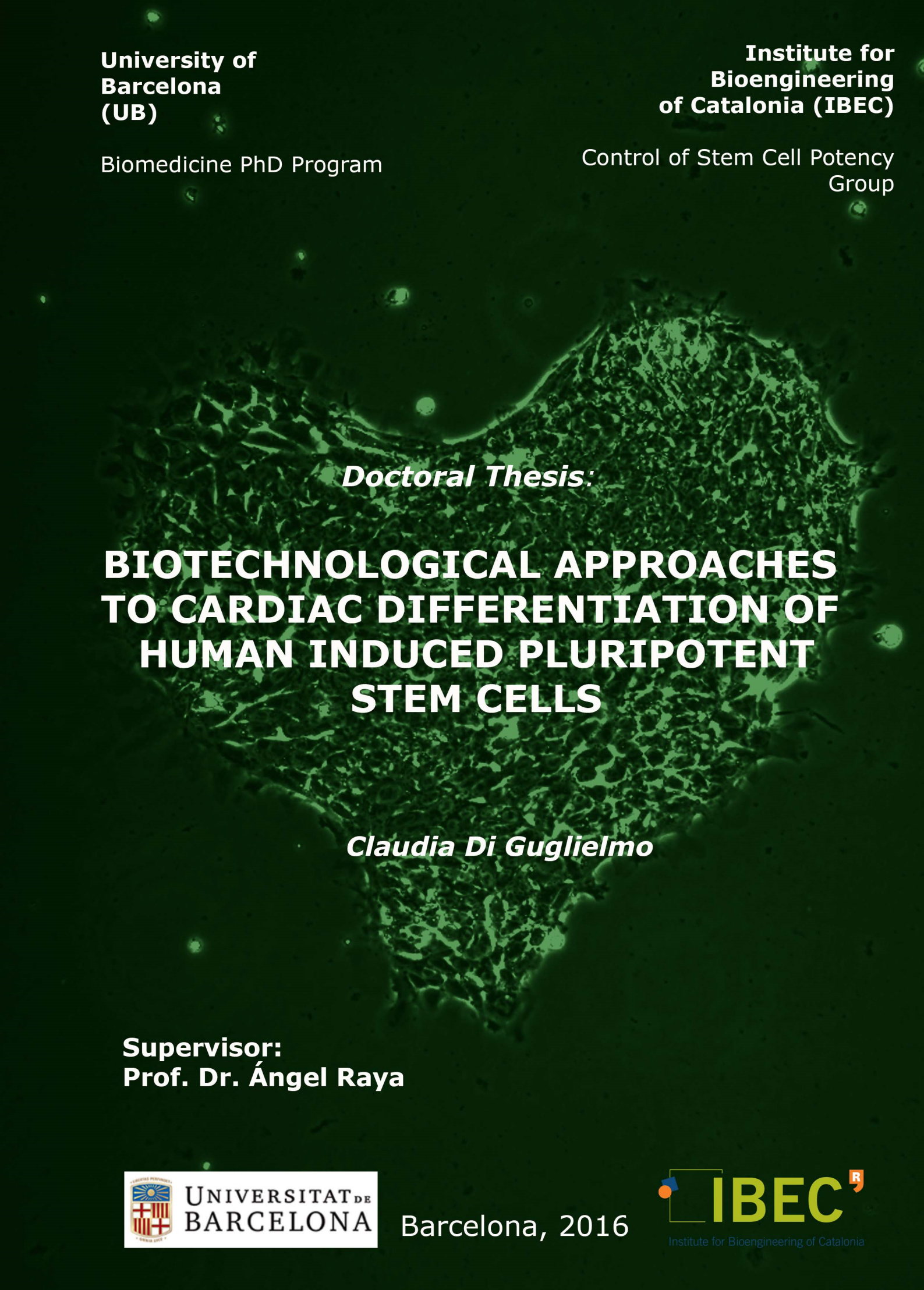

Doctoral Thesis:

BIOTECHNOLOGICAL APPROACHES TO CARDIAC DIFFERENTIATION OF HUMAN INDUCED PLURIPOTENT STEM CELLS

Claudia Di Guglielmo

Supervisor:
Prof. Dr. Ángel Raya

Barcelona, 2016

Cover image: Tuned bright-field image of a colony of human induced pluripotent stem cells with heart's symbol shape.

Doctoral Thesis:

Biotechnological approaches to cardiac differentiation of human induced pluripotent stem cells

PhD Candidate:

Claudia Di Guglielmo

University of Barcelona

Biomedicine PhD Program

Institute for bioengineering of Catalonia

(IBEC)

Control of Stem Cell Potency Group

Director: Prof. Dr. Ángel Raya

Barcelona, Academic Year 2015 / 2016

TABLE OF CONTENTS

I-ACKNOWLEDGEMENTS

The work on the perfusion bioreactor has been developed in collaboration with Maria Valls Margarit, PhD student in the "Biomimetic systems for cell engineering" group at IBEC (Institue for Bioengineering of Catalonia), under the supervision of Dr. Elena Martínez. We also thank Maria López Cavanillas, "Reparative therapy of the heart" group at VHIR (Vall d'Hebrón Institut de Recerca) led by dr. Manuel Galiñanes, for kind collaboration in teaching the neonatal rat cardiomyocytes derivation protocol and Leventon S.A. (Werfen Group), for donating the de-bubbling systems for the bioreactor presented in this work.

II-LIST OF ABBREVIATIONS

2D	two-Dimensional
3D	Three-Dimensional
AAS	Alpha Sarcomeric Actinin
ALKs	Activin receptor-like kinases
AP	Action Potential
APD	Action Potential Delay
ASA	Alpha Sarcomeric Actin
AV	Atrioventricular
BEHM	Bioengineered heart muscle
BMP	Bone Morphogenetic Protein
BTCs	Bio-artificial cardiac tissues
CBFHH	Calcium and Bicarbonate-Free Hank's Balanced Salt Solution with HEPES
CMs	Cardiomyocytes
cTNI	Cardiac Troponin I
cTNT	Cardiac Troponin T
Dkk-1	Dickkopf-1
dNTP	Deoxynucleotide
ECC	Engineered cardiac construct
ECM	Extracellular Matrix
EDTA	Ethylenediaminetetraacetic acid
EBs	Embryoid Bodies
EHT	Engineered heart tissue
ESC	Embryonic Stem Cells
FBMEs	Fibrin-based mini-EHTs
FBs	Fibroblasts
FGF	Fibroblast Growth Factor
FN	Fibronectin
GAG	Glycosaminoglycans
GFP	Green Fluorescent Protein
GSK3	Glycogen Synthase Kinase 3
hESC	Human Stem Cells
HFF	Human Foreskin Fibroblasts
hiPSC	Human Induced Pluripotent Stem Cells
hPSC	Human Pluripotent Stem Cells
iPSC	Induced Pluripotent Stem Cells
KiPS	Keratinocytes Induced Pluripotent Stem Cells
LM	Laminin
LV	Lentivirus
MEF	Mouse Embryonic Fibroblasts
MEMS	Micro electro-mechanical systems
mES	Mouse Embryonic Stem Cells

MI	Myocardial Infarction
mRNA	Messenger Ribonucleic Acid
Neo	Neomycin
NKM	Non-cardiomyocytes medium
O.N.	Over night
PBS	Phosphate-Buffered Saline
PDMS	Polydimethylsiloxane
PGA	Polyglycolic acid
PLA	Polylactic acid
PU	Polyurethane
RA	Retinoic Acid
Rcf	Relative centrifugal force
RNA	Ribonucleic Acid
RT	Room Temperature
RT-qPCR	Reverse transcription quantitative polymerase chain reaction
SCs	Stem Cells
SEM	Scanning Electron Microscopy
SMC	Smooth Muscle Cell
SMs	Skeletal Myoblasts
SN	Supernatant
SR	Sarcoplasmic Reticulum
TBS	Tris-Buffered Saline
TdP	Torsade de pointes
TE	Tissue Engineering
TGF	Transforming Growth Factor
VEGF	Vascular Endothelial Growth Factor
Wnt	Wingless/Int

III-ABSTRACT

The heart can be considered the most important organ of our body, as it supplies nutrients to all the cells. When affected from injuries or diseases, the heart function is hampered, as the damaged area is substituted by a fibrotic scar instead of functional tissue. Understanding the mechanisms leading to heart failure and finding a cure for cardiac diseases represents a major challenge of modern medicine, since they are the leading cause of death and disability in Western world. Being the heart a vital organ it is difficult to have access to its cells, especially in humans. In order to model it or find therapeutic strategies many approaches and cell sources have been studied. For example cardiac stem cells, skeletal myoblasts, bone marrow-derived cells and peripheral blood mononuclear cells have been tested in pre-clinical and clinical trials, without significant tissue regeneration. Human pluripotent stem cells (hPSC) are thought to be the most promising cell type in the field, thanks to their unlimited capacity of self-renewal and retention of differentiation potency. Induced pluripotent stem cells (iPSC) are pluripotent cells derived through reprogramming from adult cells, easily accessible from patients, like keratinocytes. iPSC can be differentiated to cardiac cells, through stage-specific protocols that reproduce embryonic development, offering a very useful platform for modelling diseases of patients with heart failure, for testing new drugs, and for cellular therapy in the future. However, properly mimicking cardiac tissue is very complex, since not only the correct cardiac cell type has to be reproduced, but also its overall cellular composition, architecture and biophysical functions.

In order to study these aspects, we applied biotechnological strategies such as the use of transgenic cell lines for obtaining pure and scalable differentiated cells to be cultured in a 3D scaffold with a perfusion bioreactor. Although it is well known that iPSC can give rise to cardiomyocytes *in vitro*, not every cell line can be efficiently differentiated. Thus, a cell line-specific differentiation protocol has to be identified and optimized. We finally identified a fast and efficient stage-specific differentiation protocol suitable for the iPSC lines used in this work, derived from human keratinocytes. With this protocol, we can reproducibly obtain close to 50% cardiomyocytes after 15 days of differentiation. One important feature of currently available differentiation protocols is that the target cell type is obtained among a heterogeneous cell population. To track the cardiac population of interest we generated transgenic cell lines where the reporter protein GFP

follows the expression of different genes specific for stages of differentiation, such as T (Brachyury) for mesoderm; NKX2.5 for cardiac progenitors; and MHC for cardiomyocytes. Moreover, cardiomyocytes obtained from hPSC using currently available differentiation protocols are typically immature, mostly resembling embryonic or fetal cardiomyocytes, arguably because of the lack of mechanical and electrical stimuli that only a 3D environment can provide. In order to create a piece of tissue in 3D we used a collagen and elastin-based scaffold, to mimic the structural proteins of endogenous extracellular matrix. We also built a perfusion bioreactor to culture the construct. After initial validation with primary cultures of rat neonatal cardiomyocytes, we tested iPSC-derived cardiac cells at different stages of differentiation. While early mesoderm or cardiac progenitors could not survive in our system, iPSC differentiated to cardiomyocytes, could be retained and maintained alive within the scaffold for at least 4 days.

In conclusion, in this work we combined biotechnological tools in order to obtain a test platform for studying the mechanisms underlying cardiac differentiation, maturation, as well as providing valuable *in vitro* systems for disease modelling, drug screening of patient-specific heart muscle cells and cell therapy.

Words count: 597 words.

IV-RESUMEN

El corazón es el órgano mas importante del cuerpo: impulsando la sangre, aporta oxigeno y nutrientes a cada célula del organismo. En caso de fallo cardiaco la función del corazón no puede recuperarse, ya que los cardiomiocitos son reemplazados por una cicatriz fibrosa no funcional. Las enfermedades cardiacas representan la mayor causa de muerte y enfermedad en el mundo occidental y entender los mecanismos de las patologías cardiacas, así como encontrar curas para ellas, es un desafío de primaria importancia para la medicina moderna. Siendo el corazón un órgano vital y difícilmente accesible, resulta imprescindible encontrar una fuente celular alternativa. Las células madre humanas con pluripotencia inducida (iPSC – induced pluripotent stem cells) parecen óptimas, porque se derivan de simples biopsias de piel de pacientes y se pueden diferenciar a cualquier tipo celular, cardiomiocitos incluidos. Aún así, diferenciar el tejido cardiaco es muy complejo: no solamente se debe de reproducir el tipo celular, sino también su composición celular, su arquitectura y sus funciones biofísicas. Para estudiar estos aspectos, por un lado obtuvimos tres líneas celulares de iPSC reporteras de genes específicos de diferentes estadios de diferenciación cardiaca (T para mesodermo, NKX2.5 para progenitores cardiacos y alpha-MHC para cardiomiocitos), y por otro desarrollamos un biorreactor adecuado para el cultivo de células cardiacas en 3D. Utilizamos las líneas transgénicas como herramienta para seleccionar células en diferentes estadios de diferenciación y las co-cultivamos con fibroblastos en un andamio compuesto de colágeno y elastina (imitando la matriz extracelular cardiaca y la composición celular del corazón). En conjunto, este estudio revela que las iPSC pueden ser retenidas y cultivadas en nuestro sistema 3D. Mientras células de mesodermo temprano y progenitores cardiacos no completaron la diferenciación cardiaca, los cardiomiocitos derivados de iPSC con cultivo convencional y cultivados en el biorreactor pudieron ser mantenidos viables en el mismo al menos 4 días. La aproximación experimental aquí presentada representa una base para desarrollar plataformas de estudio *in vitro* paciente-especificas para modelar enfermedades cardiacas humanas y estudios de fármacos, así como ofrecer una herramienta de estudio de los mecanismos de la diferenciación y maduración cardiacas.

Recuento de palabras: 345 palabras.

1- INTRODUCTION

1.1 Induced pluripotent stem cells (iPSC)

1.1.1 Embryonic Stem Cells (ESC) and Induced Pluripotent Stem Cells (iPSC)

Stem cells are cells that, together with the ability to self-renew through mitotic cell division and to remain undifferentiated, have the capacity to give rise to cell types different from its own. Proper stem cell maintenance and differentiation is critically dependent on the surrounding biochemical/biophysical environment.

The ability of a cell to differentiate into other types is called potency.

The potency of a cell specifies its differentiation potential and it is progressively restricted during development. According to this, cells are classified into (**Figure 1.1**):

- Totipotent, if they can give rise to any cell type, embryonic and extra-embryonic, like spores or zygotes.
- Pluripotent, if they can give rise to any cell type that forms an embryo.
- Multipotent, when they can differentiate only into cells of a closely related family, like progenitor cells.
- Oligopotent, if their differentiation potential is restricted to a few cells, like lymphoid or myeloid stem cells.
- Unipotent, when they can only produce one cell type, but still have the property of self-renewal, like spermatogonial stem cells.

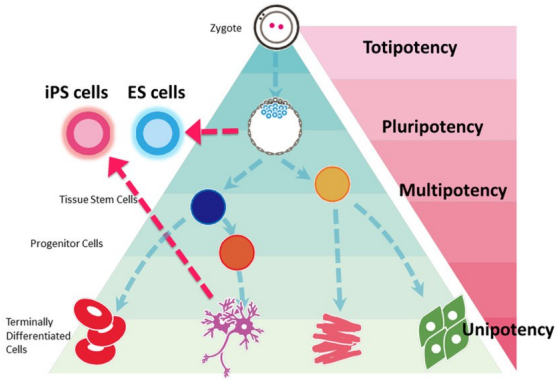

***Figure 1.1*: Stem Cell Potency**
Stem cell potency is the ability of a cell to differentiate into other cell types. The zygote (fusion of female and male gamete) is a totipotent cell, and can give rise to a whole organism. Pluripotent cells arise from totipotent cells, and differentiate to the cells that constitute the entire organism, which during development restrict their differentiation potential from multipotent to unipotent.
Being ESC cells and iPSC cells pluripotent, they can be used in vitro to obtain different cell types.

Pluripotent cells are normally found in early embryos, where they constitute the inner cell mass of the blastocyst. In the early 80's and in the late 90's, embryonic stem cells (ESC) lines were derived from mouse and human embryos, respectively (Evans & Kaufman, 1981), (Thomson et al., 1998). ESC are capable of unlimited proliferation and allowed to work *in vitro* with those cells. As well as native pluripotent cells, ESC can be differentiated into any cell type of the organism and they could be used in the treatment of diseases like diabetes or Parkinson's diseases (Thomson et al., 1998).
ESC cells opened great possibilities in research, but they imply the use of live embryos, which raises ethical concerns. Moreover in case of transplantation in patients there would be problems of tissue rejection.

The discovery of induced pluripotent stem cells (iPSC) circumvented these issues, in addition to opening new views on personalized medicine and disease modelling. iPSC are pluripotent stem cells derived from adult cells through reprogramming. The strategy was discovered and developed in 2006 by the Japanese laboratory of Yamanaka (K. Takahashi & Yamanaka, 2006).

To reprogram a cell to pluripotency means to reset an adult cell type to its pluripotent state by inserting a set of defined factors (Oct-4, Sox2, Klf4 and optionally cMyc), which was selected among an array of 24 genes highly expressed during pluripotency by the pioneers of the technique (K. Takahashi & Yamanaka, 2006).
This discovery was made with mouse fibroblasts, then iPSC have also been derived from other species, proving that the mechanism is evolutionary conserved: examples are rats (W. Li et al., 2009), pigs (Z. Wu et al., 2009), rhesus monkeys (H. Liu et al., 2008), and importantly humans (K. Takahashi et al., 2007). Induced pluripotency can be achieved from all adult tissues, in fact beyond fibroblasts, other cell types that have been reprogrammed are keratinocytes (Aasen et al., 2008), neural progenitor cells (Eminli, Utikal, Arnold, Jaenisch, & Hochedlinger, 2008), stomach and liver cells (Aoi et al., 2008), melanocytes (Utikal, Maherali, Kulalert, & Hochedlinger, 2009) and lymphocytes (Hanna et al., 2008).

Differences and similarities between iPSC and ESC have to be considered for their research and clinical applications. iPSC and ESC are very similar in their morphology, feeder dependence (see 1.1.3 "Stem cells culture" paragraph), surface markers expression, and *in vivo* teratoma formation capacity (J. Yu et al., 2007) (K. Takahashi et al., 2007). Nevertheless iPSC demonstrated different *in vitro* differentiation potential in comparison with ESC. For example, they showed reduced and more variable efficiency in neural (Hu et al., 2010) and cardiovascular (Narsinh et al., 2011) differentiation, raising the question if iPSC are indeed functionally and molecularly equivalent to ESC.
In fact, iPSC genome expression profile is affected by residual transgene expression (Soldner et al., 2009), but this issue can be solved using transgene-free iPSC. Another important difference between iPSC and ESC is that the formers retain an "epigenetic memory" from the somatic cell of origin: epigenetic marks persist after reprogramming of fibroblasts, adipose tissue and keratinocytes (Polo et al., 2010) and affect the resulting iPSC gene expression. Indeed, even if DNA methylation patterns between human iPSC and ESC are similar, differentially methylated regions were identified (Lister et al., 2011). Nearly one half are due to a failure to reprogram the somatic cell epigenome (epigenetic memory), and the remaining half are specific to iPSC, meaning that they are not found in the somatic cell of origin or in ESC.

1.1.2 Reprogramming methods

Since its discovery in 2006, the iPSC cell technology has evolved, being improved in terms of safety (integrative versus non-integrative methods) and efficiency (Rais et al., 2013).

1.1.2.1 Integrative methods

Integrative methods of reprogramming are those methods that rely on the integration of the foreign trans-genes into the host genome. They were applied during the derivation of the very first iPSC cell lines, when retroviruses and lentiviruses were used to introduce foreign genes into the host genome of cells (K. Takahashi et al., 2007). Also the iPSC used in the experiments of this thesis are obtained through retroviruses infection. The integration of the Yamanaka factors into host genome leads to the overexpression of these exogenous genes. However, those viral strategies carry the major drawback of possible mutations and silencing of indispensable genes and/or the induction of tumorigenicity (Maherali & Hochedlinger, 2008). It has also been shown that the integrated provirus can alter expression of neighbouring host genes (Hanley, Rastegarlari, & Nathwani, 2010). Despite these limitations, lots of developments have been suggested and successfully proven to be viable. Examples are drug-inducible transgenic systems (Brambrink et al., 2008) (Sommer et al., 2009) (Stadtfeld, Nagaya, Utikal, Weir, & Hochedlinger, 2008) (Wernig et al., 2008) and the usage of reprogramming cassettes that can also be LoxP-flanked (Soldner et al., 2009) (Sommer et al., 2010). Other additional gene delivery systems have been described, like the piggyback (PB) transposon/transposase and the Sendai virus, a non-viral and viral system, respectively (Woltjen et al., 2009) (Yusa, Rad, Takeda, & Bradley, 2009) (Ban et al., 2011). They are useful strategies to deliver large genetic elements and to increase reprogramming efficiencies in mammalian cells (Kaji et al., 2009).

1.1.2.2 Non-integrative methods

With the potential to impact clinical applications, iPSC cell derivation strategies shifted from genome-modifying to that of non-integrative methods, including the use of

chemical compounds (Hou et al., 2013), proteins (D. Kim et al., 2009) (Zhou et al., 2009) and plasmids (J. Yu et al., 2009) (Okita, Hong, Takahashi, & Yamanaka, 2010). In fact, somatic cell reprogramming does not require genomic integration or the continued presence of exogenous reprogramming factors. A fourth method for integration-free iPSC cell derivation was developed in 2010 (Warren et al., 2010) and then further optimized. It consists in applying synthetic modified mRNA molecules, each encoding the Yamanaka factors, to differentiated cells over an extended period of time. This novel method allows controlling stoichiometry of the Yamanaka factors in a timely manner. In addition, it opens up novel directed differentiation and trans-differentiation procedures and addresses a critical safety concern for its possible use in regenerative medicine.

1.1.3 Stem Cells Culture

hESC and iPSC need special culture conditions to maintain their pluripotency, stable karyotype and phenotype. Apart from proper culture media, they can need feeder cells for attachment, nourishment and pluripotency maintenance. Originally hESC were derived and cultured on top of mouse embryonic fibroblast (MEF) feeder cells in a culture media containing fetal bovine serum (FBS) (Thomson et al., 1998) (Reubinoff, Pera, Fong, Trounson, & Bongso, 2000). Later on, human based feeders (Human Foreskin Fibroblasts, HFF) have been used to replace MEFs (Hovatta et al., 2003) (Inzunza et al., 2005) (Skottman & Hovatta, 2006) and KnockOut Serum Replacement (SR) (Invitrogen, Carlsbad, CA, USA) has replaced FBS in hESC culture medium. FBS contains unknown components and different serum batches vary in their capability to maintain pluripotency or even differentiate hESC, being a tricky reagent to be used. Although SR still contains animal-based components, it is more defined than FBS and has also beneficial effects on hESC proliferation (Koivisto et al., 2004). In addition to feeder-dependent methods, hESC and iPSC can be cultured on feeder-free culture systems (International Stem Cell Initiative et al., 2010) (Thomas et al., 2009) with commercially available Matrigel (BD Biosciences), laminin and fibronectin (Amit, Shariki, Margulets, & Itskovitz-Eldor, 2004) (Rosler et al., 2004) or similar components like Vitronectin ™. Commercially feeder-free media are also available, like mTeSR™ that assure batch-to-batch consistency and experimental reproducibility, since they are

chemically defined (Ludwig et al., 2006) (G. Chen et al., 2011).

Passaging of hESC or iPSC is another challenging step in ESC maintenance *in vitro*. Pluripotent stem cells grow in colonies (**Figure 1.2**) and these colonies have to be broken either mechanically or enzymatically for passaging. Mechanical cutting of the colonies into smaller pieces is much more laborious but does not expose the cells to xenogeneic enzymes (e.g. trypsin or Accutase), which dissociate them in a more uniform way but at the same time disrupt their cell surface adhesion molecules and communication with other cells. Moreover, dissociation of hESC into single cells may lead to karyotype abnormalities (Brimble et al., 2004).

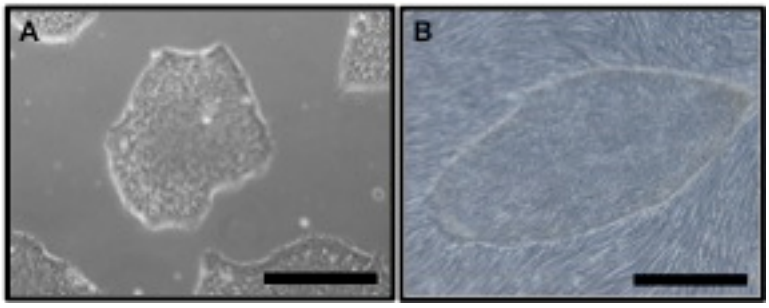

***Figure 1.2*: Colonies of human iPSC**

Human embryonic stem cells grow as cell colonies. A: Colonies of iPSC growing on a Matrigel layer. B: Colony of iPSC cultured on a layer of HFF. (Scale Bar: 500 um)

1.1.4 Differentiation Potential of iPSC and hESC

The possibility to obtain, *in vitro,* a defined cell population from pluripotent stem cells in a clinically relevant number, offered exciting prospects for modelling mammalian development and regenerative medicine. Nevertheless, the other side of the coin of hESC plasticity is that it is regulated by fine mechanisms, which are extremely difficult to study and to reproduce or tune in experimental conditions.

Many articles have been published describing differentiation protocols to defined cell types, such as cardiomyocytes, neurons, hematopoietic cells, hepatocyte-like cells, endothelial cells, retina, etc. But evaluating the effective differentiation potential of iPSC cell lines and if they are comparable to hESC is hard. In fact many variables have to be considered.

First of all, each laboratory adopts its differentiation protocol and uses different cell lines and culture conditions, so it is difficult to compare lines between different works. Then, each cell line behaves differently, making hard to compare results (Osafune et al., 2008) (Cao et al., 2008). Finally, different approaches can be applied to evaluate the outcome of differentiation: counting the quantity of cells that express one desired differentiation marker to score the number of differentiated cells (like cardiac troponin T or I, alpha-sarcomeric actin or actinin) or proving the quality of the differentiation through fine functional testing of the cells obtained (such as evaluating the beating capacity of cardiac cells through visual analysis of spontaneously contracting outgrowths (Lian et al., 2012)). So, in order to establish a standard of differentiation it is necessary to adapt all these variables to the cell line in use. Also, hESC response to differentiation stimuli might be different from that of iPSC. In addition to the extent of reprogramming, this could also be due to the fact that the majority of differentiation protocols have been established with hESC, and to the epigenetic memory of iPSC (Bilic & Izpisua Belmonte, 2012) (Hu et al., 2010).

1.2 Cardiac development and cardiac stem cell differentiation

1.2.1 Cardiac development *in vivo* and differentiation markers

Since human life without heart is not possible, the ontogeny and phylogeny of this organ have attracted exceptional interest in research. Of the two large conduction systems that allow life in vertebrate bodies, the nervous system employs electric signals for its traffic to and from the brain, while the vascular system uses vessels to aid blood flow to and from the heart. And whereas the vertebrate brain presents variety of sizes, shapes, and forms, the scheme of cardiovascular system is uniform in all vertebrates and it is recapitulated equally during embryogenesis. The evolution of multi-cellularity and of complex body reflected into the evolution of the development of a complex cardiovascular system, in order to provide cellular nutrition and general physiological homeostasis. In vertebrates, the heart is the first organ to form and its circulatory function is essential for the viability of the embryo (Buckingham, Meilhac, & Zaffran, 2005). Heart beating is triggered with spontaneous contractions in the first days of the

third week of gestation in humans. At the very beginning of embryo development, after the hollow cell cluster (blastula) begins the migration and invagination of cells (gastrulation), unspecialized cells create 3 germ layers: the endoderm, that forms lung, gut, liver and pancreas, the ectoderm (skin and nervous system), and mesoderm (muscles – cardiac, smooth and skeletal; bone; tendon and hematopoietic system). So, myocardial cells are derived from mesoderm, one of the three germ layers that form during gastrulation from the primitive streak. The initial form of the heart is the heart tube, shaped as a vessel. It then undergoes multi-phased looping and finally forms the four-chambered heart (Buckingham et al., 2005). Studies of early stages of heart differentiation are hampered by the lack of early stage cardiac cell markers (Lough & Sugi, 2000). Transient expression of T(Brachyury) is widely used to mark mesoderm and furthermore cardiac lineage formation (Kispert & Herrmann, 1994). Two cardiac progenitor cell lineages, called the heart fields, contribute to the formation of the heart (Buckingham et al., 2005). One population contributes to the formation of the left ventricle, partly the right ventricle, the atrio-ventricular canal and atria. The other lineage (named the second or secondary heart field) forms the outflow tract and the whole right ventricle and atria. It is marked by Islet-1 (Isl-1, Insulin Gene Enhancer protein gene) which expression plays an important role in the embryogenesis of pancreatic islets of Langerhans. The secondary field forms two thirds of the embryonic heart, including the cardiac muscle, smooth muscle and endothelial cells (Cai et al., 2003). (The developmental steps in heart formation are illustrated in **Figure 1.3**). Other early markers for cardiac progenitors are mesoderm posterior 1 and 2 (MESP1 and MESP2), which are transiently expressed in newly formed mesoderm at the primitive streak (Kitajima, Takagi, Inoue, & Saga, 2000). In mammals, bone morphogenic proteins (BMPs), transforming growth factor betha superfamily (TGF-betha) and the fibroblast growth factors (FGFs) have been found to be essential for heart development. These factors regulate the activation of myocardial regulatory genes such as NK2 transcription factor related gene, locus 5 (NKX2.5) and GATA binding protein-4 (GATA4) (Brand, 2003).

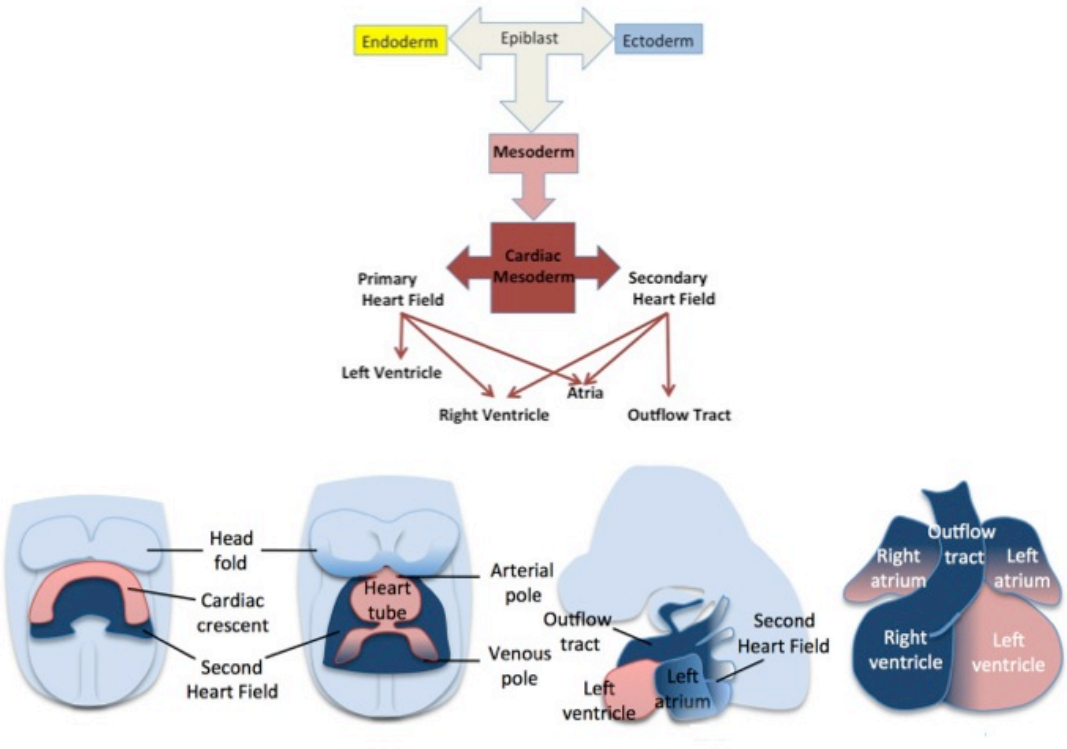

***Figure 1.3*: Heart Development**
Scheme of developmental steps in heart formation. Embryonic stem cells in the epiblast can differentiate into cell types of all three germ layers: endoderm, mesoderm or ectoderm. Mesoderm is the origin of cardiac cells. Two cardiac progenitor cell populations, the heart fields, contribute to the formation of the heart. The left ventricle is formed only from the primary heart field, whereas the atria and the right ventricle are formed from both of the progenitor cell populations. The cartoon shows addition of second heart field progenitor cells (blue) to the arterial and venous poles of the heart tube, showing its contribution to heart development.

1.2.2 Cardiac development *in vitro*

Cardiac differentiation is possible nowadays thanks to the pioneer works with murine model, since they have generated a large part of the known factors and issues about human cardiomyogenesis (Doetschman, Eistetter, Katz, Schmidt, & Kemler, 1985; Gepstein, 2002). *In vivo* developmental stages are recapitulated *in vitro* in the murine and human models as described in **Figure 1.3**. The improvement of the protocols has derived from spontaneously differentiated beating clusters of a percentage of the

differentiating cells on a dish that resulted in nearly pure cardiomyocytes (CMs) culture.

Data collected from experiments using both the Embryoid Bodies (EBs) and monolayer methodologies (see paragraph 1.2.3 "Protocols for cardiac differentiation of human pluripotent stem cells") revealed the major signalling pathways (families of proteins and growth-factors), which are thought to control early stages of mesoderm formation and cardiomyogenesis. Two key molecules that are added to experiments for in mesoderm induction *in vitro,* are the defined growth factors Activin A and BMP4. They are members of the transforming growth factor (TGF) betha superfamily and they act through downstream effectors (Smad proteins) depending on their function, referred as receptor regulated R Smads, co-mediator Co- Smads and inhibitory I-Smads. An alternative molecular pathway to follow in order to enhance cardiomyocytes generation, is to inhibit glycogen synthase kinase 3 (GSK3) pathway with small molecules inhibitors like CHIR99021, since it prepare for mesoderm specification (Lian, Zhang, Azarin, et al., 2013).

Later during differentiation, Dickkopf-1 (DKK-1) or IWP4 can further enhance CMs differentiation by terminating the canonical wingless/INT proteins (Wnt) signal and direct mesoderm to cardiac mesoderm (Yang et al., 2008). During the subsequent period also, fibroblast growth factor (FGF) 2 and vascular endothelial growth factor (VEGF) are important mitogens (Noseda, Peterkin, Simoes, Patient, & Schneider, 2011). Nevertheless, optimal concentrations of those cytokines must be optimized individually for each cell line to induce efficient cardiac development (Lian et al., 2012) (Paige et al., 2010). The signalling pathways have to be followed strictly: proteins of TGF-betha, Wnt inhibition and the FGFs all have highly specific temporal windows for effectiveness and genetic disruption of their signalling has dramatic effects on cardiac development (reviewed by Olson (Olson & Schneider, 2003)).

Cardiac progenitor cells already form an extremely organized primary and secondary heart field, ready to form the heart tube and start the looping procedure. This 3D organization is important to follow the endothelial and CMs commitment of the cells, which is dependent on VEGF and FGF signalling along with the Wnt inhibition from the previous stage of development (S. M. Wu, Chien, & Mummery, 2008) (Yang et al., 2008). Mesodermal specification has a very close contact to the hematopoietic and vascular lineages of the cardiovascular system. The resulting CMs in this stage are

immature and, in the early fetal stages of development; they exhibit spontaneous contraction, fetal-type ion channel expression (Beqqali, Kloots, Ward-van Oostwaard, Mummery, & Passier, 2006), and fetal-type electrophysiological signals (Davis, van den Berg, Casini, Braam, & Mummery, 2011).

In the following paragraphs, molecular pathways involved in key steps of cardiac differentiation will be described.

1.2.2.1 Bone morphogenetic protein and mesoderm formation

The BMPs form a large part of the TGF-betha superfamily. In particular, BMP4 is a critical signalling molecule required for the early differentiation of the embryo and establishing the dorsal-ventral axis (D. Chen, Zhao, & Mundy, 2004). It is an inducing osteogenesis polypeptide that was originally identified in cartilage and bone development and it is one of the paracrine signals from endoderm cells (S. M. Wu et al., 2008). Further on in the development, it is essential for the establishment of primary mesoderm, and thus of the cardiac differentiation pathway (P. Zhang et al., 2008). BMP4' s downstream effectors (Smad1/5) play an essential role in human embryonic development; a simplified pathway is illustrated in **Figure 1.4A**. The signalling receptor has a serine–threonine kinase domain. Among other receptor subtypes, there are many type I receptors (Activin receptor-like kinases [ALKs]) which mediate BMP binding (Shi & Massague, 2003). The activated type I receptors directly phosphorylate Smad transcription factors (Smad1/5/8 for BMPs (Miyazono, Kamiya, & Morikawa, 2010); Smad2/3 for TGF-betha and Activin A), which then form a complex with a common partner or co-Smad (Smad4). They translocate to the nucleus, where they interact with other transcription factors (D. Chen et al., 2004). The aforementioned classes can be inhibited by inhibitory Smads (Smad6/7): accumulating in the nucleus, they regulate the transcriptional activity of their target genes. The inhibitory Smads are natural inhibitors of TGF-betha-induced Smad-mediated signalling (ten Dijke & Hill, 2004). Despite the origin of BMP4, its *in vitro* application in the cardiac differentiation protocols described, activate signalling pathways that induce formation of pre-cardiac mesoderm with the typical early cardiac marker NKX 2.5. Inhibition of the BMP pathway affects negatively cardiac differentiation decreasing the percentage of cardiac Troponin T

positive (cTNT) cells in a concentration-dependent manner in *Danio* (Hao et al., 2010). Furthermore, blocking BMP activity in serum with BMP antagonist enhances neural differentiation (Pera et al., 2004).

1.2.2.2 Activin signalling pathway

Activin and Nodal, like BMPs, are members of the TGF-betha family. The TGF-betha pathway integrates signalling from TGF-betha, BMP, nodal and Activin. Activin has three isoforms: Activin A, Activin B, and Activin AB. The Activin to Smad pathway is essential for normal embryonic and extra embryonic growth and differentiation (Noseda et al., 2011). A simplified pathway is illustrated in **Figure 1.4B**. Activin acts through Activin receptor-like transmembrane serine-threonine kinases, to specific intracellular kinase, in a complex with type I receptor (ALK4). The pathway is restricted to Smad-dependent signalling. After ligand binding, activated ALK4 transduces the signal by phosphorylating Smad2 and Smad3. R-Smads interact with Smad4 and the R-Smad/Smad4 complex then undergoes nuclear translocation and stimulates various target gene expression; it also promotes cooperative DNA binding by the fork head winged-helix protein FoxH1, which mediates many effects of the pathway (Kitisin et al., 2007). Inibition of Activin A receptor-like kinase ALK5, and its relatives ALK4 and ALK7 block CMs specification (Inman et al., 2002). Activin was initially reported as a cardiomyocytes differentiation actor together with BMP4, with an important role in mesoderm formation (Sugi & Lough, 1995).

1.2.2.3 Wnt family

The Wingless-type Integration gene (Wnt) family takes its name from the Drosophila gene wingless (wg) and the orthologous int-1, an oncogene in mammary tumours activated by proviral insertion (Nusse et al., 1991). Cellular responses to these proteins are often categorized based on their utilization of betha-catenin, a co-activator of transcriptional effectors. Activity of the Wnt/betha-catenin “canonical” pathway maintains transcriptional programs that enable stem cells to remain multipotent (Cole, Johnstone, Newman, Kagey, & Young, 2008) (Van der Flier et al., 2007). Wnt

simplified pathways are illustrated in **Figure 1.4C**. Non-canonical Wnt signalling pathways in vertebrates are less well understood, but appear to have no certain function in heart development. The pathway is started upon the binding of the Wnt protein to the frizzled receptor at the cell surface. In the absence of ligand, betha-catenin is targeted for proteasome degradation via its phosphorylation by glycogen synthase kinase 3-betha (GSK3-betha) and CK1 (casein kinase 1), in a destruction complex also including Axin1 and the adenomatous polyposis coli complex (APC axin) tumour suppressor protein. Inhibitors specific for canonical Wnts include the extracellular protein dickkopf homologue (Bao, Zheng, & Wu, 2012) and small molecule inhibitor of Wnt response, like IWP4. Wnt Inhibitor IWP-4 was identified in a high throughput screen for antagonists of the Wnt/betha-catenin pathway. Germ line mutations in the Wnt pathway cause several hereditary diseases, and somatic mutations are associated with cancer of the intestine and a variety of other tissues. Despite the pathway being active in the initial period of mesoderm differentiation, Wnt signalling inhibition is essential for cardiogenic activity in the phase of cardiac progenitor cells (Lanier et al., 2012).

1.2.2.4 Fibroblast Growth Factors

Fibroblast growth factors (FGFs) constitute a large family of signalling polypeptides that are expressed in various cell types from early embryos to adults. Across vertebrates, FGFs are highly conserved and promiscuously bind to four high-affinity trans-membrane receptor tyrosine kinases, known as FGFR1, 2, 3, and 4. During embryonic development, FGFs act in multiple biological processes like cell proliferation, differentiation, and migration (Bottcher & Niehrs, 2005). FGFR1 plays an essential role in early development, mainly in mesoderm patterning and cell migration during gastrulation, and it is also involved in cell differentiation at several levels during early stages of organogenesis (Dvorak et al., 2005) (**Figure 1.4D**). The signal cascade downstream of FGFRs involves tyrosine phosphorylation of the docking protein FRS2 followed by recruitment of several Grb2 molecules. Activated Grb2 molecules bound to FRS2 recruit the nucleotide exchange factor SOS. The formation of FRS2-Grb2-SOS complexes results in activation of the Ras-Raf-p38 mitogen activated kinases (MAPK) signalling pathway followed by cell response. In parallel, phosphorylated FGFRs also activate phospholipase gamma, protein kinase C (PKC), and Grb2 molecule recruits the

docking protein Gab1 that activates the phosphatidyl-inositol 3 kinase (PI3K)-Akt cell survival pathway (Dvorak & Hampl, 2005). Human ESC express substantial levels of mRNAs coding for FGF2 and its three high-affinity receptors, FGFR1, FGFR3, and FGFR4. In addition, hESC express mRNA for the docking protein FRS2 that represents a major target of activated FGFRs (see **Figure 1.4**). The mitogen-activated protein kinase (MAPK) pathway was described as relevant for cardiac differentiation in later stages (Yook et al., 2011). Through the MEK-ERK pathway, the FGF-2 signalling pathway switches the outcome of the BMP4-induced differentiation of hESC by maintaining Nanog levels (P. Yu, Pan, Yu, & Thomson, 2011). FGF2 maintains pluripotency in hESC alone (Dvorak et al., 2005), or in combination with Activin A (Vallier, Alexander, & Pedersen, 2005). FGF2 with BMP4 cooperate to promote mesoderm induction during the initial part of the differentiation (Barron, Gao, & Lough, 2000). Combined use of Activin A, FGF2, BMP4, and VEGF specifically promotes the formation of multipotent mesoderm-committed progenitor cells, able to generate all mesoderm cell types, including cardiomyocytes, smooth muscle cells, and endothelial cells (Evseenko et al., 2010). FGF2 has a complex role in the mesoderm specification along with FGF8 (Reifers, Walsh, Leger, Stainier, & Brand, 2000), being part of the highly conserved FGF pathway.

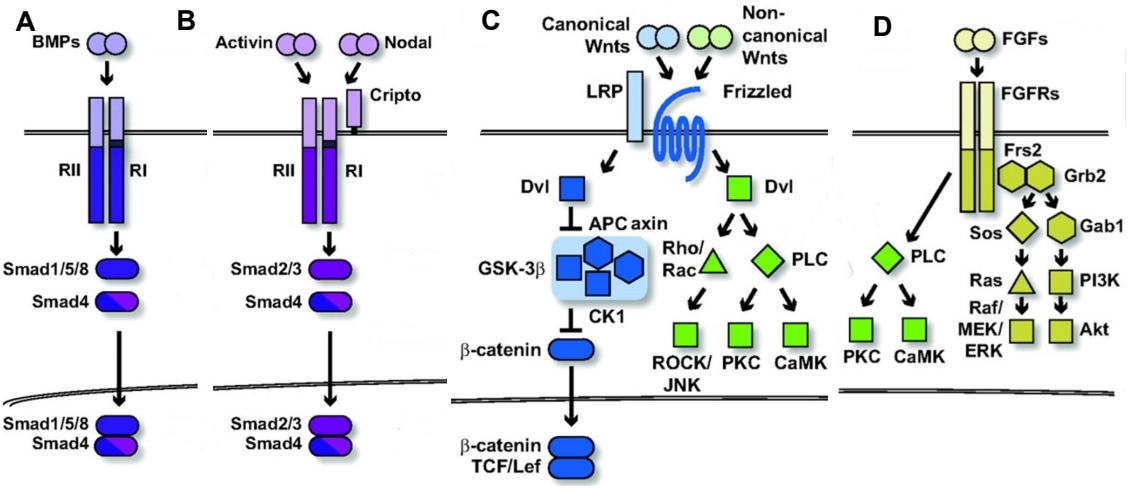

***Figure 1.4*: Signal pathways that underlie cardiac differentiation of stem cells**

A: BMP Pathway; B: Actin and Nodal Pathway; C: Wnt Pathway; D: FGF Pathway. Circle indicates ligand; oval transcription factors; rectangle receptor ligand-binding and signalling domains (light and dark, respectively), square represents protein kinases; triangle G-proteins; hexagon scaffold protein. Adapted from Noseda et al.

1.2.3 Protocols for cardiac differentiation of human pluripotent stem cells

The efficiency of the outcome of a differentiation protocol to obtain cardiomyocytes from hESC or iPSC depends, in part, on the individual cell line used and, also, on the methods used for propagation prior to differentiation. The differentiation methods that have been developed are based on three main techniques: spontaneous differentiation in EBs, differentiation in mouse visceral-endoderm-like cell (END2) co-culture and differentiation with defined factors. Apart from being differentiated from pluripotent cells, cardiomyocytes have been trans-differentiated directly from adult cell types.

In 2001 the group of Kehat published the possibility of getting CMs from human ESC cells (Kehat et al., 2001). Human ESC (Wisconsin line H9.2) were dissociated using collagenase IV into small clumps (less than 20 cells) and grown for 7 – 10 days in suspension to form EBs. Then they were plated onto gelatin-coated culture dishes. Those started spontaneous contractions after 11–14 days (four days after plating). A maximum in the number of beating areas was observed at 27–30 days of differentiation, with 8.1% EBs scored as contracting. Spontaneous differentiation to CMs in aggregates was soon after observed by others, claiming better efficacy and using different cell lines (R. H. Xu et al., 2002) (Q. He, Li, Bettiol, & Jaconi, 2003). Counting beating EBs may not be accurate, as individual EBs may contain significantly different numbers of cardiac cells, and the temperature of the microscope counting stage may also vary, but still it is considered a method for evaluating the outcome of a protocol.

First, a directed method for the derivation of CMs from the hESC cell lines has been described by Mummery et al. (Mummery et al., 2002) (Mummery et al., 2003) and (Passier et al., 2005). Beating areas were cultured in co-culture of hES[2] cells with END2. Endoderm secreted signals play an important role in the differentiation of cardiogenic precursor cells that are in the adjacent mesoderm during the embryonic development. Earlier co-culture of END2 cells with murine ESC had shown that beating areas appeared in aggregated cells and that culture medium conditioned by the END2 cells contained cardiomyogenic activity (van den Eijnden-van Raaij et al., 1991). Mitotically inactivated END2 cells were co-cultured with the human ESC cell line hES2 and gave beating areas after 12 days in co-culture. Later on, a third main way of differentiation was introduced in monolayer form, using the Matrigel-coated plates. The basic strategies for CMs differentiation are shown in **Figure 1.5**.

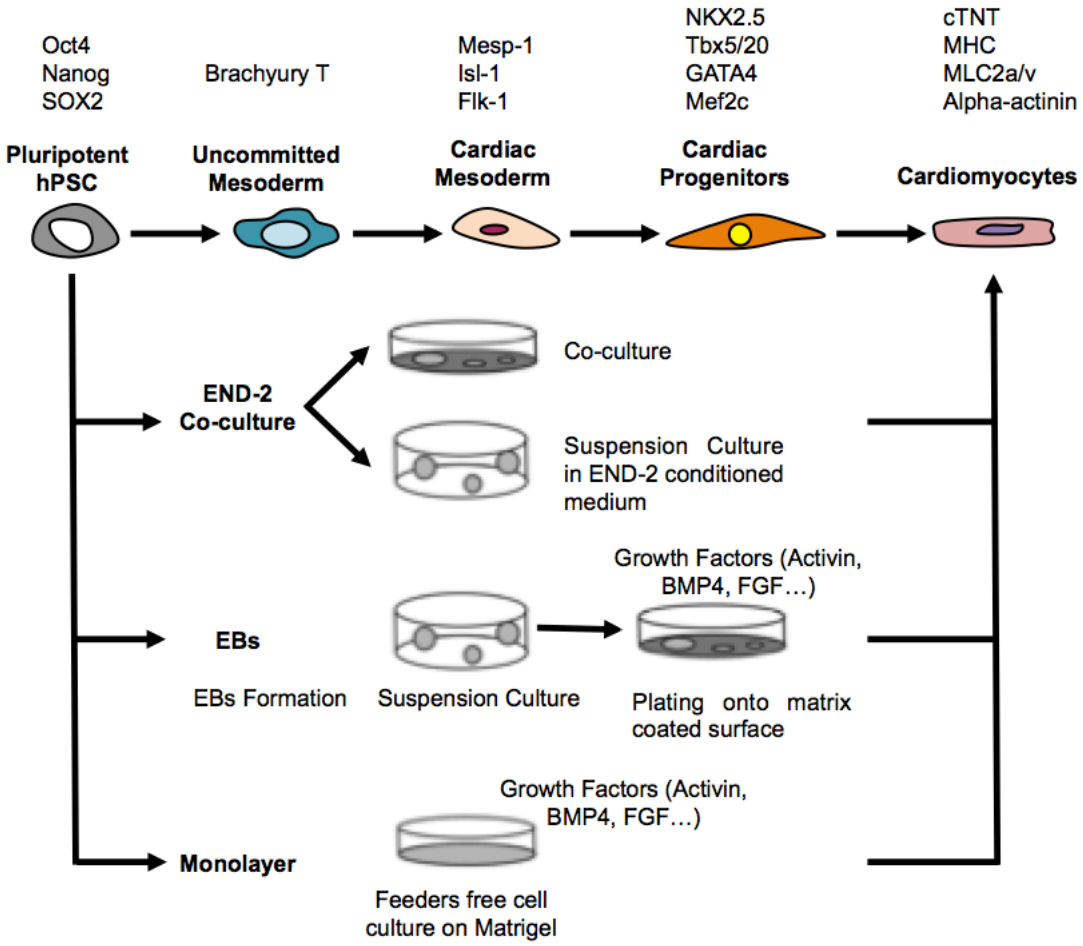

***Figure 1.5**: Cardiac differentiation cascade and differentiation methods*

From the top: Markers of different stages of cardiac differentiation, steps in cardiac differentiation and the differentiation methods. END-2 differentiation has two variables, hESC are either plated on top of END-2 cell layer or are cultured as EBs in suspension in END-2 conditioned medium. In EBs method, differentiation can be performed spontaneously or with differentiation inducing growth factors. Monolayer differentiation is initiated with feeder free hESC cultures. Culturing and differentiation of hESC are preformed on top of Matrigel.

Different cytokine approaches were tested, in agreement with differentiation pathways discussed in the previous session. After initial spontaneous indirect pathways (Kehat et al., 2001) and non-selective endoderm-inducing conditions of END2 cells (Mummery et al., 2002), mesodermal induction with Activin A and BMP4 were approached. Early differentiation was accomplished by those two factors alone. But shortly after initial 48 hours – 96 hours period, cells still express low levels of pluripotency markers such as

Oct4 and Nanog. This strategy resulted in the low amount of contracting colonies / EBs and various levels of cardio specific proteins in the samples. In order to specify more the mesodermal differentiation pathway, Wnt inhibitors (DKK1), VEGF and bFGF were studied and used as cardiac progenitor selective agents. So-called "small molecules" have various effects on cardiac differentiation. Among others, retinoic acid (RA) has been shown to accelerate hESC differentiation into CMs (Wobus et al., 1997). Enhancement was also seen using a retinoid X receptor agonist (Honda et al., 2005). RA is regulating the expression of NKX2.5, and has an effect on spatial organization of the primitive cardiac cells, as well as atria and ventricles organization in the animal model (Yutzey, Rhee, & Bader, 1994). Similarly, ascorbic acid (AA) has shown positive effects especially on EB based cultures (T. Takahashi et al., 2003), but the specificity of the AA and its possible pathway is discussed.

Until 2008, serum has been present in the culture medium of all differentiation protocols. Serum was reported to be un-favourable to maintenance of primary CMs (Piper, Jacobson, & Schwartz, 1988). The switch to serum free methods eliminated the "batch bias" and was also required for possible clinical applications. A switch to a serum-free differentiation medium in mouse EBs resulted in a 4.5-fold increase in the percentage of beating clusters (Sachinidis et al., 2003). Similarly, insulin (originally in the differentiation media) was omitted without losing CMs yield and was further shown to have even a negative effect on cardiac differentiation (X. Q. Xu, Graichen, et al., 2008).

In addition to classical cardiac differentiation of pluripotent stem cells, cardiac cells have been obtained directly from other adult cell types. The direct trans-differentiation idea came from the observation that the generation of hiPSC had shown that a relatively small set of defined genes could epigenetically alter the global gene expression of a cell. If a somatic cell could be reprogrammed into a stem/progenitor cell, probably could undergo also direct cardiac reprogramming. A combination of three developmental transcription factors (referred as GMT) was shown to reprogram murine post-natal cardiac and dermal fibroblasts directly into differentiated cardiomyocyte-like cells [zinc-finger transcription factor recognizing the GATA motif – Gata4, myocyte enhancer factor 2C (Mef2c) and T-box transcription factor 5 (Tbx5)] (Szabo et al., 2010) (Qian et al., 2012). This attitude stresses that cardiac fibroblasts comprise over 50% of all the cells in the heart (Snider et al., 2009). Mouse tail-tip dermal fibroblasts

were also able to generate CMs (the same way as murine cardiac fibroblasts) (Szabo et al., 2010). More recently, direct reprogramming of human fibroblasts has also been achieved (Islas et al., 2012). Several studies showed that the murine direct reprogramming factors Gata4, Mef2c, and Tbx5 (GMT), or GMT plus Hand2 (GHMT), were insufficient to transform human fibroblasts into CMs (Nam et al., 2013) (Wada et al., 2013), indicating that the differences between mouse and human cardiovascular development need to be considered for optimal transdifferentiation to human CMs. Better results were obtained adding to the cocktail small-non coding RNA miR-1, and miR-133m that converted human adult dermal fibroblasts into induced cardiomyocyte-like cells . The transduction of these factors promoted substantial cardiac troponin T expression in at least 9% of the source population (Nam et al., 2013). Shortly afterward, introduction of GMT plus Mesp1 and myocardin (GMTMM) was also shown to successfully convert human fibroblasts to iCMLs (Wada et al., 2013). Since then, alternative approaches have succeeded in generating human iCMs with gene expression profiles and functional characteristics similar to those detected in ESC-CMs (Fu et al., 2013).

1.2.4 Enrichment of differentiated cardiomyocytes

Due to the inefficient differentiation, the resulting cell populations that arise from a differentiation protocol, are a mixture of different cell types and the yield of hES/iPSC-CM cultures can be very low. EB differentiation in serum containing medium yields <1% and the more defined ActivinA/BMP-4 protocol yielded > 30% of cardiomyocytes (Laflamme et al., 2007). Therefore differentiation methods need considerable up-scaling and effective enrichment and purification methods should be developed before differentiated cardiomyocytes can undergo testing and clinical use in the future.

For certain research purposes, it is adequate to enrich the hES/iPSC-CM by mechanically dissecting beating areas from the differentiation cultures (Kehat et al., 2001) (Mummery et al., 2003).

Percoll^{TM} gradient separation based on density gradient separation has been used in combination with the generation and maintenance of cardiac bodies (C. Xu, Police, Hassanipour, & Gold, 2006). After separation and 7 days of suspension maintenance, 50% of the cultured EBs contained beating areas. However, this method has been

difficult for others to reproduce (van Laake, Hassink, Doevendans, & Mummery, 2006), and also in our hands.

Transgenic selection is one technique to enrich cardiomyocytes from hESC differentiation cultures. This method utilizes transgenic hESC/iPSC lines where a gene of green fluorescent protein (GFP) or an antibiotic resistance gene is located under the control of a cardiac specific promoter (D. Anderson et al., 2007; Kolossov et al., 2005) (Huber et al., 2007) (X. Q. Xu, Zweigerdt, et al., 2008) (Kita-Matsuo et al., 2009). Although this method is efficient, genetic modification is neither easy for hESC or human iPSC cell lines nor suitable for possible future clinical use (Mummery, 2010) (Vidarsson, Hyllner, & Sartipy, 2010). In a study from 2009, they sorted cardiomyocytes from mixed cell populations by using the endogenously expressed surface marker activated leukocyte cell-adhesion molecule, ALCAM (CD166) (Rust, Balakrishnan, & Zweigerdt, 2009). And in 2011 SIRPA (CD172a) was found to be a marker for cardiac cells from a screening of 370 known CD antibodies (Dubois et al., 2011). However, there is a lack of cardiac specific surface proteins and therefore a lack of antibodies to make sorting possible (Mummery, 2010). Nevertheless, fluorescence-activated cell sorting (FACS) was successfully used in selection by utilizing the high mitochondria content of cardiomyocytes (Hattori et al., 2010).

1.2.5 Characterization of differentiated cardiomyocytes

1.2.5.1 Functional and structural analysis

hES/iPSC-CM have the capacity to beat spontaneously (Kehat et al., 2001) (Mummery et al., 2003). Beating cells are at an early stage relatively small and round and situated in circular accumulations in the EBs. At later stages, EBs gradually develop to be larger and the cells turn to be more elongated in shape and tend to accumulate in strands. Electron microscopy studies reveal that cardiomyocytes contain myofibrils, which are first randomly and in a varying manner distributed throughout the cytoplasm. However, organized sarcomeric structures occur at later stages of differentiation with A, I and Z bands (see paragraph "1.3.2.2 Contractile apparatus" and **figure 1.7**). Mitochondria are also present close to the sarcomeres and cells have intercalated disks with gap junctions and desmosomes (Kehat et al., 2001) (Snir et al., 2003).

1.2.5.2 Expression of cardiac markers

Gene expression profiles of the hESC/iPSC during cardiac differentiation (Beqqali et al., 2006) (Synnergren et al., 2008) and the differentiated cardiomyocytes have been studied by DNA microarray (Cao et al., 2008) (Synnergren et al., 2008) (Kita-Matsuo et al., 2009) (X. Q. Xu, Soo, Sun, & Zweigerdt, 2009). These studies reveal that the molecular signature of hESC-CM resembles the cardiomyocytes from the human heart (Vidarsson et al., 2010). hESC/iPSC-CM differentiation can be predicted by the transient expression of the early mesodermal marker T (Brachyury). T (Brachyury) expression peak is detected at the time point of 3 days in END-2 co-cultures (Beqqali et al., 2006), a day later in EBs (Bettiol et al., 2007) and at day 1 in GSK pathway inhibition based protocols on iPSC monolayers (Lian et al., 2012; Lian, Zhang, Zhu, Kamp, & Palecek, 2013). T (Brachyury) belongs to the family of transcription factors, which are encoded by the T-box genes (Showell, Binder, & Conlon, 2004). This protein family plays roles in many developmental processes and has a sequence similarity with the DNA-binding domain, the T-domain (Showell et al., 2004). Brachyury T can be nominated as a classic transcription factor. It is localized in the nucleus and is an endogenous activator of mesodermal genes (Conlon et al., 1994) (Showell et al., 2004) (Kispert, Koschorz, & Herrmann, 1995). In the embryo, T (Brachyury) expression is suggested to be induced by TGF-beta and FGF signalling (Hemmati-Brivanlou & Melton, 1992) (Amaya, Stein, Musci, & Kirschner, 1993). Overall, very few direct targets for T-box genes have been identified. However, embryonic FGF (eFGF) (Casey, O'Reilly, Conlon, & Smith, 1998), has been suggested as downstream target for Brachyury T. Differentiation cascade can be further followed by the expression of cardiac regulatory transcription factors such as Islet-1 (Isl-1), Mesp 1, GATA4 and NKX2.5 (Graichen et al., 2008) (Yang et al., 2008).

Cardiac troponin T (cTNT) is encoded by the TNNT2 gene (Thierfelder et al., 1994). It is the tropomyosin-binding subunit of the troponin complex and can therefore be used for characterizing hESC/hIPSC-CM. Troponin complex is located on the thin filament of striated muscles and regulates muscle contraction in response to alterations in intracellular calcium ion concentrations (Farah & Reinach, 1995) (Tobacman, 1996). In addition to cTNT, other cardiac specific structural proteins are used for confirming cardiac phenotype of the beating hES/iPSC-CM such as cardiac troponin I, myosin or cardiac alpha-actinin (Kehat et al., 2001) (Mummery et al., 2003). Also, proteins of contractile apparatus, like cardiac alpha actin, proteins of gap junctions and ion

channels can be used in characterization. Gap junctions are formed from connexin proteins and have an important role in signal transduction. Connexin 43 (Cx43) is the most common form in the ventricle, Cx40 predominates in the atria and Cx45 is found in both atria and ventricle (Gaborit et al., 2007).

1.2.5.3 Electrophysiology and excitation-contraction coupling

Human ESC as well as iPSC cell-derived cardiomyocytes exhibit heterogenic action potential (AP) morphologies which can be divided into nodal, atrial and ventricular subtypes according to the shape of AP (J. Q. He, Ma, Lee, Thomson, & Kamp, 2003) (J. Zhang et al., 2009) (Zhang et al., 2009). If compared to the human neonatal or adult atrial or ventricular cardiomyocytes, hESC-CM have relatively positive maximum diastolic potential and slow maximum rate of rise of the AP, and are therefore called embryonic atrial- and ventricular like cells (J. Q. He et al., 2003). Differentiated beating cells exhibit spontaneous APs and contractile activity and therefore express cardiac structural proteins and ionic currents (Kehat et al., 2001) (Mummery et al., 2003) (J. Q. He et al., 2003). During differentiation, the expression of some ion channel genes increases suggesting that hESC-CM reach a more mature state with time in culture (Sartiani et al., 2007). Traditionally, patch clamp has been used in analysing the action potential and also the electrophysiological properties of cardiomyocytes. Microelectrode array (MEA) technology provides another useful platform to study cell electrophysiology, especially ESC-derived cardiomyocytes (Hescheler et al., 2004) (Reppel et al., 2004). In MEA, cells are plated on top of electrodes in a cell culture well-type platform and can be cultured and measured repeatedly for long periods of time.

Regarding excitation-contraction coupling, hESC/iPSC-CM have functional, even if immature, calcium handling components when compared to adult cardiomyocytes (Dolnikov et al., 2006) (J. Liu, Fu, Siu, & Li, 2007) (Satin et al., 2008). For clinical applications, the calcium system should be functioning properly to hESC-CM to integrate properly after transplantation since poor integration to the host myocardium could have serious arrhythmias as a consequence. Nevertheless, a better understanding of calcium properties of the differentiated hESC-CM is needed.

1.2.6 Fetal vs. post-natal cardiomyocytes

There are marked phenotypic differences between fetal and post-natal CMs, including age-dependent changes in protein kinase expression, betha-adrenergic signalling (Schaffer & Williams, 1986), contractile apparatus maturity, and the hyperplastic (Rybin & Steinberg, 1994) versus hypertrophic (Pandya, Santani, & Jain, 2005) responses to mechanical stress. The accumulation of maturation specific isoforms of sarcomeric proteins including cardiac myosin heavy chain, sarcomeric actin and actinin, titin, cardiac troponin-T and -I, and the maturation of sarcolemmal and sarcoplasmic reticulum (SR) ion channels (Hagege & Menasche, 2000) (Tenhunen et al., 2006) (Assmus et al., 2002) allow the functional characterization of cardiomyocytes identity and maturation. These characteristics determine the overall phenotypic appearance of CMs, which can differ depending on their location.

Regarding stem cell derived-cardiomycytes, there is currently no standard to what a stem cell derived-CM is. Many groups use the expression of early cardiac genes: NKX2.5 or GATA4 and the presence of rhythmic beating. This is not necessarily sufficient because skeletal and smooth muscle also contracts. Also, it has been widely accepted that terminally differentiated mature cardiac muscle does not express proteins that are specific to skeletal muscle. However, studies have shown that several skeletal muscle specific proteins, such as skeletal muscle specific troponins or ion channels, are transiently present in the developing heart (Haufe et al., 2005) (Saggin, Gorza, Ausoni, & Schiaffino, 1989). Similarly, “cardiac” and “skeletal” excitation-contraction coupling mechanisms co-exist in the developing skeletal muscle with the “cardiac” type dominant in the early phases of myogenesis and the “skeletal” dominating in more mature muscle (Cognard, Rivet-Bastide, Constantin, & Raymond, 1992). These studies suggest the co-existence of many cardiac and skeletal muscle specific proteins (MHCs, troponins, etc.) as well as excitation-contraction coupling mechanisms within the developing tissue, but also within cultured cells, especially those that are considered to be immature. Thus, the functional characterization of CMs for their research and clinical application is an important issue to be taken in account.

1.2.7 Applications for hESC or iPSC derived cardiomyocytes

1.2.7.1 Functional and structural analysis

Since the establishment of the first permanent hESC line (Thomson et al., 1998) there has been a great hope of replacing damaged heart tissue by hESC derived cardiomyocytes. However, many major problems need to be solved before hESC-CMs are usable in clinics. Before clinical use becomes a reality, it is likely that the derived cardiomyocytes will be applicable for drug discovery and safety pharmacology applications (Braam, Passier, & Mummery, 2009). Nevertheless, cardiac differentiation and the beating cells are already a useful tool for developmental biology and to study the pathophysiology of human cardiac diseases. In addition, iPSC technology enables the production of patient specific cell lines, which extends the potential use even further.

1.2.7.2 Pathophysiology of cardiac diseases

Many cardiac diseases are caused by gene mutations or gene-environment interactions. So far, these severe diseases have been studied in animal models, especially with transgenic mice. Even though mouse models can provide valuable information, differences between human and mouse physiology limit the applicability of the results, for example the much faster beating rate of the mouse may override the effects of arrhythmias which would be severe for humans (Freund & Mummery, 2009). Cardiomyocytes derived from genetically modified hiPSC could be used as a disease model. To derive a mutated hiPSC line and the disease model, it needs to be genetically manipulated. However, genetic manipulation of hESC has proven to be more challenging if compared to mouse ESC cells and only a few reports of successful gene targeting and manipulation have been published (Braam et al., 2008) (Giudice & Trounson, 2008). To obtain disease specific lines, the genetic manipulation step can be circumvented by deriving iPSC cell lines from patients with genetic diseases (Ebert et al., 2009; Freund et al. 2010; Park et al., 2008). The differentiation of these model iPSC cells to the desired cell type makes it possible to study the development and the pathophysiology of the disease. In addition, the factors affecting the development and the progress of the disease can be studied (Freund et al., 2010).

1.2.7.3 Safety pharmacology and drug discovery

The heart has been proven to be very sensitive to the side effects of pharmaceutical compounds. Severe reactions, such as syncope, arrhythmia and sudden death, related polymorphic ventricular tachycardia, torsade de pointes (TdP), have led to the refusal of approval or the withdrawal from the market of many pharmaceutical agents (Roden, 2004). In the absence of a complete understanding and direct analysis of TdP, the regulatory authorities have adopted the QT prolongation as a marker for the possible development of drug-induced TdP even though it is not a perfect marker for arrhythmogenesis (Finlayson, Witchel, McCulloch, & Sharkey, 2004). Prolongation of the QT interval resulting from a delay in ventricular repolarization, whether drug-induced or, for instance, congenital arising from mutation of genes, may be associated with TdP (Roden, 2004) (Zareba & Cygankiewicz, 2008), although the relationship is complex (Shah & Hondeghem, 2005). However, the QT interval is the cornerstone of the guidelines for the assessment of new chemical compounds in regard to pro-arrhythmic potential (Food & Drug Administration, 2005a) (Food & Drug Administration, 2005b). Currently, a number of preclinical models and assays have been employed by pharmaceutical companies (Carlsson, 2006; Pollard et al., 2008). These assays include *in vivo* QT assays, such as ECG of conscious dogs (Miyazaki et al., 2005), and *in vitro* assays, such as repolarization assay, which detects changes in the action potential delay (APD) of cardiac tissues (isolated animal Purkinje fibres, papillary muscle or cardiac myocytes).

Those methods are not fully adequate (Redfern et al., 2003) (Lu et al., 2008). In addition, the *in vivo* assays are ethically questionable because of the large number of animals used. Therefore there is a need for an *in vitro* method based on human cardiac cells that would bring additional value and reliability for testing novel pharmaceutical agents. Cardiomyocytes derived both from hESC and iPSC cells have many potential applications in the pharmaceutical industry including target validation, screening and safety pharmacology. These cells would serve as an inexhaustible and reproducible human model system and preliminary reports of the validation of hESC-CM system already exist (Braam et al., 2010). However, much optimization and development remains to be done, especially because of the immature phenotype of these cells and

problems due to the differentiation efficiency, heterogeneous hESC/iPSC-CM populations and enrichment methods (Braam et al., 2009).

1.2.8 Regenerative medicine

In principle, it would be possible to restore the function of the damaged heart by transplanting differentiated hESC or iPSC cells. However, this may be one of the most challenging tasks to put into practice. The needed number of transplantable cells is high and they should be immunocompatible. In addition, the transplanted graft should integrate into the host myocardium and receive blood flow to remain vital, couple with host myocardium and contract in synchrony in response to the conduction system (Braam et al., 2009). Using iPSC cells as source, immunomatched cells can be produced but reprogramming methods with viral vectors (K. Takahashi et al., 2007) (J. Yu et al., 2007) preclude consideration of their use in transplantation medicine. To this aim, iPSC obtained with non-integrating methods have to be used. hESC-CM have been transplanted into healthy myocardium of rodents. Cells survived and proliferated but they were usually separated from the rodent myocardium by a layer of fibrotic tissue (Laflamme et al., 2005) (van Laake et al., 2007). When transplanted into infracted rat or mouse hearts, some beneficial effects for the function of the heart occurred (van Laake et al., 2007) (Laflamme et al., 2007). However, after longer follow-up the positive effects were no longer present (van Laake et al., 2007) (van Laake, Passier, Doevendans, & Mummery, 2008) (van Laake et al., 2009). The doubt is if these temporary benefits are due to the formed myocardium or paracrine effects. In addition to the above-mentioned issues, the timing of cell therapy and the delivery methods still needs to be determined. Other attempts to stimulate *in vivo* the regeneration of injured cardiac tissues were pursued on animal models by: 1) injection of differentiated cells or stem cells (SCs) in situ (Hassink, Dowell, Brutel de la Riviere, Doevendans, & Field, 2003) (Hassink, Brutel de la Riviere, Mummery, & Doevendans, 2003); 2) mobilization of endogenous stem cells with cytokines (Orlic, Kajstura, Chimenti, Limana, et al., 2001); 3) activation of cardiomyocytes cell cycle (Pasumarthi & Field, 2002) (Field, 2004) obtained, e.g., by inducing permanent coronary artery occlusion (Hassink et al., 2008) or performing apical ventricular resection (Kikuchi et al., 2010) (Porrello et al., 2011). However, the application of these strategies is still limited since providing cells with the

fundamental signalling without resorting to structural supports is challenging (Bilodeau & Mantovani, 2006). It is likely, therefore, that cells need supportive material during transplantation: biomaterial research is also needed before clinical studies can be properly designed (Passier, van Laake, & Mummery, 2008).

1.3 Cardiac Tissue Engineering

The innovative field of cardiac tissue engineering (TE) could represent an effective alternative to overcome the limitations of the current clinical therapies and research application of hiPSC derived cardiomyocytes. This strategy, in fact, has shown the potential to generate both functional cardiac tissue substitutes for use in the failing heart, and biological in vitro model systems to investigate the cardiac tissue-specific development and diseases, allowing to perform accurate and controlled in vitro tests for cell and tissue-based therapies, drug screening, predictive toxicology and target validation. In the last decade, a great deal of progress was made in this field due to new advances in interdisciplinary areas such as biology, genetic engineering, biomaterials, polymer science, bioreactor engineering, and stem cell biology. Each of these areas has contributed to the development of the three main components of the cardiac TE: cells, scaffolds and culture environment, that can be used individually or in combination: 1) cells synthesize the new tissue; 2) scaffolds provide physical support to cells and a structural and biochemical cue tailored to promote cell adhesion, migration, proliferation and differentiation; 3) biomimetic in vitro culture environments, designed to replicate the *in vivo* situations by using biologically mimicking requirements, influence and drive cells to differentiate towards the desired phenotype and to express their functions, promoting extracellular matrix formation and tissue maturation.

1.3.1 Clinical motivation of cardiac tissue engineering

Cardiac disease is the leading cause of morbidity and mortality in the Western World (Ptaszek, Mansour, Ruskin, & Chien, 2012) (Roger et al., 2012). The inability of fully differentiated, supporting cardiac tissues for *in vivo* regeneration, and the limitations of the current treatment therapies greatly motivate the urgent demand for more efficacious

treatments to heart disease and new methods to repair damaged cardiac tissue. Novel approaches being developed include cell and gene therapy, and cardiac TE strategies. Cell therapy, due to the inability of adult cardiomyocytes to proliferate and regenerate injured myocardium, has emerged as an alternative treatment option. Differentiated cardiomyocytes would be, therefore an ideal cell source for injection, since they contain a developed contractile apparatus and can integrate through gap junctions and intercalated discs with the host CMs (Radisic M, 2011). However, large numbers of clinically relevant autologous CMs are unavailable. Other alternatives for appropriate cell sources, useful for the regeneration of infarcted myocardium, have been tested in animal models by transplantation of skeletal myoblasts (Dorfman et al., 1998), as well as CMs derived from ESC (Klug, Soonpaa, Koh, & Field, 1996), and bone marrow-derived mesenchymal stem cells (Toma, Pittenger, Cahill, Byrne, & Kessler, 2002). On the other hand, gene therapy approaches based on either delivering exogenous genes capable of expressing therapeutic proteins (Losordo et al., 1998) (Miao, Luo, Kitsis, & Walsh, 2000), or on blocking genes involved in the pathological process (Akhtar et al., 2000) (Mann & Dzau, 2000), are becoming alternative strategies.

However, current cell and gene therapeutic cardiac strategies have limitations. Cell therapy involves intramyocardial or coronary injection of cells suspended in an appropriate liquid (saline or culture medium). The main challenges associated with this procedure are poor survival of the injected cells (Muller-Ehmsen, Whittaker, et al., 2002) and washout from the injection site (Reffelmann & Kloner, 2003). According to some estimates, around 90% of the cells delivered through a needle leak out of the injection site (Muller-Ehmsen, Whittaker, et al., 2002) (Muller-Ehmsen, Peterson, et al., 2002). In addition, a significant number of cells die within days after injection (Muller-Ehmsen, Whittaker, et al., 2002; M. Zhang et al., 2001). Thus, developing improved delivery and localization methods (for example hydrogels) and effective anti-death strategies, could significantly improve effectiveness of cell injection procedures. Similarly, gene therapy approaches for myocardial infarction (MI), especially acute MI, are limited by the available delivery techniques. In general, in fact, the time it takes for transcription and translation is too long for a successful intervention in acute MI (Melo et al., 2004). Moreover, targeting a single gene as most commonly used in gene therapy may have conceptual limitations as well. Most pathological processes are complex and involve expression or down-regulation of multiple genes. In many cases, this genetic

complexity is not well understood and thus is difficult to predict what the ultimate effect of overexpressing or blocking of a single gene will be. In this respect, combination of gene and cell therapy may be a preferred approach in the treatment of heart diseases (Radisic 2011). But, the innovative field of cardiac TE, aiming to generate cardiac muscle cell-constructs to be used as three-dimensional (3D) models for in vitro physiological and pharmacological studies and eventually for repair of damaged heart muscle in vivo, could represent an effective alternative to overcome the current clinical limitations. Mammalian hearts have a regenerative potential only for a brief period after birth that is lost during development (Porrello et al., 2011). On the contrary, *in vitro* tissue development was proven to be more effective and adaptive, with its three main components, (cells, scaffolds and culture environment) that can be used individually or in combination (Lyons, Partap, & O'Brien, 2008): 1) cells synthesize the new tissue; 2) scaffolds provide physical support to cells and a structural and biochemical cue tailored to promote cell adhesion, migration, proliferation and differentiation (e.g., allowing the application of physical stimuli on the engineered construct); 3) biomimetic in vitro culture environments, designed to replicate the *in vivo* milieu by using biologically inspired requirements, influence and drive cells to differentiate towards the desired phenotype and to express their functions, promoting extracellular matrix (ECM) formation and tissue maturation (Grayson, Martens, Eng, Radisic, & Vunjak-Novakovic, 2009) (Egli & Luginbuehl, 2012). Due to the structural and functional complexity of cardiac tissues, for the effective production of organized and functional cardiac engineered constructs *in vitro*, two fundamental requirements need to be satisfied. First, cardiac TE implies the use of biomaterials that might present native-like tissue mechanical properties and/or topographical cues (D. H. Kim et al., 2010), as well as applying physiologic conditions such as perfusion (Radisic, Marsano, Maidhof, Wang, & Vunjak-Novakovic, 2008), electrical (Tandon et al., 2009) and mechanical stimulation (Fink et al., 2000) (Gonen-Wadmany, Gepstein, & Seliktar, 2004) (Birla, Huang, & Dennis, 2007) (Zimmermann, Schneiderbanger, et al., 2002) during cell culture (Massai et al., 2013). Consequently, a suitable dynamic environment is essential for applying these physiological conditions, and can be achieved and maintained within bioreactors, technological devices that, while monitoring and controlling the culture environment and stimulating the construct, attempt to mimic the physiological environment (Massai et al., 2013).

It has been demonstrated that the possibility to monitor and control the physicochemical environment, to provide a wide range of physical stimuli, and, eventually to adapt culture conditions to tissue maturation, allows to obtain engineered constructs with improved morphological and functional properties (Carrier et al., 1999) (Dumont et al., 2002) (Bilodeau & Mantovani, 2006). Moreover, in recent years, several studies have shown that the use of bioreactors in industrial processes for TE is sustainable both clinically and economically (Archer & Williams, 2005) (Portner, Nagel-Heyer, Goepfert, Adamietz, & Meenen, 2005) (Olmer et al., 2012). In addition, cardiac TE has shown the potential to generate thick-contractile myocardium-like constructs that might be used as functional substitutes or as biological *in vitro* model systems (Bursac et al., 1999) (Habeler et al., 2009) (Smits et al., 2009) (Hirt et al., 2012) to investigate the cardiac tissue-specific development and diseases, and to offer accurate and controlled *in vitro* tests for cell and cardiac tissue-based therapies (Tulloch & Murry, 2013), drug screening, predictive toxicology and target validation (Elliott & Yuan, 2011) (Hansen et al., 2010). Literature (Pok & Jacot, 2011) (Venugopal et al., 2012) reports also the beneficial effects of the use of patches for the injured myocardium. Within this scenario, the bioreactor described in this work, provide an example for generating a patch to be used as biological *in vitro* research model systems for assessing fundamental myocardial biology and physiology, and to be implemented for use in pharmacological research.

1.3.2 Anatomy and properties of human heart

The anatomy notions here mentioned are referred to (Weinhaus 2009). The mammalian heart is a muscular pump which serves two primary and vital functions: 1) collect blood from the tissues of the body and pump it to the lungs; and 2) collect blood from the lungs and pump it to all other tissues in the body. Human heart lies in the thorax, posterior to the sternum and costal cartilages, and rests on the superior surface of the diaphragm. It assumes an oblique position in the thorax, with two-thirds to the left of midline. It occupies a space between the pleural cavities called the middle mediastinum, defined as the space inside of the pericardium, the covering around the heart. This serous membrane has an inner and an outer layer, with a lubricating fluid in between. The fluid allows the inner visceral pericardium to ‘‘glide’’ against the outer parietal

pericardium. The internal anatomy of the heart reveals four chambers composed of cardiac muscle or ‘‘myocardium’’. The two upper chambers (or atria) function mainly as collecting chambers; the two lower chambers (ventricles) are much stronger and function to pump blood. The role of the right atrium and ventricle is to collect blood from the body and pump it to the lungs. The role of the left atrium and ventricle is to collect blood from the lungs and pump it throughout the body. There is a one-way flow of blood through the heart; this flow is maintained by a set of four valves. The atrioventricular or AV valves (tricuspid and bicuspid) allow blood to flow only from atria to ventricles. The semilunar valves (pulmonary and aortic) allow blood to flow only from the ventricles out of the heart and through the great arteries. During ventricular systole, AV valves close in order to prevent the regurgitation of blood from the ventricles into the atria. During ventricular diastole, the AV valves open as the ventricles relax, and the semilunar valves close. The semilunar valves prevent the backflow of blood from the great arteries into the resting ventricles.

Although the heart is filled with blood, it provides very little nourishment and oxygen to the tissues of the heart. The walls of the heart are too thick to be supplied by diffusion alone. Instead, the tissues of the heart are supplied by a separate vascular supply committed only to the heart. The arterial supply to the heart arises from the base of the aorta as the right and left coronary arteries (running in the coronary sulcus). The venous drainage is via cardiac veins that return deoxygenated blood to the right atrium. The coronary arteries arise from the ostia in the left and right sinuses of the aortic semilunar valve, course within the epicardium, and encircle the heart in the AV (coronary) and interventricular sulci.

A cross-section cut through the heart reveals a number of layers (**Figure 1.6).** From superficial to deep these are: 1) the parietal pericardium with its dense fibrous layer, the fibrous pericardium; 2) the pericardial cavity (containing only serous fluid); 3) a superficial visceral pericardium or epicardium; 4) a middle myocardium; and 5) a deep lining called the endocardium. The endocardium is the internal lining of the atrial and ventricular chambers, and is continuous with the endothelium of the incoming veins and outgoing arteries. It also covers the surfaces of the AV valves, pulmonary and aortic valves, as well as the chordae tendinae and papillary muscles. The endocardium is a sheet of epithelium called endothelium that rests on a dense connective tissue layer consisting of elastic and collagen fibers. These fibers also extend into the core of the

previously mentioned valves.

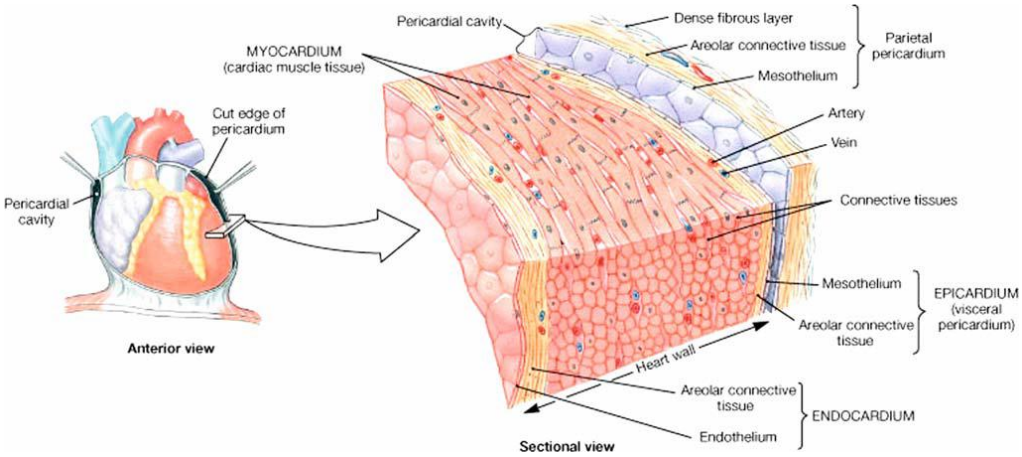

***Figure 1.6:* Internal anatomy of the heart**

The walls of the heart contain three layers—the superficial epicardium, the middle myocardium composed of cardiac muscle, and the inner endocardium (Weinhaus and Roberts, 2009).

1.3.2.1 Cellular composition of the heart

The bulk of heart tissue is the contractile myocardium, a highly differentiated tissue, around 1 cm thick in humans, with an asymmetrical and helical architecture (Buckberg, 2002) (Akhyari, Kamiya, Haverich, Karck, & Lichtenberg, 2008) composed of tightly packed cardiomyocytes (CMs) that form myofibers. Together with cardiomyocytes, transmission and scanning electron microscopy have identified five types of non-muscle cells within the adult myocardium: endothelial cells, fibroblasts, pericytes, smooth muscle cells, and macrophages, which comprise approximately 65-70% of ventricular cells (C. A. Beltrami et al., 1994). CMs are highly metabolically active; therefore oxygen and nutrients are depleted within a relatively thin layer of viable tissue (Carrier et al., 2002a). They comprise only 20–40% of the total cells in the heart but they occupy 80–90% of the heart volume (Nag, 1980). Morphologically, intact CMs have an elongated, rod shaped appearance.

Fibroblasts, of mesenchymal origin, constitute the bulk of non-myocyte cell population (Souders, Bowers, & Baudino, 2009). Their main function is to secrete and maintain extra cellular matrix (ECM) components, including collagen, fibronectin, and laminin (see next paragraph). Unlike CMs and endothelial cells, fibroblasts are found natively in the stromal space and lack basement membranes. This feature gives them their unique ability to migrate and populate injury sites, such as a myocardial infarct, and quickly restore tissue volume and ECM proteins (van den Borne et al., 2010). In the developing fetal heart, cardiac fibroblasts contribute to ECM rich structure including valves and atrial ventricular walls. As the heart matures, a 3D network of collagen and fibroblasts, known as the cardiac skeleton, begins to take shape. This network allows cardiac fibroblasts to exert forces on the myocytes, as well as, to respond to external stimuli through degradation and synthesis of ECM. These processes help to maintain the mechanical integrity of the heart through cell-cell and cell-ECM interactions. More importantly, cardiac fibroblasts forms heterotypic gap junctions with nearby CMs or fibroblasts, whereby the conductivity of these junctions can be modulated by the differential expression and coupling of connexins isoforms, including Cx45, Cx43 and Cx40 (Kohl, 2003) (Louault, Benamer, Faivre, Potreau, & Bescond, 2008). The cell-cell interaction between cardiac fibroblasts and cardiomyocytes helps to ensure the long range synchronization of myocardium contraction. Cardiac fibroblasts also play a pivotal role during cardiac repair. Residence fibroblasts can mobilize in response to

tissue damage and differentiate into smooth muscle-like cells called myofibroblasts (Tomasek, Gabbiani, Hinz, Chaponnier, & Brown, 2002). These are not true smooth muscle cell, but they are more contractile and active compared to fibroblast. The ability of myofibroblasts to contract collagen and produce new ECM helps stabilizing wound site and form scar tissue. In myocardial infarcts, these cells are responsible for the formation of granulation tissue. However, their eventual loss through apoptosis results in the weakening of the scar and the ultimately leads to heart wall thinning (van den Borne et al., 2010) (Kakkar & Lee, 2010). Therefore, the dynamic balance between fibroblast and myofibroblasts' phenotype is a critical factor in wound healing outcome.

1.3.2.2 Extracellular Matrix

Extracellular matrix (ECM) refers to the non-cellular components found in tissues. It is a complex mixture of molecules including proteins such as collagen, elastin, laminin, fibronectin and polysaccharides such as glycosaminoglycans (GAG). The composition and architecture of ECM varies depending on the native tissue. The primary purpose of ECM is to provide structural integrity to tissues. However, it is now known that ECM components such as collagen and laminin also play a crucial role in functional cell signalling through ECM receptors, such as the integrins, on cell membranes (Baronas-Lowell, Lauer-Fields, & Fields, 2004; Garlanda & Dejana, 1997; Ichii et al., 2001; Raines, 2000). The majority of ECM components in the heart are secreted by cardiac fibroblasts and myofibroblasts. They provide a wide range of ECM molecules for various functions, including fibrillar collagen and elastin for structural integrity, laminin and collagen IV for basement membrane maintenance, and proteoglycans for cell signalling modulation (Hutchings, Ortega, & Plouet, 2003; Orecchia et al., 2003). Moreover, these ECM components are able to transmit external stimuli to the myocytes and fibroblast and trigger intracellular signalling that can alter cellular functions. Ott *et al.* demonstrated that decellularized native cardiac tissue can be repopulated with cardiomyocytes and cardiac fibroblasts and give rise to functional tissue that possesses the microarchitecture of native tissue (Ott et al., 2008). This suggests that both the composition and organization of ECM molecules are important for proper tissue development.

1.3.2.2.1 Collagen

It is the most abundant protein in the body and accounts for 20 to 30% of total body weight (Harkness, 1966). Collagen has a simple amino acid sequence consisting of tripeptide repeats. This leads to a high degree of homology among collagens from different species. For example, type I collagen from bovine and porcine skin has been demonstrated to be highly compatible with human cells (Prockop & Kivirikko, 1995). The abundance and compatibility of collagen makes it an ideal matrix substrate for tissue engineering applications.

The widespread presence of collagen in the ECM is attributed to its unique micro and macro structure. Collagen is secreted mainly by fibroblasts, smooth muscle cells and enothelial cells, and it is present only in the ECM. The basic primary structure of collagen consists of repeating tri- peptide units of -Gly-X-Y-, where the amino acid X and Y are often represented by proline and hydroxyproline (Prockop & Kivirikko, 1995) respectively. Based on amino acid sequence, microstructure and functional attributes, collagen can be subdivided into several types. Type I collagen is the most abundant collagen. Together type I, II, III and V collagen share the same triple-helix structure and are referred to as fibrous forming collagens. In cardiac tissue, over 90% of collagen belongs to either type I or III (Espira & Czubryt, 2009). Other types of short fibrous collagen (type IX, XI, XII and XIV) serve as anchor fibers to secure cells and other ECM components to the larger, continuous collagen fibers. Type IV collagen is found in basement membrane and has unique globular structures along the triple-helix backbone (C. H. Lee, Singla, & Lee, 2001) resulting in the formation of sheet-like structure. There are many characteristics that make collagen a desirable material for tissue engineering scaffolds. Collagen is an excellent substrate for cell attachment. Certain amino acid sequences found in collagen are targets for integrin receptor binding. Collagen can be readily remodelled by matrix metalloproteinase secreted from implanted cells or native tissues surrounding the implant. Various experimental and commercially available collagen products are designed to gradually degrade and be absorbed by peri-implant tissues.

In the adult myocardium, the five most common types of collagen, in descending order of abundance, are type I, III, IV, V and VI. Collagen plays several essential roles in cardiac ECM. It mediates the fibrotic response of cardiac fibroblasts by forming

complexes with non-adhesive signalling protein, such as osteopontin, through the integrin receptors (Hsueh, Law, & Do, 1998). Type I collagen is the major component of the perimysium, a sheath-like connective tissue which surrounds and interconnects groups of myocytes to help maintain the ordered laminar structure of muscle bundles in the myocardium (LeGrice et al., 1995) (Pope, Sands, Smaill, & LeGrice, 2008). Each laminar layer consists of several fiber bundles stacked together. The layers are organized in varying directions depending on their locations. Fibers located on the epicardial and endocardial surfaces run in a base-apex orientation, whereas fibers in the mid-wall run in a circumferential orientation (Nielsen, Le Grice, Smaill, & Hunter, 1991). This structure gives rise to the anisotropy of the myocardium and also magnifies the shorting of each fiber bundle into the whole ventricular wall thickening (Coppola & Omens, 2008).

From a biomaterial perspective, collagen is a highly versatile material. It can be easily extracted from a wide variety of sources and can be processed into many different forms from sheets to discs, and hydrogel sponge to electrospun mesh. The amino acid residues on the collagen polypeptide backbone can be readily crosslinked or modified with synthetic polymers to modulate its mechanical and biological properties. For example, an interpenetrating network made from poloxamine, a synthetic hydrogel, and natural collagen fiber has been shown to improve the mechanical strength of the resulting composite hydrogel while maintaining cytocompatability (Sosnik & Sefton, 2005).

1.3.2.2.2 Elastin and Other ECM Proteins

Elastin fibers provide flexibility and elasticity to tissues such as blood vessels, skin and cardiac tissue. In arteries, elastin fibers constitute up to 50% of its dry weight and is secreted mainly by vascular smooth muscle cells (Alberts, 2002). Moreover, elastin fibers are long-lasting and have a low turnover rate, thus making it an important structural ECM component. Like collagen, elastin is synthesized in a soluble pro-protein form known as tropoelsatin. Tropoelastin is bound by a 67 kD galatolectin chaperone protein on the cell membrane to prevent premature coacervation (Hinek & Rabinovitch, 1994). Tropoelastin consist of alternating Lys-Ala rich hydrophilic and Val-Pro-Gly rich hydrophobic domains (B. Li & Daggett, 2002). Unlike collagen, no proteolytic

processing of tropoelstin is required for elastogenesis. Instead, the lysine/alanine rich domain takes on the alpha-helix structure, where the lysyl residues are readily deaminated by extracellular lysyl oxidase to form translysyl crosslinkages (Debelle & Tamburro, 1999). On the other hand, hydrophobic domains from adjacent tropoelastin molecules form loose interpenetrating chain structures that are responsible for the elasticity of elastin fibers (Keeley, Bellingham, & Woodhouse, 2002). Once crosslinked, elastin forms an insoluble elastin fiber.

Besides collagen and elastin, fibronectin (FN) is the next most abundant ECM component. FN molecules form homodimers and consist of several distinctive functional domains. FN exists in both insoluble and soluble forms. In its insoluble ECM form, FN associates with collagen fibers with its collagen-binding domain, while interacting with cell surface adhesion molecules such as integrin through its Arg-Gly-Asp (RGD) domain. This bifunctional nature allows FN to serve as a biological crosslinker between cells and the ECM (Schwarzbauer, 1991). Also, by using integrin as a transmembrane adapter protein, the actin cytoskelekton exerts forces on extracellular FN fibrils to aid in its polymerization and organization. Soluble FN circulates through the blood stream and participates in thrombosis and wound healing.

Another bifunctional ECM component is laminin (LM). Laminin is found associated with type IV collagen in the basal lamina. Like FN, laminin can bind to both ECM components and cell surface receptors and it is believed to influence cell attachment, migration and differentiation (Alberts, 2002).

1.3.2.3 Contractile apparatus

Contractile apparatus of cardiomyocytes consists of sarcomeres arranged in parallel myofibrils (Severs, 2000). So, sarcomere is the smallest functional, contractive unit of a myofibril. Sarcomeres occur as repeating units, extending from one Z line (Z for from the German "Zwischenscheibe", *the disc in between* the I bands) to the next along the length of the myofibril (**Figure 1.7**). The central bipolar thick filaments are composed primarily of myosin, with each thick filament surrounded by six parallel thin filaments originating from the Z-disc at both ends of the sarcomere. Thin filaments from adjacent sarcomeres are crosslinked by alpha-actinin at the Z-disc. Six giant titin proteins lie along the entire length of the thick filament and beyond, spanning the centre of the sarcomere to the Z-disc, where they interact with α-actinin (Kontrogianni-Konstantopoulos, Ackermann, Bowman, Yap, & Bloch, 2009). A and I bands have been named for their properties under a polarizing microscope. A-band (A for anisotropic) is seen as a dark segment that corresponds to the thick filament, and the I-band (I for isotropic) is seen as a light segment, spanned by thin filaments and titin only (Hwang & Sykes, 2015).

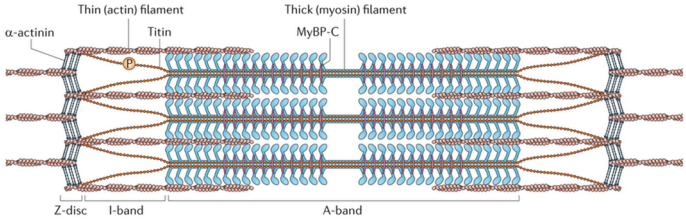

***Figure 1.7:* Sarcomere Structure**

Z discs delimitate sarcomere units. Myosin forms the central thick filaments, and actin forms thin filaments originating from the Z-disc at both ends of the sarcomere. Thin filaments from adjacent sarcomeres are crosslinked by α-actinin at the Z-disc. Six giant titin proteins lie along the entire length of the thick filament and beyond, spanning the centre of the sarcomere to the Z-disc, where they interact with α-actinin. Surrounding the Z-line is the region of the I-band. I-band is the zone of thin filaments that is not superimposed by thick filaments. Following the I-band is the A-band. An A-band contains the entire length of a single thick filament.

Electrical signals propagate through a 3D syncytium formed by CMs. Rapid impulse propagation is enabled by specialized junctions between cells, gap junctions, which are composed of different forms of connexin protein. The most abundant protein in ventricular CMs is connexin-43. Groups of specialized CMs (pace makers), which are located in the sinoatrial node, drive periodic contractions of the heart. The majority of the CMs in the myocardium are non-pace maker cells and they respond to the electrical stimuli generated by pace maker cells. Excitation of each cardiomyocyte causes an increase in the amount of cytoplasmic calcium, which triggers mechanical contraction. The result is an electrical excitation leading to a coordinated mechanical contraction to pump the blood forward (Odedra D, 2011).

Therefore, the heart can be considered as a dynamic electromechanical system where the myocardial tissue undergoes mechanical stretch during diastole and active contraction during systole, consuming large amounts of oxygen.

1.3.2.4 Physiological and electrical properties

The physiological stimuli that affect the entire cardiac system submit it to continuous stresses that require an enormous strength, flexibility and durability of the structures, as well as a high degree of adaptive capacity to face changes due to growth, physical activity and pathological conditions (Bouten et al., 2011). In details, in the normal human heart during one cardiac cycle, the left ventricular pressure ranges between 10 and 120 mmHg, and the cavity volume varies between 40 and 130 ml (Fortuin, Hood, & Craige, 1972) (Bouten et al., 2011), respectively. The right ventricle pressure ranges between 5 to 30 mmHg (Schneck, 2003), and the cavity volume changes from 24 to 86.5 ml (Mahoney et al., 1987). Local mechanical loads can reach 50 kPa (Bouten et al., 2011), with 22.9% longitudinal and 59.2% radial mean strain (Kuznetsova et al., 2008). However, exhaustive quantitative measures of the mechanical properties of human heart are still an open challenge.

With regard to the electrical properties, tissue in general is surrounded by extracellular fluid with relatively high electrical conductivity (Durand, 2000). For vertebrates, the physiologically significant range of endogenously produced electrical field strengths is 0.1-10 V/cm (Tandon et al., 2009). The electrical stimuli present in the heart can be

classified as: 1) direct current signals, which affect and direct cell migration during the development of the cardiac primitive streak and left-right asymmetry; and 2) the pulsatile signals implicated in the development of the cardiac syncytium (Nuccitelli, 1992). In terms of frequency, the typical resting heart rate in adults is 60-100 beats per minute (bpm) that corresponds to 1-1.7 Hz (Schneck, 2008). In terms of pulse duration, 1-2 ms is sufficiently long to excite heart tissue cells (Tandon et al., 2009).

1.3.3 Functional cardiac tissue engineering approaches

Cardiac morphogenesis depends on complex cell-cell and cell-matrix interactions within a dynamic four dimensional environment (three dimensional (3D) plus time). Previous studies have shown that close cell-cell interactions and 3D culture conditions are often necessary prerequisites for cardiomyocytes differentiation (Akins et al., 2007) (P. A. Anderson et al., 2007) (Steinberg, 1963) and that cardiac cells within 3D cultured tissues display distinct features that are more representative of native tissues (Tobita et al., 2006) (Zimmermann et al., 2000) than are cells within 2D culture (Claycomb, 1983). 3D growth of cells in aggregate spheres has been shown to direct and facilitate cell-cell interactions as well as to modify the differential expression of both morphogenic and angiogenic pathways in CMs (Akins et al., 2007). Cell aggregate culture has been shown to enhance cardiomyocytes gene expression patterns (Akins et al., 2007), increase the synthesis and release of ECM components (Watzka et al., 2000), and accelerate cardiomyocytes differentiation efficiency of embryonic stem cells (Carpenedo, Sargent, & McDevitt, 2007). Aggregate culture has also been used to enhance survival and differentiation of various stem cell types (Carpenedo et al., 2007) (Kehat et al., 2001), versus static culture. These studies suggest that aggregation confers many of the necessary structural cues required for maintaining differentiated phenotype, including proper dimensionality, shape, cell–ECM, and cell–cell interactions. Bursac et al. investigated the effect of 3D vs. 2D culture on cardiomyocytes properties and found that the 3D microenvironment plays critical role in maintenance of cardiomyocytes metabolism, sarcomere formation, cell-to-cell connections, and electrophysiological properties (Bursac et al., 2003). Eschenhagen et al. described physiologic contractile force and action potentials in 3D neonatal engineered heart tissue (Zimmermann et al.,

2006) (Zimmermann et al., 2000) (Eschenhagen, Didie, Heubach, Ravens, & Zimmermann, 2002) (Eschenhagen et al., 1997) (Eschenhagen & Zimmermann, 2005) (Zimmermann, Melnychenko, & Eschenhagen, 2004). These studies show that a 3D environment is required for the proper cell-cell and cell-matrix interactions that drive proper cardiomyocytes differentiation and maturation with contractile function. Tissue engineering offers these advantages as well as flexibility of size and shape, high cell retention, and the ability to monitor three-dimensional tissue formation and function *in vitro*. Studies using various cell types and scaffolds, both natural and synthetic, have been successful in creating engineered cardiac tissue that resembles the native heart muscle in morphological, biochemical, and functional properties (Zimmermann et al., 2006) (Tobita et al., 2006) (Eschenhagen & Zimmermann, 2005) (Radisic et al., 2004) (E. J. Lee, Kim do, Azeloglu, & Costa, 2008) (Schwarzkopf et al., 2006) (Huang, Khait, & Birla, 2007) (Naito et al., 2006).

1.3.3.1 Cell sources

Various types of cells have been used in cardiac tissue engineering, including primary cardiac myocytes (Tobita et al., 2006) (Eschenhagen et al., 1997) (Radisic et al., 2004) (E. J. Lee et al., 2008; Shimizu et al., 2002) (Kofidis et al., 2002) (Feng, Matsumoto, & Nakamura, 2003; Ishii, Shin, Sueda, & Vacanti, 2005; McDevitt, Woodhouse, Hauschka, Murry, & Stayton, 2003; Zimmermann, Schneiderbanger, et al., 2002). Freshly isolated primary cardiac myocytes are used because of their structural and physiologic attributes as well as their intrinsic contractile properties.

Neonatal rat cardiomyocytes are often chosen for their natural electrophysiological, structural, and contractile properties (Ravichandran et al., 2013), however they have a limited capacity to proliferate and not clinical relevance. Embryonic stem cells (ESCs) (Boheler et al., 2002) (Guo et al., 2006; Mummery et al., 2002; Zimmermann & Eschenhagen, 2007) and iPSC (Mauritz et al., 2008) (Narazaki et al., 2008) (Martinez-Fernandez et al., 2009) (Zwi-Dantsis, Mizrahi, Arbel, Gepstein, & Gepstein, 2011) represent valid cell candidates for cardiac TE thanks to their autologous nature, ability to propagate in large quantities, and to differentiate into cardiomyocytes. However, their still high risk of tumorigenicity and the complexity of their differentiation protocols still

make it not an easy cell source to be used for safe and standardized cardiac TE. Human adult stem cells share most of the positive features with iPSC making them an eligible cell candidate for cardiac TE with the extra benefit of low oncogenesis, but have shown to have still a limited and not highly reproducible in vitro differentiation potential into fully mature cardiomyocytes (Orlic, Kajstura, Chimenti, Jakoniuk, et al., 2001) (A. P. Beltrami et al., 2003) (Planat-Benard et al., 2004). Skeletal myoblasts (SMs) are widely use in cardiac TE thanks to their high proliferative potential, high resistance to ischemia, and their fate restriction to the myogenic lineage, with the capacity to develop a complete contractile apparatus, virtually eliminates the risk of tumorigenicity (Menasche, 2004) (Menasche, 2008). On the other hand, the major disadvantage of SMs is that they do not electrically couple with the host cardiomyocytes (Durrani, Konoplyannikov, Ashraf, & Haider, 2010), and this obviously raises the major question of the mechanisms by which, in case of cell transplantation, the myoblasts can improve left ventricular function (Menasche, 2004).

1.3.3.2 Cardiac Patches

Cardiac patches have been investigated with the double aim of creating a tissue replacing strategy in case of large damaged hearts for therapy or to reproduce *in vitro* pieces of reliable heart tissue for research or drug screening options. Possible approaches explored for engineering a cell-based and functional scaffolds are cell self-assembly, porous and fibrous scaffolds, cultivation of thin films (sheets) of functionally coupled cells, and cells grown on composite scaffolds (Radisic and Sefton, 2011).

In cardiac TE approaches, most studies suggest that some type of scaffold is necessary to support assembly of cardiac tissue *in vitro*. An important scaffold-free approach includes stacking of confluent monolayers of cardiomyocytes (Shimizu et al., 2002). Even if cardiac patches obtained in this way generate high active force, engineering patches more than two or three layers remains a problem. Shimizu and colleagues also described the polysurgery approach. Vascularized cardiac patches can be formed by sequential layering of cell sheets in multiple surgeries (Shimizu et al., 2006). Despite this strategy demonstrates that thick tissues (around 1 cm) can in principle be created from cell sheets, the approach will be difficult to implement in the clinical setting.

Thick relevant contractile cardiac patch was obtained by combining cardiomyocytes cell sheets with CM-seeded small-intestinal submucosa (SIS) by Hata and colleagues. Stacked cardiomyocytes sheets contracted spontaneously and synchronously with seeded SIS after adherence, and a large portion of analysed constructs showed a defined contraction direction, parallel to the longitudinal axis (Hata et al., 2010). Stevens and colleagues managed to generate a cardiac patch based on human ESC-derived CMs by self-assembly of isolated cells in orbitally mixed dishes (Stevens, Pabon, Muskheli, & Murry, 2009), essentially creating cell aggregates that could be deployed as a patch. Engineered cardiac constructs have been created in different forms like free floating monolayers, chambers, ring-like structures, rectangular patches, and cylinders (Shimizu et al., 2002) (Zimmermann et al., 2006) (Tobita et al., 2006) (Radisic et al., 2004) (Yildirim et al., 2007). These have been constructed with many different natural and synthetic scaffolds, such as gelatin, fibrin glue, collagen, porous alginate, polyglycolic acid, and polyurethane (Kofidis et al., 2002) (McDevitt et al., 2003; Zimmermann, Schneiderbanger, et al., 2002) (Carrier et al., 1999; Christman, Fok, Sievers, Fang, & Lee, 2004; Dar, Shachar, Leor, & Cohen, 2002; Leor & Cohen, 2004; R. K. Li et al., 1999). Among all the biomaterials used, collagen sponges were the most common. In the pioneering approach of Li et al., fetal rat ventricular CMs were expanded after isolation, seeded on collagen sponges, and cultivated in static dishes for up to 4 weeks (R. K. Li et al., 1999). The cells proliferated with time in culture and expressed multiple sarcomeres. Similarly, fetal cardiac cells were also cultivated on porous alginate scaffolds in static 96-well plates. After 4 days in culture the cells formed spontaneously beating aggregates in the scaffold pores (Leor et al., 2000). Cell seeding densities of the order of 10^8 cell/cm^3 were achieved in the alginate scaffolds using centrifugal forces during seeding (Dar et al., 2002). Neonatal rat CMs seeded on collagen sponges formed spontaneously contracting constructs after 36h of culture (Kofidis et al., 2003) and maintained their activity for up to 12 weeks.

In a standard TE approach, fibrous polyglycolic acid (PGA) scaffolds were combined with neonatal rat CMs and cultivated in spinner flasks and rotating vessels (Carrier et al., 1999). The scaffold was 97% porous and consisted of non-woven PGA fibers 14 um in diameter. Peripheral layer of the constructs seeded with neonatal rat or embryonic chick CMs showed relatively homogeneous electrical properties and sustained macroscopically continuous impulse propagation on a centimeter-size scale (Bursac et

al., 1999). Electrospun scaffolds have gained significant attention as they allow the control over structure at sub-micron levels as well as control over mechanical properties, both of which are important for cell attachment and contractile function. Zong and colleagues (Zong et al., 2005) used electrospinning to fabricate oriented biodegradable non-woven polylactic acid (PLA) scaffolds. Neonatal rat CMs cultivated on oriented PLA matrices had remarkably well-developed contractile apparatus and demonstrated electrical activity.

A significant step towards a clinically useful cardiac patch was the cultivation of ESC-derived CMs on thin polyurethane (PU) films. Cells exhibited cardiac markers (sarcomeric actinin) and were capable of synchronous macroscopic contractions (Amaya et al., 1993). The orientation and cell phenotype could further be improved by micro-contact printing of ECM components as demonstrated for neonatal rat CMs cultivated on thin PU and PLA films (McDevitt et al., 2002; McDevitt et al., 2003). Similarly, thin (10-15 um diameter) several millimeter long cardiac organoids, positive for cardiac troponin I and capable to spontaneously contract, were obtained through microfluidic patterning of hyaluronic acid on glass substrates (Khademhosseini et al., 2007). In a recent study, Feinberg and colleagues seeded a layer of neonatal rat ventricular cardiomyocytes on a polydimethylsiloxane (PDMS) membrane that could be detached from a thermo-sensitive layer at room temperature. Called “muscular thin films”, these cell-covered sheets could be designed to perform tasks such as gripping, and pumping by careful tailoring of the tissue architecture, this film shape, and electrical-pacing protocol (Feinberg et al., 2007). Scaffold structure can be used to effectively guide orientation of CMs and yield anisotropic structure similar to the native myocardium even in the absence of specific physical cues such as electrical or mechanical stimulation. Engelmayr et al. constructed an accordion-like scaffold using laser boring of PGS layer (Engelmayr et al., 2008). The scaffolds were pre-treated with cardiac FBs followed by seeding of enriched CMs. During pre-treatment, rotating culture was used, while static culture was used upon cardiomyocytes seeding. Contractile cardiac grafts with mechanical properties closely resembling those of the native rat right ventricle were obtained after the culture period. In addition, the cells in the pores were aligned along the preferred direction. Bian and colleagues created a cell/fibrin hydrogel micromolding approach where PDMS molds, containing an array of elongated posts, were used to fabricate relatively large neonatal rat skeletal muscle

tissue networks. As the cells compacted the hydrogel, the presence of high-aspect-ratio posts forced them to elongate and align, thus imparting a high degree of anisotropy to the cells and the tissue. This approach has been extended to cultivation of cardiac patches based on mouse ESC-derived progenitor cells (Bian, Liau, Badie, & Bursac, 2009) (Bian et al., 2009). To combine the advantages of the presence of naturally occurring ECM and the stability of porous scaffolds, neonatal rat CMs were inoculated into collagen sponges or synthetic PGS scaffolds using Matrigel (Radisic et al., 2006). The main advantage of a collagen sponge is that it supports cell attachment and differentiation. Nevertheless the scaffold tends to swell when placed in culture medium; making complicated the creation of a parallel channel array resembling a capillary network. For that reason a biodegradable elastomer (Wang, Ameer, Sheppard, & Langer, 2002) with high degree of flexibility was used. Boublik et al. have reported mechanical stimulation of hybrid cardiac grafts based on knitted hyularonic acid- based fabric and fibrin (Boublik et al., 2005). The grafts exhibited mechanical properties comparable to those of native neonatal rat hearts. In a subcutaneous rat implantation model the constructs exhibited the presence of CMs and blood vessel ingrowth after 3 weeks.

1.3.3.3 Bioreactors

Cardiac patches, in order to be cultured *in* vitro, need special support, that only proper devices can provide. An engineered cardiac patch should 1) have dimensions (typically 10-50 cm^2 of surface area and millimetres of thickness) and contractile features, thus vascularization is fundamental for its survival; 2) have a compliant response adequate to assure adaptation to systolic strength and diastolic relaxation; and 3) guarantee structural and electrical integration with the hosting myocardium (Vunjak-Novakovic et al., 2010; Zimmermann et al., 2006) or replicate electrical characteristics of native tissue. The complexity of the cardiac tissue makes the fulfilment of these requirements very challenging, since adult CMs quickly dedifferentiate *in vitro* and the maintenance of their differentiation *in vitro* is still an open issue, and neonatal cells are still immature to obtain effective results from their culture. These open issues have driven the development of the biomimetic paradigm of cardiac TE, which involves the application of physiologically-relevant chemical and physical stimuli to cultured cells (Tandon et al., 2009).

A synergistic combination of cells, scaffolds and culture conditions within tailored bioreactors allows obtaining cardiac engineered constructs, which are close to the native tissue in morphology and function, thus offering new perspectives to basic cardiac research and tissue replacement therapy.

In their pioneering studies (Eschenhagen, Didie, Heubach, et al., 2002; Eschenhagen et al., 1997; Zimmermann et al., 2000), Eschenhagen, Zimmermann and coworkers proposed a method for the *in vitro* production of coherently contracting 3D engineered heart tissues (EHTs) made of CMs from embryonic chicken (Eschenhagen et al., 1997) and neonatal rats (Zimmermann, Didie, et al., 2002; Zimmermann et al., 2000) mixed with collagen type I and, only when cultivating rat cells, Matrigel. Going beyond the limitations of monolayer cultures, sheet-shaped EHTs provided a simplified model suitable for the investigation of heart-like features of the constructs and for an analysis of the consequences that culture environment and genetic manipulations have on contractility. In order to measure EHT contractile forces, EHTs were then immersed in thermo stated organ bathes, and subjected to stable isometric preloads and electrical pulses. EHTs exhibited well-organized myofilaments with intercellular connections, and coherent contractions after 2-3 days (Eschenhagen et al., 1997; Zimmermann et al., 2000).

The influence of chronic mechanical stretch on morphological and functional behavior of CMs was evaluated by Fink et al. (Fink et al., 2000), who subjected EHTs to phasic unidirectional stretch (1-20%, 1.5 Hz) for 6 days and then to isometric force measurement (as in (Eschenhagen et al., 1997; Zimmermann et al., 2000)). Stretched EHTs exhibited improved organization of CMs into parallel arrays of rod-shaped cells, increased cell length and width, and a marked improvement of the contractile function. They (Eschenhagen, Didie, Heubach, et al., 2002; Eschenhagen, Didie, Munzel, et al., 2002) (Zimmermann, Didie, et al., 2002) proved the *in vivo* feasibility of the EHT implantation on rats. Implanted EHTs maintained a network of differentiated CMs and were strongly vascularized (Eschenhagen, Didie, Heubach, et al., 2002; Eschenhagen, Didie, Munzel, et al., 2002; Zimmermann, Didie, et al., 2002). Moreover, EHTs grafted on the heart of syngeneic rats (Zimmermann, Didie, et al., 2002) preserved contractile function *in vivo*. By adopting a multi-chamber bioreactor to impart controlled simultaneous cyclic strains, Gonen-Wadmany et al. (Gonen-Wadmany et al., 2004) developed a bioartificial engineered cardiac construct (ECC) capable of synchronized

multidirectional contraction. Based on previous studies (Zimmermann et al., 2000; Zimmermann, Schneiderbanger, et al., 2002), ECCs were prepared mixing neonatal rat CMs and sheep aortic smooth muscle cells (SMCs) with type I collagen gel, enriched with growth factors and hormones. ECCs, molded over silicone bulbs, were mechanically stimulated by inflating and deflating the silicone bulbs with repetitive pneumatic pressure at 1 Hz for 6 days. Cell distribution was found to be homogeneous throughout the ECCs, and the use of SMCs resulted in a significant compaction of the collagen gels and in a cardiac substitute containing a high cell density. Moreover, the authors demonstrated that cellular and morphological reorganization is highly dependent on the amplitude of strain stimulation.

In 2007, Birla et al. (Birla et al., 2007) proposed a multi-chamber bioreactor capable of controlling tissue stimulation in order to correlate the degree of mechanical stretch to changes in the contractile performance of 3D bioengineered heart muscle (BEHM) constructs. Neonatal rat CMs were plated on fibrin-coated surfaces of cell culture plates, with the addition of thrombin, and maintained in incubator for 2 weeks. Spontaneous contractions of the primary CMs resulted in compaction of the fibrin gel promoting BEHM formation. For another 7 days, BEHMs were mechanically stimulated within the bioreactor with different time intervals per day (2, 6, and 24 hours). The active force was evaluated by stimulating the BEHMs between parallel platinum electrodes. No apparent physical damage was found in BEHMs stretched using a stretch protocol of 10% stretch and 1 Hz, with no significant changes in the active force, specific force, pacing characteristics, or morphological features, demonstrating the structural stability of the constructs in response to applied stretch protocol.

By performing 3D suspension cultures of neonatal rat CMs on cell supports within rotating bioreactor, Akins et al. (Akins et al., 1999) investigated the capacity of isolated heart cells to re-establish tissue architectures *in vitro*. They observed the formation of 3D aggregates of mixed populations of ventricular cells, replicating the distribution observed *in vivo*, and presenting spontaneous and rhythmic contraction, suggesting that cardiac cells possess an innate capacity to re-establish complex 3D cardiac organization *in vitro*.

Motivated by the need to optimize seeding and perfusion of 3D scaffolds, Carrier et al. (Carrier et al., 1999) used different bioreactors (flasks, xyz gyrator, and rotating

bioreactors) to investigate the *in vitro* morphogenesis of engineered cardiac muscle in a cell-polymer bioreactor model system. Porous nonwoven meshes of fibrous PGA were seeded with rat heart cells. Constructs cultivated within rotating bioreactors showed significantly improved structural and functional properties, with uniformly distributed cellularity, improved maintenance of metabolic parameters, elongated cell shape, and ultra structural features peculiar of native cardiac tissue.

Papadaki et al. (Papadaki et al., 2001) cultivated highly concentrated neonatal rat cardiomyocytes, seeded on laminin-coated PGA scaffolds, within rotating bioreactors. By using a specific apparatus (Bursac et al., 1999), they stimulated and recorded extracellular potentials. The engineered cardiac muscle presented a peripheral region containing CMs electrically connected through functional gap junctions. These constructs did not exhibit spontaneous beating, but responded to electrical stimulation and showed conduction velocity of propagating electrical impulses comparable with native tissue. However, due to the concentration gradients associated with diffusional transport of nutrients and oxygen, the engineered tissues mentioned above were limited to approximately 100 um-thick peripheral layers around a relatively cell-free construct interior. To overcome this limitation, Carrier et al. investigated the effects of direct perfusion (Carrier et al., 2002a) and oxygen concentration (Carrier et al., 2002b) on engineered cardiac tissues obtained from fibrous PGA scaffolds seeded with neonatal rat CMs. It was found that direct medium perfusion through the constructs, located within cartridges, guarantees the following: 1) a reduction of diffusional gradients over macroscopic distances; 2) the control of local levels of pH and oxygen; 3) the spatial uniformity of cell distribution; and 4) an increase of construct thickness (Carrier et al., 2002a). It was also proven that a marked positive correlation exists between medium pO_2 and the aerobicity of cell metabolism, DNA and protein content, and the expression of cardiac-specific markers (Carrier et al., 2002b). However, the system in (Carrier et al., 2002b) had two important limitations: 1) direct perfusion exposes cardiac cells to hydrodynamic shear stress values higher than the physiological ones; 2) cell density of engineered tissue was approximately only the 20-25% of the density in native cardiac tissue (Carrier et al., 1999; Carrier et al., 2002b) (Carrier et al., 2002a). To improve cell density Radisic et al. (Radisic et al., 2003; Radisic et al., 2008) developed a new seeding strategy within the same perfusion system as in (Carrier et al., 2002b). Using Matrigel as vehicle for cell delivery, neonatal rat CMs were seeded into collagen

sponges and cultured in perfused cartridges with alternating medium flow. Initial cell densities corresponding to those normally present in the adult rat heart (about 10^8 cells/cm^3) were reached, with rapid and spatially uniform cell distribution throughout the perfused constructs. The result of the direct medium perfusion (0.5 ml/min) approach was high cell viability, differentiated function of CMs and cell protection from critical hydrodynamic shear. As for the electrophysiological function, it was observed that constructs cultured in perfusion maintained constant frequency of contractions, whereas constructs cultivated in orbitally mixed dishes presented episodes resembling arrhythmia.

A growing research branch focuses on bioreactors' application for *in vitro* generation of cardiac-tissue-like 3D constructs at smaller scales. Recently, miniaturized screening platforms were developed to study the impact of physical and chemical parameters on the maturation, structure, and function of the cardiac tissue. The basic idea is to provide advanced high-throughput, low-volume *in vitro* models for drug testing and, in combination with recent iPSC technology, disease modelling. Important requisites towards a screening platform are miniaturization, reduced manual handling, and automated readout. In 2010, Hansen et al. (Hansen et al., 2010) developed a drug-screening platform based on large series of miniaturized EHTs, fabricated as strips, where the contractile activity can be automatically monitored. Neonatal rat heart cells were mixed with fibrinogen/Matrigel plus thrombin and pipetted into rectangular casting moulds in which two flexible silicone posts were positioned. During cultivation, fibrin-based mini-EHTs (FBMEs) demonstrated cell spreading inside the matrix and newly formed cell-cell contacts that led to the formation of condensed FBMEs and to the imposition of direct mechanical load to cells. Elongation of cells was observed, accompanied by single cells coherent beating activity, and, after 8-10 days, FBMEs started to rhythmically deflect the posts. Analysis of a large series of FBMEs revealed high reproducibility and stability for weeks.

In 2011, Kensah and co-workers (Kensah et al., 2011) developed a multimodal bioreactor for mechanical stimulation of miniaturized bio-artificial cardiac tissues (BCTs) and for real-time measurement of contraction forces during tissue maturation, enabling small- scale stem cell-based cardiac TE. Each module connected a cultivation chamber (with a glass bottom for microscopic assessment) to both a linear motor with integrated position measurement and a force sensor. BCTs were prepared with neonatal

rat CMs mixed with type I collagen and Matrigel, according to (Zimmermann, Schneiderbanger, et al., 2002). BCTs were subjected to cyclic stretch stimulation (10%, 1 Hz) with daily real-time spontaneous active force measurement. The bioreactor was designed for including additional functions such as electric pacing and culture medium perfusion. More recently, using the same bioreactor, Kensah et al. (Kensah et al., 2013) cultured highly purified murine and human pluripotent stem cell-derived CMs to generate functional BCTs and to investigate the role of fibroblasts, ascorbic acid, and mechanical stimuli. For the first time, a stimulation strategy for tissue maturation was combined with a novel concept of tissue formation from non-dissociated cardiac bodies, which has led to a dramatic increase in contractile forces, comparable with native myocardium. BCTs underwent constant static stress, and an additional mechanical stretch was then applied within the bioreactor using either uniaxial cyclic stretch or stepwise growing static stretch, mimicking the increasing systolic and diastolic pressure in the developing embryonic heart.

In this complex context, in this study we present a bioreactor suitable for homing hiPSC derived CMs, to be further implemented in order to provide electrical and mechanical stimuli that would favour cardiac cells maturation, so to obtain a cardiac tissue-like *in vitro* system.

2-OBJECTIVES

The main aim of this work was to create an "*in vitro"* tissue engineered cardiac patch that would promote the maturation of human iPSC derived cardiomyocytes and be useful for future advanced functional studies. Our specific objectives for this purpose were:

1) Optimize a differentiation protocol to obtain large numbers of iPSC-derived cardiomyocytes. We will test different stage-specific cardiac differentiation protocols on ESC and iPSC and select the most reproducible and efficient one.

2) Generate transgenic human iPSC lines in order to purify a homogeneous cardiac cell population. We will test different methods to generate reporter induced pluripotent stem cell iPS for genes specific for different stages of differentiation.

3) Build a 3D system to support the growth of cardiomyocytes derived from hPSC. We will develop a perfusion bioreactor system for 3D culture and test its performance using neonatal rat and human iPSC-derived cardiomyocytes.

3- METHODS

3.1. Maintenance of human ESC and iPSC cells on Feeder Layer

The human ES lines and the KiPS lines, ES[4] ((Aasen et al., 2008) (Raya et al., 2008) (Raya et al., 2009)) and KiPS 3F.7 were obtained from the Centre of Regenerative Medicine of Barcelona (CMRB). ES [4] were derived from a male human embryo on day 2 and KiPS 3F.7 from retroviral transfection of Oct-4, Sox2 and Klf-4 into human foreskin keratinocytes. They were maintained on irradiated (55Gy) human foreskin fibroblasts (HFF) (embryonic feeder cells in **HES medium** consisting of Knockout^{TM} DMEM (Life technology) supplemented with 20% KnockOut Serum Replacement (Life technologies), 100 µM Nonessential amino acids (Life Technologies), 2 mM GlutaMax (Life Technologies), 50 U/mL penicillin, 50 µg/mL streptomycin (Life Technologies), 50µM 2-mercaptoethanol (Life Technologies), and 10 ng/mL bFGF (Peprotech) in 10cm Petri Dishes. Cultures were maintained at 37ºC 5%O2 5%CO2 and media were changed every day.

Cells were passed to new feeders every 10-14 days by mechanical disruption with The STRIPPER® (Origio), a 150um-diameter plastic pipette.

3.2. Maintenance of human ESC and iPSC cells on Matrigel

Cells were cultured on 10 cm Petri dishes coated with Matrigel (BD Bioscience) diluted 1:40 in KnockOut DMEM, with **cHES medium** consisting of HES medium (described in section *"Maintenance of human ES and iPS cells on Feeder Layer"*) conditioned 24 hours with irradiated (55Gy) mouse embryonic fibroblasts (MEF) and filtered through a 0,22 um Millipore Filter. Cell cultures were maintained at 37ºC, 5%CO2, 5% O2 and conditioned medium was changed every day, excluding the day right after passaging. If required, cells were exposed during a week to Geneticin 50ug/mL (G-418 Disulphate (Melford)) for

positive selection. Cells were split 1:10 when confluent, approximately every 7 days.

Splitting was done incubating cells with 0.05% trypsin-EDTA (Life Technologies) for 1 minute and pipetting the desired amount of cells into a plate with fresh medium.

3.3. Cardiac Differentiation via ActivinA (Protocol 1)

hPSC were cultured as monolayer on plates coated with Matrigel (BD Biosciences), diluted 1:40 in Knockout^{TM} DMEM (Life technology) and kept under 5% O_2 for 1 week. To induce cardiac differentiation, cells were cultured for 5 days under 5% O_2 in RPMI medium (Life technologies) with B27 supplement 50X (Life technologies) supplemented with 50 ng/ml of human recombinant Activin A (PeproTech) and 10 ng/ml of BMP4 (PeproTech). After 5 days, cells were transferred to ambient oxygen atmosphere and the RPMI/B27 medium was changed every 2 days. Cluster of beating areas were observed with a Leica optical microscope at 10x magnitude.

3.4 Cardiac Differentiation via EBs using ActivinA and BMP4 (Protocol 2)

3.4.1 Home-made tools fabrication

Prior to differentiation, EBs (embryoid bodies) were generated by mechanical detachment of ESC or iPSC colonies from the feeder layer of fibroblasts using home-made glass tools.

Such tools were fabricated prior to each experiment from a 230 mm glass Pasteur pipette following the steps described in ***figure 3.1***.

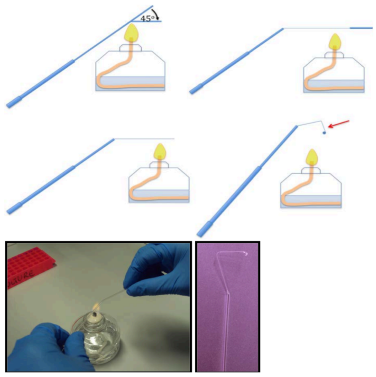

***Figure 3.1*:Fabrication of home-made tools to scrape EBs from hPSC colonies growing on HFF.**

Glass tools are fabricated from a long (230 mm) glass Pasteur pipette. With an alcohol lamp, pull the pipette at a 45° angle and elongate the hot glass to make it thin. Cut the distal part of the pipette with the flame. Fold and seal the end of the tool making sure that the part to be used for lifting the colonies (red arrow) is straight and thin.

3.4.2 EBs' formation

Glass tools were sterilized with Ethanol and used to gently manually detach the colonies of pluripotent stem cells from HFF feeder layer. This procedure was performed with the help of Leica stereomicroscope connected to a screen under a laminar flux cell culture hood. By scraping, colonies assumed a roundish/spherical shape and remained in suspension in culture medium. After having scraped all the colonies from a well, EBs were harvested and cultured in a low attachment 60mm petri dish (Corning) with 5 ml of cHES medium in order to obtain compact and defined shaped EBs.

3.4.3 EBs' differentiation

EBs were cultured in suspension for two days and then they were plated on 6 well plates coated with 0,1% gelatin (Chemicon, Millipore). Around 20 EBs were seeded in each well.

To differentiate EBs, the following cytokines were added to stemPro-34 (Invitrogen) medium supplemented with 2mM Glutamax (Life technologies),

0.5ng/ml ascorbic acid (Sigma) and 50µg/ml monothiogyocerol (Sigma): days 0-4, 10 ng/ml BMP4 (Peprotech), 5ng/ml bFGF (Peprotech), 3ng/ml for ES[4] or 6ng/ml for iPSC activin A (Peprotech); days 4-8 150 ng/ml DKK1 (Peprotech), 10ng/ml VEGF (Peprotech); days 8-12, 10ng/ml VEGF (Peprotech), 10ng/ml bFGF (Peprotech); after day 12 10ng/ml VEGF (Peprotech) for the duration of the experiment.

After 20 days of differentiation, cells were maintained in **EB medium** supplemented with Ascorbic Acid. EB medium consisted of HES medium (described in section *"Maintenance of human ES and iPSC cells on Feeder Layer"*), without bFGF, and with FBS (HyClone) instead of KnockOut Serum Replacement.

Cells were maintained in an environment of 5% CO_2, 5% O_2, 90% N_2 up to day 12 and then transferred into an environment of 5% CO_2, 21% O_2, 74% N_2. Cluster of beating areas were observed with a Leica optical microscope at 10x magnitude.

3.5 Cardiac differentiation via small molecules (Protocol 3)

Pluripotent cells maintained on Matrigel (BD Biosciences) in mTeSR1 (STEMCELL Technologies) were dissociated into single cells with Accutase (Invitrogen) at 37 °C for 5 min and then were seeded onto a Matrigel-coated 12 well plate at 200,000–250,000 cell/well in mTeSR1 supplemented with 5 uM ROCK inhibitor (Y-27632; Stemgent) (day −3). Cells were cultured in mTeSR. When achieved confluence, cells were treated with CHIR 99021(Selleck) in RPMI/B27 -insulin (Life technologies) for 24 h (day 0 to day 1). On day 1, medium was changed to RPMI/B27 -insulin alone. At day 3, 5 uM IWP4 (Stemgent) was added. At day 5, IWP4 was removed by medium changing with RPMI/B27-insulin. Starting from day 7, cells were maintained the RPMI/B27 (Life technologies), with medium changed every 3 d. Appearance of beating clusters was monitored through Leica optical microscope observation. Imaging of cell cultures was performed with a Leica DM IRBE microscope, supported by

a Cool-SNAP-fx CCD camera (Photometrics) under the control of MetaMorph® Software (Molecular Devices).

3.6 RNA extraction

Total RNA was isolated from cells using TRIZOL reagent from Life Technologies or TRI Reagent from SIGMA, following this protocol: 1) HOMOGENIZATION: cells pellets from a well of a 6 or 12 well plate, was lysed in 1ml of TRIZOL or TRI Reagent by repetitive pipetting. In case of thick tissue-like cell cultures in the more advanced stages of differentiation, pipetting with a syringe and a needle was performed. 2) PHASE SEPARATION: homogenized samples was incubated for 5 minutes at RT, 200ul of chloroform was added and tubes were vigorously shaken by hand for 15 seconds. Samples were incubated at RT for 2 to 3 min and centrifuged at 12000g per 15 min at 4°C. (Two phases formed: RNA in the upper aqueous phase) 3) RNA PRECIPITATION: the aqueous phase was transferred to a fresh tube and RNA was precipitated by adding and mixing with 500ul of isopropyl alcohol. Samples were incubated at RT for 10 minutes or at -20ºC O.N. and centrifuged at 12000g for 10 min at +4°C. 4) RNA WASH: after removing the supernatant, RNA pellet was washed twice with 100ul of 75% ethanol, centrifuging at 12000 rcf per 5 min at +4°C. 5) REDISSOLVING THE RNA: the RNA pellet was air dried and dissolved 30ul of RNase-free water. 6) RNA concentration was assessed through uv/visible spectrophotometry, measured at 260 nm and 280 nm with Nanodrop ND-1000 equipment (Thermo Scientific).

3.7 RT-qPCR

1) Retrotranscription of RNA into cDNA. The reaction was performed using the SuperScript III® kit (Invitrogen), following manufacturer's instructions. The following components were added to a nuclease-free microcentrifuge tube (Mix A): 1ug of total RNA, 1ul of random primers, 1 ul of 10 mM dNTP Mix (10 mM

each dATP, dGTP, dCTP and dTTP at neutral pH), sterile distilled water to 1o µl. Mixture was heated to 65°C for 5 min and quickly chilled on ice for 1 minute. Mix B was prepared with 2ul of l0X First-Strand Buffer, 2 ul of 0.1M DTT, 4ul of $MgCl_2$, 1ul of RNAse OUT and 1ul of SuperScript III® retrotranscriptase. Mix A and B were mixed gently, spinned down and incubated at RT for 10 minutes, followed by 50 minutes at 50ºC. Reaction was inhibited by 5 minutes of incubation at 85ºC and cDNA samples were immediately processed or stored at -20ºC.

2) qPCR Reaction. The obtained cDNA was diluted 1:10 and used as a template for real time amplification in quantitative PCR. Mix 1 was prepared with 1ul of diluted cDNA and 3,8ul of water. Mix 2 was prepared with 0,6 ul of Forward Primer 10uM, 0,6 ul of Reverse Primer 10uM and 6ul of "LightCycler® 480 SYBR Green I Master". Mix 1 and 2 were mixed, according to specific desired amplification, into a microtube 96 well plate (MicroAmp® Fast Optical 96-well reaction plate with barcode -0.1 ml-) which was covered with an optical film, and the reaction was run in a StepOnePlus Real-Time PCR Machine (Applied Biosystems). It consisted of an initial denaturation at 95°C for 10 minutes and 40 cycles of 15 seconds at 95°C and 1 min at 60ºC. Primers Melting curve was performed with an extra step at 95ºC for 15 seconds, 60ºC at 1 minute and 95ºC for 15 seconds. Relative fold increase in gene expression was calculated with the "Delta Delta Ct Method", and normalized to GAPDH endogenous gene.

3.8 PCR

PCR reactions were performed with Go Taq® Flexi DNA PolymerasePCR Reaction kit. The following were added to a PCR reaction tube for a final reaction volume of 25 ul: 5ul of 5X Green GoTaq® Flexi Buffer, 3 ul of $MgCl_2$ 25mM, 1,5 ul of 10uM dNTP Mix, 3 ul amplification primer F (5 uM), 3 ul amplification primer R (5 uM), 6 ul (0,3 ug) cDNA (from first-strand reaction), 0.3 ul GoTaq® Flexi DNA Polymerase, autoclaved distilled water to 25 ul. Reaction was mixed gently and briefly spun down. PCR amplification was performed in a DNA thermal cycler (GeneAmp PCR System 9700, Applied BioSystems) and consisted of an initial denaturation at 95°C for 5 min, 30 cycles

of denaturation for 1min at 95°C, annealing for 1 min s at 55ºC, 57ºC, 60ºC or 62ºC depending on the primer's pair, and extension for 1minute/1000 base pair, depending on the size of the amplified fragment at 72ºC. Final extension proceeded for 10 min at 72ºC. All the products were run on a 1, or 2% agarose gel and visualized by ethidium bromide staining. Fermentas DNA ladders were used as reference.

3.9 Primers List

Primers are listed in the following table (5' – 3'):

GAPDH F	GCACCGTCAAGGCTGAGAAC
GAPDH R	AGGGATCTCGCTCCTGGAA
GFP F	GAACCGCATCGAGCTGAA
GFP R	TGCTTGTCGGCCATGATATAG
NANOG F	ACAACTGGCCGAAGAATAGCA
NANOG R	GGTTCCCAGTCGGGTTCAC
T F	TGCTTCCCTGAGACCCAGTT
T R	GATCACTTCTTTCCTTTGCATCAAG
NKX2.5 F	TGGAGAAGACAGAGGCGGACAA
NKX2.5 R	ACAGGTACCGCTGCTGCTTGAA
TNNT2 F	TGCAGGAGAAGTTCAAGCAGCAGA
TNNT2 R	AGCGAGGAGCAGATCTTTGGTGAA
MHC F	ACAAGAAGGAGGGCATTGAGTGGA
MHC R	GCGTGGCTTCTGGAAATTGTTGGA
pNKX2.5 F	ACTCAGCATAACAGAATCAGG
GFP R	TTTACTTGTACAGCTCGTCC
pKanNeo R	GAAGAACTCGTCAAGAAGGC

Table 3.1: Primers list

3.10 Immunofluorescence for standard 2D cell cultures

Cells were fixed with 4% paraformaldehyde in PBS at RT for 15 min and permeabilized for 15 min in 0.5% Triton in PBS. Cells were blocked in PBS 0,5% Triton-X100 with 3% donkey serum for 2 h, and incubated with primary antibodies O.N. The following antibodies were used: mouse IgM anti-Alpha-Actin (Sarcomeric) (Sigma A2172, 1:200), mouse anti-Alpha-actinin (Sarcomeric) (Sigma A7811, 1:100), mouse anti-

Alpha-tubulin (Sigma T6074, 1:500), goat anti-Brachyury (R&D Systems AF2085, 1:25), PE-human anti-CD172a (Biolegend 323805, 1:250), mouse anti-connexin 43 (Sigma C8093, 1:200), rabbit anti-GATA4 (Santa Cruz sc-9053, 1:50), chicken anti-GFP (Aves Labs, 1: 500), rabbit anti-TroponinI (cTNI) (Santa Cruz sc-15368, 1:25), mouse anti-Heavy Chain Cardiac Myosin (MHC) (AbCam ab15, 1:100), mouse anti-TroponinT (cTNT) (Thermo Scientific MS-295-P, 1:200). Cells were blocked for 1 hour and incubated with secondary antibodies for two hours. Secondary antibodies used were anti-rabbit IgG, anti-mouse IgG and anti-goat IgG Alexa Fluor 488 (Jackson 711-545-152, 115-546-071, 705-545-147, 1:200), anti-chicken IgY Dy-Light 488 (Jackson 703-485-155, 1:200), anti-mouse IgM and anti-rabbit IgG Cy3 (Jackson 715-165-140 and 711-165-152, 1:200), anti-mouse IgM DyLight 649 (Jackson 115-495-075, 1:200). To visualize nuclei, slides were stained with 0.5 mg/ml DAPI (4',6-diamidino-2-phenylindole) for 15 minutes and then mounted with PVA-DABCO (Polyvinyl Alcohol - 1,4-diazabicyclo[2.2.2]octane). Images were taken using a Leica SP5 confocal microscope. For quantification of cTNT positive cells, randomly 5 20X magnification areas were counted.

3.11 Immunofluorescence "in toto" for 3D cell cultures

In order to be analysed by immunofluorescence, scaffolds were fixed O.N. with 4% paraformaldehyde (SIGMA) in PBS at 4ºC and included in 4% agarose (low melt point, agarose D1, CONDA) for 5 minutes at 4ªC. 200 um cross sections were obtained cutting the blocks with a vibratome (0'075 mm/s advance rate, 81 Hz vibration and 1mm amplitude). Slices were washed three times for 30 minutes with TBS 1X, blocked in TBS 0,5% Triton-X100 with 6% donkey serum for 2 hours RT, and incubated with primary antibodies for 48 hours at ºC. Slices were blocked for 2 hours and incubated with secondary antibodies O.N. The antibodies are mentioned in 3.10 paragraph "Immunofluorescence for standard 2D cell cultures". To visualize nuclei, slides were stained with 0.5 mg/ml DAPI (4',6-diamidino-2-phenylindole) for 1 hour, incubated with mounting medium mixed with TBS 1:1 and then mounted. Images were taken using a Leica SP5 confocal microscope.

3.12 Genomic DNA extraction

Total DNA from cells infected with Lentivirae was extracted with QIAamp DNA Mini Kit (QUIAGEN, #51304) following instructions and finally resuspended in 200ul of TE Buffer (10mM Tris 1mM EDTA).
Total DNA from cells transfected with plasmid was extracted with Genomic DNA Purification Kit (Fermentas #K0512) following manufacturer's protocol for "cell cultures", and finally resuspended in 100 ul of Tris-EDTA Buffer. Quality and quantification of DNA was determined through uv/visible spectrophotometry, measured at 260 nm and 280 nm with Nanodrop ND-1000 equipment (Thermo Scientific).

3.13 Plasmids and lentiviral vectors

pNKX-GFP (Addgene plasmid # 45497, (Wu et al., 2006)) was kindly donated by Patrizia Dell'Era, from Brescia University.
T/Brachyury-eGFP Rex Neo and aMHC-eGFP-Rex-Neo vectors for lentiviral production were adquired from Addgene (plasmid # 21222 and # 21229 respectively, (Kita-Matsuo et al., 2009)).

3.14 Lipofectamine transfection of KiPS 3F.7

400.000 cells (KiPS 3F.7) were seeded in a 6wp. The day after they were transfected with Lipofectamine 2000 (Invitrogen) with 5ug of pNKX-GFP. The day after medium was changed and cells were cultured in presence of G418 (50ug/mL) to select for neomycin resistant colonies.
Transfection was performed in parallel with a pCAG-TOMATO plasmid as positive control.

3.15 Lentivirus production and infection of KiPS 3F.7

293T cells were transiently transfected with 1) transfer vector T/Brachyury-eGFP Rex Neo or aMHC-eGFP-Rex-Neo 2) the second generation packaging construct pCMVR8.74 (Addgene plasmid # 22036), and 3) the VSV envelope–expressing construct pCMV-VSV-G (Addgene plasmid # 8454)VSV-G, by calcium phosphate, in order to produce High-titre vesicular stomatitis virus (VSV)–pseudotyped LV stocks, that were purified by ultracentrifugation and resuspended to a final volume of 50ul of PBS. KiPS 3F.7 were cultured with cHES medium in a 10cm petri dish coated with Matrigel at 80/90% of confluence. They were split with trypsin 0.05%, counted and resuspended to a final concentration of $1x10^6$ cells/mL. 0,2 $x10^6$ cells were transferred into an eppendorf tube (in a volume of 200 ul of PBS) and infected with 5ul of viral particles. Tubes were incubated 1 hour at 37ºC and gently shacked every 10 minutes. Cells were then plated into a well of a six well plate coated with Matrigel, and cultured with 1 ml of cHES medium. After 24 hours medium was replaced with 2ml of cHES and cells were cultured as usual. After 4 days from infection, selection with G418 (SIGMA) was performed during 10 days, diluting it 1:1000 into culture medium to a final concentration of 50ug/mL.

3.16 Flow cytometry and cell sorting

Dissociation procedure for day 0 to day 12 of cardiac differentiation. EBs and CMs generated from hPSC differentiation experiments were dissociated with 0.25% trypsin/EDTA.

Dissociation procedure for day 13 and more. EBs and CMs generated from hPSC differentiation cultures were incubated in collagenase type II (1 mg/ml, Life Technologies) in Hanks solution (NaCl, 136 Mm; $NaHCO_3$, 4.16 mM; $NaPO_4$, 0.34 mM; KCl, 5.36 mM; KH_2PO_4, 0.44 mM; dextrose, 5.55 mM; HEPES, 5 mM) for 30 minutes to 2 hours at 37°C with gentle shaking. The equivalent amount of dissociation solution (in Hanks solution: taurin, 10 mM, EGTA 0.1 mM, BSA 1 mg/ml, collagenase type II 1 mg/ml) was then added to the cell suspension and the EBs were pipetted gently to dissociate the cells. After dissociation, cells were centrifuged (1,000 r.p.m., 5 min), filtered and used for analysis. Cells were analyzed using an FC500 or a Gallios flow

cytometer (Beckman Coulter). For FACS, the cells were sorted at a concentration of 10^6 cells/ml in IMDM/6% FCS using a FACSAriaTMII (Becton Dickinson) cell sorter. To prevent cell death due to pressure and shear stress, all sorts were performed with a 100 μm nozzle.

3.17 Primary culture of neonatal rat CM and CM Cell culture

For 50 hearts: Sprague Dawley rats (p2 or p3) were scarified by decapitation with scissors. Pups' upper torax was opened and the heart was squeezed outside the body. It was detached with tweezers and collected in cold freshly prepared, 0,22um filtered, CBFHH (Calcium and Bicharbonate-Free Hank's Balanced Salt Solution with HEPES) Buffer (consisting of NaCl 3,42M, KCl 0,54M, $MgSO_4(H_2O)7$ 0.081M, KH_2PO_4 0,044M, $Na_2HPO_4(H_2O)_2$ 0.034M, Glucose 0,56M, HEPES (Sigma) 0.2M). Hearts were washed with CBFHH buffer and auricles and rests of other tissues (lungs, thyme, vessels…) were eliminated. Hearts were cut into two parts to let as much blood as possible to flow away, and they were washed with CBFHH. Under a sterile flow culture hood hearts were cut sharply into very small pieces (< $1mm^3$) with scissors avoiding smash the tissue. 2ml of CBFHH was added and tissue was collected into a falcon tube with a Pasteur pipette and was washed 3 times.

Rounds of predigestion and digestion of the tissue were performed as following. PREDIGESTION: Add 8ml of freshly prepared trypsin 2mg/mL in CBFHH (BD Difco). Keep rolling 8' RT. Decant tissue and discard supernatant with a Pasteur pipette. DIGESTION Perform as many digestion cycles as required, until the tissue gets whitish and small in pieces: Prepare Collection tubes putting 2,5 ml of FBS into 50mL falcon tubes and keep them in ice. Add x (see **table 3.2**) ml of trypsin 2mg/mL to the disgregation tissues – agitate at RT for x (see **table 3.2**) minutes. Collect SN in the corresponding collection tube with a glass pipette with larger tip width (custom made a glass pipette cutting and sharping the tip end of around 3mm). Add x (see **table 3.2**) ml of freshly prepared DNAse 0,014mg/mL (DNAse I, Calbiochem) – Pipette up and down 20/25 times with the pipette with special width. Decant the tissue. Collect SN in the corresponding collection tube, kept in ice.

		ml	min	n of rounds	
PreDigestion	trypsin	8	8	1	discard SN
CT1	trypsin	8	4	up to fill the tube	Collect SN
	DNase	7			Pipette, decant, recollect
CT2	trypsin	7,5	3	up to fill the tube	Collect SN
	DNase	6,5			Pipette, decant, recollect
CT3	trypsin	7	2	up to fill the tube	Collect SN
	DNase	6			Pipette, decant, recollect
CT4	trypsin	6,5	1	up to fill the tube	Collect SN
	DNase	5,5			Pipette, decant, recollect
CT5	trypsin	6	1	up to fill the tube	Collect SN
	DNase	5			Pipette, decant, recollect
CT6	trypsin	6	1	up to fill the tube	Collect SN
	DNase	5			Pipette, decant, recollect
CT7	trypsin	6	1	up to fill the tube	Collect SN
	DNase	5			Pipette, decant, recollect

Table 3.2: *Trypsin/DNase digestion cycles. CT: Collection Tube*

Collection tubes were then centrifuged for 12 minutes at 100g. SN was discarded and pellet was resuspended in 2 mL of **non-cardiomyocytes medium- NKM**, (consisting of DMEM low glucose (life technologies) supplemented with 10% Fetal Bovin Serum (HyClone), 100 µM Nonessential amino acids (Life Technologies), 2 mM GlutaMax (Life Technologies), 50 U/mL penicillin, 50 µg/mL streptomycin (Life Technologies)) and gently pipetted 20/25 times. All the tubes were recollected in one and centrifuged 12min 100g. SN was discarded and pellet resuspended in 2ml of cold NKM by pipetting 20/25 times. 300 ul of freshly prepared DNAse (1mg/mL) were added to each 30 ml of cell suspension and cells were pipetted 20/25 time. Cells were centrifuged at 100g for 12 min and resuspended in 5ml of cold NKM. Cells were filtered through a 250um stainless steel filter and recollected into a clean falcon tube. Cardiomyocytes were counted with a Neubauer Chamber, by morphology (the remaining blood cells were excluded by morphology).

CM were cultured on 0,1% gelatin coated plate or Matrigel coated glass or implied for 3D culture and cultured in **cardiomyocytes medium** consisting of DMEM 4.5 g/L (Life technologies), 10% horse serum (Life technologies), 2% chick embryo extract (egg tech) 100 uM Nonessential amino acids (Life Technologies), 2 mM GlutaMax (Life Technologies), 50 U/mL penicillin, 50 ug/mL streptomycin (Life Technologies).

3.18 Perfusion bioreactor, scaffold and seeding loop

Perfusion bioreactor and seeding loop components were assembled and sterilized following indications from Radisic el al. (Radisic, Marsano, Maidhof, Wang, & Vunjak-Novakovic, 2008). Details will be object of Maria Valls' PhD thesis. Peristaltic Pump is a REGLO Digital, 2 channels pump from Ismatec. Scaffolds were cut from 1mm thick Matriderm® sheets, with a 1cm diameter biopsy punch and hydrated 24 hours in PBS and 1 hour in culture medium before use. To perform SEM (Scanning electron microscopy) characterization, Matriderm® was directly imaged with a NOVA NANOSEM 230 (FEI) with Low Vacuum Detector.

Before cell culture, perfusion loop and bioreactor were carefully filled with culture medium. Seeding procedure: hydrated scaffolds were located into the chambers and the perfusion loop was filled in with culture medium and connected to the peristaltic pump. Cells to be seeded were prepared depending on the condition (they were derived from rats pups in case of primary culture, enzymatically or manually detached from culture dishes and eventually sorted by FACS) and mixed prior to seeding in case of co-culture. For each scaffold, a total number of 3,5 millions of cells were resuspended into 1 ml of culture medium. Cells were inoculated into the seeding loop with a syringe through the Luer manifold, upstream the perfusion chamber, and perfused through it at 1ml/min flow rate. In order to calculate seeding efficiencies, medium was recollected from the seeding loop after seeding, it was centrifuged and cells were counted. Seeding efficiencies values were calculated as a percentage on the difference between initial seeded cells number (3,5 millions) and leftover cells after seeding procedure. Seeded scaffolds were maintained for 4 hours into a humid ultra low-attachment culture dish and then placed into the bioreactor for culturing. Cell culture: cells were cultured in 35 ml of medium for bioreactor at a flow rate of 0,1 ml/min; medium was changed every 3 or 4 days.

4-RESULTS

4.1 Cardiac differentiation protocol optimization

In vitro differentiation protocols aim to replicate what happens *in vivo* to the cells of an embryo. Like every *in vitro* technique, they are, of course, a simplification of the original processes and they have to replicate them in the most possible reliable way. It is fundamental, therefore, that the proper key pathways are activated correctly in a specific time order and schedule. This implicates that experiments turn to be very delicate and time consuming. Growth factors activin A, BMP4 and FGF2 have been shown to enhance the cardiac specification of hPSCs, in a time- and dose- dependent manner (Burridge et al., 2011) (Kattman et al., 2011). However, large variations remain between the cardiogenic potential of pluripotent stem cell lines, due to differences in endogenous levels of pluripotency regulators OCT4 and NANOG (Yu, Pan, Yu, & Thomson, 2011) and signalling molecules NODAL, BMP4 and WNT3A (Kattman et al., 2011) (Paige et al., 2010). Different principal methods are available for mesoderm induction and cardiac specification of hPSCs to cardiomyocytes (Burridge, Keller, Gold, & Wu, 2012). Two of them are: 1) embryoid body (EB) formation, an efficient but technically demanding method and 2) monolayer differentiation of highly confluent hPSC cultures (easier way and faster). To identify and choose the most suitable cardiac differentiation protocol, two methods were compared, based on Activin A and Activin A, BMP4, DKK1 respectively (here referred as “Protocol 1” and “Protocol 2”) with the human embryonic stem cell line ES[4], to be then applied with human induced pluripotent stem cell line KiPS3F.7.

Apart from the two protocols here presented, other methods were tested, but in our hands they didn’t perform as promised by literature. In particular we tested the method proposed by Burridge et al. in which human ESC and iPSC are successfully differentiated to CM, through EBs formation, with an efficiency of around 95%, in terms of percentage of contracting EBs (Burridge et al., 2011). In this protocol EBs are generated by centrifuge-force forced aggregation in 96 well plates and kept in culture in this form, for the entire duration of the protocol with polyvinyl alcohol and specific

cytokines. Our cell lines could not stand this way of culture, since EBs went to spontaneous disaggregation after few days of culture.

Concerning EB based protocols, it is important to mention that EB size and cell number are important factors in cardiac differentiation outcome (Bauwens et al., 2011) (Mohr et al., 2010). For this reason we tried to further optimize our "Protocol 2" based on Activin A, BMP4 and DKK1 starting from cell-number and sized-controlled EBs obtained thanks to special designed plates described by Ungrin et al. (Ungrin, Joshi, Nica, Bauwens, & Zandstra, 2008) and commercialized as Aggrewell™ (Stemcell Technologies), but with our cells we could not manage to improve the protocol. We therefore used a manual method to generate EBs, even though it was much more delicate, tedious, time consuming, and did not confer uniformity to EBs (paragraph "3.4.1 EBs' formation" of Methods section).

After three years that we were working on this project, a novel promising protocol was published by Lian et al. (Lian et al., 2013) based on GSK3 inhibition and IWP4 for mesodermal commitment, which seemed much more feasible, easily handling and efficient. After validating that it was so also with our KiPS cell lines, we adopted this last method (Protocol 3), for experiments in 3D.

4.1.1 Cardiac Differentiation via activin A (Protocol 1)

ES[4] cells were cultured on a layer of Matrigel in cHES medium and differentiated to cardiac lineage as described in paragraph 3.3. "Cardiac Differentiation via ActivinA (Protocol 1)" of Methods section and represented in **figure 4.1** (Si-Tayeb et al., 2010). This protocol last nearly 30 days, since it requires a period of adaptation of the cell culture in hypoxia conditions and beating areas appear after 20 days of differentiation.

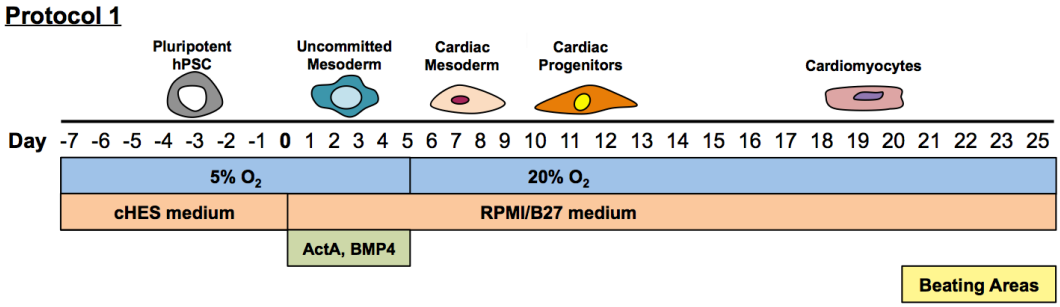

***Figure 4.1*: Schematic and timeline of protocol 1**
Pluripotent cells (in this case ES[4] cells) are cultured for 7 days on Matrigel with MEFs' conditioned medium and set to cardiac differentiation on hypoxia condition (5% O_2). Cardiac differentiation is triggered on day 0, shifting culture medium to RPMI/B27 and treating cells with Activin A and BMP4 cytokines. After 5 days cells are moved to atmospheric oxygen concentration (20%) and growth factors are retired. Cardiac fate is shown with the appearance of beating areas around 20 days after the beginning of the differentiation.

Cardiac differentiation was monitored by observation of the evolution of the cell cultures and RT-qPCR of genes for cardiac differentiation at different time points: days 0, 5 and 10 (only cell morphology evaluation), 15, 20 and 25 of differentiation. Evaluation of beating areas, as well as immunofluorescence analysis for cardiac marker cTNT and at the end of the protocol were performed.

Cell culture observation shows how after 5 days of culture typical mesodermal structures appear (**Figure 4.2**), they evolve progressively to a cardiac mesodermal and cardiac fate until day 20, when they spontaneously start to beat. On day 25 it is possible to observe very complex and multilayer structures.

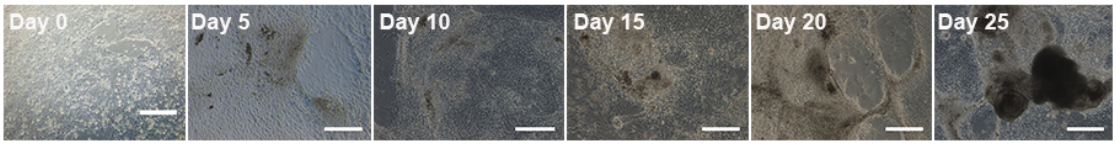

***Figure 4.2*: hES differentiating to cardiomyocytes with Protocol 1**
Bright-field images of ES[4] cells at day 0, day 5, day 10, day 15, day 20 and day 25 of differentiation. Scale bars: 500 um.

Those complex structures are the ones that can have beating capacity. One way to evaluate the outcome of a differentiation protocol is to evaluate the percentage of

beating areas among all the complex structures. Beating areas were scored at days 14, 15, 18, 20 and 25 of differentiation. **Figure 4.3** shows the results of the counting of beating areas of 3 differentiation protocols as a percentage on all the complex structures. The number of structures varied between 11 and 28, and the beating areas between 0 and 7 per condition. Maximum efficiency was reached at day 25.

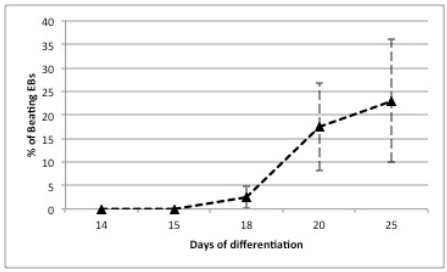

***Figure 4.3*: Beating areas evaluation of Protocol 1**
Percentage of beating areas at different time points of differentiation. Cells started contracting at day 18 and their number increased progressively until day 25, reaching 22,5% of efficiency. Error bars: standard deviation, n=3.

In order to monitor loss of pluripotency, mesodermal and cardiac fate, RT-qPCR analysis was performed for NANOG, T (Brachyury), NKX2.5 and TNNT2 (cTNT, cardiac Troponin T). Results are shown in **Figure 4.4**.

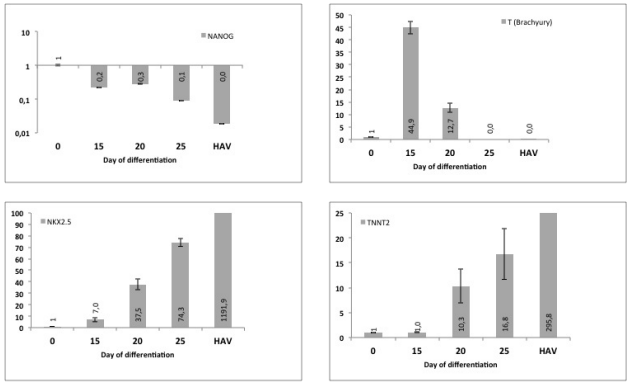

***Figure 4.4*: RT-qPCR analysis of NANOG, T (Brachyury protein), NKX2-5 and TNNT2 (cTNT protein) in ES[4] cells at different stages of differentiation with Protocol 1.**
Graphs represent fold increase in gene expression of NANOG, T, NKX2.5 and TNNT2 in hES differentiating to cardiomyocytes Vs. undifferentiated cells (Day 0 of Differentiation). Cells were analysed at day 0, 15, 20 and 25 in order to evaluate the efficiency of the protocol. (HAV: human adult ventricle, as positive control). Error bars represent standard deviation.

NANOG is a marker of pluripotency and it was down-regulated when cells were submitted to differentiation. T (Brachyury) is a marker of mesoderm induction, which expression was firstly enhanced to be down-regulated once committed cardiac fate was taken. NKX2.5 expression marks cardiac progenitors and it increased while cells are undertaking more strict cardiac differentiation. Finally, TNNT2 gene (coding for cardiac Troponin T – cTNT- protein) was expressed in the late stages of the differentiation, when cells already showed beating capacity.

cTNT expression and structural organization was confirmed by immunofluorescence. Cells analysed at the end of the experiment showed expression of cTNT, with its characteristic sarcomeric organization (**Figure 4.5**).

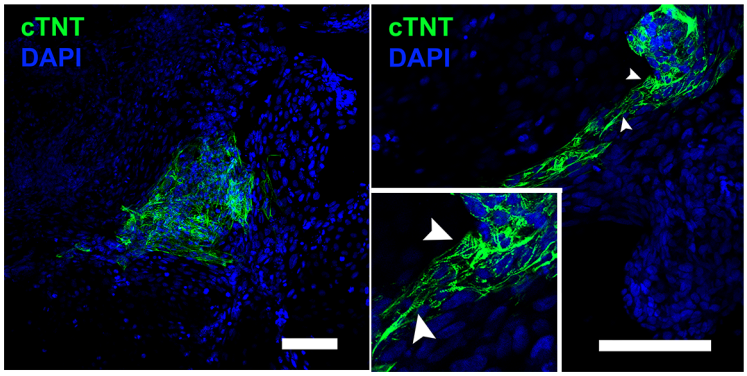

***Figure 4.5*: Immunostaining for cTNT on cardiac ES[4] cell cultures at day 25 of differentiation with protocol 1.**
Images of two different areas. Scale bars: 75 um. Arrows indicate the presence of cardiac troponin bands, indicating a developed contractile apparatus.

4.1.2 Cardiac Differentiation via activin A, BMP4 and DKK1 (Protocol 2)

Cardiac differentiation via Activin A BMP4 and DKK1 is possible through a staged protocol developed in the laboratory of G.Keller (Yang et al., 2008). It is a more specific protocol and it promised to obtain cardiomyocytes in a more efficient way. As mentioned in the introduction section, each differentiation protocol should be adapted to each laboratory's cell lines and conditions. In order to obtain sufficient amount of cardiomyocytes we needed to adapt such protocol to our cell lines. The original protocol contemplates to 1) feeders deplete ES cells from MEFs prior to the experiment by

culturing them on Matrigel 2) Generate EBs by enzymatic disgregation with collagenase and trypsin, and culture them in aggregation media consisting of StemPro with BMP4 and Ascorbic Acid 3) Start mesoderm induction after 24 hours, supplementing Stem Pro medium with ActivinA, BMP4 and bFGF for 4 days. 4) Specify cardiac mesoderm with VEGF and DKK1during days 4 to 8. 5) Maintain cardiac fate with VEGF and bFGF. Cells are maintained in hypoxia conditions until day 10/12 of differentiation.

Such conditions were unsuitable to our cells, since EBs generated by enzymatic disgregation could not survive in Stem Pro medium. We therefore tried different strategies to adapt the protocol to our cells. The main obstacle was to obtain EBs by enzymatic disgregation and to grow them in the induction medium. We therefore applied a standard culture technique, which was previously tested with our cell lines. It consisted of 1) maintaining the hPSC on a layer of HFF, 2) obtaining EBs by mechanical separation of the pluripotent colonies with hand made glass tools, 3) keeping EBs in suspension culture to allow them to compact in cHES medium 4) plating the EBs, ready to be differentiated 5) starting the differentiation. The scheme of this final outcome is illustrated in **figure 4.6.**

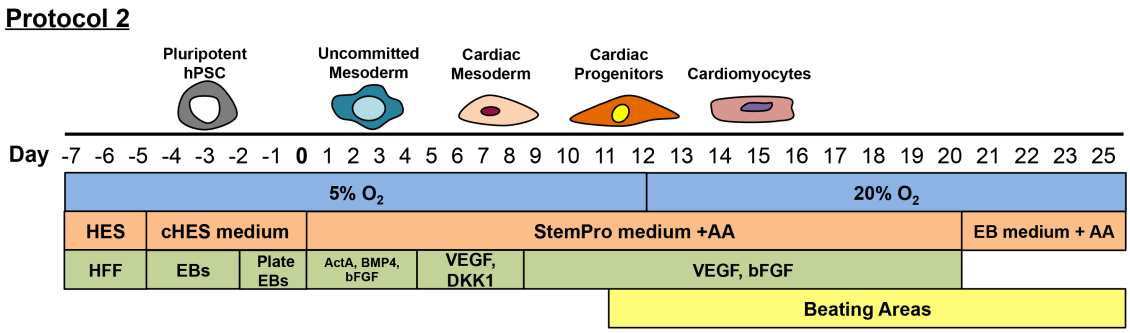

***Figure 4.6*: Schematic and timeline of protocol 2**
Pluripotent cells (in this case ES[4] cells) are maintained in hypoxia condition on a layer of HFF with HES medium. In order to induce cardiac differentiation, colonies are scraped into EBs and cultured in cHES for 2 days. EBs are then plated in six well plates and cardiac differentiation is induced after 2 days, by switching the medium to Stem Pro with Ascorbic Acid (AA) and treating cells with Activin A (ActA), BMP4 and bFGF, which commit cells to a mesodermal fate. On day 4, cardiac mesoderm is induced by treating cells with VEGF and DKK1. Cardiac fate is then maintained with VEGF and bFGF from day 8. Beating areas start appearing on day 11. On day 12 cells are moved to atmospheric oxygen concentration. From day 20 on, cells are maintained with EB medium supplemented with Ascorbic Acid (AA).

In order to evaluate the efficiency of the protocol and to have a comparison with the previous protocol based on Activin A (protocol 1), the same analysis were performed. **Figure 4.7** shows the evolution of cell cultures.

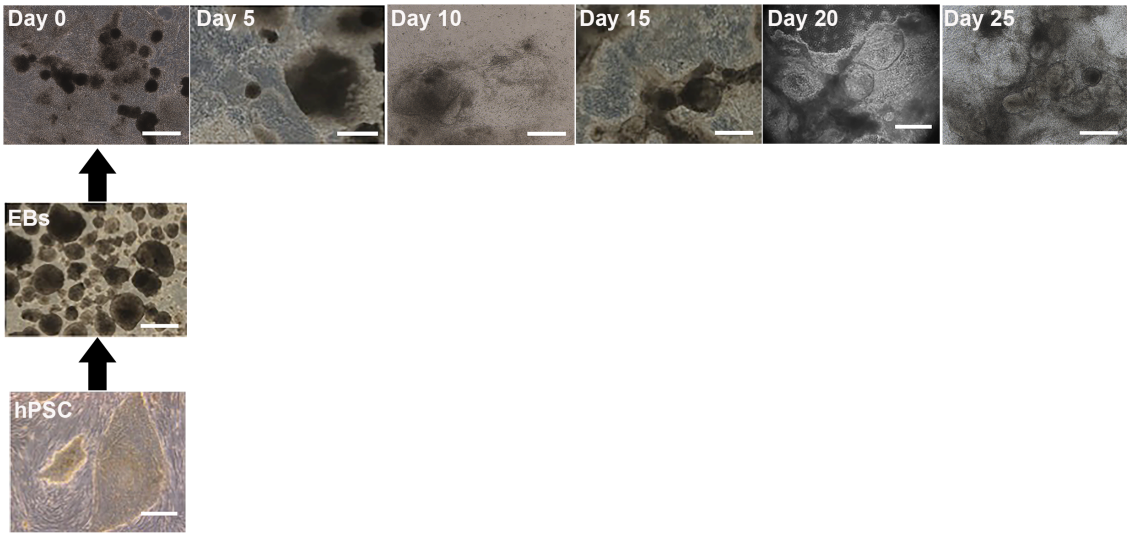

***Figure 4.7*: hPSC differentiating to cardiomyocytes with Protocol 2**
Bright-field images of the typical morphology of pluripotent colonies on HFF, manually scraped EBs and cells differentiating at day 0, day 5, day 10, day 15, day 20 and day 25. ES[4] cells are shown at ×10 magnification. Scale bars: 500 um.

Pluripotent cells were cultured on a monolayer of HFF and manually scraped to form EBs prior to experiment. When EBs were seeded on gelatin coated plates they attached on the well and cells spread from the borders of the EBs (Day 0), covering the whole plate surface. After mesoderm induction and cardiac specification, EBs generated mesodermal structures that evolved progressively and started to contract from day 11-14. In the attached **video 4.1** and **video 4.2** (10x and 20x magnification respectively) it is possible to observe beating differentiated EBs at day 20, as an example. **Figure 4.8** shows the first frame of video 4.1 and video 4.2.

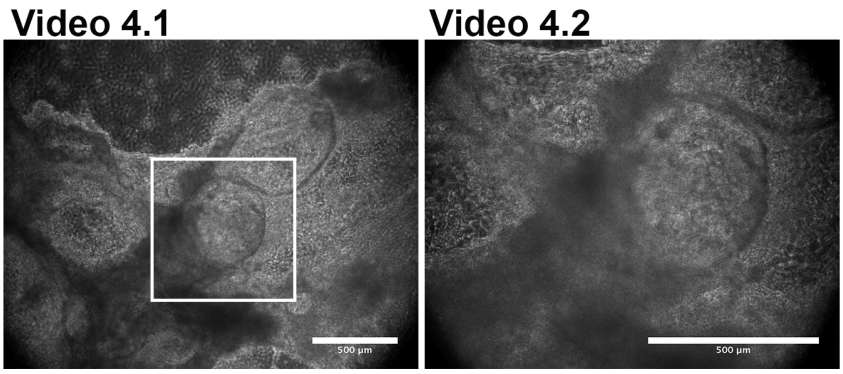

***Figure 4.8*: First frame of the attached videos 4.1 and 4.2.**
Time-lapse captures of beating structures at day 20 of cardiac differentiation with Protocol 2. Magnifications: 10x (video 4.1) and 20x (video 4.2). White square indicates the zoomed region. Scale bars: 500 um.

Figure 4.9 shows the results of beating areas' scoring of 3 differentiation protocols as a percentage on all the mesoderm-like cell structures. The number of structures ranged from 10 and 27, and the beating areas from 1 to 8 per condition. Maximum efficiency was reached at day 20.

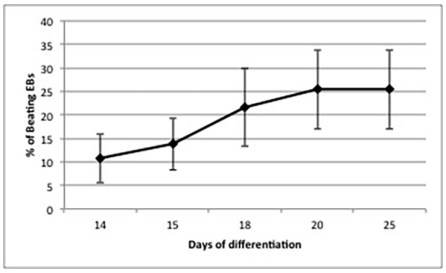

***Figure 4.9*: Beating areas evaluation with Protocol 2**
Percentage of beating areas at different time points of differentiation. Cells started contracting at day 11 and their number increased progressively until day 20, reaching 25% of efficiency. Error bars: standard deviation from a mean of 3.

RT-qPCR analysis was performed for NANOG, T(Brachyury), NKX2.5 and TNNT2 (cardiac Troponin T). Results are shown in **Figure 4.10**.

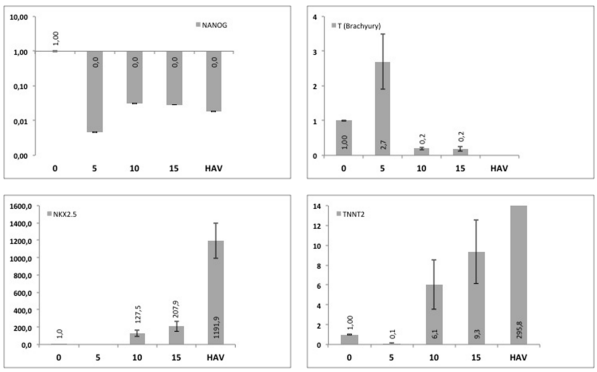

***Figure 4.10*: RT-qPCR analysis of NANOG, T(Brachyury), NKX2-5 and TNN2 in ES[4] cells at different stages of differentiation with Protocol 2**. *Graphs represent fold increase in gene expression of hES differentiating to cardiomyocytes Vs. undifferentiated cells. Cells were analysed at day 0, 5, 10 and 15 in order to evaluate the efficiency of the protocol. (HAV: human adult ventricle, as positive control). Error bars represent standard deviation.*

NANOG was correctly down-regulated when cells were submitted to differentiation. T (Brachyury) was enhanced at day 5 and then promptly silenced. NKX2.5 was expressed at day 10, when cardiac fate was undertaken. TNNT2 was expressed in the late stages of the differentiation, as expected.

In **Figure 4.11**, cTNT expression in ES[4] cells on day 25 of differentiation with protocol 2 is shown by immunofluorescence. cTNT positive areas have a wide extension and, at a higher magnification analysis it is possible to appreciate sarcomeric organization of the bands.

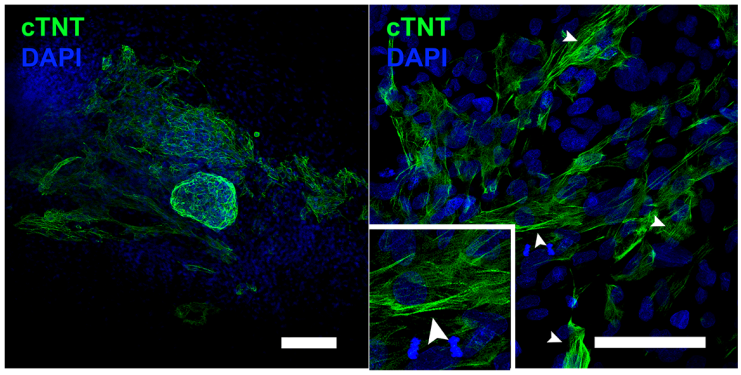

***Figure 4.11*: Immunostaining for cTNT on cardiac ES[4] cell cultures at day 25 of differentiation with protocol 2.**
Scale bars: 150 um. Arrows indicate the presence of cardiac troponin bands, indicating a developed contractile apparatus.

The overall analysis of the results, together with the observation of the evolution of the protocols, showed that 1) mesodermal-like structures formed faster and in a more defined way with Protocol 2; 2) cluster of beating cells were first observed after 20 or 11 days of differentiation using Protocol 1 or Protocol 2, respectively. The percentage of beating cluster was higher with protocol 2; 3) expression of cardiac related genes happened earlier in time with protocol 2, confirming that it is a faster protocol; 4) cardiac marker cTNT, analysed by immunofluorescence was more frequent to find in cells cultures differentiated with protocol 2, with a more marked presence of sarcomeric bands.

Therefore, results indicated that Protocol 2, based on ActivinA, BMP4 and DKK1 was faster and more efficient than Protocol 1, based only on Activin A. Therefore we chose protocol 2 for our experiments with iPSC.

4.1.2.1 Protocol 2 optimization for iPSC

Once we chose the Activn A, BMP4 and DKK1 based protocol as the most suitable for our embryonic stem cells, we fine-tuned the morphogens' concentrations by titrating the doses of BMP4 and Activin A, key factors for mesoderm induction, in order to adapt and optimize the protocol for induced pluripotent stem cell line KiPS3F.7.

According to what published by Kattman and colleagues (Kattman et al., 2011), we tested different doses of the two morphogens in the time window of day 0-4. The tested concentrations are 0, 3, 6, 10 and 30 ng/mL of Activin A and 0, 10 and 30 ng/mL of BMP4. We analysed the outcome of the titration by beating bodies evaluation and cardiac troponin T expression by immunofluorescence and RT-qPCR.

Figure 4.12 reports the final results of beating areas' evaluation, immunofluorescence, and RT-qPCR results.

	Evaluation of beating areas at day 20		cTNT immunofluorescence		
Dosis of Activin A and BMP4	Number of beating Areas	Qualitative evaluation of beating Areas	% Staining cTNT (mean of 3 counts)	Number of Stained areas (up to 5)	Final Score of cTNT staining
Act0 B0	0	-			
Act0 B10	0	-			
Act0 B30	1	++	8,5	2	17
Act3 B0	1	+	19,3	2	38,6
Act3 B10	0	-			
Act3 B30	0	-			
Act6 B0	2	++++	44,6	3	133,8
Act6 B10	**7**	**+++++**	**48,0**	**5**	**240**
Act6 B30	2	++++	66,0	3	198
Act10 B0	0	-			
Act10 B10	0	-			
Act10 B30	0	-			
Act30 B0	1	+	46,0	4	184
Act30 B10	1	++	36,6	3	109,8
Act30 B30	1	++	-	-	-

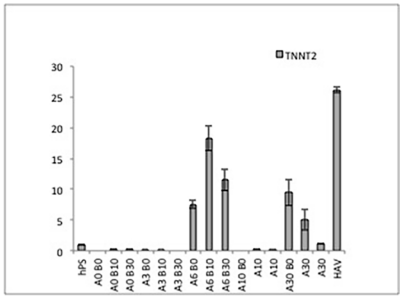

Figure 4.12: Results of Activin A And BMP4 titration for protocol 2.
Table: 15 combinations of doses of Activin A (Act) and BMP4 (B) were tested, varying from 0 ng/mL to 30 ng/mL (0, 3, 6, 10, 30) as indicated in the column "Dosis of Activin A and BMP 4". At Day 20, beating areas per well were scored. Their quality was assessed considering the extension of area and the power of beating with 0 to 5 crosses. Immunofluorescence for cTNT was performed. cTNT positive cells were scored from 3 20x area. cTNT positive cells percentage Vs total nuclei was obtained (% Staining cTNT (mean of three counts)). The number of positive cTNT areas in the entire slide was determined ("Number of Staines areas"). A final score was obtained by multiplying the number of the percentage of cTNT positive cells for the number of stained areas. The higher score was obtained for the concentration of 6ng/mL of Activin A and 10 ng/ml of BMP4, highlighted in grey in the table.
Graph. Y-axis: fold increase in gene expression for TNNT2, coding for cTNT protein. X-axis: hPS = KiPS 3F.7 pluripotent stem cells; different doses combinations (ng/mL) of ActivinA (A) and BMP4 (B); HAV: human heart ventricle, as positive control. cTNT expression analysis confirms that the best dose of morphogens is 6ng/mL for Activin A and 10ng/mL for BMP4.

The obtained results led us to increase the concentration of Activin A from 3 to 6 ng/ml for further experiments.

Further differentiations of KiPS3F.7 cell lines confirmed such differentiation efficiencies. Representative beating areas and immunofluorescence of cardiac marker cTNT are shown in **figure 4.13**. Bright field image corresponds to the first frame of the attached **video 4.3**.

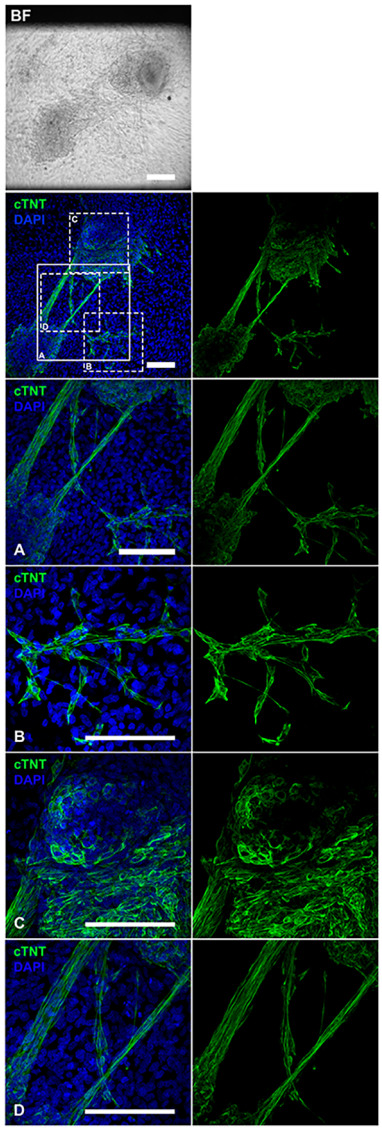

***Figure 4.13*:Bright field image and immunostaining for cTNT of beating areas from cardiac KiPS 3F.7 cell cultures at day 20 of differentiation with protocol 2.**
Beating areas expressing cardiac marker cTNT. Different magnifications are showed in squares A, B, C and D, in which characteristic bands of the sarcomere structures typical of sarcomeric organization are visible. Scale bars: 75 um.

4.1.3 Cardiac Differentiation of iPSC with GSK3 inhibitor and IWP4 (Protocol 3)

Protocol 2, based on Activin A, BMP4 and DKK1 molecules, was suitable to KiPS 3F.7 cell line, but it is an extremely time consuming and tedious to perform. To obtain the high number of cells needed for 3D tissue culture (described in the following sections), a great amplification on HFF through manual picking of the colonies was required: up

to 90 wells of cells, that means 3 to 6 weeks of waiting for the cells to grow, and that had to be manually scraped in order to obtain EBs (which takes around 8 hours to an expert hand).

Nevertheless in 2013, new protocol was published (Lian et al., 2013), based on GSK3 pathway inhibition and IWP4 mesoderm induction, here named protocol 3 (shown in **figure 4.14**). It was supposed to be much more efficient and feasible than protocol 2, since it is based on monolayer cell culture. We tested it with our KiPS 3F.7 cell line and compared it with protocol 2.

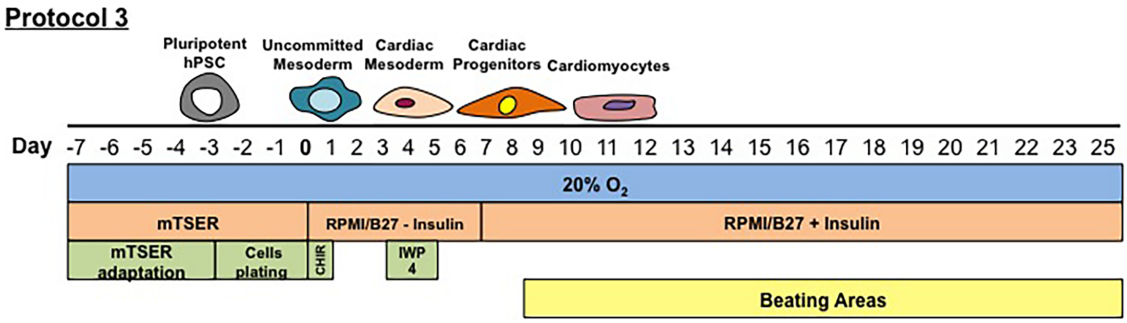

***Figure 4.14*: Schematic and timeline of protocol 3**
*Pluripotent cells (KiPS3F.7 cells) are adapted to mTSER prior to experiment. In order to induce cardiac differentiation, cells are enzymatically detached and seeded onto 12wp (cells plating). When confluence is reached (afeter 2 or 3 days), differentiation can be induced. Medium is shifted to RPMI/B27 without Insulin and cells are treated with CHIR*99021(CHIR)*, a GSK3 pathway inhibitor. On day 3, IWP4 is added to inhibit WNT pathway. From day 7 on, cells are cultured with Insulin. Beating areas appear from day 8-10.*

Figure 4.15 shows the evolution of cell cultures.

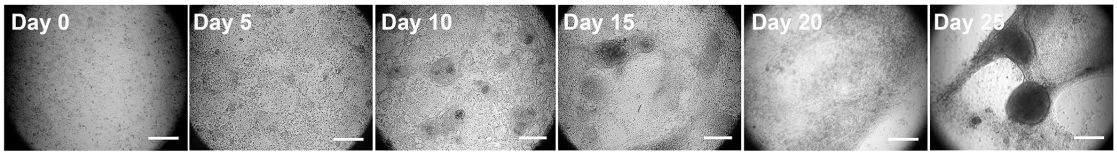

***Figure 4.15*: KiPS 3F.7 differentiating to cardiomyocytes with Protocol 3**
Bright-field images of the typical morphology of day 0, day 5, day 10, day 15, day 20 and day 25. Scale bars, 200 um.

On day 0 cells were a confluent monolayer. On day 5 cells were already committed to mesoderm and on day 10 beating structures were present. They appeared as beating clusters that soon spread as a beating monolayer. For this reason it was not possible to count beating areas. Monolayers continued contracting until day 25 and on. In the attached videos **video 4.4 – 4.9** it is possible to observe beatings structures on day 10, 20 or 25 as an example. **Figure 4.16** shows the first frames of the videos.

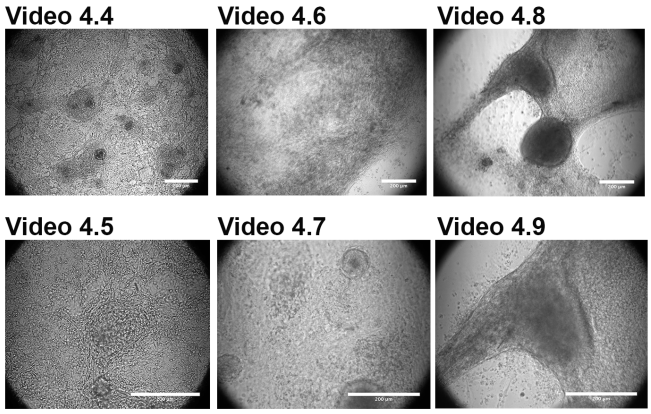

***Figure 4.16*: First frame of the attached videos 4.4 - 4.9.**
Time-lapse captures of KiPS 3F.7 at day 1 0(videos 4.4 and 4.5), 20 (videos 4.6 and 4.7) and 25 (videos 4.8 and 4.9) of cardiac differentiation with Protocol 3. Magnifications: 10x (video 4.4, 4.6 and 4.8) and 20x (video 4.5, 4.7and 4.9). Scale bars: 200 um.

Kinetic analyses of the differentiation cultures through RT-qPCR analysis (**figure 4.17**) revealed a fast primitive streak–like population defined by T (BRACHYURY) that was already down-regulated at day 4 and emergence of mesoderm at day 4, marked by up-regulation of NKX2.5. NANOG pluripotency gene was down regulated during all the differentiation. Contracting cardiomyocytes were first detected between days 8 and 10 of differentiation, coincident with the up-regulation of TNNT2. cTNT protein is expressed as shown in **figure 4.18**, indicating marked sarcomeric organization.

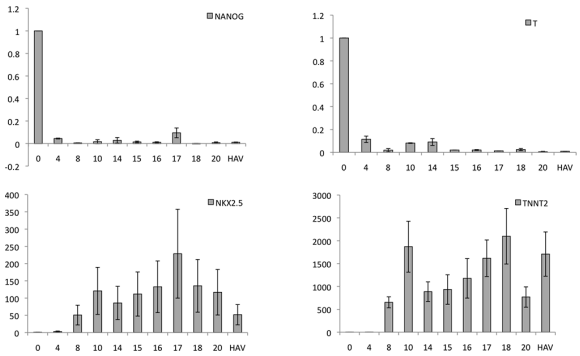

***Figure 4.17*: RT-qPCR analysis of NANOG, T (Brachyury), NKX2-5 and TNN2 in KiPS 3F.7 cells at different stages of differentiation with Protocol 3**. *Fold increase in gene expression analysed at day 0, 4, 8, 10, 14, 15, 16, 18 and 20. (HAV: human adult ventricle, as positive control). Error bars represent standard deviation.*

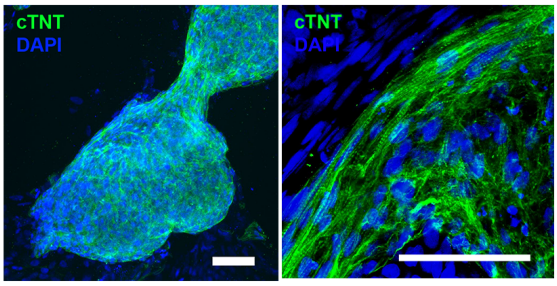

***Figure 4.18*: Immunostaining for cTNT of beating areas from cardiac KiPS3F.7 cell cultures at day 20 of differentiation with protocol 3.**
Beating areas expressing cardiac marker cTNT with sarcomere structures typical of sarcomeric organization. Scale bars: 75 um.

Overall analysis results of the three protocols indicates that protocol 3, based on GSK3 pathway inhibition and mesoderm specification with IWP4, is much more efficient and reliable for differentiating iPSC to cardiomyocytes, both in terms of handling and time consumption that in terms of cardiomyocyte generation. Beating structures appeared between day 8 and 10 and they covered at least the 50% of the entire area of the culture plate, indicating that differentiated cardiomyocytes initiate connections between them to spread cardiac contractions. While, with protocols 1 and 2, beating areas stayed confined to clustered beating structures. RT-qPCR analysis of genes involved in cardiac differentiation confirmed faster and efficient differentiation for protocol 3, as well as immunofluorescence analysis. All those considerations led us to shift to this last protocol for our experiments in 3D.

4.2 Transgenic cell lines

During in vitro differentiation of hPSC, many different cell types arise in culture in a non-synchronized way. For this reason, a critical factor in differentiation protocols is to monitor the effectiveness of differentiation during time, to select and expand only the cell population of interest. A major hindrance to the generation of adult specialized and functional CMs is that the mechanisms that regulate the differentiation to particular cell types are not well known. In addition to this, cardiomyocytes (CMs) obtained from hPSC using currently available differentiation protocols are typically immature, mostly resembling embryonic or fetal CMs (Cao et al., 2008) (Davis, van den Berg, Casini, Braam, & Mummery, 2011). In this context we generated a set of transgenic hPSC that allowed monitoring populations of cells during different steps of the differentiation process. In these cell lines, promoters of genes expressed in the cardiac lineages drive the expression of Green Fluorescence Protein (GFP) (see **figure 4.19**). We implied such cells in our tissue engineering experiments, in order to put the basis to develop protocols that would allow a more efficient maturation of cardiac cells, together with adequate electrophysiological stimuli.

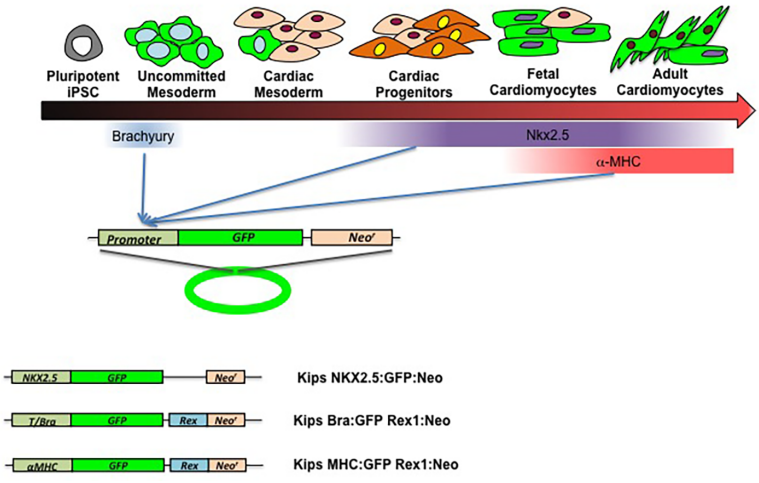

***Figure 4.19*: Scheme of cardiac differentiation outline and vectors used in order to obtain transgenic induced pluripotent stem cell lines.**
Plasmid vector (NKX2.5:GPF_Neo^r) and lentiviral vectors (T/Bra:GFP_Rex1:Neo^r and alphaMHC:GFP_Rex1:Neo^r) scheme, in which the promoter of a gene for mesoderm (T), cardiac progenitors (NKX2.5) or mature cardiomyocytes (alpha-MHC) drives the expression of the reporter gene GFP. When differentiating to cardiomyocytes, cells that are following the proper differentiation path can be monitored thanks to the expression of GFP, in correspondence of the used promoter.

4.2.1 KiPS 3F.7:NKX2.5:GFP:Neo^r cell line

To achieve cardiac-progenitor specific GFP expression, KiPS 3F.7 cells were transfected with lipofectamine with pNKX-GFP plasmid, carrying the neomycin resistance gene, in which reporter protein expression is driven by a 2.1 kb enhancer located 9.5 kb upstream of the translation start site of murine NKX2.5, that is activated concomitant with the endogenous gene (Lien et al., 1999). After transfection, antibiotic selection with G418 was performed, in order to select cells that had integrated the plasmid into their genome.

To prevent loss of NKX2.5:GFP expression in bulk-transduced KiPS, we generated clonal lines of pNKX2.5-GFP-transfected KiPS (KiPS 3F.7 NKX2.5:GFP Neo^r cells). In order to obtain clonal colonies, two weeks after transfection and antibiotic selection, cells from single colonies were treated with trypsin 0,05% and manually picked with "*THE STRIPPER*" to be plated on human feeder fibroblasts in twelve-well plates. Six independent colonies were then picked and expanded. Plasmid integration in each clonal line as well as in the bulk-line was screened by two PCR reactions on genomic DNA using primers specific to the vector sequence corresponding to the promoter-GFP (primers pNKX2.5 F and GFP R in materials and methods) and to the promoter-Neo^r cassette (primers pNKX2.5 F and pKanNeo R) (see **figure 4.20**). The bulk cell line and three clones (clones 1, 2 and 6) showed integration (**figure 4.20**). Clone 6 showed integration only of a fragment of the vector. We submitted cell lines derived from clones 1 and 2 to cardiac differentiation with protocol 2 and verified transgene expression. In clone 1 we detected a faint expression of GFP, while clone 2 showed a strong expression that started on the day 4/5-7 time window and lasted at least until day 20, as expected by literature (Dubois et al., 2011). Differentiated cells at day 20 also expressed cTNT, as shown by immunofluorescence (**figure 4.20**). We therefore selected clone 2 for further experiments. It is possible to see GFP expression in beating cardiac areas (**video 4.10 and 4.11**), which first frames are here shown in **figure 4.21**.

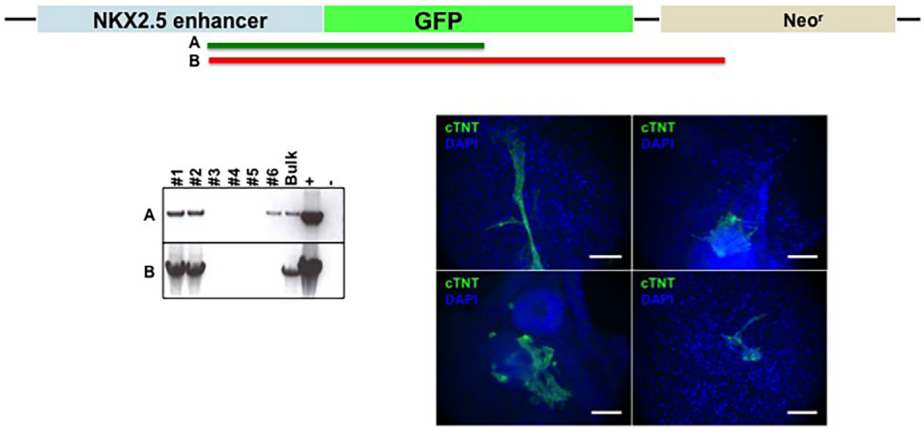

***Figure 4.20*: KiPS 3F.7 NKX2.5:GFP:Neo^r cell line: integration of the vector and cTNT expression.**
Plasmid vector pNKX-GPF scheme. A and B represent amplified fragments amplified in PCR reaction made on genomic DNA from KiPS 3F.7 NKX2.5:GFP:Neo^r bulk cell line and clones #1 to #6. Vector was completely integrated in clones #1 and #2 and partially in clone #6. +: pNKX-GFP plasmid as positive control. -:water used as negative control for PCR reaction. Immunofluorescence shows cTNT expression in different experiments of KiPS 3F.7 NKX2.5:GFP:Neo^r cell line differentiated with protocol 2. Scale bars: 100um.

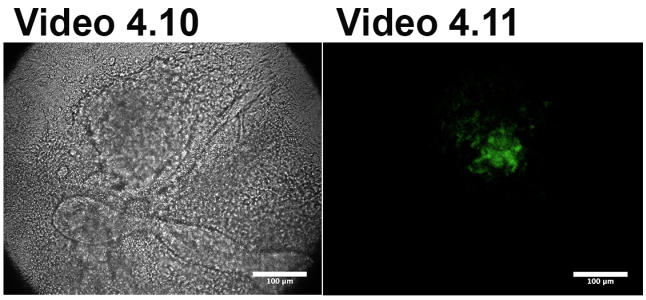

***Figure 4.21*: First frame of the attached videos 4.10 and 4.11.**
Bright Field and Fluorescence Time-lapse captures of KiPS 3F.7 NKX2.5:GFP:Neo^r, #2 at day 14 of cardiac differentiation with Protocol 2. Transgenic cell lines express GFP driven by cardiac progenitor's promoter NKX2.5, which is visible in beating areas. Magnifications: 20x. Scale bars: 100 um.

In order to characterize time expression of NKX2.5 driven GFP, and to further sort cardiac progenitors to be cultured in 3D environment, a titration via cytometry was performed. The higher expression was detected at day 8, with the 18% of cells expressing GFP the value was maintained up to day 12. After then expression decreased to 4% at day 14 and equivalent values were maintained up to day 20 (**Figure 4.22**).

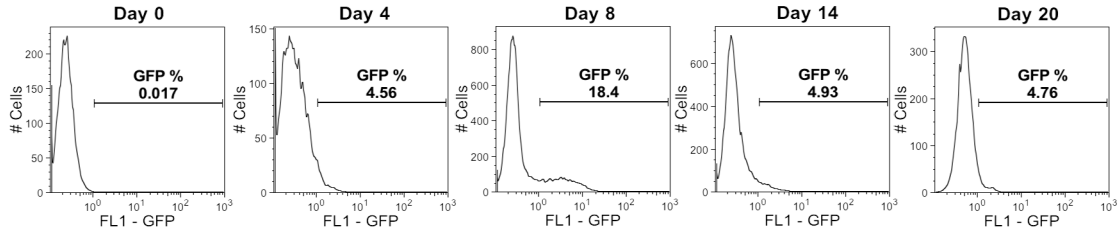

***Figure 4.22*: GFP expression titration of KiPS 3F.7 NKX2.5:GFP:Neo^r, #2 cells.**
Cytometry analysis of KiPS 3F.7 NKX2.5:GFP:Neo^r, #2 cells. GFP expression started at day 4 and it was maintained at least up to day 20. Maximum expression occurred on day 8, with the 18% of positive cells.

4.2.2 KiPS 3F.7 T/Bra:GFP_Rex1:Neo^r cell line

In order to obtain a stable cell line with a reporter for early mesoderm, KiPS 3F.7 cells were transduced with a lentiviral vector expressing GFP under the control of T/Brachyury promoter. To establish a stable transduced cell line, the same clonal strategy of NKX2.5:GFP reporter line was used, taking advantage of the Neomycin resistance cassette under the control or Rex1 pluripotency gene promoter.
PCR reactions on genomic DNA using primers specific to the vector sequences (GFP F and R) confirmed lentiviral integration in cells' genome. 24 clones were produced, and 6 were submitted to cardiac differentiation both with protocols 2 and 3 to select the most efficient line. We selected clone #4 for further experiments in 3D. To characterize this cell line we differentiated it with Protocol 3, based on GSK3 inhibition and IWP4. In **figure 4.23**, we can see the evolution of differentiating cells. GFP is expressed following T expression, during the first 4 days of differentiation, and then it is silenced.

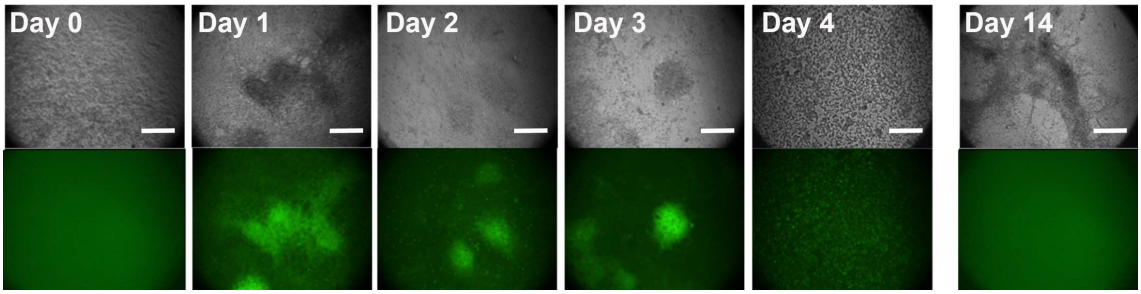

***Figure 4.23*: KiPS 3F.7 T/Bra:GFP_Rex1:Neo^r cells differentiating with protocol 3**
Bright-field and fluorescence images of the typical morphology of pluripotent stem cells on Matrigel monolayer at day 0 and cells differentiating at day 1day 2, day 3, day 4, day 14 and day 25. GFP expression is promptly triggered at day 1, staying active until day 4. Later it is not expressed. Scale bar: 100nm.

GFP expression was analysed and quantified through cytometry. **Figure 4.24** shows the obtained titration. GFP was expressed between days 1 and 4. From day 5 transgene's expression is significantly silenced and it is maintained down-regulated over time.

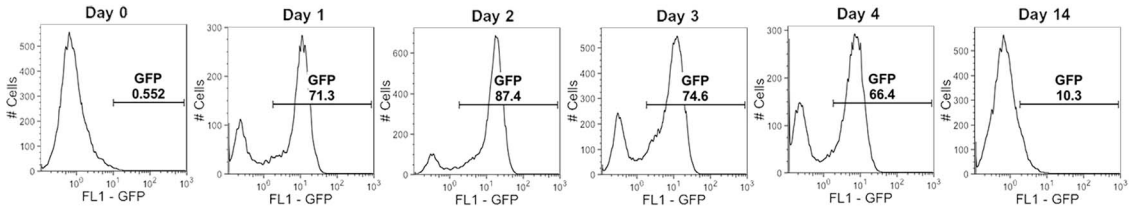

***Figure 4.24*: GFP expression titration of KiPS 3F.7 T/Bra:GFP_Rex1:Neo^r cells.**
Cytometry analysis shows that GFP expression started at day 1 with 71.3% of positive cells, peaked at day 2 (87.4%) and decreased on day 4 (66,4%). On day 14 only 10,3% of the cells expressed GFP.

To confirm that GFP followed T expression pattern, semi-quantitative RT-PCR of T and GFP analysis was been performed on cDNA (**figure 4.25**). T mRNA was transcribed on day 1 and 2. GFP levels started one day earlier, because the sample had been collected after adding GSK3 inhibitor, and had already had some mesoderm inducing effect. GFP mRNA expression decreased on day 3 and showed a fade band on day 4, coherent with the decrease of protein expression detected by fluorescence microscopy and cytometry.

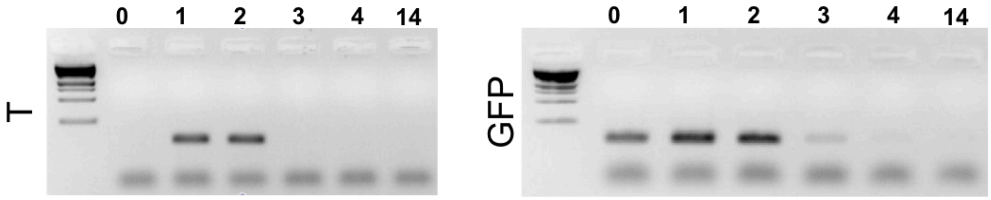

***Figure 4.25*: T and GFP mRNA expression in of KiPS 3F.7 T/Bra:GFP_Rex1:Neo^r cells.**
mRNA transcripts of T and GFP were evaluated on days 0, 1, 2, 3, 4 and 14 of cardiac differentiation with Protocol 3.

To prove the co-expression of Brachyury protein and GFP we performed an immunofluorescence analysis of the two proteins on KiPS 3F.7 T/Bra:GFP_Rex1 Neo^r at day 2 of differentiation, when maximum expression occurred (**Figure 4.26**).

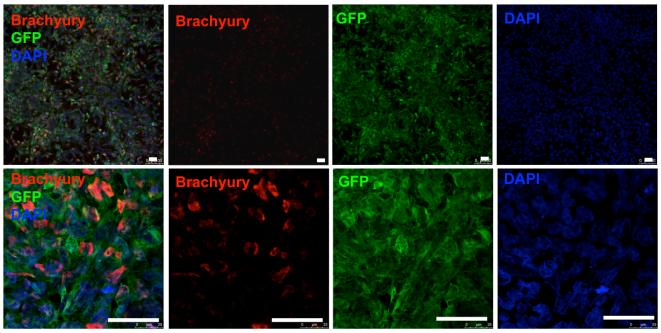

Figure 4.26: T and GFP immunofluorescence analysis of KiPS 3F.7 T/Bra:GFP_Rex1:Neo^r cells at day 2 of differentiation.
Brachyury is a transcription factor, expressed in nuclei, while GFP expression is driven in the cytoplasm. Immunofluorescence analysis showed that the two proteins were expressed in the same cells. Scale bar:50 um

4.2.3 KiPS 3F.7 MHC:GFP_Rex1:Neo^r cell line

KiPS 3F.7 MHC:GFP_Rex1:Neo^r cell line was obtained by lentiviral transduction, with a lentiviral vector expressing GFP under the control of alpha-MHC protein. PCR reactions on genomic DNA using primers specific to the vector sequences (GFP F and R) confirmed lentiviral integration in cells' genome. The same clonal strategy was applied: 24 clones were produced, and 6 were submitted to cardiac differentiation both with Activin A, BMP4 and DKK1 based protocol (protocol 2) and with GSK3 and IWP4 based protocol (protocol 3) to select the most efficient line. We selected clone #9 for further characterization and experiments in 3D.

KiPS 3F.7 MHC:GFP_Rex1:Neo^r cell line was characterized with the same experiments. Different time points were analysed, considering the later expression of the gene in cardiac differentiation. Fluorescent cells had beating capacity (**Videos 4.12 and 4.13**)

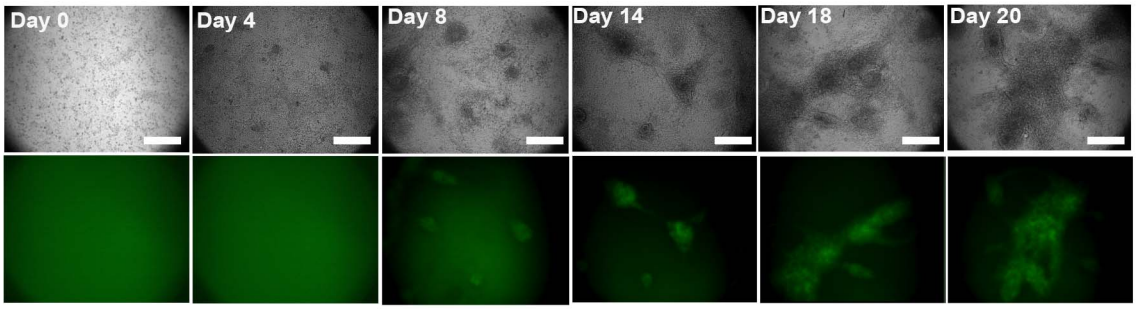

***Figure 4.27*: KiPS 3F.7 MHC:GFP_Rex1:Neo^r cells differentiating with protocol 3**
Bright-field images of the typical morphology of pluripotent stem cells on Matrigel monolayer at day 0 and cells differentiating at day 4, day 8, day 14, day 18, and day 20. Fluorescence imaging shows that GFP expression began on day 8 and stayed active later on. Bright field and fluorescence images of cells at day 20 are the first frames of ***videos 4.12*** *and* ***4.13*** *respectively. Scale bar: 100 nm*

Cytometry titration of GFP expression shows that it started on day 8, together with the appearance of beating structures, as MHC is a structural sarcomeric protein. GFP level increased as differentiation proceeded.

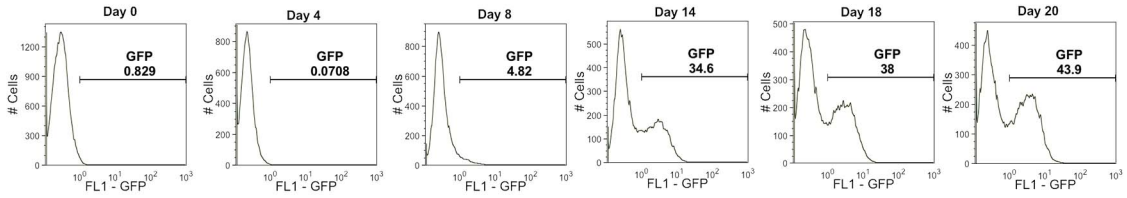

***Figure 4.28*: GFP expression titration of KiPS 3F.7 MHC:GFP_Rex1:Neo^r cells.**
Cytometry analysis shows that GFP expression starts at day 8 with 4,82% of positive cells, and increase progressively. On day 20 it reaches 43,90% of expression

On day 20 we sorted for GFP positive cells, in order to analyse its mRNA to better correlate the specificity of the transgene to its promoter. Moreover we analysed alpha-MHC and GFP expression at other time points by semi-quantitative RT-PCR (**figure 4.29**).

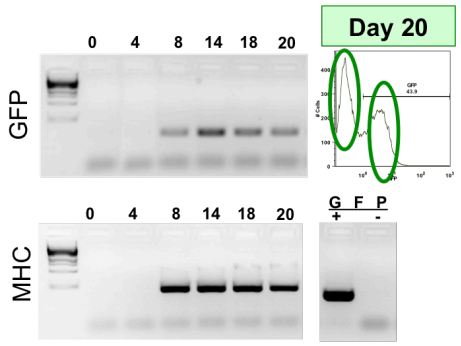

***Figure 4.29*: MHC and GFP mRNA expression in of KiPS 3F.7 *MHC:GFP_Rex1:Neo^r* cells.**
mRNA transcripts of MHC and GFP were evaluated on days 0, 4, 8, 14, 18 and 20 of cardiac differentiation with Protocol 3. On day 20 cells were sorted according to their expression of GFP. MHC expression was evaluated in GFP positive (+) and negative (-) cells. MHC expression was detected only on the positive population.

Alpha-MHC and GFP expression were synchronized and coincided with the day of appearance of beating structures. As expected, MHC was expressed in GFP positive cells, while it was absent in GFP negative ones.

Immunofluorescence analysis on cells at day 11 of differentiation with protocol 3 (**figure 4.30**) confirmed that GPF followed the expression of the endogenous MHC protein, validating our cell line.

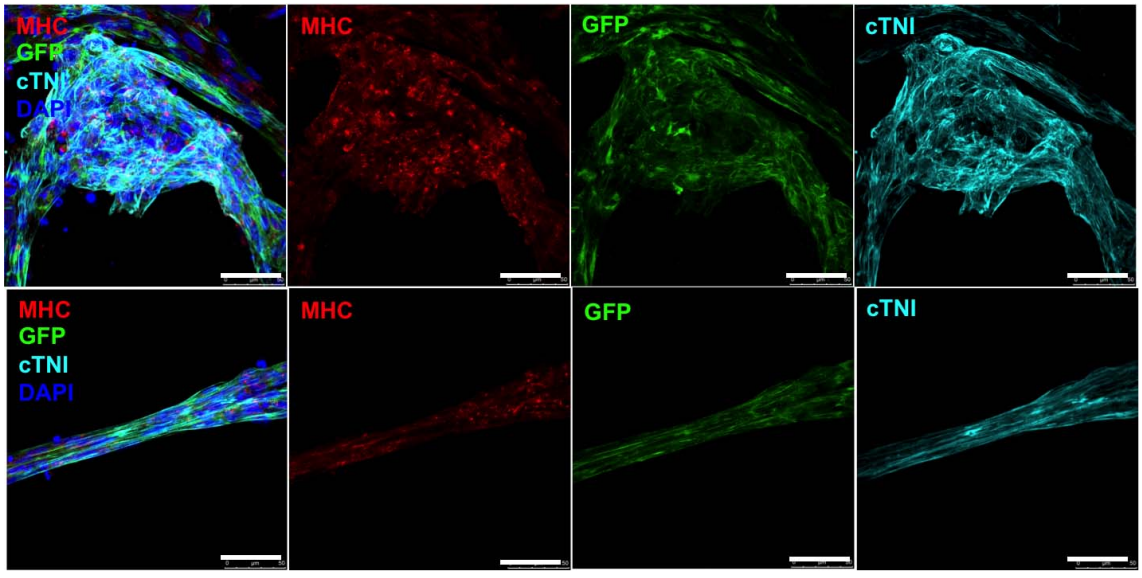

***Figure 4.30*: MHC and GFP immunofluorescence analysis of KiPS 3F.7 *MHC:GFP_Rex1:Neo^r* cells at day 11 of differentiation.**
GFP expression matched with MHC expression as well as with cardiac Troponin I (cTNI), another important cardiac marker.

In summary, In order to monitor the correct commitment of the differentiating hPSC to the cardiac lineage during differentiation protocols, and to select pure population of labelled cardiac cells, we obtained homogeneous transgenic iPSC through transfection of plasmid or infection with lentiviruses into iPSC cell line KiPS3F.7. Specifically, we completed the characterization of NKX2.5–GFP cell line, expressing green fluorescent protein under the control of NKX2.5 promoter, a marker for cardiac progenitors. PCR analyses of genomic extract demonstrated the integration of the vector. Through fluorescence microscopy is was possible to observe the appearance of green cells starting from 4/5-7 days of differentiation, using ActivinA. BMP4 and DKK1- based protocol (Protocol 2), which was maintained at least up to day 20. To sort the maximum number of cardiac progenitors we titrated the expression of GFP by flow cytometry during time. The higher expression was detected at day 8, with the 18% of cells expressing GFP the value was maintained up to day 12.

This line was tought to be well established but after some passages it stopped to perform good since the fluorescence was significantly diminished. We thought that this was due to the method with which we obtained the cell line: plasmid transfection with lipofectamine. So we changed our approach and we tried to obtain more stable lines by transduction of human iPSC with lentiviral vectors.

Apart from NKX2.5 we transduced cells with reporters of Brachyury (T), a mesoderm marker, and alpha-Myosin Heavy Chain (MHC) cardiomyocytes marker. We differentiated those cells both with ActivinA, BMP4 and DKK1 based protocol (protocol 2) and GSK3 and IWP4 based protocol (protocol 3), to test the efficiency of differentiation of the lines and of the markers. GFP was expressed following the expected timing under the control of T and alpha-MHC promoters, but significantly later (day 20 instead than day 5) in the case of NKX2.5. We characterized and validated the two working cell lines through cytometry, immunofluorescence and RT–PCR analysis. The reporter gene (GFP) was expressed within the desired time window, and expression of GFP and T (almost 90% on day 2) or MHC (nearly 45% at day 20) proteins were synchronized and co-localized.

4.3 Bioreactor for human iPSC derived cardiomyocytes culture

Properly mimicking naïve cardiac tissue is very complex, since not only the correct cardiac cell population has to be reflected, but also its exact total cellular composition, its architecture and biophysical functions. Tissue engineering approaches offer tools and possibilities to mimic tissues and organs environments, combining a proper scaffold in which cells can grow, within a bioreactor.

In order to support the growth of cardiomyocytes derived from hiPSC, we optimized a perfusion bioreactor system, validating it with rat neonatal cardiomyocytes. This work was developed together with Maria Valls Margarit, PhD student in the "Biomimetic systems for cell engineering" group at IBEC, under the supervision of Dr. Elena Martínez. Detailed description and characterization of the device are objects of Maria Valls' doctoral thesis and will be elucidated by her.

4.3.1 Bioreactor structure

In the context of cell therapy for heart repair and tissue replacement, bioreactors have been developed, to support *in vitro* growth of artificial cardiac tissue. In particular, Vunjak-Novakovic's laboratory developed a perfusion system in which neonatal rat cardiomyocytes could be cultured (Radisic, Marsano, Maidhof, Wang, & Vunjak-Novakovic, 2008). We optimized that device inserting a de-bubbling system to avoid air bubble formation and creating a multiple chamber system, in which up to 5 experiments could be run in the same bioreactor. **Figure 4.31** shows the bioreactor and its components. Cells are cultured into a porous scaffold and homed into a chamber that consists of a Millipore filter cartridge.

Maria Valls Margarit has carried out the characterization of the physical parameters of the bioreactor in the context of her doctoral thesis, actually in progress.

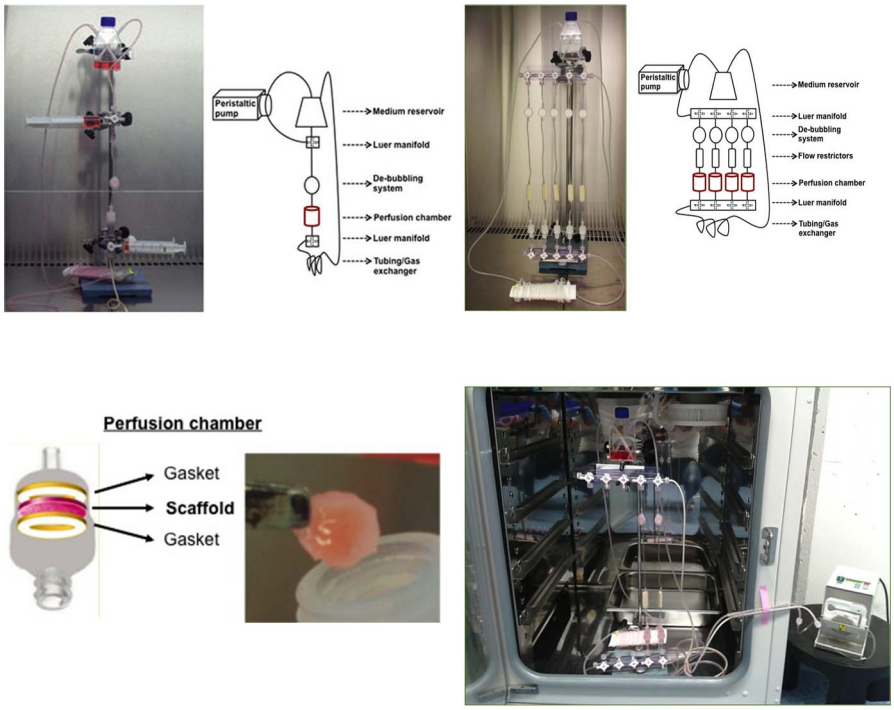

***Figure 4.31*: Perfusion Bioreactor system**
Upper left: Perfusion bioreactor system and cartoon scheme describing its components. Upper Right: multi-chamber parallel bioreactor system and cartoon describing its components). Lower left: Cartoon of the Perfusion Chamber (credit to Maria Valls) and detailed picture of a scaffold in a Millipore filter cartridge. Lower Right: Multi-chamber parallel perfusion bioreactor connected to a peristaltic pump into a cell culture incubator.

Different components were custom built and assembled together through Luer connections or parafilm sealing. Medium reservoir was obtained from a T25 cell culture flask, opening two holes at the sides in order to allow tubing insertions. Tubes were fixed with parafilm in order to prevent leaking and/or contamination. Along the tubing system, Luer three-ways stopcocks systems permit the connection of other components as well as syringes, used for changing culture medium.

An important issue in tissue engineering is to avoid formation of air bubbles, as they could hamper medium flow through the scaffold, as well as the correct supply of nutrients to the cells. For this reason we assembled a high fidelity de-bubbling system inserting it upstream to the culture chamber. The de-bubbling system is a porous membrane, original component of a portable elastomeric pump used in clinic chemotherapy for ambulatory patients ("Dosi-Fuser®" system from Leventon'). Following the perfusion flow, after the de-bubbling system we find the core of the

bioreactor: the perfusion chamber. It consists of a Millipore filter cartridge in which two silicon gaskets tightly hold the scaffold. It is extremely important that all the components of the chamber reflect the precise size requirements, since the smallest mismatch could induce air bubbles' formation or leaking, collapsing the entire system. Oxygen refreshing and gas exchange after the perfusion chamber is possible thanks to a two coponents: 1) a 3 meter long silicon tubing, coiled around a holder 2) the filter cap of the medium reservoir. Tubing system is connected to a perfusion pump, set to pull the medium following this direction: Luer manifold to de-bubbling system, to perfusion chamber, to gas exchange tubing, to medium reservoir. Pump's flow rate was set to 0,1 mL/ minute, a value that assures proper nutrients' exchange and prevents cells from suffering shear stress.

In order to be able to perform multiple experiments at once, we needed to increase the number of perfusion chambers that one single bioreactor could supply, from 1 to 5. We therefore inserted Luer manifolds and micro fluidic resistances into the system to guarantee a homogeneous distribution of medium into the 5 chambers. Microfluidic resistances are also components of Dosi-Fuser systems. We tested medium re-distribution into the 5 chambers and we proved that flow rate was homogeneous and constant into the 5 chambers: setting 0,5 mL/minute as flow rate in the peristaltic pump, the flow rate of interest of 0,1 ml/min is guaranteed to the 5 chambers.

4.3.2 Scaffold

In order to reproduce extracellular environment of the heart, it is important to mimic naïve extracellular matrix of the tissue of interest. In the context of tissue engineering applications, different scaffolds are used for different purposes. Heart extracellular matrix is composed mainly of type I, III, IV, V and VI (in order of abundance) collagen and elastin. The scaffold we chose for our experiments, Matridem®, is a commercially available three-dimensional bovine collagen-elastin matrix, which composition partially reflects heart's extracellular matrix proteins, being made of collagen type I, III and V and elastin. Although being a commercially available product used in clinics, its porosity wasn't described. We characterized Matriderm® porosity through SEM analysis: pores have a homogenous distribution, with Feret diameter ranging from 5 to 35 um (**Figure 4.32**).

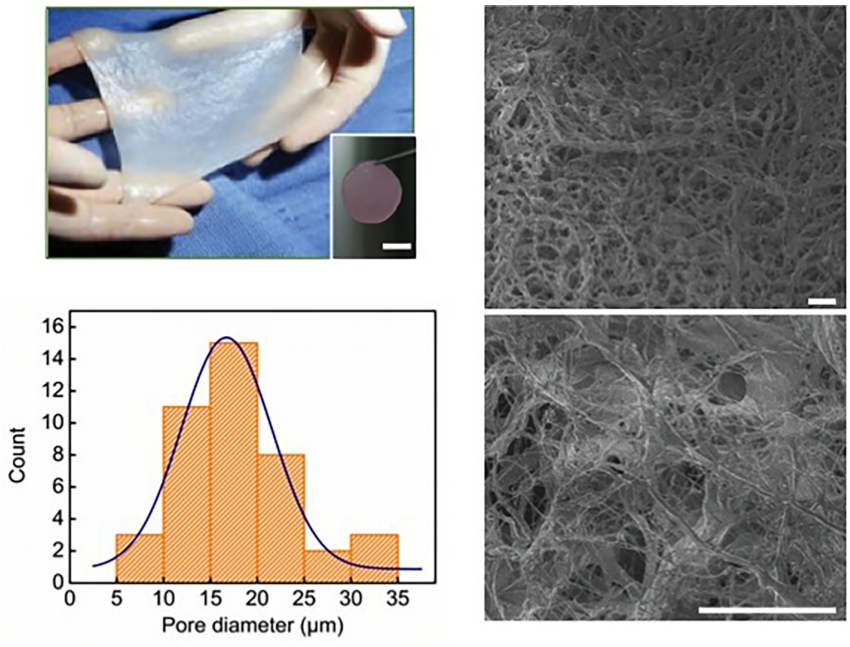

***Figure 4.32*: Scaffold porosity**
Upper left: Hydrated Matriderm® sheet and hydrated Matriderm® cut scaffold (scale bar: 5mm). Upper and Lower Right: SEM images of Matriderm® scaffold surface. Scale bar: 100um. Lower left: Graph representing pore size distribution of Matriderm® according to their Feret diameter (credit to Maria Valls Margarit).

4.3.3 Seeding optimization and cells viability

In order to mimic a piece of original tissue, cells have to be homogeneously distributed throughout the scaffold, with a proper cell density. Cell density of a rat's heart is of 10^8 cells/cm^3. To obtain such conditions, we tested two methods for inoculating our cells into the scaffold: static and under perfusion. We used to this purpose primary cultures of neonatal rat cardiomyocytes. Static seeding resulted in confining the cells into the upper part of the scaffold, where cells are then unable to colonize the biomaterial. Perfusion seeding was tested to obtain a wider cell distribution within the scaffold. We assembled a perfusion loop that enabled a forward-reverse culture medium flow. Following indications from Vunjak-Novakovic's paper (Radisic, Marsano, Maidhof, Wang, & Vunjak-Novakovic, 2008) 3,5 millions of cells were concentrated in 1 ml of culture medium and perfused into the scaffold by peristaltic pump's pressure at 1 ml/min. The original procedure indicates to apply forward-reverse perfusion during 2 hours. Actually in our hands, such prolonged forward-reverse perfusion resulted in washing out cells. We therefore adapted the procedure introducing the cells into the

scaffold with a single forward step of perfusion. Cell seeding is performed within a culture chamber into the seeding loop; later the scaffold is moved to the bioreactor itself. In order for the cells to adhere to the scaffold, recently seeded scaffolds are incubated 4 hours before being perfused, as sudden perfusion would impede cellular adhesion and favour cells detachment.

To understand how many cells the scaffold retained right after cell seeding, medium was retired from the scaffold and cells were counted. Remaining cells were subtracted from the initial number of seeded cells (3,5 millions) and seeding efficiency was calculated as percentage of total cells retained into the scaffold. Seeding efficiencies of primary cultures varied from 60 to 90%. **Figure 4.33** represents the seeding loop and Matriderm® scaffolds seeded with neonatal rat primary cardiac cells.

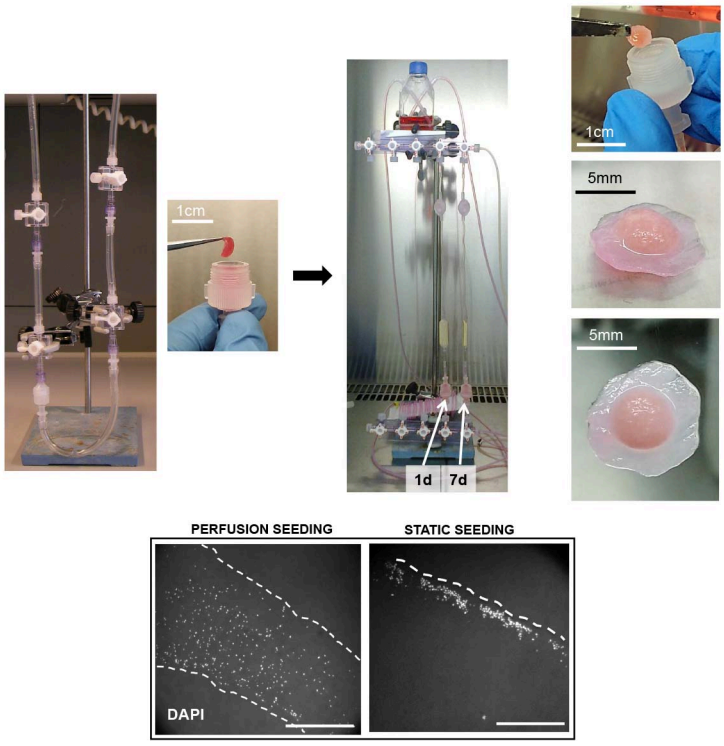

***Figure 4.33*: Seeding of primary culture of neonatal rat cardiomyocytes**
Upper-left: Perfusion loop. Empty hydrated scaffold is placed into a perfusion chamber. Cells are seeded connecting the perfusion loop to a peristaltic pump. After seeding, Matriderm is retired from the chamber of the perfusion loop and placed into a bioreactor. Upper-right: On different time points, according to the experiment (for example 1 or 7 days), Matriderm® is retired for analysis. After 7 days of culture, rat cardiomyocytes proliferate into the scaffold and form a thick tissue-like structure. Lower line: cross sections of Matriderm scaffold seeded with rat cardiomyocytes in perfusion or with static seeding. Perfusion seeding allows homogeneous distribution throughout the scaffold. Limits of Matriderm scaffold are marked. Scale bar: 1 mm.

4.3.4 Rat cardiomyocytes growth

In order to assess cardiac cells' viability into the bioreactor, two Collagen-Elastin scaffolds were seeded with primary cell culture from neonatal rats and cultivated in the bioreactor for 1 and 4 days respectively. Cells distributed homogeneously through the scaffold, although in a small amount. We marked cardiomyocytes (CMs) that eventually survived or proliferated into the scaffold for 1 or 4 days through immunofluorescence for cardiac troponin T (cTNT). The original control cell population contained 31,9% of cardiomyocytes, after 1 day of culture into the bioreactor the percentage was 27,0% and this value was maintained for 4 days, indicating that cardiomyocytes are able to survive and colonize the scaffold, maintaining a population of cells similar to that of the native tissue. 3D culture does not affect endogenous cell composition, since also in native hearts; cardiac cells represent 30% of the total (**figure 4.35**). After 7 days of culture, cardiac population was retained into the scaffold: cTNT is expressed together with connexin 43, which suggests that the tissue can stay functional into the bioreactor. Connexin 43 is a gap junction protein that allows ion exchange through cells. Moreover, rat CMs here cultured maintain beating capacity. **Video 4** Shows rat CMs beating in ordinary 2D conditions, while **video 4 s**hows Matriderm® scaffold with primary culture of rat CM that maintain their beating capacity. **Figure 4.34** shows first frames of those videos.

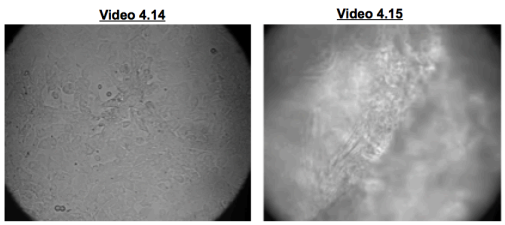

***Figure 4.34*: First frame of the attached videos 4.14 and 4.15.**
Bright Field Time-lapse captures of primary culture of rat CM cultured for 7days on a petri dish (video 4.14) or into perfusion bioreactor (video 5.15).

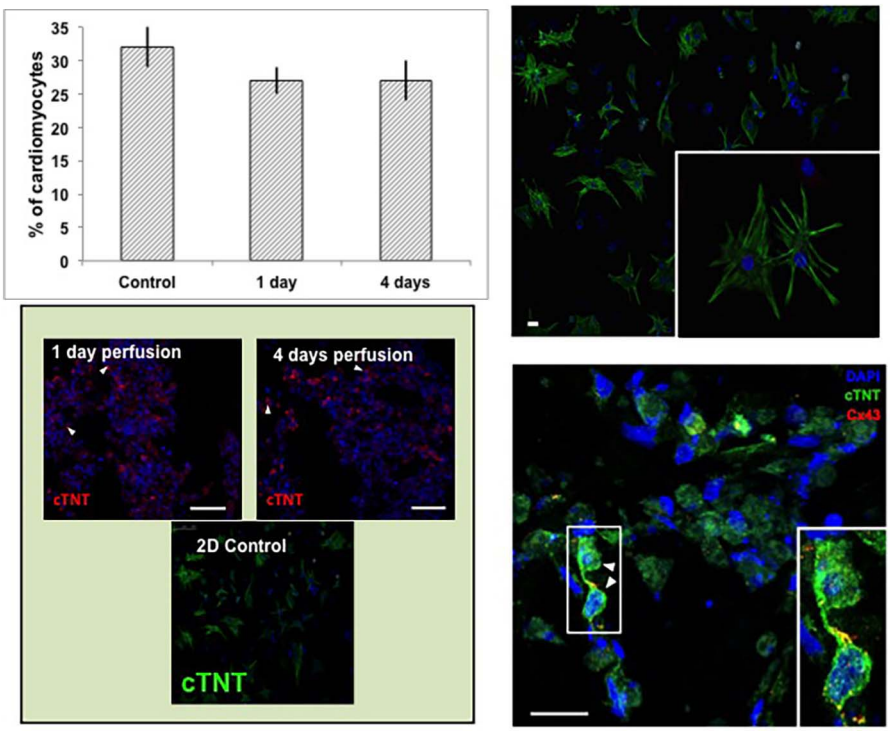

***Figure 4.35*: Rat CM behaviour in perfusion bioreactor**
Upper left: Graph showing cardiomyocytes percentage in primary rat cardiomyocyte cultured for 1 and 4 days into perfusion bioreactor. 30% of cardiac population is maintained in the two conditions, as well as in 2D cell culture of control. Lower left: immunofluorescence for cTNT of Matriderm® scaffolds cultured with primary rat cardiomyocytes used to calculate cardiac population percentage retained into the scaffold. 2D control, sown as control. Lower right: Immunofluorescence for cTNT and Connexin 43 in rat CM cultured 7 days into the bioreactor. Scale bar:25 um, CM cultured in 2D are shown as control in the upper-right panel.

In summary we optimized a perfusion bioreactor system useful to culture functional rat neonatal cardiomyocytes.

4.3.5 Cardiac differentiation of human iPSC-derived cardiac progenitors in 3D

As we wanted to evaluate the capacity of cardiac cells derived from iPSC to be cultured and in 3D, we first tried to culture cardiac progenitors derived from KiPS 3F.7 NKX2.5:GFP_Neo^r cell line, following the hypothesis that a 3D environment could provide better condition of early cardiac precursors.

Differentiated cells at day 8 with Activin A, BMP4 and DKK1 (protocol 2) were sorted and seeded into the bioreactor. At day 8, 15% of the cells were GFP positive. We inoculated into the bioreactor an enriched population of sorted GFP positive cells and GFP negative cells, to increase the percentage of cardiac progenitors with the aim of increasing the percentage of cardiac cells in culture and leave a 70% proportion of non-cardiomyocytes cells. Seeding efficiency was 70%. Through DAPI staining we could detect the presence of cells after 7 days of 3D culture, but immunofluorescence for cardiac markers did not show progresses into the differentiation, as we could not find any cTNT positive cell. We therefore repeated the experiment, using cells three days older, even though GFP expression was lower. Seeding efficiencies were around 80%.
Figure 4.36 is a representative image of a scaffold populated with iPSC, but negative for cardiac markers.

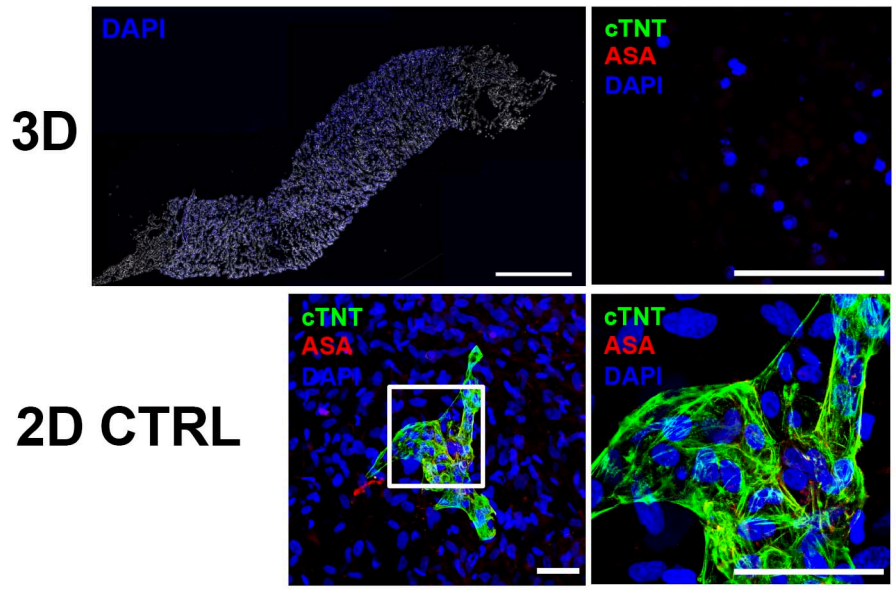

***Figure 4.36**: KiPS 3F.7 NKX2.5:GFP:Neo^r, #2 cells sorted derived progenitors into the bioreactor*
3D: KiPS 3F.7 NKX2.5:GFP:Neo^r, #2 cells sorted for GFP at day 8 of differentiation, enriched in cardiac progenitors and cultured into the bioreactor for 7 days. DAPI staining of a cross section of the scaffold shows that differentiated iPSC can populate Matriderm® (left, scale bar 1cm), but cells are negative for cardiac markers cTNT and alpha sarcomeric actin (ASA), indicating that they cannot complete their differentiation in 3D (right, scale bar 75 um). 2D CTRL: immunofluorescence of control cell culture for cardiac markers cTNT and ASA shows that KiPS 3F.7 NKX2.5:GFP:Neo^r, #2 cells have cardiac potential.

Since we validated our system with neonatal rat CM, that are more advanced in differentiation, we attributed the unsuccessful result to the age of early cardiac progenitors. In order to select more differentiated cells at day 20 of differentiation with protocol 2, we manually scraped beating areas. To obtain the high required cell number, 90 wells had to be differentiated, and 720 beating areas detached, which represent an enormous consumption of time and reagents. Again, we could detect cardiac cells positive for cardiac markers at seeding times, but not at later time points.

4.3.6 Cardiac differentiation of human iPSC-derived early mesodermal cells in 3D

Activin A, BMP4 and DKK1 cardiac differentiation protocol (protocol 2) is based on EB formation and differentiation of iPSC. According to cell morphology it is possible to observe that cardiac differentiation is restricted to the EBs clusters. On the other hand, GSK3 and IWP4 differentiation protocol (protocol 3) is used on monolayers of cells, and results in much more extended beating areas. We though that such more robust stimuli, could be reflected into the stability of iPSC culture to survive into the bioreactor, therefore we switched to protocol 3 to continue our experiments.

Since high amount of cardiac cells are required to populate a 3D device, and since it is not easy to obtain such amount of cells form advanced differentiating protocols, we wanted to see if early mesoderm committed cells were able to follow cardiac differentiation in 3D. To pursue this aim, we took advantage of KiPS3F.7 T/Bra:GFP:Rex1:Neo cell line. We started cardiac differentiation with Protocol 3 and asses, by fluorescent microscopy observation and cytometry analysis that at day 2, 90% of the cells were committed to mesoderm.

In order to provide support to cells, such cell population was co-cultured 1:1 with human foreskin fibroblasts (HFF) for 6, 13, 17 and 20 days in 3D, (with the same media and cytokines used in normal current Protocol 3 differentiation in 2D) in order to follow its possible cardiac fate. Cells were successfully seeded, as seeding efficiencies was around 90% in each condition, and they colonized Matriderm®: observing the scaffold (**figure 4.37**) it is possible to appreciate a thick tissue-like structure, that proliferate after 20 days of culture. DAPI staining of the nuclei confirms the observation: after 20 days cells proliferate into the culture chamber.

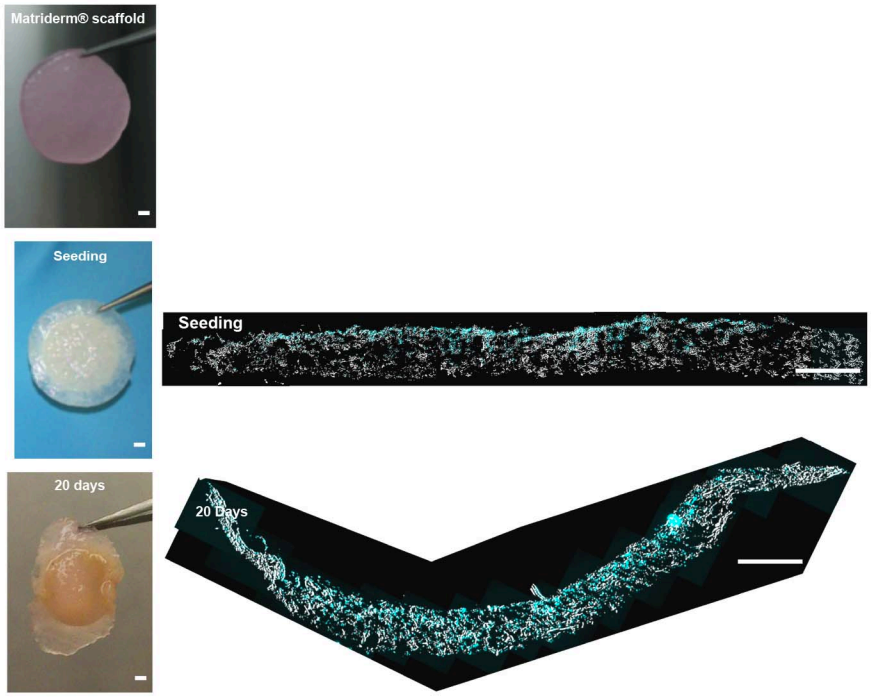

***Figure 4.37*: human iPSC-derived cell culture in perfusion bioreactor**
Left panels: hydrated Matriderm® scaffolds without cells, after seeding and after 20 days of culture into the perfusion bioreactor. Right panels: cross-sections of DAPI stained scaffolds seeded with co-culture 1:1 of KiPS 3F.7 T/Bra:GFP_Rex1:NEo^{r} #4 cells and Human Foreskin Fibroblasts at seeding time and after 20 days of culture. Scale bars 1mm.

In order to analyse cells morphology in 3D and to discriminate iPSC-derived cells from HFF, we performed immunofluorescence for the ubiquitous protein alpha-tubulin and for specific markers, respectively. Mesodermal cells were efficiently retained into Matriderm® scaffold, as shown by immunostaining for GFP (see **figure 4.38**). Nevertheless, in such 3D conditions mesodermal cells could not complete cardiac differentiation. 2D control shows that, if cultured in 2D, the cell line can differentiate to cardiac cells, as shown by expression of mesodermal and cardiac markers alpha sarcomeric actin (ASA) and cTNT.

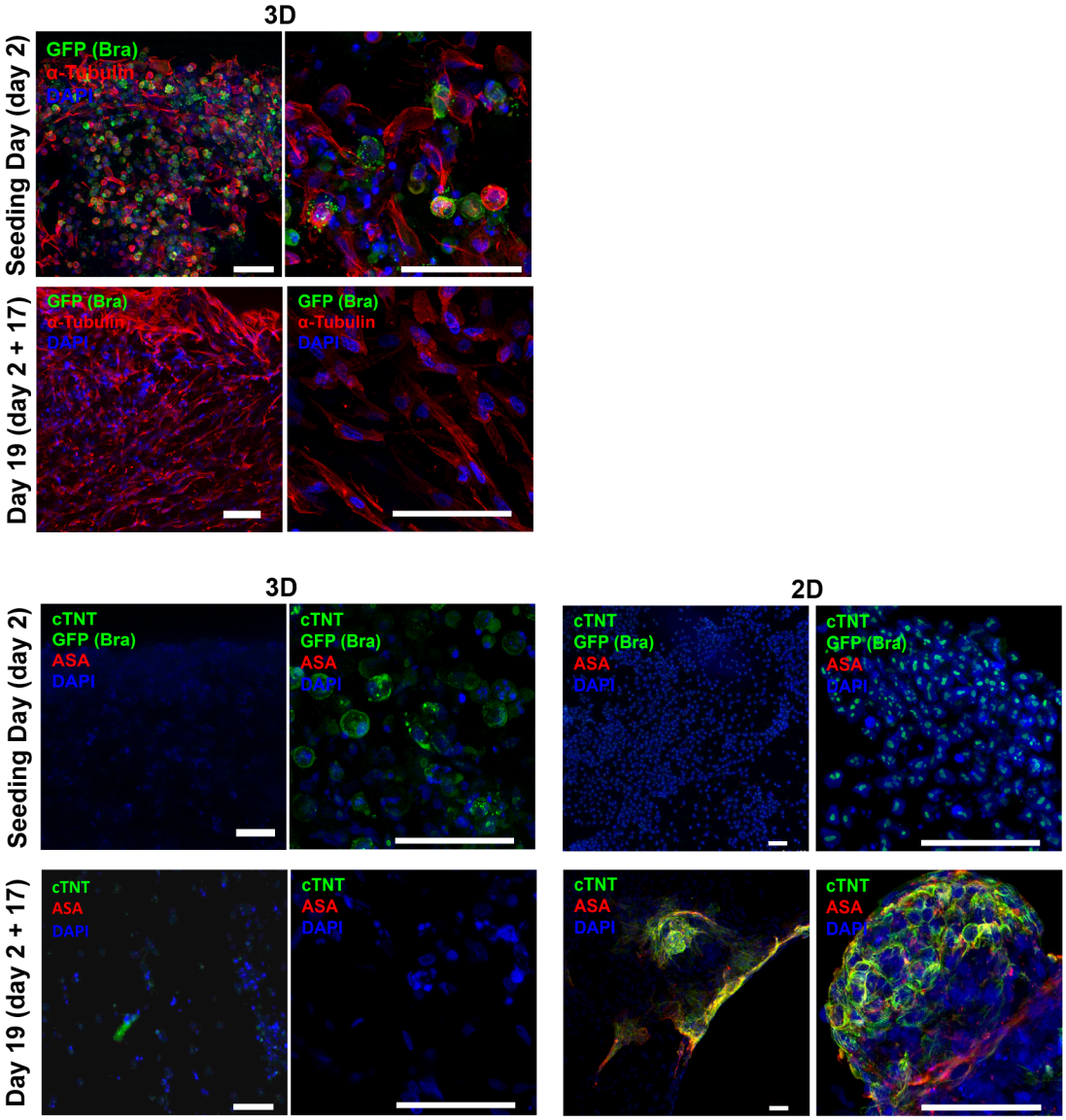

***Figure 4.38*: KiPS 3F.7 T/Bra:GFP_Rex1Neo^r cells differentiation into the bioreactor.**

3D culture of uncommitted mesoderm derived iPSC cells. Upper Left: immunostaining for GFP (reporter of T/Brachuyry: GFP(Bra)) and alpha tubulin of KiPS 3F.7_T/BRA:GFP_Rex1:Neo^r #4 iPSC cells co-cultured 1:1 with human foreskin fibroblasts. Cells at day 2 of differentiation with protocol 3, seeded into Matriderm Scaffold (Seeding Day (day2)) and cells differentiated to cardiac lineage for 19 days in total: seeded at day 2 of differentiation and cultivated into the bioreactor for 17 days (Day 19 (day 2+17)). Lower Left: immunostaining for alpha sarcomeric actin (ASA) and cardiac troponin T (cTNT) of KiPS 3F.7_T/BRA:GFP_Rex1:Neo^r #4 iPSC cells co-cultured 1:1 with human foreskin fibroblasts. Cells at day 2 of differentiation and seeded into Matriderm Scaffold (Seeding day (Day 2)) and cells differentiated to cardiac lineage for 19 days in total: seeded at day 2 of differentiation and cultivated into the bioreactor for 17 days (day 19 (day 2+17)). Lower Right: Differentiation control on normal 2D conditions at day 2 and at day 19. Scale bars: 75um.

Since, at least, we assessed that the cardiogenic potential of the cell line was solid, we decided to start co-culture of cells with human fibroblasts at day 15 of cardiac differentiation with Protocol 3. Also in this case seeding efficiency was between 80 and 98% for each condition. We analysed scaffolds at seeding time, to be sure that cardiac cells survived all the seeding procedure, and after 4 days. Results are shown in **figure 4.39**. Immunofluorescence for mesodermal and cardiac markers GATA4, alpha sarcomeric actin (ASA), and cTNT confirms cardiac differentiation of the cells in 2D conditions. In 3D, clusters of cardiac cells, expressing ASA are found right after seeding. After 4 days cardiac markers are still present.

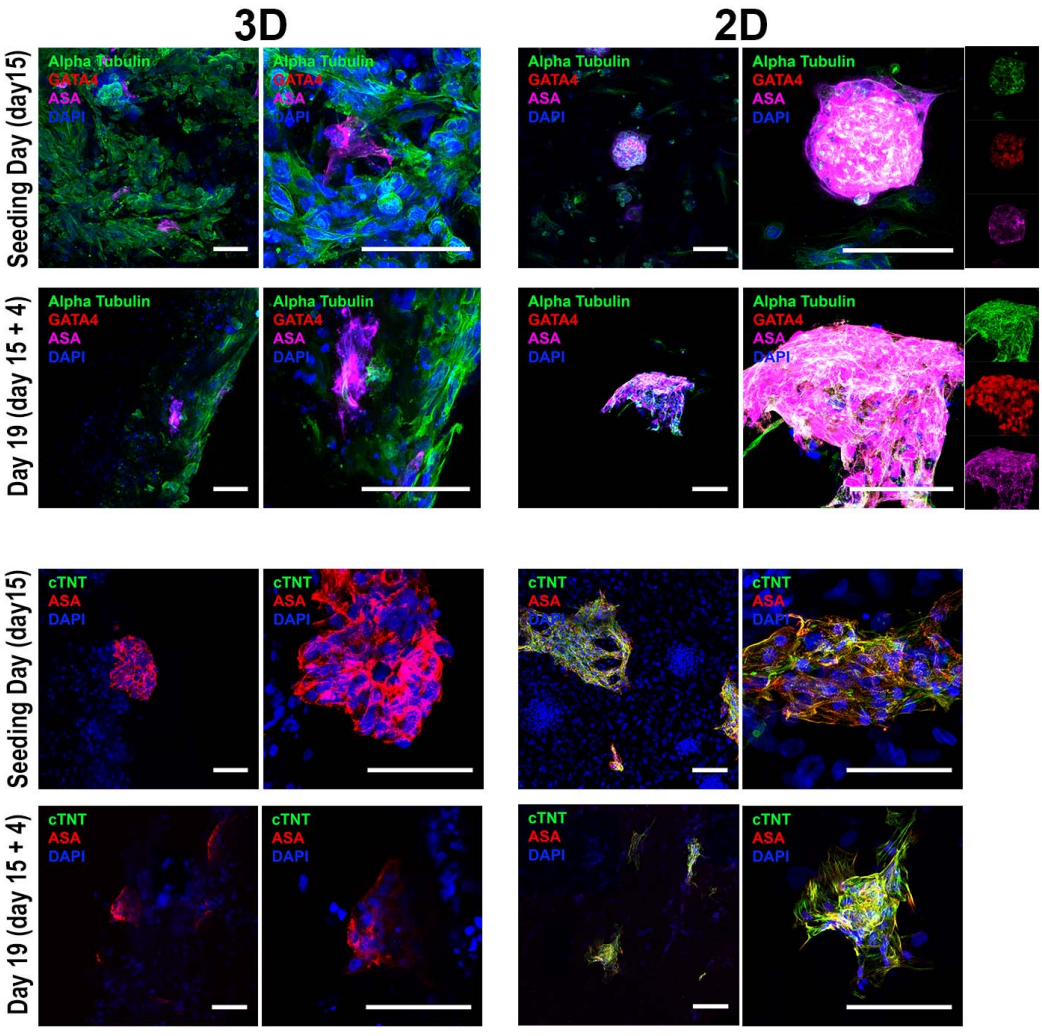

***Figure 4.39*: KiPS 3F.7 T/Bra:GFP_Rex1Neo^r derived cardiomyocytes culture into the bioreactor.**
Upper Left: immunostaining for alpha tubulin, GATA4 and alpha sarcomeric actin (ASA) of KiPS 3F.7_T/BRA:GFP_Rex1:Neo^r #4 iPSC cells co-cultured 1:1 with human foreskin fibroblasts. Cells at day 15 of differentiation with protocol 3, seeded into Matriderm Scaffold (Seeding Day (day15))and cells differentiated to cardiac lineage for 19 days in total: seeded at day 15 of differentiation and cultivated into the bioreactor for 4 days (Day 19 (day 15+4)). Lower Left: immunostaining for cardiac troponin T (cTNT) and alpha sarcomeric actin (ASA) of KiPS 3F.7_T/BRA:GFP_Rex1:Neo^r #4 iPSC cells co-cultured 1:1 with human foreskin fibroblasts. Cells at day 15 of differentiation and seeded into Matriderm Scaffold (Seeding day (Day 15)) and cells differentiated to cardiac lineage for 19 days in total: seeded on day 15 of differentiation and cultivated into the bioreactor for 4 days (day 19 (day 15+4)). Upper and Lower Right: Differentiation controls on normal 2D conditions at day 15 and of the co-culture at day 19. Scale bars: 75um.

4.3.7 Sorted cardiac GFP:MHC population

Our bioreactor device was developed within the aim of reproducing a more physiological environment that could favour maturation of iPSC derived CMs. In order to deal with this issue we tried to culture sorted GFP positive differentiated cardiomyocytes, where the GFP reports for MHC positive cells. We therefore submitted KiPS cells to differentiation for 24 days and co-culture iPSC derived sorted cardiomyocytes with human fibroblasts in a 1:1 proportion. As we can see from **figure 4.40**, overall cells well colonized the scaffolds (alpha tubulin staining is strongly present and diffused). Moreover staining of cardiac markers ASA and cTNI reveals that the cardiac population survives the 3D conditions for 24 hours.

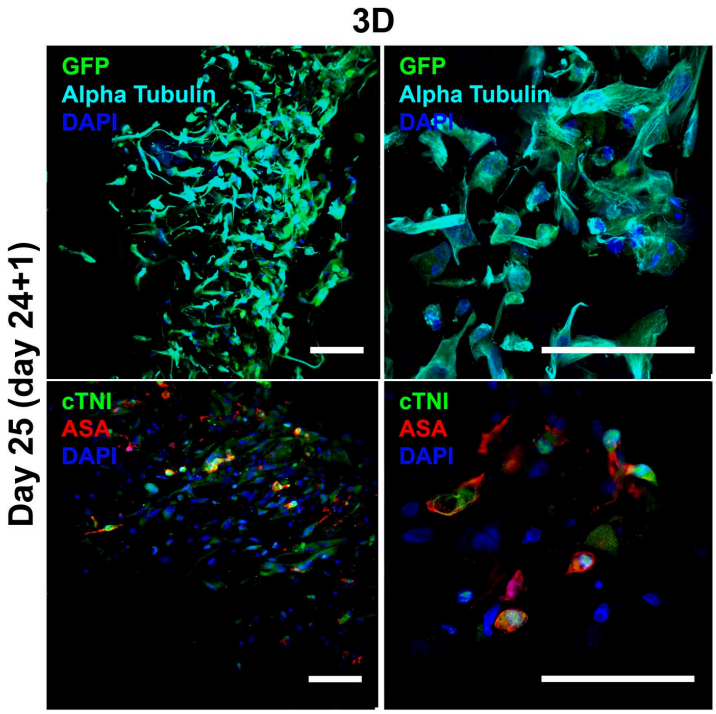

***Figure 4.40*: KiPS 3F.7 MHC:GFP_Rex1Neo^r derived cardiomyocytes culture into the bioreactor.**
Upper line: Immunostaining for GFP and alpha tubulin of KiPS 3F.7 MHC:GFP_Rex1:Neo^r #9 iPSC cells differentiated to cardiac lineage for 25 days in total: seeded at day 24 of differentiation and cultivated into the bioreactor for 1 day. Lower line: Immunostaining for alpha sarcomeric actin and cTNI of KiPS 3F.7 MHC:GFP_Rex1:Neo^r #4 iPSC cells differentiated to cardiac lineage for 25 days in total: seeded at day 24 of differentiation and cultivated into the bioreactor for 1 day. Scale bar: 75um

4.3.8 Human iPSC-derived CMs culture in 3D

To confirm that iPSC-derived cardiomyocytes could be cultured in 3D, we analysed the evolution the cell culture after 4 days. Beating structures from Kips 3F.7 MHC:GFP_Rex1:Neo^r at day 30 of differentiation were co-cultured with fibroblasts, seeded into the bioreactor and cultured for 1 and 4 days.

As shown in **figure 4.41**, iPSC derived CMs can colonize and be retained by the scaffold. Mesodermal and cardiac markers cTNI and Alpha Sarcomeric Actin (ASA) permit to identify the cardiogenic population among the fibroblasts marked with Alpha tubulin. We confirmed the result by analysing co-staining of cTNI with a second specific cardiac marker (alpha sarcomeric actinin - AAS). The same cell population, co-cultured in 2D reflects what occurs in 3D. Cell morphology in 3D

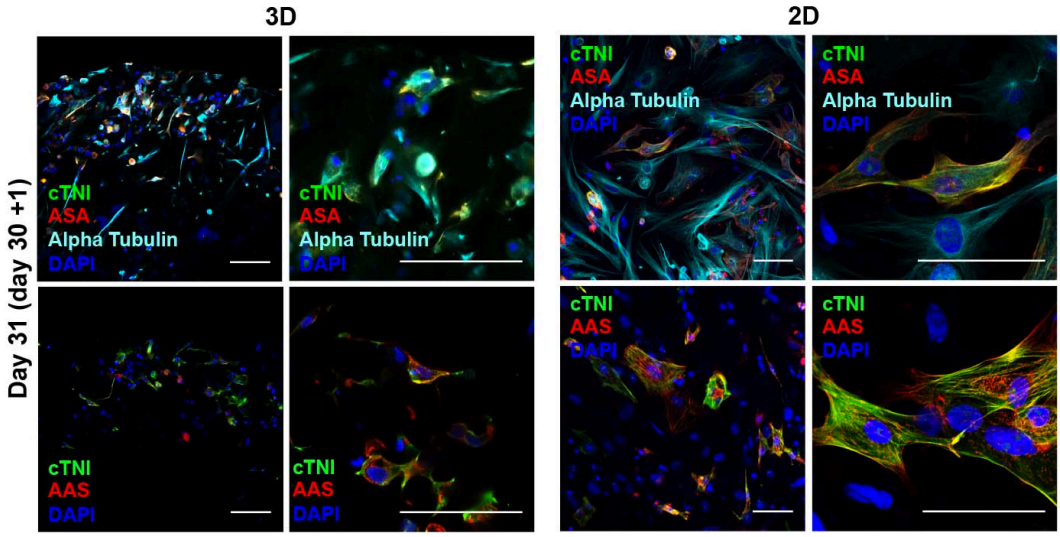

***Figure 4.41*: KiPS 3F.7 MHC:GFP_Rex1Neo^r derived cardiomyocytes culture into the bioreactor for 1 day and conventional 2D culture control.**
Immunostaining for cardiac troponin I (cTNI), Alpha sarcomeric Actin (ASA), alpha tubulin and cTNI and alpha sarcomeric actinin (AAS) of KiPS 3F.7 MHC:GFP_Rex1:Neo^r #9 iPSC cells differentiated to cardiac lineage for 30 days and cultivated into the bioreactor for 1 day (Day 31 (Day 30+1)). Left panels: cells that are cultured in 3D into our bioreactor device. Right panels: analysis of the same cells in a conventional 2D culture. Scale bars: 75um

Figure 4.42 shows the same analysis after 4 days of culture.

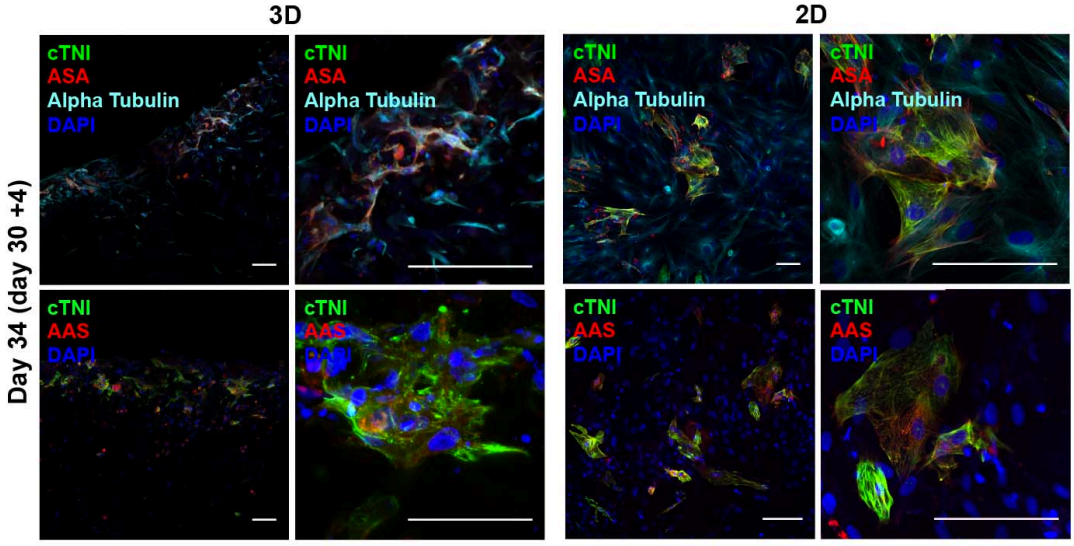

***Figure 4.42*: KiPS 3F.7 MHC:GFP_Rex1Neo^r derived cardiomyocytes culture into the bioreactor for 4 days and conventional 2D culture control.**
Immunostaining for cardiac troponin I (cTNI), Alpha sarcomeric Actin (ASA), alpha tubulin and cTNI and alpha sarcomeric actinin (AAS) of KiPS 3F.7 MHC:GFP_Rex1:Neo^r iPSC cells differentiated to cardiac lineage for 30 days and cultivated into the bioreactor for 4 more days (Day 34(day 30+4). Left panels: cells that are cultured in 3D into our bioreactor device. Right panels: analysis of the same cells in a conventional 2D culture Scale bar: 75um

After 4 days, human iPSC- derived CMs, not only are retained into the scaffold, but organize themselves forming clusters of aggregated cells. In 2D such clusters show beating capacity. We didn't observe such phenotype in the bioreactor, but this trial represents a first approach that demonstrates that cardiac cell population derived from iPSC can be cultured into a 3D device. We believe that by further optimization of cell culture conditions, this tool would be a valid study platform in the context of cardiac tissue engineering.

5-DISCUSSION

The aim of this thesis was to create an "*in vitro*" tissue engineered cardiac patch that could be useful for advanced functional study and maturation of human iPSC derived cardiomyocytes, as well as to be used as platform for drug screening or study of cardiac disease. This is a multi tasking and multidisciplinary challenge; it implies knowledge and expertise in different delicate fields, like medicine, cell biology, biotechnologies, engineering and physics that have to be combined.

In the context of clinical and biological aspects, it is worth to mention that heart disease is, and is predicted to remain, the main leading cause of death globally (Mathers & Loncar, 2006). The fact that patients develop severe impairment of pump function indicates that the ability of human heart to regenerate itself following injury is inadequate, despite persistence of endogenous cardiomyogenesis into adulthood (Bergmann et al., 2009). Different cell sources have been considered for cardiac-field repair: cardiac stem cells, skeletal myoblasts, bone marrow derived cells and mononuclear cells, being tested in pre-clinical and clinical trials, without significant tissue regeneration (Malliaras & Marban, 2014) (Taghavi et al., 2015). Bone marrow is an example of source of adult stem cells, consisting of different cell types that potentially can migrate and transdifferentiate into cells of various phenotypes. But the extent to which these cells could differentiate into cardiac myocytes is unsure, and findings on animal studies have not been replicated consistently (Balsam et al., 2004). Bone marrow cells can be directly aspirated from bone marrow or can be obtained from the peripheral circulation, being relatively easily accessible. In the hearts of humans and other mammalian species, clusters of surviving resident cardiac stem cells or progenitor cells have been identified (Smith, Barile, Messina, & Marban, 2008b) (Smith, Barile, Messina, & Marban, 2008a) (Barile, Messina, Giacomello, & Marban, 2007): although they have a high proliferative potential, it is insufficient to compensate for extensive injury, like myocardial infarct. This have been studied with cardiospheres, which are spherical clusters of cells that can be obtained with a cardiac biopsy, that are plated and grown in culture to provide cardiosphere-derived cells together with other populations of resident cardiac progenitors (Smith et al., 2008b). A proof-of-concept study showed that cardiospheres could be isolated, cultured, and expanded to provide a potentially

useful source of autologous cardiac stem cells (Messina et al., 2004), but their benefit are inconsistent. The first cell type to be injected into ischemic myocardium was skeletal myoblasts (Menasche et al., 2003). It improved left ventricular function and volumes, probably through mechanical or scaffolding effect, but there was little evidence of transdifferentiation to cardiomyocytes (Menasche, 2008) and cells weren't able to electrically integrate, arising chances of arrhythmias (Menasche et al., 2008). The greatest potential for organ regeneration is a characteristic of embryonic stem cells, which are derived from the inner mass of a developing embryo during the blastocyst stage (Segers & Lee, 2008). Their transplant in animal models of experimental myocardial infarction and non-ischemic cardiomyopathy, caused a significant improvement in cardiac function and structure (Behfar & Terzic, 2007). But, for clinical translation, they have the disadvantage of the immunological mismatch due to their allogeneic origin (Saric, Frenzel, & Hescheler, 2008). Moreover, embryonic stem cells are obtained with methods that have raised social and ethical concerns, hampering the research both in the preclinical and clinical areas (Murry & Keller, 2008; Passier, van Laake, & Mummery, 2008). That's why iPSC represent a fundamental breakthrough, because they are cells with characteristics similar to embryonic stem cells, but they are generated from somatic tissue, like adult fibroblasts. iPSC are obtained through reprogramming using ectopic expression of genes related to pluripotency (Hochedlinger & Jaenisch, 2006) (Takahashi et al., 2007). They provide an alternative source, easily accessible from patients through a simple skin biopsy, from which it is possible to generate cell lines with cardiogenic potential without the use of embryos. In addition, this strategy can be used to develop patient-specific stem cells, which could be a unique resource in studying genetic mechanisms of disease development, drug mechanisms, and regenerative medicine.

iPSC can be obtained by overexpressing 4 or 3 pluripotent genes, called the "Yamanaka Factors": Klf4, Sox2, Oct3 and optionally the oncogenic cMyc. The iPSC cell line used in this study (KiPS 3F.7) is derived from keratinocytes, and obtained through retroviral transduction of the 3 reprogramming factors. Being cMyc a proto-oncogene it is more advisable not using it especially for clinically aimed purposes, in order to prevent teratoma formation. Clinical applications of iPSC are nowadays favoured thanks to more recent transgene-free and viral-free reprogramming technologies (Kim et al., 2009), that avoid to disrupt the genome or cause unpredictable results by preventing

integration into the host genome. In fact, genomic integration or continuous presence of exogenous reprogramming factors, aren't requirements for human somatic cells reprogramming (J. Yu et al., 2009).

KiPS 3F.7 cells come form the Centre of Regenerative Medicine of Barcelona and were fully characterized in order to guarantee full pluripotency. Pluripotent stem cells (ESC as well as iPSC) can be differentiated into functional cardiomyocytes, even though the differentiation potential of the cell lines differs from each other, or even between passages of the same line due to differences in endogenous levels of pluripotency regulators OCT4 and NANOG and signalling molecules (Kattman et al., 2011) (P. Yu, Pan, Yu, & Thomson, 2011) (Paige et al., 2010). Different protocols have been developed in order to reproduce embryonic development, recapitulating stage specific molecular signalling. In this study we tested various differentiation protocols. Apart from the three protocols reported, we tried differentiation protocols based on EBs obtained through forced aggregation by centrifugation (Bauwens et al., 2011) (Burridge et al., 2007). Even though the published protocols reported high cardiac differentiation rates, we could not adapt them to differentiate our cell lines. Whereas EBs formed by forced aggregation could undergo endodermal and ectodermal differentiation ((annex 1), (Sanchez-Danes et al., 2012)), our cell lines only can stand EBs cardiac differentiation by mechanical scraping of the colonies: this forced us to adapt the original protocol developed by G. Keller's laboratory (Yang et al., 2008) to a more tedious, but successful form (Cardiac differentiation via Activin A, BMP4 and DKK1 protocol). This confirms that it is fundamental to adapt each protocol to specific cell line and laboratory conditions. With cardiac differentiation protocols via Activin A, and via Activin A, BMP4 and DKK1, the differentiation rate we obtained was sufficient for preliminary studies. With both protocols we could differentiate cells with beating capacity and that expressed cardiac marker cTNT.

The first steps of both protocols happen in cell incubators with 5% of oxygen concentration. The oxygen level to which embryonic stem cells are exposed is an important environmental parameter to take into account. Under conditions that maintain undifferentiated phenotype, low oxygen reduces spontaneous differentiation of human ESCs, while reduces pluripotency gene expression in mouse ESCs, although reports are conflicting. Oxygen level in the gas phase is often different than that experienced by the

cells, with mechanisms that are unclear, which makes interpretation of the literature difficult. What is demonstrated is that differentiation under low oxygen condition increases generation of various cell types like cardiomyocytes, but also neurons, hematopoietic progenitors, endothelial cells, and chondrocytes (Millman, Tan, & Colton, 2009).

The first approach by which we analysed differentiation's progress is observing cell morphology. In the case of EBs' based differentiation protocols, EBs attach to the plate's surface and single cells protrude from the main structure to spread and colonize the surroundings. The final aspect is a "two and a half" dimension cell culture in which monolayers of cells are spread together with multilayered clusters. Following cytokines inducing signals, mesodermal structures appear and start beating when cardiomyocytes differentiate. In the case of monolayer based differentiation protocols, mesodermal structures form as an effect of cytokines induction, creating a "two and a half" dimension cell culture first, which then evolves to a beating layer. With Activin A, BMP4 and DKK1 protocol, this evolution pathway is faster in comparison with Activin A protocol, that's why, in order to compare the global efficiency of the protocol, we analysed cell cultures at earlier time points. In the GSK3 pathway inhibition protocol this process is accelerated with beating structures appearing earlier and covering at least the 50% of the entire area of the culture plate, indicating that differentiated cardiomyocytes initiate connections between them to spread cardiac contractions. In fact it had been shown that pre-treatment of hPSC with a GSK3 inhibitor greatly enhanced cardiac differentiation (Lian et al., 2012).

Cardiomyocytes obtained in our study, express sarcomeric proteins cardiac troponin T (cTNT), cardiac troponin I (cTNI), sarcomeric actin (ASA), sarcomeric actinin (AAS) and myosin heavy chain (MHC). These results indicate that differentiated cells share characteristics similar to those of functional cardiomyocytes. Cardiac population that originates is not homogeneous, since part of the cells expressed the markers in a not organized way, indicating a more immature phenotype. Electron microscopy analysis would help in studying A, I and Z-bands presence, in order to detail degrees of myofibrillar organization to name early or late stage cardiomyocytes (Kehat et al., 2001) (Snir et al., 2003).

To tissue engineering applications, one requisite is to reproduce a compact tissue, with a cell density similar to the native one. In case of the heart it is 10^8 cells for cm^3 (Guo et al., 2009), a challenging high amount. For this reason, to apply iPSC-derived cardiomyocytes to tissue engineering we found GSK inhibition pathway's protocol to be the more appropriate. Apart from being much more efficient (beating areas expressing cardiac markers are spread in the entire area of the well and not confined to beating clusters), it is faster, since beating areas differentiate in 8-10 days (Vs. 12-14 of Activin A, BMP4, DKK1 protocol and 20-25 of Activin A protocol) and considering the overall time and reagents consumption for preparing the cells to differentiation, it allow to gain one month for each cell differentiation.

During differentiation protocols, cell fate is committed by cytokines and it is progressively restricted stage by stage. Nevertheless, not all the cells respond to the stimuli in the same way, and the outcome is a heterogeneous population, in which some cells differentiate correctly, and some others undergo unwanted pathways. For this reason, we found ideal the use of reporter genes. There are a wide variety of different methods used to accomplish genetic editing. Each method presents advantages and disadvantages; therefore the method of choice for transgene delivery requires careful consideration. Within the frame of our study we tried different approaches (electroporation, DNA plasmid transfection, lentiviral transduction) in order to obtain transgenic lines for genes of different cardiac differentiation stages: Oct4 for pluripotency, T (Brachyury) for early mesoderm, NKX2.5 for cardiac progenitors and alpha-MHC for cardiomyocytes. Our first intention was to generate double transgenic lines, in order to monitor not only one cell population, but also cells differentiating at two different stages. Unfortunately we could not succeed in this goal, since iPSC are very delicate to be genetically edited. We decided, therefore, to focus on early mesoderm, progenitors and cardiomyocytes for separate, in order to obtain tools with which carry out our study in 3D. In particular we obtained the KiPS 3F.7 NKX2.5:GFP_Neo^r cell line, by DNA plasmid transfection and KiPS 3F.7 T/Bra:GFP_Rex1:Neo^r and KiPS 3F.7 MHC:GFP_Rex1:Neo^r by lentiviral transduction. After transfection of bulk cells, we selected for stable cell lines thanks to the presence in the vector of Neomycin resistance cassettes.

The homeobox gene NKX2.5 is the earliest known marker of cardiac lineage in vertebrate embryos. In mouse, NKX2.5 expression is first detected in mesodermal cells

specified to form the heart at embryonic day 7.5 and its expression is maintained throughout the developing and adult heart. Other tissues in which NKX2.5 is transiently expressed are the developing pharynx, thyroid and stomach (Lien et al., 1999). In cardiac differentiation protocols, NKX2.5 marks cardiac progenitors cells. T codes for Brachyury protein, that is an embryonic nuclear transcription factor that binds to a specific DNA element, the palindromic T-site. It binds through a region in its N-terminus, called the T-box, and effects transcription of genes required for mesoderm formation and differentiation (Edwards et al., 1996) (Herrmann, 1992). Alpha-myosin heavy chain is a structural sarcomeric protein expressed in adult tissue (Mahdavi, Chambers, & Nadal-Ginard, 1984), and together with beta-myosin heavy chain is a core structural component of the contractile skeleton in cardiomyocytes.

We obtained 6 clonal lines of KiPS NKX2.5:GFP:Neo^r, 24 of KiPS 3F.7 T/Bra:GFP_Rex1:Neo^r and KiPS 3F.7 MHC:GFP_Rex1:Neo^r, submitted 2 (for KiPS NKX2.5:GFP:Neo^r) or 6 (for KiPS 3F.7 T/Bra:GFP_Rex1:Neo^r and KiPS 3F.7 MHC:GFP_Rex1:Neo^r) of them to cardiac differentiation and selected the one that performed better by monitoring transgenes expression and beating areas. After some passages, KiPS NKX2.5:GFP:Neo^r stopped to perform properly, and GFP related fluorescence became detectable only by flow cytometry and not by fluorescence microscopy. We attributed this issue to the transfection method and we switched to the more reliable approach of lentiviral transduction for producing KiPS 3F.7 T/Bra:GFP_Rex1:Neo^r and KiPS 3F.7 MHC:GFP_Rex1:Neo^r cell lines.

Conventional differentiation protocols give rise to cardiomyocytes with more immature than adult phenotype (Rajala, Pekkanen-Mattila, & Aalto-Setala, 2011), but research and clinical applications require to achieve a more mature phenotype. It is thought that biomechanical and biophysical stimuli can affect proper maturation process (Bilodeau & Mantovani, 2006) (Massai et al., 2013), so we developed a tissue-engineered device that could support 3D culture of cardiomyocytes. Tissue engineering is a fast-evolving field of biomedical science and technology, with future promise to manufacture living tissues for replacement, repair, and regeneration of diseased organs. In this context, bioreactors provide a fluidic environment for cells, and guarantee their viability. Different types of bioreactors have been developed, that vary greatly in size, complexity, and functional capabilities. The device presented here offers room to cardiomyocytes to

be cultured in an environment similar to the native tissue, as the scaffold we used mimics cardiac extracellular matrix (cardiomyocytes function, morphology, and survival are also influenced by extracellular matrices (Bick, Snuggs, Poindexter, Buja, & Van Winkle, 1998)) and the porosity of the biomaterial, together with flow perfusion imitates vascular supply. Matriderm® pore size ranges between 3 and 35 um, optimal for homing human stem cells, which measure 14 um (Zwaka & Thomson, 2003) in diameter. In tissue engineering approaches it is also important to reproduce the role of non-myocyte cells in the heart: during early embryonic development, cardiomyocytes require direct cell-to-cell contact or paracrine signalling from non-cardiac endoderm cells to differentiate into working cells (Arai, Yamamoto, & Toyama, 1997) (Lough & Sugi, 2000). A similar observation was reported in cardiomyocytes induction from stem cells (Iijima et al., 2003) (Rudy-Reil & Lough, 2004). Other studies showed that non-cardiac cells, such as fibroblast and/or endothelial cells, are required for cardiomyocytes to maintain contractile function and cell survival (Armstrong, Lee, & Armstrong, 2000) (Eisenberg & Eisenberg, 2006) (Narmoneva, Vukmirovic, Davis, Kamm, & Lee, 2004). Therefore, cell-cell interactions, both homo-and hetero-typic, and proper cell-ECM contact under 3D environment are fundamental for assuring functional cardiomyocytes differentiation, maturation, and survival.

We demonstrated that rat neonatal cardiomyocytes could survive in our device, which reflects all the above-mentioned considerations. Experiments are in progress (by PhD student Maria Valls) in order to improve the system with electrodes, to add electrical stimuli that are a key factor for cardiac cells maturation. Testing differentiating iPSC in 3D, we confirmed the fundamental role of non-cardiomyocyte cells, as in preliminary experiments performed without fibroblast or non-cardiogenic cells, iPSC derived cardiac cells couldn't colonize the scaffold.

Even though our results indicate that committed early mesoderm cells or cardiac progenitors can not complete cardiac differentiation in our bioreactor, we managed to retain into the scaffold iPSC-derived cardiomyocytes, indicating that only more advanced differentiated cells can be cultured under these conditions. Probably, in order to culture more immature cell types or stem cells, cytokines and nutrients doses should be re-adjusted, taking into account that their consumption rate could be influenced by perfusion. Also, flow rate of 0,1 ml/min, which is optimal for culturing neonatal rat cardiomyocytes and cardiomyocytes derived from iPSC, could rather cause shear stress to uncommitted mesoderm or cardiac progenitor cells. In our experiments, we also

found how sudden continuous perfusion hampers cell adhesion to the scaffold right after cell seeding, affecting cells capacity to establish cell adhesion to scaffold surface.

Our final results show that cardiomyocytes derived from iPSC can be retained into the scaffold and cultured for four days. We believe that refining cardiac cell population with MHC:GFP transgenic cell line will permit to increase the number of cardiac cells retained into the scaffold, providing a tool with a dual purpose. Firstly, it could be used as model systems to investigate *in vitro* the effects of drugs and other stimuli on cardiac cell culture and cardiac tissue formation and maturation, and secondly, once optimal culture conditions have been identified, bioreactors could be used as production systems for *in vitro* engineered functional cardiac tissues with clinical aim. The use of iPSC would allow studying patient specific cardiomyopathies. The clinical motivation of this work comes from the potential significance of combining these two complementary aspects of cardiac tissue engineering: in the near future, to develop innovative technological and biological tools to be used as model systems could strongly support the investigation of the still unknown mechanisms of cardiac tissue development, and in the late future, such approach could represent an effective therapeutic strategy to the reestablishment of the structure and function of injured cardiac tissues in the clinical practice, potentially contributing to the improvement of quality of life.

Taken together, the results of the experiments described here implement our knowledge on the generation of *in vitro* tissue engineered cardiac patches. Such 3D culture systems could be very useful to promote the functional maturation of human iPSC-derived cardiomyocytes, and could allow investigating the pathogenic mechanisms that underlie cardiac diseases and screen for new drugs using patient-specific cells.

6-CONCLUSIONS

The main aim of this work was to create an "*in vitro"* tissue engineered cardiac patch that would promote the maturation of human iPSC derived cardiomyocytes and be useful for future advanced functional studies. Based on the results of the experiments performed, the following conclusions can be drawn:

1) We have successfully differentiated cardiomyocytes from human iPSC using three different stage-specific differentiation protocols, the protocol relying on GSK3 pathway inhibition being the most efficient in our hands.

2) We have successfully generated stable transgenic human iPSC lines reporter for cardiac-specific markers. These transgenic iPSC lines can be efficiently differentiated to cardiomyocytes and represent valid tools to monitor and/or select homogeneous populations of cells at different stages of cardiac differentiation.

3) We have developed a 3D culture system based on the continuous perfusion of a porous scaffold that supports the maintenance of neonatal rat cardiomyocytes or human iPSC-derived cells for at least 3 weeks.

4) The environment of perfusion bioreactor developed in our studies is not supportive for the cardiac differentiation of human mesoderm progenitors (T/Brachyury-positive cells) or early cardiac precursors (NKX2.5-positive cells) differentiated from iPSC.

5) The environment of perfusion bioreactor developed in our studies supports the maintenance of human cardiomyocytes differentiated from iPSC for at least 4 days, thus providing the basis for improving cardiomyocyte maturation and opening the way to future studies on functional human cardiac cells.

7-ANNEXES

I was involved in the publication of the work here attached, entitled "Disease-specific phenotypes in dopamine neurons from human iPS-based models of genetic and sporadic Parkinson's disease" (Sanchez-Danes et al., 2012).

In this context I participated to the experiments culturing iPSC and preparing Embryoid Bodies for dopaminergic neurons dfferentiation.

EMBO Molecular Medicine
Research Article
iPS cell-based model of Parkinson's disease

Disease-specific phenotypes in dopamine neurons from human iPS-based models of genetic and sporadic Parkinson's disease

Adriana Sánchez-Danés[1], Yvonne Richaud-Patin[2,3†], Iria Carballo-Carbajal[4,5†], Senda Jiménez-Delgado[2,3], Carles Caig[5,6], Sergio Mora[2,3], Claudia Di Guglielmo[2,3,7], Mario Ezquerra[5,6], Bindiben Patel[8], Albert Giralt[5,9,10,11], Josep M. Canals[5,9,10,11], Maurizio Memo[7], Jordi Alberch[5,9,10,11], José López-Barneo[5,12], Miquel Vila[4,5,13], Ana Maria Cuervo[8], Eduard Tolosa[5,6,10,11], Antonella Consiglio[1,7], Angel Raya[2,3,13]***

Keywords: autophagy; disease modeling; LRRK2 mutation; neurodegeneration; pluripotent stem cells

DOI 10.1002/emmm.201200215

Received July 15, 2011
Revised January 04, 2012
Accepted January 10, 2012

Induced pluripotent stem cells (iPSC) offer an unprecedented opportunity to model human disease in relevant cell types, but it is unclear whether they could successfully model age-related diseases such as Parkinson's disease (PD). Here, we generated iPSC lines from seven patients with idiopathic PD (ID-PD), four patients with familial PD associated to the *G2019S* mutation in the *Leucine-Rich Repeat Kinase 2* (*LRRK2*) gene (LRRK2-PD) and four age- and sex-matched healthy individuals (Ctrl). Over long-time culture, dopaminergic neurons (DAn) differentiated from either ID-PD- or LRRK2-PD-iPSC showed morphological alterations, including reduced numbers of neurites and neurite arborization, as well as accumulation of autophagic vacuoles, which were not evident in DAn differentiated from Ctrl-iPSC. Further induction of autophagy and/or inhibition of lysosomal proteolysis greatly exacerbated the DAn morphological alterations, indicating autophagic compromise in DAn from ID-PD- and LRRK2-PD-iPSC, which we demonstrate occurs at the level of autophagosome clearance. Our study provides an iPSC-based *in vitro* model that captures the patients' genetic complexity and allows investigation of the pathogenesis of both sporadic and familial PD cases in a disease-relevant cell type.

(1) Institute for Biomedicine (IBUB), University of Barcelona, Barcelona, Spain
(2) Control of Stem Cell Potency Group, Institute for Bioengineering of Catalonia (IBEC), Barcelona, Spain
(3) Center for Networked Biomedical Research on Bioengineering, Biomaterials and Nanomedicine (CIBER-BBN), Spain
(4) Neurodegenerative Diseases Research Group, Vall d'Hebron Research Institute, Barcelona, Spain
(5) Center for Networked Biomedical Research on Neurodegenerative Diseases (CIBERNED), Madrid, Spain
(6) Movement Disorders Unit, Department of Neurology, Hospital Clinic of Barcelona, Barcelona, Spain
(7) Department of Biomedical Science and Biotechnology, University of Brescia, Brescia, Italy
(8) Department of Developmental and Molecular Biology and Institute for Aging Studies, Albert Einstein College of Medicine, Bronx, NY, USA
(9) Faculty of Medicine, Department of Cell Biology, Immunology and Neuroscience, Universitat de Barcelona, Barcelona, Spain
(10) Institut d'Investigacions Biomèdiques August Pi i Sunyer (IDIBAPS), Universitat de Barcelona, Barcelona, Spain
(11) Cell Therapy Program, Faculty of Medicine, Universitat de Barcelona, Barcelona, Spain
(12) Instituto de Biomedicina de Sevilla, Hospital Universitario Virgen del Rocio/CSIC/Universidad de Sevilla, Sevilla, Spain
(13) Institució Catalana de Recerca i Estudis Avançats (ICREA), Barcelona, Spain
***Corresponding author:** Tel: +34 93 403 9842; Fax: +34 93 403 4570; E-mail: aconsiglio@pcb.ub.es
****Corresponding author:** Tel: +34 93 402 0537; Fax: +34 93 402 0183; E-mail: araya@ibecbarcelona.eu

†These authors contributed equally to this work.

INTRODUCTION

Parkinson's disease (PD) is a common and devastating neurodegenerative disorder characterized by motor clinical manifestations, although non-motor features are also important in later stages of the disease (Lees et al, 2009; Obeso et al, 2010; Schapira & Tolosa, 2010). Movement alterations in PD stem from the selective loss of dopaminergic neurons (DAn) from the pars compacta of the substantia nigra, a specific subtype of neurons patterned as ventral midbrain DAn (vmDAn). Neuronal loss is typically progressive and accompanied by α-synuclein (SNCA)-containing intraneuronal inclusions known as Lewy bodies and Lewy neurites. While the majority of PD cases are sporadic, likely resulting from complex interactions among gene susceptibility and environmental factors, around 10% of patients present monogenic forms of the disease (Lesage & Brice, 2009). Pathogenic mutations in the *Leucine-Rich Repeat Kinase 2* (*LRRK2*) and *SNCA* genes have been identified and associated to PD, while mutations in four genes (*Parkin*, *DJ-1*, *PINK1* and *ATP13A2*) cause early onset parkinsonism (Lees et al, 2009). In particular, *LRRK2* mutations cause an autosomal dominant, late-onset familial PD, whose clinical and pathological features are indistinguishable from those of the common, sporadic form of PD (Paisan-Ruiz et al, 2004; Zimprich et al, 2004). While over 50 variants have been identified throughout the different *LRRK2* domains in PD patients, the mutation *G2019S* has been regarded as the most common cause of dominant familial PD and accounts for up to 2% of sporadic PD cases (Cookson, 2010).

The pathogenic mechanisms that lead to neurodegeneration in PD are not well understood, since current experimental PD models do not recapitulate key neuropathological features of the disease (Dawson et al, 2010). In particular, the special susceptibility of DAn to neurodegeneration and the progressive nature of this process in PD, together with the presence of Lewy bodies, have proven especially difficult to model in animal models of PD. The advent of induced pluripotent stem cell (iPSC) technology (Takahashi & Yamanaka, 2006) has made it possible to reprogram human somatic cells to pluripotency (Park et al, 2008b; Takahashi et al, 2007; Yu et al, 2007), thus enabling the generation of disease-specific iPSC (Lee & Studer, 2010). In this way, disease-relevant cell types have been generated from iPSC representing a variety of early onset diseases, and shown to display specific features of the disease *in vitro* (Carvajal-Vergara et al, 2010; Ebert et al, 2009; Ku et al, 2010; Lee et al, 2009; Marchetto et al, 2010; Moretti et al, 2010; Rashid et al, 2010; Raya et al, 2009; Zhang et al, 2011). Disease-specific iPSC have also been generated from sporadic cases of PD, but DAn differentiated from these cells did not show any conspicuous phenotype (Soldner et al, 2009), prompting uncertainty as to whether iPSC technology might be useful to model diseases of non-monogenic, complex etiology and/or late onset. Here, we generated iPSC lines from both idiopathic PD (ID-PD) and familial PD associated to the *G2019S* mutation in the *LRRK2* gene (the most frequent cause of familial PD, Cookson, 2010), as well as from age- and sex-matched healthy individuals. We show that, over long-time culture, DAn differentiated from PD-iPSC display specific PD pathology related phenotypes and, thus, provide proof-of-concept for iPSC-based cellular models that capture PD patients' genetic complexity and allow investigation of the PD pathogenesis in disease-relevant cell types.

RESULTS

Generation of PD-specific iPS cell lines

We recruited a total of 15 individuals into this study: 7 patients diagnosed with ID-PD, with no family history of disease and no known PD-related mutations; 4 unrelated patients diagnosed with familial PD carrying the *G2019S* mutation in the *LRRK2* gene (LRRK2-PD); and 4 healthy individuals with no history of neurological disease (Ctrl). Individuals in each group were also selected so that no significant bias in gender or age occurred (Table 1). Primary cultures of epidermal keratinocytes and dermal fibroblasts were established from all individuals and were used for reprogramming at passages 2–4. We used retroviral delivery of OCT4, KLF4 and SOX2 to generate 2–6 independent iPSC lines per individual, totalling 50 iPSC lines. Of those, 2 lines per patient were thoroughly characterized and shown to be fully reprogrammed to pluripotency, as judged by colony morphology and growth dynamics, sustained long-term passaging (>20 passages), karyotype stability, alkaline phosphatase (AP) staining, expression of pluripotency associated transcription factors (OCT4, SOX2, NANOG, CRIPTO and REX1) and surface markers (SSEA3, SSEA4, TRA1-60 and TRA1-81), silencing of retroviral transgenes, demethylation of *OCT4* and *NANOG* promoters, *in vitro* pluripotent differentiation ability and generation of teratomas comprising derivatives of the three main embryo germ layers (Table 1 and Fig 1A–N).

The efficiency of iPSC generation varied among different individuals, but did not depend on the presence or type of disease, nor on the age of donors. Whereas, most of the iPSC lines analyzed met our criteria for *bona fide* pluripotent stem cells, those that failed to silence the reprogramming transgenes, did not differentiate appropriately *in vitro*, or presented karyotype alterations were identified and excluded from further studies (Table 1). Overall, iPSC generated from PD patients or from healthy individuals were indistinguishable in all tests performed, with the exception that LRRK2-PD iPSC lines carried the $LRRK2^{G2019S}$ mutation (Fig 1O).

Generation of PD-specific vmDA neurons

For the directed differentiation of iPSC towards vmDA neurons (the cell type most affected in PD), we used a 30-day protocol recently implemented in our laboratory that relies on lentiviral-mediated forced expression of the ventral midbrain determinant LMX1A, together with DA neuron patterning factors (Sanchez-Danes et al, 2012). All iPSC lines tested generated DAn using this differentiation protocol, as judged by co-staining with the neuron-specific class III-β-tubulin (TUJ1) and tyrosine hydroxylase (TH; Fig 2A–C). Moreover, DAn differentiated in this way were mature and mostly of the A9 subtype, as revealed by expression of dopamine transporter (DAT), G protein-activated

Table 1. Summary of iPSC lines generated

	Patient			Disease					iPSC						
	Code	Sex	Age[a]	Age onset	Family history	Mutation	Initial symptoms[b]	LDopa response	# of Lines	Clones selected	Karyotype	Transgene silencing[c]	Pluripotency markers[c]	*In vitro* differentiation[c]	Teratoma assay[c]
CONTROL	SP09	M	66						4	SP09.2	46,XY	Passed	Passed	Passed	N/P
										SP09.4	46,XY	Passed	Passed	Passed	Passed
	SP11	F	48						3	SP11.1	46,XX	Passed	Passed	Passed	Passed
										SP11.4	46,XX	Passed	Passed	Passed	N/P
	SP15	F	47						4	SP15.2	46,XX	Passed	Passed	Passed	Passed
										SP15.3	46,XX	Passed	Passed	Passed	N/P
										SP15.4	47,XX+20	Passed	Passed	N/P	N/P
	SP17	M	52						3	SP17.1	47,XY+20	Passed	Passed	Passed	N/P
										SP17.2	46,XY	Passed	Passed	Passed	Passed
										SP17.3	46,XY	Passed	Passed	Failed	N/P
ID-PD	SP01	F	63	58	No	No	T and B	N/A	4	SP01.1	46,XX	Passed	Passed	Passed	Passed
										SP01.4	46,XX	Passed	Passed	Passed	N/P
	SP02	M	55	48	No	No	T	N/A	2	SP02.1	46,XY	Passed	Passed	Passed	Passed
										SP02.2	46,XY	Passed	Passed	Passed	N/P
	SP04	M	46	40	No	No	B	Good	2	SP04.1	46,XY	Passed	Passed	Passed	N/P
										SP04.2	46,XY	Passed	Passed	Passed	Passed
	SP08	F	66	60	No	No	T	Good	4	SP08.1	46,XX	Passed	Passed	Passed	Passed
										SP08.2	46,XX	Passed	Passed	Passed	N/P
										SP08.3	46,XX	Failed	N/P	N/P	N/P
	SP10	M	58	50	No	No	D	Good	2	SP10.1	46,XY	Passed	Passed	Passed	N/P
										SP10.2	46,XY	Passed	Passed	Passed	Passed
	SP14	M	55	51	No	No	B	Good	2	SP14.1	46,XY	Passed	Passed	Passed	Passed
										SP14.2	46,XY	Passed	Passed	Passed	N/P
	SP16	F	51	48	No	No	B	N/A	4	SP16.2	46,XX	Passed	Passed	Passed	Passed
										SP16.3	46,XX	Passed	Passed	Passed	N/P
LRRK2-PD	SP05	M	66	52	Yes	LRRK2	B	Good	2	SP05.1	46,XY	Passed	Passed	Passed	Passed
										SP05.2	46,XY	Passed	Passed	Passed	N/P
	SP06	M	44	33	Yes	LRRK2	T	Good	6	SP06.1	46,XY	Passed	Passed	N/P	N/P
										SP06.2	46,XY	Passed	Passed	Passed	Passed
	SP12	F	63	49	Yes	LRRK2	T	Good	4	SP12.3	46,XX	Passed	Passed	Passed	Passed
										SP12.4	46,XX	Passed	Passed	Passed	N/P
	SP13	F	68	57	Yes	LRRK2	T	Good	4	SP13.2	46,XX	Passed	Passed	Passed	N/P
										SP13.4	46,XX	Passed	Passed	Passed	Passed

N/A, information not available; N/P, test not performed.
[a]Age at biopsy.
[b]T, tremor; B, bradykinesia; D, foot dystonia.
[c]Tests performed as exemplified in Fig 1.

inward rectifier potassium channel 2 (GIRK2) and FOXA2, respectively (Fig S1 of Supporting information). We found a large variability in the numbers of DAn obtained from different iPSC lines, ranging from 9 to 29% of all differentiated cells, which did not depend on the presence or type of disease (Fig 2D), nor on the efficiency of lentiviral infection (Fig S2 of Supporting information), but rather appeared to depend on the specific iPSC clone used (Fig S3 of Supporting information), consistent with previous results on differentiation to other neuronal lineages (Hu et al, 2010). Thus, our results so far confirm previous data on the similar ability of control and ID-PD iPSC to give rise to DAn (Soldner et al, 2009, 2011) and extend these findings to iPSC derived from LRRK2-PD patients.

Spontaneous phenotypes of PD-specific vmDA neurons

Because SNCA is the main component of Lewy bodies, and immunolabelling with antibodies against SNCA has become the standard and most sensitive immunohistochemical method for the neuropathological diagnosis of PD (Lees et al, 2009), we first investigated whether SNCA could be detected in DAn differentiated from PD-specific iPSC. The majority of DAn differentiated from Ctrl-iPSC and ID-PD iPSC exhibited barely detectable levels of endogenous SNCA in their cytoplasm, while ~20% of DAn showed cytoplasmic staining (Fig 3A, B and D). However, most DAn derived from LRRK2-PD iPSC exhibited diffuse cytoplasmic accumulations of SNCA (Fig 3C and D), which did not form obvious aggregates or inclusions. This finding is consistent with results from animal studies that reported post-translational regulatory interactions of mutant LRRK2 and SNCA (reviewed in Cookson, 2010). In this line, the accumulation of SNCA in our model of LRRK2-PD iPSC-derived DAn did not appear to depend on transcriptional regulation of SNCA expression, which was upregulated during DAn differentiation to a similar extent compared with Ctrl-iPSC- and ID-PD iPSC-derived cells (Fig S4 of Supporting information), which also showed similar LRRK2 levels (Fig S5 of Supporting information).

Since neuronal degeneration in PD patients takes decades to occur, we next attempted to maintain iPSC-derived DAn over longer culture times. For this purpose, we co-cultured them over a monolayer of mouse post-natal cortical astrocytes (Johnson et al, 2007), which supported viable cultures of vmDA neurons

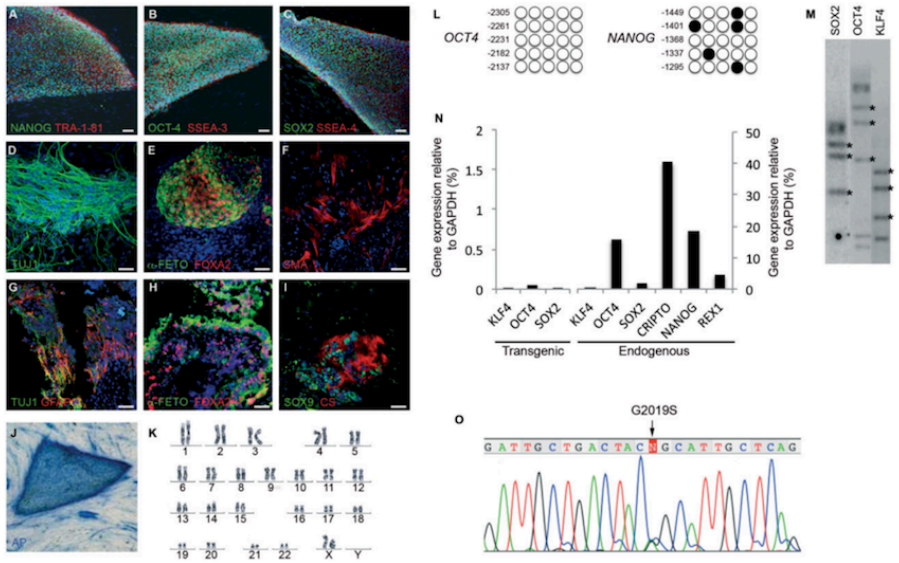

Figure 1. Generation and characterization of PD patient-specific iPSC lines.

A-C. Representative colonies of passage-20 LRRK2-PD-iPSC (cell line SP13.4) stained positive for the pluripotency-associated markers NANOG, OCT4 and SOX2 (green), TRA-1-81, SSEA3 and SSEA4 (red).

D-F. Immunofluorescence analyses of LRRK2-PD-iPSC (cell line SP13.4) differentiated *in vitro* show the potential to generate cell derivatives of all three primary germ cell layers including ectoderm (D, stained for TUJ1, green), endoderm (E, stained for α-fetoprotein, green, and FOXA2, red) and mesoderm (F, stained for smooth muscle actin, SMA, red).

G-I. Immunofluorescence analyses of sections from a teratoma induced by injecting LRRK2-PD-iPSC (cell line SP13.4), showing derivatives of the three main embryo germ layers: ectoderm (G, stained for TUJ1, green, and GFAP, red), endoderm (H, stained for α-fetoprotein, green, and FOXA2, red) and mesoderm (I, stained for SOX9, green, and chondroitin sulphate, CS, red). In (**A–I**) nuclei are counterstained with DAPI, shown in blue. Scale bars, 50 μm.

J. LRRK2-PD-iPSC (cell line SP13.4) stained for alkaline phosphatase (AP) activity.

K. Normal karyotype of LRRK2-PD-iPSC (cell line SP13.4) at passage 20.

L. Bisulphite genomic sequencing of the *OCT4* and *NANOG* promoters showing demethylation in LRRK2-PD-iPSC (cell line SP13.4).

M. Southern blot analysis of LRRK2-PD-iPSC (cell line SP13.4) showing genomic integrations (asterisk) of the indicated retroviruses.

N. RT-qPCR analyses of the expression levels of retroviral-derived reprogramming factors (transgenic) and endogenous expression levels (endogenous) of the indicated genes in LRRK2-PD-iPSC (cell line SP13.4).

O. Direct sequence of genomic DNA from LRRK2-PD-iPSC (cell line SP13.4) identifying the *LRRK2*^{G2019S} mutation.

for up to 75 days (latest time point analysed, see Fig S6 of Supporting information). Under these conditions, Ctrl-iPSC gave rise to DAn that were morphologically homogeneous and showed the expected features of mature DAn, including complex dendritic arborizations (Fig 4A and F). However, DAn differentiated from ID-PD or LRRK2-PD iPSC developed a range of altered morphologies over long-term culture that were not evident at shorter time points (Fig S7 of Supporting information). After detailed analysis, we categorized the morphologies of individual DAn in these cultures in three types: type 1 were neurons with mature morphology and long neurites with complex arborization, similar to those differentiated from Ctrl-iPSC; type 2 DAn showed fewer and simpler processes, reminiscent of immature neurons; and type 3 were DAn with clear signs of degeneration, including very short or absent neurites, vacuolated soma, fragmented nucleus and positive staining for cleaved caspase-3 (Fig 4A–D and Fig S7 of Supporting information). In aged (~75 days) cultures, most of DAn differentiated from ID-PD or LRRK2-PD iPSC were of altered type 2 or type 3 morphologies (Fig S7 of Supporting information), with a significant percentage of them undergoing apoptosis (Fig 4E).

To rule out any subjectivity that might have occurred in the adscription of different morphologies to iPSC-derived DAn, we also directly measured the number and length of neurites. For this, we used high-power confocal images of TH-stained single

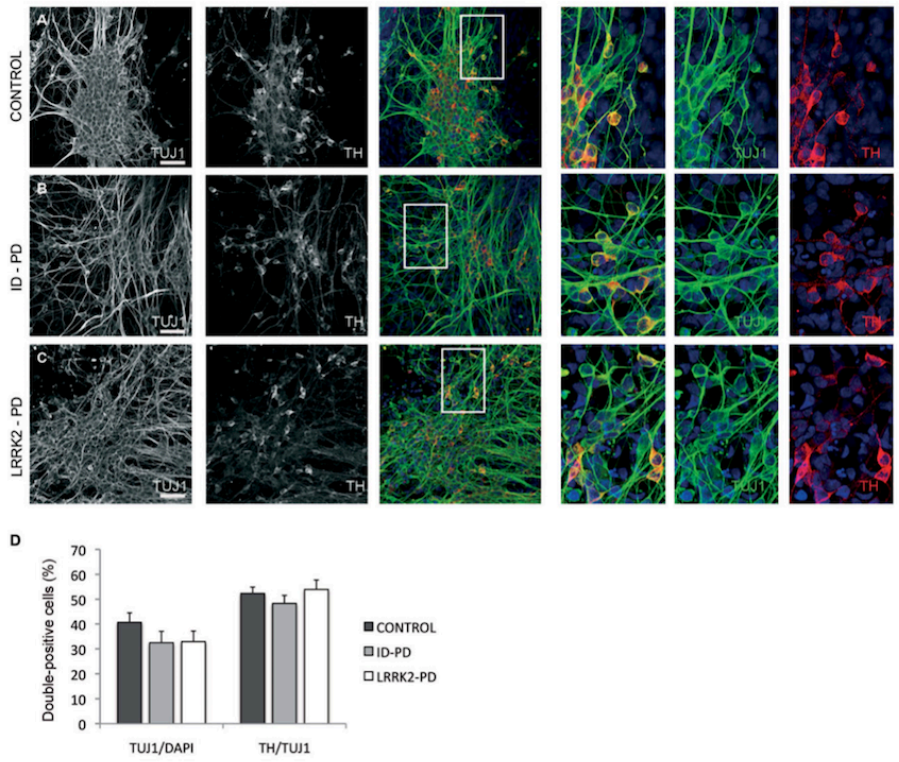

Figure 2. Differentiation of DA neurons from PD patient-specific iPSC. Ctrl-, ID-PD and LRRK2-PD iPSC were differentiated into DA neurons and analysed by immunofluorescence for expression of TUJ1 (green) and TH (red) at the end of the 30-day differentiation protocol.

A-C. All iPSC-derived neurons express TUJ1 and TH. Shown are representative images of differentiation experiments from Ctrl-iPSC (cell line SP11.1), ID-PD iPSC (cell line SP08.1) and LRRK2-PD iPSC (cell line SP06.2). Nuclei are counterstained with DAPI, shown in blue. Scale bars, 50 μm.

D. Quantitative analyses of cells stained positive for TUJ1 (left bars) or TUJ1 and TH (right bars). TUJ1-positive cells are represented as the percentage of total number of cells (stained with DAPI). Bars represent average with SEM as error bars. Data for CONTROL is the average of 4 iPSC lines, for ID-PD from 7 iPSC lines and LRRK2-PD from 4 iPSC. No significant differences were found in the ability of iPSC to generate neurons [$F(2,12) = 0.953$; $p = 0.413$] or DA neurons [$F(2,12) = 0.679$; $p = 0.526$] after 30 days of differentiation.

neurons, randomly chosen, differentiated from all the PD patient-specific and control iPSC lines and used software-assisted analysis (Fig 4F, see also Chu et al, 2009). These analyses confirmed that both the number and length of neurites of Ctrl-iPSC-derived DAn were significantly higher than those of DAn differentiated from ID-PD or LRRK2-PD iPSC (Fig 4G and H). The causative role of the genetic background of patient-specific cells was further investigated by ectopically expressing mutated $LRRK2^{G2019S}$ in DAn differentiated from Ctrl-iPSC. In these experiments, DAn differentiated for 65 days were co-transfected with plasmids encoding wild-type (WT) LRRK2 or $LRRK2^{G2019S}$ and GFP, and cells were analysed after 10 days. Even though the transfection efficiency (as evaluated by GFP/TH double positive cells) was low in all cases, we could readily detect DAn transfected with WT LRRK2, which were morphologically indistinguishable from untransfected DAn (Fig 4I–K and M). In contrast, few DAn transfected with mutant $LRRK2^{G2019S}$ were found after 10 days, suggesting that the expression of pathogenic LRRK2 is deleterious for these cells (Fig 4M). Indeed, surviving DAn expressing mutated $LRRK2^{G2019S}$ displayed evident morphological alterations, including fewer and shorter neurites compared to untransfected DAn or DAn expressing WT LRRK2 (Fig 4I–L and N). So far, our data show that, even though PD-specific iPSC differentiate

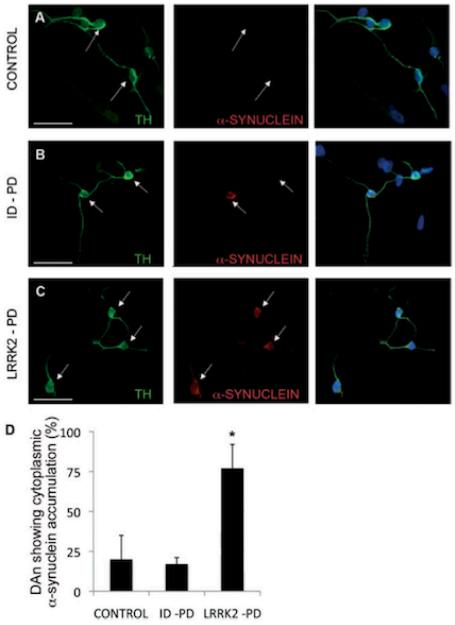

Figure 3. Abnormal SNCA accumulation in DA neurons from LRRK2-PD iPSC.

A-C. Immunofluorescence analyses of DA neurons after 30 days of differentiation from Crtl-iPSC (**A**), ID-PD iPSC (**B**) and LRRK2-PD iPSC (**C**), co-stained for TH (green) and SNCA (red). Arrows point to DA neurons, as identified by TH positive staining.

D. Quantitative analyses of DA neurons showing cytoplasmic accumulation of SNCA. Bars represent average with SEM as error bars. Data is the average of at least two-independent experiments using 3 Ctrl-iPSC lines, 4 ID-PD iPSC lines and 3 LRRK2-PD iPSC lines. The differences in the number of DA neurons showing accumulation of SNCA are statistically significant (asterisk) when comparing those derived from LRRK2-PD iPSC with either those from Ctrl-iPSC ($p = 0.019$) or from ID-PD iPSC ($p = 0.002$) [$F(2,16) = 6.888$; $p = 0.007$].

normally into vmDA neurons, they display evident signs of morphological alterations upon long-time culture.

Impaired autophagy of PD-specific vmDA neurons

We next investigated the bases for the altered morphology and shorter/fewer neurites of PD iPSC-derived DAn compared to those differentiated from Ctrl-iPSC. Given that autophagy has been shown to play key roles for maintaining neurite length (reviewed in Chu et al, 2009) and that several lines of evidence indicate that dysregulated autophagy may be a pathogenic mechanism in PD (Menzies et al, 2011), we first analysed the autophagosome content in iPSC-derived DAn. For this purpose, we used immunofluorescence labelling with antibodies to the light chain type 3 protein (LC3), a marker of autophagosomes (Kabeya et al, 2000). After 75 days of culture, DAn differentiated from Ctrl-iPSC showed a diffuse cytoplasmic LC3 staining with very few autophagosomes (LC3-positive puncta, Fig 5A). In contrast, a marked increase in LC3-positive puncta was evident in untreated DAn differentiated from ID-PD or LRRK2-PD iPSC (Fig 5B–E). The fact that autophagosomes were evident even in the absence of inhibitors of lysosomal proteolysis in these neurons suggests either massive upregulation of autophagosome formation, or a compromise in the clearance of autophagic compartments in these cells. To distinguish between these possibilities, we compared levels of p62 in the three groups of cells. A large fraction of p62 undergoes degradation through autophagy because it serves as a cargo-recognizing protein that it is sequestered in autophagosomes along the cytosolic cargo. Immunostaining for p62 revealed a marked increase in the levels of this protein in DAn differentiated from ID-PD or LRRK2-PD iPSC, where it showed a punctuate pattern reminiscent of the one observed for LC3 (Fig 5F–J).

To directly analyse autophagic clearance we compared the rates of degradation of LC3-II in the different cells by immunoblot (LC3-flux assay), even though we were aware that neural-specific changes could be underestimated in this type of analysis, as DAn represent only a fraction of the cells present in whole-culture lysates. Part of the LC3 located in the inner membrane of the autophagosome is degraded along with the cargo when these compartments fuse to lysosomes, consequently the increase in levels of LC3-II upon blockage of lysosomal proteolysis provides information on autophagic clearance. As expected, immunoblot for LC3 confirmed an increase in basal steady-state levels of LC3-II in the PD-derived cells (Fig 5K and L). Blockage of lysosomal degradation resulted in an increase in LC3-II levels in all cells but, despite some level of individual variability, the autophagic flux was significantly reduced in PD-derived cells (Fig 5K and M). To separately analyse autophagosome formation independently of clearance, we also compared changes in LC3-II at two different times after blockage of lysosomal degradation (under these conditions, any increase in LC3-II would directly result from autophagosome formation as degradation is no longer occurring). Although we found a consistent trend for increased autophagosome formation in DAn differentiated from ID-PD or LRRK2-PD, when compared to Crtl-iPSC (Fig 5K and N), this increase was not statistically significant and clearly less pronounced that the changes observed on clearance. Our findings thus support that the marked increase in the abundance of these compartments in PD-iPSC-derived neurons when compared with control was due, for the most part, to blockage on their clearance.

Ultrastructural analysis by electron microscopy confirmed marked differences in the autophagic system between DAn differentiated from Ctrl-iPSC and those of PD origin. As shown in Fig 6A–C, autophagic vacuoles were in general more abundant in the PD groups. In control cells, most of the autophagic profiles corresponded to autophagolysosomes (autophagic vacuoles already fused to lysosomal compartments; Fig 6A and D). In contrast, in the case of the ID-PD and LRRK2-PD, autophagosomes (prior to lysosomal fusion) were predominant (Fig 6B–D), supporting that the increase in LC3-positive structures is

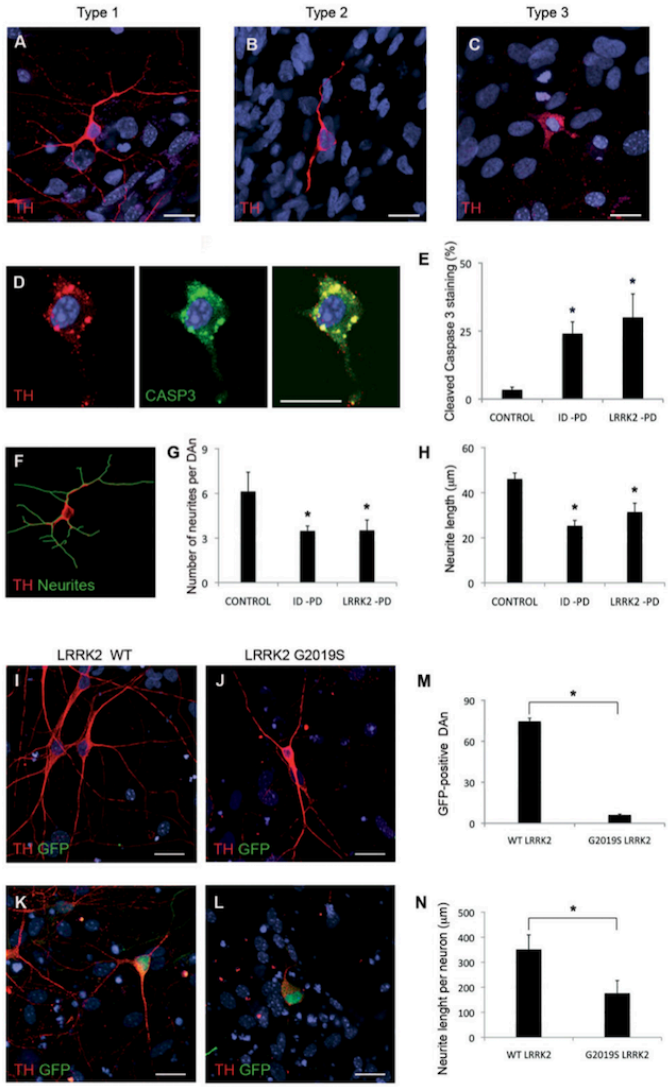
Type 1
Type 2
Type 3
A
B
C
TH
D
TH
CASP3
E
Cleaved Caspase 3 staining (%)
50
25
0
CONTROL
ID -PD
LRRK2 -PD
F
TH Neurites
G
Number of neurites per DAn
9
6
3
0
CONTROL
ID -PD
LRRK2 -PD
H
Neurite length (µm)
60
40
20
0
CONTROL
ID -PD
LRRK2 -PD
LRRK2 WT
LRRK2 G2019S
I
J
TH GFP
M
GFP-positive DAn
90
60
30
0
WT LRRK2
G2019S LRRK2
K
L
TH GFP
N
Neurite lenght per neuron (µm)
500
400
300
200
100
0
WT LRRK2
G2019S LRRK2

Figure 4.

likely due to problems in the maturation of autophagosomes. An increase in intracellular lipid droplets, previously shown to undergo degradation by macroautophagy (Singh et al, 2009), and the presence of dilated ER in the PD cells are also common features of cells with compromised autophagy (Fig 6B, C and E).

Lastly, defective autophagosome clearance was also confirmed analyzing the co-localization of autophagosome (LC3) and lysosomal (LAMP-1) markers in DAn differentiated from ID-PD, LRRK2-PD or Crtl-iPSC. The very low levels of LC3 puncta detected in basal conditions in the control cells (Fig S8 of Supporting information) precluded evaluating LC3/LAMP-1 co-localization in these cells. To be able to compare the autophagic flux among the three groups of cells, we reduced degradation of LC3 in lysosomes by treatment with leupeptin (which does not modify autophagosome/lysosome fusion). Under these conditions, we detected a significantly lower level of LC3/LAMP-1 co-localization in both ID-PD and LRRK2-PD iPSC-derived DAn, when compared to control cells (Fig 7A–D). These results confirm compromised maturation of autophagosomes into autophagolysosomes in these cells.

To evaluate whether morphological alterations and autophagy defects in DAn were mechanistically linked, we next reproduced in Ctrl-iPSC-derived DAn the blockage of autophagic clearance observed in ID-PD and LRRK2-PD iPSC, by inducing autophagosome formation through mTOR inhibition with rapamycin and, at the same time, blocking lysosomal degradation with leupeptin. This treatment resulted in ~20% of Ctrl-iPSC-derived DAn showing higher number of autophagosomes, which stained positive for LC3 as well as for LAMP-1 (Fig S9 of Supporting information). This combined treatment had an even more marked effect in DAn differentiated from ID-PD or LRRK2-PD iPSC. In either case, rapamycin/leupeptin treatment induced a significant shortening in the average total neurite length of DAn (Fig 7E). Importantly, the increased susceptibility of ID-PD and LRRK2-PD iPSC-derived DAn to rapamycin/leupeptin treatment appeared to be cell type-specific, since patients' fibroblasts showed an increase of LC3-positive puncta and changes in LC3 levels comparable to control cells upon this treatment (Fig S10 of Supporting information), further supporting that the compromise in autophagosome clearance may be specific for DAn. These results indicate that DAn differentiated from either ID-PD or LRRK2-PD iPSC have a deficient competence for autophagic clearance compared with Ctrl-iPSC-derived DAn, and suggest that the PD pathology related phenotypes revealed in our *in vitro* model are caused, at least in part, by an impairment in the autophagy pathway.

DISCUSSION

In this study, we describe the generation and characterization of a collection of iPSC lines representing age- and sex-matched patients of sporadic and LRRK2-associated PD, as well as control individuals. Consistent with previous studies describing the generation of patient-specific iPSC in the context of PD (Park et al, 2008a; Soldner et al, 2009, 2011) or other conditions (Dimos et al, 2008; Park et al, 2008a; Raya et al, 2010), the efficiency of iPSC generation varied among different individuals, but did not depend on the presence or type of disease, nor on the donor age. We chose retroviral delivery of reprogramming transgenes to secure the derivation of iPSC lines from valuable biopsy material, because of the higher efficiency of this system in our hands compared to that of lentivirus-based systems. A clear advantage of the latter is the possibility of using inducible excisable lentivirus (Soldner et al, 2009), so that iPSC are free of reprogramming transgenes. However, we reasoned that a careful analysis of the silencing of integrated transgenes in our iPSC lines, together with the generation of independent iPSC lines from several patients representing each condition, would rule out any confounding effects due to residual transgene

Figure 4. Morphological alterations of PD-iPSC-derived DA neurons after long-term culture.

A-C. Immunofluorescence analyses of Ctrl-iPSC (cell line SP11.1, **A**), ID-PD iPSC (cell line SP08.1, **B**) and LRRK2-PD iPSC (cell line SP06.2, **C**), differentiated towards DA neurons and cultured for 75 days on cortical astrocytes, stained for TH (red). Images are representative of the three morphologies of DA neurons found under these conditions.

D. Immunofluorescence analysis of DA neurons differentiated from LRRK2-PD iPSC (cell line SP06.2) for 75 days, co-stained for TH (red) and cleaved caspase-3 (green). In **A–D** nuclei are counterstained with DAPI, shown in blue. Scale bar, 12.5 μm.

E. Quantitative analyses of the percentage of DA neurons differentiated for 75 days showing cleaved caspase-3 staining. Data for CONTROL is the average of 4 iPSC lines, for ID-PD from 7 iPSC lines and LRRK2-PD from 4 iPSC. Asterisks denote statistically significant differences between CONTROL and ID-PD ($p = 0.004$) or LRRK2-PD ($p = 0.011$) [$F(2,12) = 5.668$; $p = 0.018$].

F. Image of the same DA neuron shown in (**A**), with neurites outlined by green traces as processed by NIH ImageJ software.

G. Quantitative analyses of the number of neurites in DAn differentiated for 75 days. Data for CONTROL is the average of 87 DAn from 4 iPSC lines, for ID-PD is from 119 DAn from 7 iPSC lines and for LRRK2-PD is from 91 DAn from 4 iPSC. Asterisks denote statistically significant differences between CONTROL and ID-PD ($p < 0.001$) or LRRK2-PD ($p < 0.001$) [$F(2,294) = 21.096$; $p < 0.001$].

H. Quantitative analyses of the neurite length in DA neurons differentiated for 75 days. Data for CONTROL is the average of 540 neurites from 4 iPSC lines, for ID-PD is from 409 neurites from 7 iPSC lines and for LRRK2-PD is from 303 neurites from 4 iPSC. Asterisks denote statistically significant differences between CONTROL and ID-PD ($p < 0.001$) or LRRK2-PD ($p < 0.001$) [$F(2,1249) = 42.161$; $p < 0.001$]. (**E**, **G** and **H**) bars represent average with SEM as error bars.

I-L. DAn (TH positive, red) and GFP (green) from Ctrl-iPSC (SP11.1) co-transfected with plasmids encoding WT LRRK2 (WT, **I** and **K**) or mutant LRRK2^{G2019S} (**J** and **L**) and GFP. (**I** and **J**) Images showing GFP negative DA neurons. (**K** and **L**) Co-transfected DA neurons being GFP positive. Nuclei are counterstained with DAPI, shown in blue. Scale bar, 12.5 μm.

M. Quantitative analysis of the number of GFP positive neurons present in co-transfected cells.

N. Quantitative analyses of the neurite length per neuron in co-transfected DAn. For (**M** and **N**) data are average of two-independent experiments using two different Ctrl-iPSC lines. Bars represent average with SEM as error bars. Statistically significant differences are indicated with asterisks ($p = 0.003$ in **M**; $p = 0.006$ in **N**).

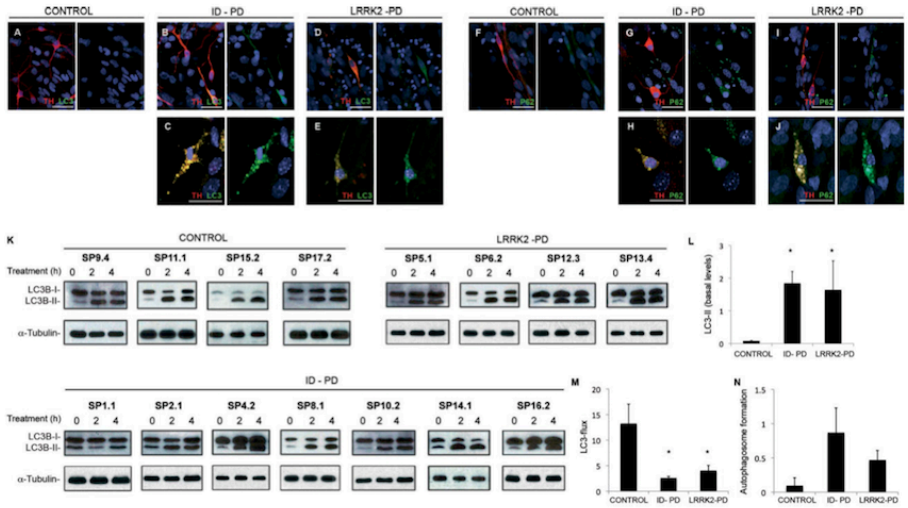

Figure 5. Alterations in autophagic clearance in DA neurons from PD patient-specific iPSC.

A-E. Immunofluorescence analyses of Ctrl-iPSC (cell line SP17.2, **A**), ID-PD iPSC (cell line SP16.2, **B** and **C**) and LRRK2-PD iPSC (cell line SP12.3, **D** and **E**), differentiated towards DA neurons and cultured for 75 days on cortical astrocytes, co-stained for LC3 (green) and TH (red). Images are representative of the most abundant morphologies of DA neurons found under these conditions.

F-J. Immunofluorescence analyses of Ctrl-iPSC (cell line SP17.2, **F**), ID-PD iPSC (cell line SP10.2, **G** and **H**) and LRRK2-PD iPSC (cell line SP06.2, **I** and **J**), differentiated towards DA neurons and cultured for 75 days on cortical astrocytes, co-stained for p62 (green) and TH (red). Images are representative of the morphologies of DA neurons found under these conditions. In **A–J**, nuclei are counterstained with DAPI, shown in blue. Scale bars, 35 μm.

K. Western blot analysis for LC3 in DA neuron cultures at 75 days of differentiation from the indicated iPSC lines, treated with leupeptin and NH_4Cl during the indicated period of time. α-tubulin is used as a loading control.

L. Quantification analyses of the basal levels (treatment time = 0) of LC3-II relative to α-tubulin. Asterisks denote statistically significant differences between CONTROL and ID-PD ($p = 0.003$) and between CONTROL and LRRK2-PD ($p = 0.046$) [$F(2,12) = 4.253$; $p = 0.046$].

M. Quantification of LC3 flux normalized to α-tubulin. Asterisks denote statistically significant differences between CONTROL and ID-PD ($p = 0.002$) and between CONTROL and LRRK2-PD ($p = 0.029$) [$F(2,12) = 9.614$; $p = 0.003$].

N. Quantification of the autophagosome formation normalized to α-tubulin. No significant differences were found among groups [$F(2,12) = 1.570$; $p = 0.248$]. (**L–N**) Data per each group is the average of the blots shown in **K**. Bars represent average with SEM as error bars.

expression in individual iPSC lines, while still allowing a high efficiency of iPSC generation. In any case, we omitted c-MYC from the reprogramming cocktail due to the possibility of its interaction with LRRK2 in the context of eukaryotic initiation factor 4E (eIF4E) function regulation (Imai et al, 2008; Ruggero et al, 2004).

All the iPSC lines tested in our study were competent to give rise to DAn, although the efficiency at which they did so varied among lines. Similar findings have been reported for iPSC in a variety of differentiation protocols, including neuronal lineages other than DAn (Hu et al, 2010), cardiomyocytes (Zhang et al, 2009) and haematopoietic cells (Woods et al, 2011). Importantly, the variability in differentiation efficiency of our iPSC lines was independent of the presence or type of disease, indicating inter-line variation, rather than a result of the disease. Moreover, DAn differentiated from Ctrl- or PD-iPSC appeared morphologically and phenotypically indistinguishable after 30 days in culture, in agreement with a previous report that analysed the DAn differentiation ability of IP-PD iPSC (Soldner et al, 2009), and extending these findings to iPSC derived from LRRK2-PD patients. Despite this similarity, we found anomalous accumulation of SNCA in DAn differentiated from LRRK2-PD iPSC, compared to those from Ctrl- or ID-PD iPSC. The identification of this PD-related phenotype in LRRK2 mutant DAn is consistent with the notion that LRRK2 and SNCA may participate in intersecting pathways (reviewed in Cookson, 2010), and with the fact that LRRK2 can accelerate mutant SNCA-induced neuropathology in mice in a dose-dependent manner (Lin et al, 2009). Moreover, these results demonstrate the ability of iPSC-based cellular systems to recapitulate PD-related pathology and to model a monogenic form of PD.

Probably the most significant finding of our work is the identification of spontaneous phenotypes in long-term cultures of DAn from both idiopathic and LRRK2-associated PD. To our

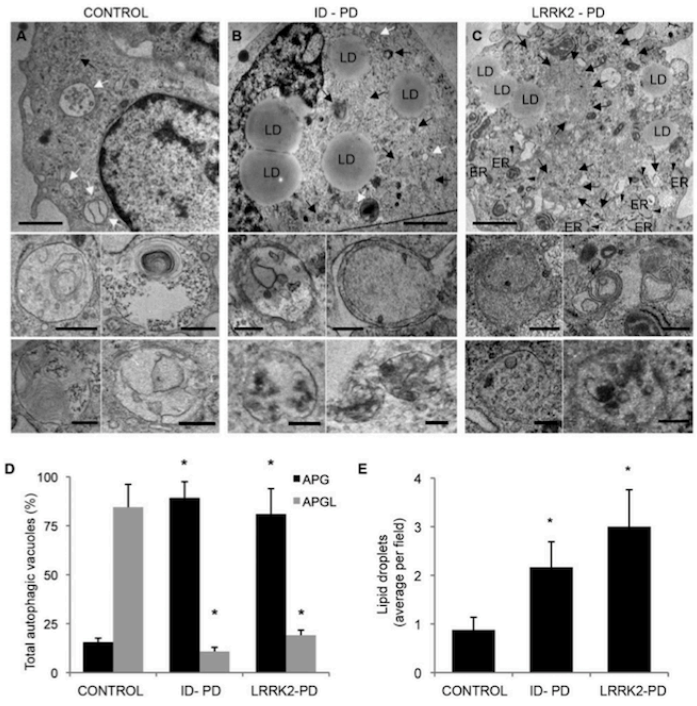

Figure 6. Autophagic system in iPSC-derived neurons.

A-C. Ultrastructure of DA neurons at 75 days of differentiation from Ctrl-iPSC (**A**), ID-PD iPSC (**B**) and LRRK2-PD (**C**) iPSC. Lower inserts show higher magnification images to illustrate individual examples of autophagic vacuoles. Black arrows: autophagosomes; white arrows: autophagolysosomes; arrowheads: dilated ER; LD: lipid droplets. Scale bars: 0.5 μm (top) and 0.2 μm (bottom).

D. Percentage of autophagosomes (APG) and autophagolysosomes (APGL) relative to the total amount of autophagic vacuoles per field. Asterisks denote statistically significant differences in the percentage of autophagosomes [$F(2,16) = 28.274$; $p < 0.001$] and of autophagolysosomes [$F(2,16) = 8.894$; $p = 0.003$] between CONTROL and ID-PD (autophagosomes, $p < 0.001$; autophagolysosomes, $p = 0.003$), and between CONTROL and LRRK2-PD (autophagosomes, $p = 0.003$; autophagolysosomes, $p = 0.010$).

E. Content of lipid droplets per field. Asterisks denote statistically significant differences [$F(2,16) = 28.274$; $p < 0.001$] between CONTROL and ID-PD ($p = 0.010$), and between CONTROL and LRRK2-PD ($p = 0.013$). Bars represent average with SEM as error bars ($n = 4$–8).

knowledge, this is the first time such phenotypes have been described. Indeed, Soldner and colleagues did not find any differences between DAn differentiated from ID-PD iPSC and from control iPSC (Soldner et al, 2009), a fact that they attributed to the short time span of cultured neurons (32–42 days). Moreover, these authors suggested that additional manipulations might be necessary to accelerate PD-pathology related phenotypes in iPSC-derived DAn *in vitro*, such as increasing oxidative stress, challenge with neurotoxins or overexpressing PD-related genes (Soldner et al, 2009). Thus, it may not appear entirely unexpected that DAn differentiated from our LRRK2-PD iPSC displayed PD-related alterations *in vitro*. However, during the writing of this manuscript, a study was published that found no alterations in DAn differentiated from iPSC from one LRRK2-PD patient, unless these were challenged with H_2O_2, 6-hydroxydopamine (a PD-related neurotoxin) or MG-132 (proteasome inhibitor; Nguyen et al, 2011). We believe that the lack of spontaneous PD pathology-related phenotypes in previous iPSC-based models of ID-PD (Soldner et al, 2009) and LRRK2-PD (Nguyen et al, 2011), in contrast with our results presented here, may be due to at least two reasons: First, the longer time span of cultured neurons (up to 75 days) in our experiments, which may have induced culture-related stress conditions mimicking *in vivo* aging in PD patients, and thus accelerated the development of PD-related phenotypes *in vitro*. In support of this, we found that DAn differentiated for 30 days from ID-PD- or LRRK2-PD iPSC, a

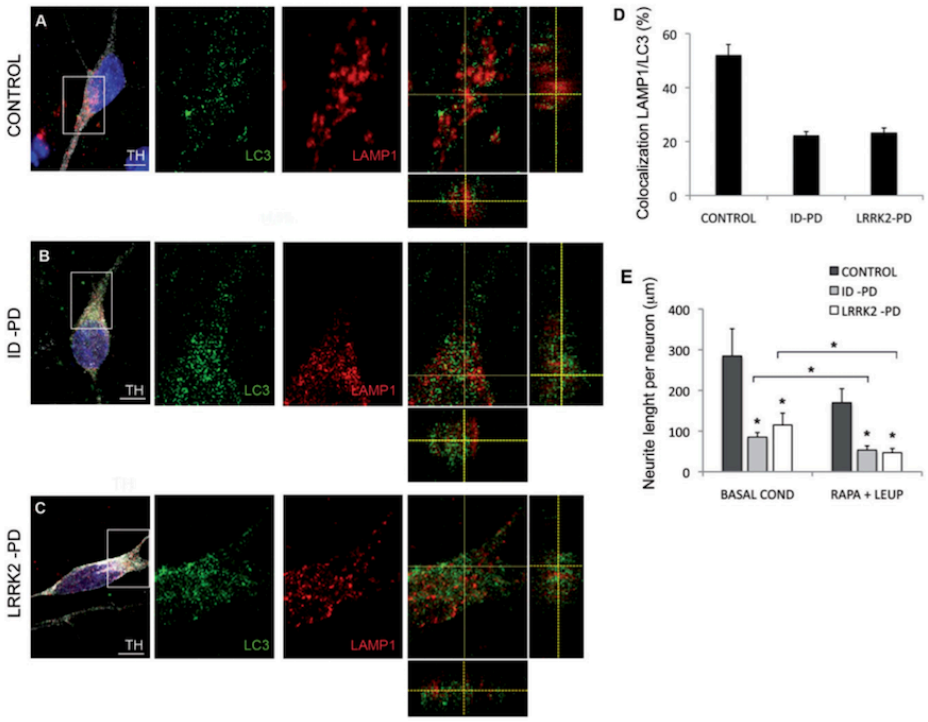

Figure 7. Defective autophagosome clearance in PD-iPSC-derived DA neurons.

A-C. DAn (TH positive, white) cultured on astrocytes for 75 days stained for LC3 (green) and LAMP1 (red) after 6 h of treatment with leupeptin from CONTROL (cell line SP11.1, **A**), ID-PD (cell line SP10.2, **B**) and LRRK2-PD (cell line SP05.1, **C**) iPSC. Z-stack views are shown on the merged images (right panels). Nuclei are counterstained with DAPI, shown in blue. Scale bars, 5 µm.

D. Quantitative analyses of the colocalization of LAMP1 and LC3. Data for each group is the average of 15, 15 and 14 DAn representing three different Ctrl-, ID-PD and LRKK2-PD iPSC lines, respectively. Asterisks denote statistically significant differences between CONTROL and ID-PD ($p < 0.001$) or LRRK2-PD ($p < 0.001$) [$F(2,41) = 41.628$; $p < 0.001$].

E. Quantitative analyses of the total neurite length per neuron with or without treatment with rapamycin and leupeptin. Under basal conditions (without treatment), data for CONTROL is the average of 97 DAn from 4 iPSC lines, for ID-PD is from 127 DAn from 7 iPSC lines and for LRRK2-PD is from 80 DAn from 4 iPSC lines. After treatment with rapamycin and leupeptin (RAPA + LEUP), data for CONTROL is the average of 60 DAn from 4 iPSC lines, for ID-PD is from 112 DAn from 7 iPSC lines and for LRRK2-PD is from 74 DAn from 4 iPSC lines. Asterisks above data bars denote statistically significant differences under basal conditions [$F(2,301) = 5.886$; $p = 0.003$] between CONTROL and ID-PD ($p = 0.003$), and between CONTROL and LRRK2-PD ($p = 0.022$), and after treatment with rapamycin and leupeptin [$F(2,243) = 48.812$; $p < 0.001$] between CONTROL and ID-PD ($p < 0.001$), and between CONTROL and LRRK2-PD ($p < 0.001$). Asterisks comparing data sets denote statistically significant differences in total neurite length after treatment with rapamycin and leupeptin in DAn from ID-PD ($p = 0.001$) and LRRK2-PD ($p < 0.001$), but not from CONTROL ($p = 0.090$). In (**D–E**) bars represent average with SEM as error bars.

time when no alterations (other than SNCA accumulation in LRRK2-PD iPSC-derived DAn) were evident, showed increased susceptibility to sub-lethal concentrations of the PD-related toxin MPP+ (Fig S11 of Supporting information). Thus, it is likely that the prolonged culture of these cells in our 75-day differentiation protocol served to amplify the intrinsic susceptibility of PD-iPSC-derived DAn to undergo neurodegeneration in response to aging, the most important PD-related susceptibility factor. Second, it should be noted that the majority of iPSC-derived neurons in our experiments were of vmDA neuron phenotype, whereas, this cell population was much rarer in previous studies, with Soldner and colleagues reporting ~10% of DAn (TH+/TUJ1+ cells) of a phenotype that was not examined in detail (Soldner et al, 2009), and Nguyen and colleagues reporting less than 1% of neurons of a vmDA phenotype (Nguyen et al, 2011). We believe that the enrichment

of vmDA neuron in our experiments facilitated the identification of PD pathology-related phenotypes, which are known to affect preferentially this specific subtype of DAn.

Our iPSC-based PD model should help investigating the pathogenic mechanisms that underlie PD neurodegeneration. Thus, although several lines of evidence suggest a causal link between impaired autophagy and the development of PD-related pathology, definitive proof for this has been elusive (reviewed in Yang & Mao, 2010). Our findings of defective autophagosome clearance in DAn from PD patient-specific iPSC, together with the positive correlation between the expansion of the autophagic compartment and the degree of morphological alterations in these cells, provide strong support for this hypothesis. In addition, the iPSC-based PD model described here should also prove an invaluable tool to investigate early functional alterations that predate the onset of neurodegeneration, which surely will help identifying potentially new therapeutic targets for the prevention, rather than rescue, of PD-related neurodegeneration.

Overall, our studies demonstrate the potential of iPSC-based technology to experimentally model the pathogenic mechanisms of late-onset diseases such as PD. Not only did we find PD pathology related phenotypes in long-term cultures of DAn representing a monogenic form of PD, but also in those from patients of ID-PD. This critical point indicates that the cause for the increased susceptibility of ID-PD-derived DAn to undergo degeneration *in vitro* after long-time culture, albeit complex, is encoded in the genome of ID-PD patients, or at least of those tested in our study. Therefore, intrinsic cell-autonomous factors, rather than environmental influences, appear to be sufficient to trigger neurodegeneration of DAn from PD patients, in a process that requires time to manifest itself, but that can be modelled within the time-frame of *in vitro* experiments. We believe that key aspects to the success of our strategy were the efficient differentiation of the PD relevant cell type, the ability to maintain DAn cultures over a long-term culture span and the use of multiple patients per condition, which allowed controlling the inherent variability of human pluripotent stem cell lines. In this way, we have identified *in vitro* phenotypes associated with ID and/or LRRK2 PD, which could be harnessed as readouts for drug screening studies. Our findings provide important conceptual and technical advances for the understanding of PD pathogenesis and, eventually, for the identification of novel therapeutic strategies in this disease.

MATERIALS AND METHODS

Description of PD patients

Studies were approved by the authors' Institutional Review Board and conducted under the Declaration of Helsinki. Patients were encoded to protect their confidentiality, and written informed consent obtained. The generation of human iPS cells was done following a protocol approved by the Spanish competent authorities (Commission on Guarantees concerning the Donation and Use of Human Tissues and Cells of the Carlos III Health Institute). PD was diagnosed according to UK Brain Bank criteria (Hughes et al, 1992). We identified subjects participating in the study among patients attending the outpatient Movement Disorder Unit at the Hospital Clinic of Barcelona (Barcelona, Spain). Four patients were known from previous studies to have LRRK2-associated PD. The remaining seven patients had a sporadic form of PD and LRRK2 mutation was excluded by direct DNA sequencing. Healthy controls were recruited among patients' spouses.

Generation of iPSC

Epidermal keratinocytes were used for iPSC generation, except for patients SP05 and SP09, for whom dermal fibroblasts were used. Keratinocytes were cultured in serum-free low calcium medium (Epilife, Invitrogen) and reprogrammed using a 1:1:1 mix of retroviruses encoding FLAG-tagged OCT4, SOX2 and KLF4, essentially as previously described (Aasen et al, 2008). Fibroblasts were reprogrammed using a 1:1:1 mix of retroviruses encoding FLAG-tagged OCT4, SOX2 and KLF4, following a previously described protocol (Raya et al, 2010). For selecting reprogrammed cells, the medium was changed to human ES cell (hESC) medium, consisting of KO-DMEM (Invitrogen) supplemented with 20% KO-Serum Replacement (Invitrogen), 2 mM Glutamax (Invitrogen), 50 μM 2-mercaptoethanol (Invitrogen), non-essential aminoacids (Cambrex) and 10 ng/ml bFGF (Peprotech). Cultures were maintained at 37°C, 5% CO_2, with media changes every other day. Colonies were picked based on morphology 45–60 days after the initial infection and plated onto fresh feeders. Lines of patient-specific iPS cells were maintained by mechanical dissociation of colonies and splitting 1:3 onto feeder cells in hESC medium or by limited trypsin digestion and passaging onto Matrigel-coated plates with hESC medium pre-conditioned by mouse embryonic fibroblasts. The iPSC lines generated and characterized in this study are currently in the process of being registered and deposited in the Spanish Stem Cell Bank, through which they will be made available to interested researchers.

Characterization of iPSC lines

Expression of retroviral transgenes and endogenous pluripotency-associated transcription factors by quantitative Polymerase Chain Reaction (after reverse transcription) (RT-PCR), integration of retroviral transgenes by Southern blot and methylation status of *OCT4* and *NANOG* promoters were assessed as previously reported (Aasen et al, 2008). *In vitro* differentiation towards endoderm, mesoderm and neuroectoderm was carried out essentially as described (Raya et al, 2008). Severe combined immunodeficient (SCID) beige mice (Charles River Laboratories) were used to test the teratoma induction capacity of patient-specific iPS cells essentially as described (Aasen et al, 2008). All animal experiments were conducted following experimental protocols previously approved by the Institutional Ethics Committee on Experimental Animals, in full compliance with Spanish and European laws and regulations.

iPSC differentiation to DA neurons

For DAn differentiation, iPSC were transduced with LV.NES.LMX1A.GFP and processed as previously described (Sanchez-Danes et al, 2011). For DAn yield analysis cells were co-cultured with PA6 for 3 weeks in N2B27 medium. For SNCA and LRRK2 staining, DAn generated on the top of PA6 for 3 weeks were trypsinized and cultured for 3 days on Matrigel-coated dishes. For long-term culture, neural progenitor cells

were seeded onto mouse primary cortical astrocytes, prepared as described elsewhere (Giralt et al, 2010), and maintained in N2B27 medium. After 9 weeks, some wells were incubated with 4 μM rapamycin (LC Labs) and/or 100 μM leupeptin (Sigma) for 6 h prior to fixation. For LC3 flux studies in DAn, neurons differentiated on murine astrocytes for 9 weeks were treated for 2 and 4 h with lysosomal inhibitors NH_4Cl (20 mM, Sigma) and leupeptin (200 μM) in N2B27 media. After the treatment a pellet was obtained using a cell scraper (BD).

Expression of wild-type or mutant LRRK2 in DAn

DAn differentiated on top of murine astrocytes were grown on coverslips and transfected at day 65 of the differentiation protocol. The transfection was done as described previously (Kaech & Banker, 2006). Briefly, transfection media consisting on 200 μl of MEM media (Invitrogen), 5 μl lipofectamine 2000 (Invitrogen), 1 μg of plasmids encoding WT LRRK2 or mutant $LRRK2^{G2019S}$ (kindly provided by Giorgio Rovelli, Novartis Pharma Ltd, Basel, Switzerland, and Philipp Kahle, Hertie Institute for Clinical Brain Research, University Clinics Tübingen, Germany) and 0.25 μg pmaxGFP plasmid (Lonza) was prepared. The media was aspirated from the wells and in each coverslip containing the DAn culture 200 μl of transfection media was added and incubated for 4 h at 37°C followed by replacement (two times) with fresh N2B27 media. GFP positive cells started to appear 2 days after transfection.

Immunohistochemistry

Cells were fixed with 4% paraformaldehyde in PBS at 4°C for 10 min and permeabilized for 15 min in 0.5% Triton in PBS. Cells were then blocked in Triton-X100 with 3% donkey serum for 2 h. The following antibodies were used: mouse anti-Tra-1-81 (Chemicon, MAB4381, 1:100), rabbit anti-Sox2 (Chemicon, AB5603, 1:500), mouse anti-SSEA-4 (MC-813-70, 1:2) and mouse anti-SSEA-3 (MC-631, 1:2) from the Developmental Studies Hybridoma Bank at the University of Iowa, mouse anti-SMA (Sigma, 1:400), mouse anti-Tuj1 (Covance, 1:500), mouse Oct-3/4 (Santa Cruz, 1:100), rabbit anti-α-fetoprotein (Dako, 1:400), goat anti-Nanog (Everest Biotech; 1:100), goat anti-FoxA2 (R&D Biosystems, 1:100), rabbit anti-TH (Sigma, 1:1000), mouse anti-TH (Chemicon, MAB5280, 1:1000), rabbit anti-Girk2 (Sigma, 1:40), rat anti-DAT (Chemicon, MAB369, 1:400), rabbit anti-cleaved Caspase-3 (Cell Signalling, 1:400), rabbit anti-LC3 (Cell Signalling, 1:100), mouse anti-LAMP1 (U. Iowa Developmental Hybridoma Bank, 1:100), rabbit anti-p62 (Enzo Life Sciences, 1:200), chicken anti-GFP (Aves Labs, 1: 500), rabbit anti-LRRK2 (MJFF C41-2, kindly provided by MJFF, 1:100), mouse anti-chondroitin sulphate (Sigma, 1:400), rabbit anti-Nurr1 (Santa Cruz, 1: 50) and mouse anti-SNCA (Ab-2, Thermo Scientific, 1:1000). Secondary antibodies used were all the Alexa Fluor Series from Invitrogen (all 1:500). Images were taken using Leica SP5 confocal microscope. For quantification of the DAn yield randomly 300 cells per differentiated aggregate were counted (average 6–8 differentiated aggregates per experiment). Data points represent the average of at least three-independent experiments. To visualize nuclei, slides were stained with 0.5 μg/ml DAPI (4′,6-diamidino-2-phenylindole) and then mounted with PVADABCO. Direct AP activity was analysed using an AP blue/red membrane substrate solution kit (Sigma) according to the manufacturer's guidelines.

Neurite analysis

Neurite analysis was performed at the indicated time-points on iPSC-derived neurons differentiated on top of cortical mouse astrocytes fixed and stained for TH. We randomly selected a minimum of 20 DAn per iPSC line (on the only condition that were isolated from surrounding DAn, so that we could unambiguously ascribe neurites to a single DAn), using a Leica SP5 confocal microscope, and analysed with the ImageJ plugin NeuronJ to determine the number and length of neurites per cell.

Fibroblast culture and treatment for autophagy studies

Fibroblasts from all patients were cultured in IMDM (Invitrogen) supplemented with 10% FBS (Gibco) and 2 mM Glutamax (Invitrogen). Fibroblasts were grown until reaching 65–75% confluence, when they were used as controls or treated for 6 h with rapamycin (0.2 or 2 μM) and 100 μM leupeptin. After the treatment, some cells were fixed and analysed by immunofluorescence for LC3 and the rest was processed as a pellet for Western blot analysis for LC3. For LC3 flux studies in fibroblasts, cells were treated for 2 and 4 h in supplemented IMDM containing lysosomal inhibitors, consisting in 20 mM NH_4Cl (Sigma) and 200 μM leupeptin, after the treatment a pellet was obtained using 0.25% trypsin–EDTA.

Protein extraction and Western blotting

Proteins were extracted using RIPA protein extraction buffer (Sigma) supplemented with protease inhibitor (Sigma) and phosphatase inhibitor cocktails (Sigma). In brief, cells were detached from culture dishes, centrifuged and washed once with cold PBS. Cell pellets were then resuspended and incubated in RIPA buffer for 20 min on ice and sonicated in one pulse of 5 s at 10% amplitude on ultrasonicator (Branson Digital Sonifier, Branson Ultrasonics Corporation, Danbury, CT, USA) to ensure high efficiency of lysis. After centrifugation, supernatants of total protein extracts were denatured in loading buffer for 10 min at 98°C. Proteins were separated using SDS–polyacrylamide gel electrophoresis (SDS–PAGE) and transferred to PVDF membrane. The membrane was probed with anti-α-tubulin (Sigma T6074; 1:10,000), anti-LC3 (Cell Signalling; 1:1000) and anti-LRRK2 (MJFF2 c41-2; 1:50).

Electron microscopy and morphometric analysis

Cells were fixed in 2.5% gluteraldehyde/2% paraformaldehyde in 100 mM sodium cacodylate, pH 7.43 (SC) and post-fixed in 1% osmium tetroxide in SC followed by 1% uranyl acetate. After ethanol dehydration and embedding in LX112 resin (LADD Research Industries), ultrathin sections were stained with uranyl acetate followed by lead citrate. All grids were viewed on a JEOL 100CX II transmission electron microscope at 80 kV. Morphometric analysis was performed using ImageJ in 15–20 different micrographs for each condition after thresholding. Autophagic vacuoles were identified using previously established criteria (Dunn, 1990; Nixon et al, 2005). Autophagic vacuoles (vesicles <0.5 μm) were classified as autophagosomes when they met two or more of the following criteria: double membranes (complete or at least partially visible), absence of ribosomes attached to the cytosolic side of the membrane, luminal density similar to cytosol and identifiable organelles or regions of organelles in their lumen. Vesicles of similar size but with a single membrane (or less than 40% of the membrane visible as double), luminal density lower

The paper explained

PROBLEM:

Parkinson's disease (PD) has a lifetime risk of 2%, making it the second most common neurodegenerative disease after Alzheimer's disease. It is associated to a selective loss of dopaminergic neurons (DAn) from the substantia nigra pars compacta responsible for controlling body movement. Around 90% of PD cases are sporadic, while 10% have a familial or genetic origin, of which mutations in the LRRK2 gene are the most frequent cause. The pathogenic mechanisms leading to PD are not well understood, to a large extent owing to the lack of suitable genetic models of this disease in animals. Therefore, there is an urgent need for developing reliable experimental models that recapitulate the salient features of PD. Recently, induced pluripotent stem cells (iPSC) have been used to model human diseases, although it is currently unclear if this approach would be able to model age-related diseases.

RESULTS:

We generated iPSC from sporadic PD patients, PD patients with LRRK2 mutation and healthy controls. All of these iPSC lines were comparable in their ability to generate DAn, and no major differences were found in these neurons under conventional culture conditions, except for increased accumulation of SNCA in neurons from LRRK2 mutant iPSC. However, when cultured for over 2.5 months (a condition mimicking aging *in vitro*), DAn differentiated from patient-specific iPSC developed evident signs of neurodegeneration, including fewer and shorter neurites and a significant increase in apoptotic cells. Most importantly, this degeneration occurred in neurons from either sporadic PD or mutant PD, but not from healthy individuals. We then show that these alterations are caused by a deficient autophagic machinery.

IMPACT:

We have generated an iPSC-based model for PD that recapitulates key pathological features of PD such as neurodegeneration and SNCA accumulation in DAn generated from PD-patients. Our findings indicate that the bases of the increased susceptibility of DAn to degenerate upon aging in sporadic PD patients should be encoded in their genome. Moreover, our iPSC-based PD model provides a valuable tool to investigate the pathogenic mechanisms of PD, such as altered autophagy, and to screen for drugs that may prevent or rescue neurodegeneration in PD.

than the surrounding cytosol, multiple single membrane-limited vesicles containing light or dense amorphous material were classified as autophagolysosomes.

RT-qPCR analyses

Total mRNA was isolated by guanidinium thiocynate–phenol–chloroform extraction (TRIzol, Invitrogen) and treated with DNaseI. One microgram was used to synthesize cDNA with the SuperScript III Reverse Transcriptase Synthesis Kit (Invitrogen). Quantitative PCR analyses were done in triplicate on 50 ng with Platinum Syber Green qPCR Super Mix (Invitrogen) in an ABI Prism 7000 thermocycler (Applied Biosystems). All results were normalized to HPRT and β-2-microglobulin. The primers used were: B2micro-F, 5′-GCCGTGTGAACCATGTGACT-3′; B2micro-R, 5′-GCTTACATGTCT CGATCCCACTT-3′; HPRT-F, 5′-TTATGGACAGGACTGAACGTCTTG-3′ HPRT-R, 5′-GCACACAGAGGGCTACAATGTG-3′; NANOG-F, 5′-ACAACTGGCCGAAGAATA GCA-3′; NANOG-R, 5′-GGTTCCCAGTCGGGTTCAC-3′; FOXA2-F, 5′-AGACTCCTGC TTCTTCAAGCACCT-3′; FOXA2-R, 5′-ACTTCCCTGCAACAACAGCAATGG-3′; LRRK2-F, 5′-GGGAGCAGATGCCAATCAAGCAAA-3′; LRRK2-R, 5′-TCCACCAATTT GGGACTGCTCTCT-3′; SNCA-F, 5′-AGCGGACCTCCACAAGTAACGAAT-3′; SNCA-R, 5′-TTGGCATCTGTCTTCCTCCCAAGT-3′; TAU-F, 5′-ACGAAGGCCTGAAGCACA GGATTA-3′; TAU-R, 5′-TCCTTTGGGACTGCCATGAGACTT-3′.

Statistical analysis

Differences among groups were evaluated by one-way ANOVA, and comparisons between two groups by Student's *t*-test, using the StatPlus build for Microsoft Excel.

Author contributions

ASD differentiated DAn from iPSC, performed neurodegeneration and autophagy studies and analyzed data; YRP and SJD generated and characterized iPSC lines; ICC and MV analysed SNCA and MPP+ susceptibility; CC, ME and ET identified and recruited the PD patients, and obtained authorization for the study; SM performed LC3 flux studies; CDG helped with iPSC cultures; BP performed electron microscopy studies; AMC designed the autophagy studies, analysed data and edited the manuscript; AG, JMC, MM, JA and JLB provided materials; AC conceived, designed and supervised the study, and edited the manuscript; AR generated iPSC lines, conceived, designed and supervised the study and wrote the manuscript.

Acknowledgements

We thank Alberto Garcia for excellent technical assistance, and Irene Fernández, Roger Torrent, Bahaa Arefai and Enric Navas for help with experiments. We also thank G. Rovelli, P. Kahle and the MJFF for the kind gift of reagents. AS-D was partially supported by a pre-doctoral fellowship from MEC. Additional support was provided by grants from MICINN (BFU2009-13277, PLE2009-0144 and ACI2010-1117 to AR; RyC-2008-02772 and BFU2010-21823 to AC; SAF2008-04360, to JA; SAF2009-07774 and PLE2009-0089, to JMC), FIS (PI10/00849 to MV; RD06/0010/0006 to JMC), NIH/NIA AG031782/AG038072 (to AMC) and Fondazione Guido Berlucchi (to

AC). The Cell Therapy Program was supported by the CMRB (Promt-0901 to JMC). The work was also part of a CIBERNED Cooperative Project (to JA, JL-B, MV, ET and AR).

Supporting information is available at EMBO Molecular Medicine online.

The authors declare that they have no conflict of interest.

References

Aasen T, Raya A, Barrero MJ, Garreta E, Consiglio A, Gonzalez F, Vassena R, Bilic J, Pekarik V, Tiscornia G, *et al* (2008) Efficient and rapid generation of induced pluripotent stem cells from human keratinocytes. Nat Biotechnol 26: 1276-1284

Carvajal-Vergara X, Sevilla A, D'Souza SL, Ang YS, Schaniel C, Lee DF, Yang L, Kaplan AD, Adler ED, Rozov R, *et al* (2010) Patient-specific induced pluripotent stem-cell-derived models of LEOPARD syndrome. Nature 465: 808-812

Chu CT, Plowey ED, Dagda RK, Hickey RW, Cherra SJ III, Clark RS (2009) Autophagy in neurite injury and neurodegeneration: *in vitro* and *in vivo* models. Methods Enzymol 453: 217-249

Cookson MR (2010) The role of leucine-rich repeat kinase 2 (LRRK2) in Parkinson's disease. Nat Rev Neurosci 11: 791-797

Dawson TM, Ko HS, Dawson VL (2010) Genetic animal models of Parkinson's disease. Neuron 66: 646-661

Dimos JT, Rodolfa KT, Niakan KK, Weisenthal LM, Mitsumoto H, Chung W, Croft GF, Saphier G, Leibel R, Goland R, *et al* (2008) Induced pluripotent stem cells generated from patients with ALS can be differentiated into motor neurons. Science 321: 1218-1221

Dunn WA Jr., (1990) Studies on the mechanisms of autophagy: maturation of the autophagic vacuole. J Cell Biol 110: 1935-1945

Ebert AD, Yu J, Rose FF, Jr., Mattis VB, Lorson CL, Thomson JA, Svendsen CN (2009) Induced pluripotent stem cells from a spinal muscular atrophy patient. Nature 457: 277-280

Giralt A, Friedman HC, Caneda-Ferron B, Urban N, Moreno E, Rubio N, Blanco J, Peterson A, Canals JM, Alberch J (2010) BDNF regulation under GFAP promoter provides engineered astrocytes as a new approach for long-term protection in Huntington's disease. Gene Ther 17: 1294-1308

Hu BY, Weick JP, Yu J, Ma LX, Zhang XQ, Thomson JA, Zhang SC (2010) Neural differentiation of human induced pluripotent stem cells follows developmental principles but with variable potency. Proc Natl Acad Sci USA 107: 4335-4340

Hughes AJ, Ben-Shlomo Y, Daniel SE, Lees AJ (1992) What features improve the accuracy of clinical diagnosis in Parkinson's disease: a clinicopathologic study. Neurology 42: 1142-1146

Imai Y, Gehrke S, Wang HQ, Takahashi R, Hasegawa K, Oota E, Lu B (2008) Phosphorylation of 4E-BP by LRRK2 affects the maintenance of dopaminergic neurons in *Drosophila*. EMBO J 27: 2432-2443

Johnson MA, Weick JP, Pearce RA, Zhang SC (2007) Functional neural development from human embryonic stem cells: accelerated synaptic activity via astrocyte coculture. J Neurosci 27: 3069-3077

Kabeya Y, Mizushima N, Ueno T, Yamamoto A, Kirisako T, Noda T, Kominami E, Ohsumi Y, Yoshimori T (2000) LC3, a mammalian homologue of yeast Apg8p, is localized in autophagosome membranes after processing. EMBO J 19: 5720-5728

Kaech S, Banker G (2006) Culturing hippocampal neurons. Nat Protoc 1: 2406-2415

Ku S, Soragni E, Campau E, Thomas EA, Altun G, Laurent LC, Loring JF, Napierala M, Gottesfeld JM (2010) Friedreich's ataxia induced pluripotent stem cells model intergenerational GAATTC triplet repeat instability. Cell Stem Cell 7: 631-637

Lee G, Studer L (2010) Induced pluripotent stem cell technology for the study of human disease. Nat Methods 7: 25-27

Lee G, Papapetrou EP, Kim H, Chambers SM, Tomishima MJ, Fasano CA, Ganat YM, Menon J, Shimizu F, Viale A, *et al* (2009) Modelling pathogenesis and treatment of familial dysautonomia using patient-specific iPSCs. Nature 461: 402-406

Lees AJ, Hardy J, Revesz T (2009) Parkinson's disease. Lancet 373: 2055-2066

Lesage S, Brice A (2009) Parkinson's disease: from monogenic forms to genetic susceptibility factors. Hum Mol Genet 18: R48-R59

Lin X, Parisiadou L, Gu XL, Wang L, Shim H, Sun L, Xie C, Long CX, Yang WJ, Ding J, *et al* (2009) Leucine-rich repeat kinase 2 regulates the progression of neuropathology induced by Parkinson's-disease-related mutant alpha-synuclein. Neuron 64: 807-827

Marchetto MC, Carromeu C, Acab A, Yu D, Yeo GW, Mu Y, Chen G, Gage FH, Muotri AR (2010) A model for neural development and treatment of Rett syndrome using human induced pluripotent stem cells. Cell 143: 527-539

Menzies FM, Moreau K, Rubinsztein DC (2011) Protein misfolding disorders and macroautophagy. Curr Opin Cell Biol 23: 190-197

Moretti A, Bellin M, Welling A, Jung CB, Lam JT, Bott-Flugel L, Dorn T, Goedel A, Hohnke C, Hofmann F, *et al* (2010) Patient-specific induced pluripotent stem-cell models for long-QT syndrome. N Engl J Med 363: 1397-1409

Nguyen HN, Byers B, Cord B, Shcheglovitov A, Byrne J, Gujar P, Kee K, Schule B, Dolmetsch RE, Langston W, *et al* (2011) LRRK2 mutant iPSC-derived DA neurons demonstrate increased susceptibility to oxidative stress. Cell Stem Cell 8: 267-280

Nixon RA, Wegiel J, Kumar A, Yu WH, Peterhoff C, Cataldo A, Cuervo AM (2005) Extensive involvement of autophagy in Alzheimer disease: an immuno-electron microscopy study. J Neuropathol Exp Neurol 64: 113-122

Obeso JA, Rodriguez-Oroz MC, Goetz CG, Marin C, Kordower JH, Rodriguez M, Hirsch EC, Farrer M, Schapira AH, Halliday G (2010) Missing pieces in the Parkinson's disease puzzle. Nat Med 16: 653-661

Paisan-Ruiz C, Jain S, Evans EW, Gilks WP, Simon J, van der Brug M, Lopez deMunain, Aparicio A, Gil S, Khan AM, *et al* (2004) Cloning of the gene containing mutations that cause PARK8-linked Parkinson's disease. Neuron 44: 595-600

Park IH, Arora N, Huo H, Maherali N, Ahfeldt T, Shimamura A, Lensch MW, Cowan C, Hochedlinger K, Daley GQ (2008a) Disease-specific induced pluripotent stem cells. Cell 134: 877-886

Park IH, Zhao R, West JA, Yabuuchi A, Huo H, Ince TA, Lerou PH, Lensch MW, Daley GQ (2008b) Reprogramming of human somatic cells to pluripotency with defined factors. Nature 451: 141-146

Rashid ST, Corbineau S, Hannan N, Marciniak SJ, Miranda E, Alexander G, Huang-Doran I, Griffin J, Ahrlund-Richter L, Skepper J, *et al* (2010) Modeling inherited metabolic disorders of the liver using human induced pluripotent stem cells. J Clin Invest 120: 3127-3136

Raya A, Rodriguez-Piza I, Aran B, Consiglio A, Barri PN, Veiga A, Belmonte JC (2008) Generation of cardiomyocytes from new human embryonic stem cell lines derived from poor-quality blastocysts. Cold Spring Harb Symp Quant Biol 73: 127-135

Raya A, Rodriguez-Piza I, Guenechea G, Vassena R, Navarro S, Barrero MJ, Consiglio A, Castella M, Rio P, Sleep E, *et al* (2009) Disease-corrected haematopoietic progenitors from Fanconi anaemia induced pluripotent stem cells. Nature 460: 53-59

Raya A, Rodriguez-Piza I, Navarro S, Richaud-Patin Y, Guenechea G, Sanchez-Danes A, Consiglio A, Bueren J, Izpisua Belmonte, JC (2010) A protocol describing the genetic correction of somatic human cells and subsequent generation of iPS cells. Nat Protoc 5: 647-660

Ruggero D, Montanaro L, Ma L, Xu W, Londei P, Cordon-Cardo C, Pandolfi PP (2004) The translation factor eIF-4E promotes tumor formation and cooperates with c-Myc in lymphomagenesis. Nat Med 10: 484-486

Sanchez-Danes A, Consiglio A, Richaud Y, Rodriguez-Piza I, Dehay B, Edel M, Bove J, Memo M, Vila M, Raya A, *et al* (2012) Efficient generation of A9 midbrain dopaminergic neurons by lentiviral delivery of LMX1A in human

embryonic stem cells and induced pluripotent stem cells. Hum Gene Ther 23: 56-69

Schapira AH, Tolosa E (2010) Molecular and clinical prodrome of Parkinson disease: implications for treatment. Nat Rev Neurol 6: 309-317

Singh R, Kaushik S, Wang Y, Xiang Y, Novak I, Komatsu M, Tanaka K, Cuervo AM, Czaja MJ (2009) Autophagy regulates lipid metabolism. Nature 458: 1131-1135

Soldner F, Hockemeyer D, Beard C, Gao Q, Bell GW, Cook EG, Hargus G, Blak A, Cooper O, Mitalipova M, *et al* (2009) Parkinson's disease patient-derived induced pluripotent stem cells free of viral reprogramming factors. Cell 136: 964-977

Soldner F, Laganiere J, Cheng AW, Hockemeyer D, Gao Q, Alagappan R, Khurana V, Golbe LI, Myers RH, Lindquist S, *et al* (2011) Generation of isogenic pluripotent stem cells differing exclusively at two early onset Parkinson point mutations. Cell 146: 318-331

Takahashi K, Yamanaka S (2006) Induction of pluripotent stem cells from mouse embryonic and adult fibroblast cultures by defined factors. Cell 126: 663-676

Takahashi K, Tanabe K, Ohnuki M, Narita M, Ichisaka T, Tomoda K, Yamanaka S (2007) Induction of pluripotent stem cells from adult human fibroblasts by defined factors. Cell 131: 861-872

Woods NB, Parker AS, Moraghebi R, Lutz MK, Firth AL, Brennand KJ, Berggren WT, Raya A, Belmonte JC, Gage FH, *et al* (2011) Brief report: efficient generation of hematopoietic precursors and progenitors from human pluripotent stem cell lines. Stem Cells 29: 1158-1164

Yang Q, Mao Z (2010) Parkinson disease: A role for autophagy? Neuroscientist 16: 335-341

Yu J, Vodyanik MA, Smuga-Otto K, Antosiewicz-Bourget J, Frane JL, Tian S, Nie J, Jonsdottir GA, Ruotti V, Stewart R, *et al* (2007) Induced pluripotent stem cell lines derived from human somatic cells. Science 318: 1917-1920

Zhang J, Wilson GF, Soerens AG, Koonce CH, Yu J, Palecek SP, Thomson JA, Kamp TJ (2009) Functional cardiomyocytes derived from human induced pluripotent stem cells. Circ Res 104: e30-e41

Zhang J, Lian Q, Zhu G, Zhou F, Sui L, Tan C, Mutalif RA, Navasankari R, Zhang Y, Tse HF, *et al* (2011) A human iPSC model of Hutchinson Gilford Progeria reveals vascular smooth muscle and mesenchymal stem cell defects. Cell Stem Cell 8: 31-45

Zimprich A, Biskup S, Leitner P, Lichtner P, Farrer M, Lincoln S, Kachergus J, Hulihan M, Uitti RJ, Calne DB, *et al* (2004) Mutations in LRRK2 cause autosomal-dominant parkinsonism with pleomorphic pathology. Neuron 44: 601-607

8-REFERENCES

Aasen, T., A. Raya, M. J. Barrero, E. Garreta, A. Consiglio, F. Gonzalez, R. Vassena, J. Bilic, V. Pekarik, G. Tiscornia, M. Edel, S. Boue and J. C. Izpisua Belmonte (2008). "Efficient and rapid generation of induced pluripotent stem cells from human keratinocytes." Nat Biotechnol **26**(11): 1276-1284.

Akhtar, S., M. D. Hughes, A. Khan, M. Bibby, M. Hussain, Q. Nawaz, J. Double and P. Sayyed (2000). "The delivery of antisense therapeutics." Adv Drug Deliv Rev **44**(1): 3-21.

Akhyari, P., H. Kamiya, A. Haverich, M. Karck and A. Lichtenberg (2008). "Myocardial tissue engineering: the extracellular matrix." Eur J Cardiothorac Surg **34**(2): 229-241.

Akins, R. E., R. A. Boyce, M. L. Madonna, N. A. Schroedl, S. R. Gonda, T. A. McLaughlin and C. R. Hartzell (1999). "Cardiac organogenesis in vitro: reestablishment of three-dimensional tissue architecture by dissociated neonatal rat ventricular cells." Tissue Eng **5**(2): 103-118.

Akins, R. E., K. Gratton, E. Quezada, H. Rutter, T. Tsuda and P. Soteropoulos (2007). "Gene expression profile of bioreactor-cultured cardiac cells: activation of morphogenetic pathways for tissue engineering." DNA Cell Biol **26**(6): 425-434.

Alberts, B. Johnson, A. Lewis, J. Raff, M. Roberts, K. and Walter, P. "Cell Junctions, Cell Adhesion, and the Extracellular Matrix". In Molecular Biology of Cell, 4th Edn, Garland Science, (2002)

Albrecht, D. R., G. H. Underhill, T. B. Wassermann, R. L. Sah and S. N. Bhatia (2006). "Probing the role of multicellular organization in three-dimensional microenvironments." Nat Methods **3**(5): 369-375.

Amaya, E., P. A. Stein, T. J. Musci and M. W. Kirschner (1993). "FGF signalling in the early specification of mesoderm in Xenopus." Development **118**(2): 477-487.

Amit, M., C. Shariki, V. Margulets and J. Itskovitz-Eldor (2004). "Feeder layer- and serum-free culture of human embryonic stem cells." Biol Reprod **70**(3): 837-845.

Anderson, D., T. Self, I. R. Mellor, G. Goh, S. J. Hill and C. Denning (2007). "Transgenic enrichment of cardiomyocytes from human embryonic stem cells." Mol Ther **15**(11): 2027-2036.

Anderson, P. A., B. J. Muller-Borer, G. L. Esch, W. B. Coleman, J. W. Grisham and N. N. Malouf (2007). "Calcium signals induce liver stem cells to acquire a cardiac phenotype." Cell Cycle **6**(13): 1565-1569.

Aoi, T., K. Yae, M. Nakagawa, T. Ichisaka, K. Okita, K. Takahashi, T. Chiba and S. Yamanaka (2008). "Generation of pluripotent stem cells from adult mouse liver and stomach cells." Science **321**(5889): 699-702.

Arai, A., K. Yamamoto and J. Toyama (1997). "Murine cardiac progenitor cells require visceral embryonic endoderm and primitive streak for terminal differentiation." Dev Dyn **210**(3): 344-353.

Archer, R. and D. J. Williams (2005). "Why tissue engineering needs process engineering." Nat Biotechnol **23**(11): 1353-1355.

Armstrong, M. T., D. Y. Lee and P. B. Armstrong (2000). "Regulation of proliferation of the fetal myocardium." Dev Dyn **219**(2): 226-236.

Assmus, B., V. Schachinger, C. Teupe, M. Britten, R. Lehmann, N. Dobert, F. Grunwald, A. Aicher, C. Urbich, H. Martin, D. Hoelzer, S. Dimmeler and A. M. Zeiher (2002). "Transplantation of Progenitor Cells and Regeneration Enhancement in Acute Myocardial Infarction (TOPCARE-AMI)." Circulation **106**(24): 3009-3017.

Balsam, L. B., A. J. Wagers, J. L. Christensen, T. Kofidis, I. L. Weissman and R. C. Robbins (2004). "Haematopoietic stem cells adopt mature haematopoietic fates in ischaemic myocardium." Nature **428**(6983): 668-673.

Ban, H., N. Nishishita, N. Fusaki, T. Tabata, K. Saeki, M. Shikamura, N. Takada, M. Inoue, M. Hasegawa, S. Kawamata and S. Nishikawa (2011). "Efficient generation of transgene-free human induced pluripotent stem cells (iPSCs) by temperature-sensitive Sendai virus vectors." Proc Natl Acad Sci U S A **108**(34): 14234-14239.

Bao, J., J. J. Zheng and D. Wu (2012). "The structural basis of DKK-mediated inhibition of Wnt/LRP signaling." Sci Signal **5**(224): pe22.

Barile, L., E. Messina, A. Giacomello and E. Marban (2007). "Endogenous cardiac stem cells." Prog Cardiovasc Dis **50**(1): 31-48.

Baronas-Lowell, D., J. L. Lauer-Fields and G. B. Fields (2004). "Induction of endothelial cell activation by a triple helical alpha2beta integrin ligand, derived from type I collagen alpha1(I)496-507." J Biol Chem **279**(2): 952-962.

Barron, M., M. Gao and J. Lough (2000). "Requirement for BMP and FGF signaling during cardiogenic induction in non-precardiac mesoderm is specific, transient, and cooperative." Dev Dyn **218**(2): 383-393.

Bauwens, C. L., H. Song, N. Thavandiran, M. Ungrin, S. Masse, K. Nanthakumar, C. Seguin and P. W. Zandstra (2011). "Geometric control of cardiomyogenic induction in human pluripotent stem cells." Tissue Eng Part A **17**(15-16): 1901-1909.

Behfar, A. and A. Terzic (2007). "Cardioprotective repair through stem cell-based cardiopoiesis." J Appl Physiol (1985) **103**(4): 1438-1440.

Beltrami, A. P., L. Barlucchi, D. Torella, M. Baker, F. Limana, S. Chimenti, H. Kasahara, M. Rota, E. Musso, K. Urbanek, A. Leri, J. Kajstura, B. Nadal-Ginard and P. Anversa (2003). "Adult cardiac stem cells are multipotent and support myocardial regeneration." Cell **114**(6): 763-776.

Beltrami, C. A., N. Finato, M. Rocco, G. A. Feruglio, C. Puricelli, E. Cigola, F. Quaini, E. H. Sonnenblick, G. Olivetti and P. Anversa (1994). "Structural basis of end-stage failure in ischemic cardiomyopathy in humans." Circulation **89**(1): 151-163.

Beqqali, A., J. Kloots, D. Ward-van Oostwaard, C. Mummery and R. Passier (2006). "Genome-wide transcriptional profiling of human embryonic stem cells differentiating to cardiomyocytes." Stem Cells **24**(8): 1956-1967.

Bergmann, O., R. D. Bhardwaj, S. Bernard, S. Zdunek, F. Barnabe-Heider, S. Walsh, J. Zupicich, K. Alkass, B. A. Buchholz, H. Druid, S. Jovinge and J. Frisen (2009). "Evidence for cardiomyocyte renewal in humans." Science **324**(5923): 98-102.

Bettiol, E., L. Sartiani, L. Chicha, K. H. Krause, E. Cerbai and M. E. Jaconi (2007). "Fetal bovine serum enables cardiac differentiation of human embryonic stem cells." Differentiation **75**(8): 669-681.

Bian, W., B. Liau, N. Badie and N. Bursac (2009). "Mesoscopic hydrogel molding to control the 3D geometry of bioartificial muscle tissues." Nat Protoc **4**(10): 1522-1534.

Bick, R. J., M. B. Snuggs, B. J. Poindexter, L. M. Buja and W. B. Van Winkle (1998). "Physical, contractile and calcium handling properties of neonatal cardiac myocytes cultured on different matrices." Cell Adhes Commun **6**(4): 301-310.

Bilic, J. and J. C. Izpisua Belmonte (2012). "Concise review: Induced pluripotent stem cells versus embryonic stem cells: close enough or yet too far apart?" Stem Cells **30**(1): 33-41.

Bilodeau, K. and D. Mantovani (2006). "Bioreactors for tissue engineering: focus on mechanical constraints. A comparative review." Tissue Eng **12**(8): 2367-2383.

Birla, R. K., Y. C. Huang and R. G. Dennis (2007). "Development of a novel bioreactor for the mechanical loading of tissue-engineered heart muscle." Tissue Eng **13**(9): 2239-2248.

Boheler, K. R., J. Czyz, D. Tweedie, H. T. Yang, S. V. Anisimov and A. M. Wobus (2002). "Differentiation of pluripotent embryonic stem cells into cardiomyocytes." Circ Res **91**(3): 189-201.

Bottcher, R. T. and C. Niehrs (2005). "Fibroblast growth factor signaling during early vertebrate development." Endocr Rev **26**(1): 63-77.

Boublik, J., H. Park, M. Radisic, E. Tognana, F. Chen, M. Pei, G. Vunjak-Novakovic and L. E. Freed (2005). "Mechanical properties and remodeling of hybrid cardiac constructs made from heart cells, fibrin, and biodegradable, elastomeric knitted fabric." Tissue Eng **11**(7-8): 1122-1132.

Boudou, T., W. R. Legant, A. Mu, M. A. Borochin, N. Thavandiran, M. Radisic, P. W. Zandstra, J. A. Epstein, K. B. Margulies and C. S. Chen (2012). "A microfabricated platform to measure and manipulate the mechanics of engineered cardiac microtissues." Tissue Eng Part A **18**(9-10): 910-919.

Bouten, C. V., P. Y. Dankers, A. Driessen-Mol, S. Pedron, A. M. Brizard and F. P. Baaijens (2011). "Substrates for cardiovascular tissue engineering." Adv Drug Deliv Rev **63**(4-5): 221-241.

Braam, S. R., C. Denning, E. Matsa, L. E. Young, R. Passier and C. L. Mummery (2008). "Feeder-free culture of human embryonic stem cells in conditioned medium for efficient genetic modification." Nat Protoc **3**(9): 1435-1443.

Braam, S. R., R. Passier and C. L. Mummery (2009). "Cardiomyocytes from human pluripotent stem cells in regenerative medicine and drug discovery." Trends Pharmacol Sci **30**(10): 536-545.

Braam, S. R., L. Tertoolen, A. van de Stolpe, T. Meyer, R. Passier and C. L. Mummery (2010). "Prediction of drug-induced cardiotoxicity using human embryonic stem cell-derived cardiomyocytes." Stem Cell Res **4**(2): 107-116.

Brambrink, T., R. Foreman, G. G. Welstead, C. J. Lengner, M. Wernig, H. Suh and R. Jaenisch (2008). "Sequential expression of pluripotency markers during direct reprogramming of mouse somatic cells." Cell Stem Cell **2**(2): 151-159.

Brambrink, T., K. Hochedlinger, G. Bell and R. Jaenisch (2006). "ES cells derived from cloned and fertilized blastocysts are transcriptionally and functionally indistinguishable." Proc Natl Acad Sci U S A **103**(4): 933-938.

Brand, T. (2003). "Heart development: molecular insights into cardiac specification and early morphogenesis." Dev Biol **258**(1): 1-19.

Brimble, S. N., X. Zeng, D. A. Weiler, Y. Luo, Y. Liu, I. G. Lyons, W. J. Freed, A. J. Robins, M. S. Rao and T. C. Schulz (2004). "Karyotypic stability, genotyping, differentiation, feeder-free maintenance, and gene expression sampling in three human embryonic stem cell lines derived prior to August 9, 2001." Stem Cells Dev **13**(6): 585-597.

Buckberg, G. D. (2002). "Basic science review: the helix and the heart." J Thorac Cardiovasc Surg **124**(5): 863-883.

Buckingham, M., S. Meilhac and S. Zaffran (2005). "Building the mammalian heart from two sources of myocardial cells." Nat Rev Genet **6**(11): 826-835.

Bursac, N., M. Papadaki, R. J. Cohen, F. J. Schoen, S. R. Eisenberg, R. Carrier, G. Vunjak-Novakovic and L. E. Freed (1999). "Cardiac muscle tissue engineering: toward an in vitro model for electrophysiological studies." Am J Physiol **277**(2 Pt 2): H433-444.

Bursac, N., M. Papadaki, J. A. White, S. R. Eisenberg, G. Vunjak-Novakovic and L. E. Freed (2003). "Cultivation in rotating bioreactors promotes maintenance of cardiac myocyte electrophysiology and molecular properties." Tissue Eng **9**(6): 1243-1253.

Burridge, P. W., D. Anderson, H. Priddle, M. D. Barbadillo Munoz, S. Chamberlain, C. Allegrucci, L. E. Young and C. Denning (2007). "Improved human embryonic stem cell embryoid body homogeneity and cardiomyocyte differentiation from a novel V-96 plate aggregation system highlights interline variability." Stem Cells **25**(4): 929-938.

Burridge, P. W., G. Keller, J. D. Gold and J. C. Wu (2012). "Production of de novo cardiomyocytes: human pluripotent stem cell differentiation and direct reprogramming." Cell Stem Cell **10**(1): 16-28.

Burridge, P. W., S. Thompson, M. A. Millrod, S. Weinberg, X. Yuan, A. Peters, V. Mahairaki, V. E. Koliatsos, L. Tung and E. T. Zambidis (2011). "A universal system for highly efficient cardiac differentiation of human induced pluripotent stem cells that eliminates interline variability." PLoS One **6**(4): e18293.

Cai, C. L., X. Liang, Y. Shi, P. H. Chu, S. L. Pfaff, J. Chen and S. Evans (2003). "Isl1 identifies a cardiac progenitor population that proliferates prior to differentiation and contributes a majority of cells to the heart." Dev Cell **5**(6): 877-889.

Cao, F., R. A. Wagner, K. D. Wilson, X. Xie, J. D. Fu, M. Drukker, A. Lee, R. A. Li, S. S. Gambhir, I. L. Weissman, R. C. Robbins and J. C. Wu (2008). "Transcriptional and functional profiling of human embryonic stem cell-derived cardiomyocytes." PLoS One **3**(10): e3474.

Carlsson, L. (2006). "In vitro and in vivo models for testing arrhythmogenesis in drugs." J Intern Med **259**(1): 70-80.

Carpenedo, R. L., C. Y. Sargent and T. C. McDevitt (2007). "Rotary suspension culture enhances the efficiency, yield, and homogeneity of embryoid body differentiation." Stem Cells **25**(9): 2224-2234.

Carrier, R. L., M. Papadaki, M. Rupnick, F. J. Schoen, N. Bursac, R. Langer, L. E. Freed and G. Vunjak-Novakovic (1999). "Cardiac tissue engineering: cell seeding, cultivation parameters, and tissue construct characterization." Biotechnol Bioeng **64**(5): 580-589.

Carrier, R. L., M. Rupnick, R. Langer, F. J. Schoen, L. E. Freed and G. Vunjak-Novakovic (2002). "Effects of oxygen on engineered cardiac muscle." Biotechnol Bioeng **78**(6): 617-625.

Carrier, R. L., M. Rupnick, R. Langer, F. J. Schoen, L. E. Freed and G. Vunjak-Novakovic (2002). "Perfusion improves tissue architecture of engineered cardiac muscle." Tissue Eng **8**(2): 175-188.

Casey, E. S., M. A. O'Reilly, F. L. Conlon and J. C. Smith (1998). "The T-box transcription factor Brachyury regulates expression of eFGF through binding to a non-palindromic response element." Development **125**(19): 3887-3894.

Chen, B., M. E. Dodge, W. Tang, J. Lu, Z. Ma, C. W. Fan, S. Wei, W. Hao, J. Kilgore, N. S. Williams, M. G. Roth, J. F. Amatruda, C. Chen and L. Lum (2009). "Small molecule-mediated disruption of Wnt-dependent signaling in tissue regeneration and cancer." Nat Chem Biol **5**(2): 100-107.

Chen, D., M. Zhao and G. R. Mundy (2004). "Bone morphogenetic proteins." Growth Factors **22**(4): 233-241.

Chen, G., D. R. Gulbranson, Z. Hou, J. M. Bolin, V. Ruotti, M. D. Probasco, K. Smuga-Otto, S. E. Howden, N. R. Diol, N. E. Propson, R. Wagner, G. O. Lee, J. Antosiewicz-Bourget, J. M. Teng and J. A. Thomson (2011). "Chemically defined conditions for human iPSC derivation and culture." Nat Methods **8**(5): 424-429.

Christman, K. L., H. H. Fok, R. E. Sievers, Q. Fang and R. J. Lee (2004). "Fibrin glue alone and skeletal myoblasts in a fibrin scaffold preserve cardiac function after myocardial infarction." Tissue Eng **10**(3-4): 403-409.

Claycomb, W. C. (1983). "Cardiac muscle cell proliferation and cell differentiation in vivo and in vitro." Adv Exp Med Biol **161**: 249-265.

Cognard, C., M. Rivet-Bastide, B. Constantin and G. Raymond (1992). "Progressive predominance of 'skeletal' versus 'cardiac' types of excitation-contraction coupling during in vitro skeletal myogenesis." Pflugers Arch **422**(2): 207-209.

Cole, M. F., S. E. Johnstone, J. J. Newman, M. H. Kagey and R. A. Young (2008). "Tcf3 is an integral component of the core regulatory circuitry of embryonic stem cells." Genes Dev **22**(6): 746-755.

Conlon, F. L., K. M. Lyons, N. Takaesu, K. S. Barth, A. Kispert, B. Herrmann and E. J. Robertson (1994). "A primary requirement for nodal in the formation and maintenance of the primitive streak in the mouse." Development **120**(7): 1919-1928.

Coppola, B. A. and J. H. Omens (2008). "Role of tissue structure on ventricular wall mechanics." Mol Cell Biomech **5**(3): 183-196.

Dahlmann, J., A. Krause, L. Moller, G. Kensah, M. Mowes, A. Diekmann, U. Martin, A. Kirschning, I. Gruh and G. Drager (2013). "Fully defined in situ cross-linkable alginate and hyaluronic acid hydrogels for myocardial tissue engineering." Biomaterials **34**(4): 940-951.

Dar, A., M. Shachar, J. Leor and S. Cohen (2002). "Optimization of cardiac cell seeding and distribution in 3D porous alginate scaffolds." Biotechnol Bioeng **80**(3): 305-312.

Davis, R. P., C. W. van den Berg, S. Casini, S. R. Braam and C. L. Mummery (2011). "Pluripotent stem cell models of cardiac disease and their implication for drug discovery and development." Trends Mol Med **17**(9): 475-484.

Debelle, L. and A. M. Tamburro (1999). "Elastin: molecular description and function." Int J Biochem Cell Biol **31**(2): 261-272.

Doetschman, T. C., H. Eistetter, M. Katz, W. Schmidt and R. Kemler (1985). "The in vitro development of blastocyst-derived embryonic stem cell lines: formation of visceral yolk sac, blood islands and myocardium." J Embryol Exp Morphol **87**: 27-45.

Dolnikov, K., M. Shilkrut, N. Zeevi-Levin, S. Gerecht-Nir, M. Amit, A. Danon, J. Itskovitz-Eldor and O. Binah (2006). "Functional properties of human embryonic stem cell-derived cardiomyocytes: intracellular Ca2+ handling and the role of sarcoplasmic reticulum in the contraction." Stem Cells **24**(2): 236-245.

Dorfman, J., M. Duong, A. Zibaitis, M. P. Pelletier, D. Shum-Tim, C. Li and R. C. Chiu (1998). "Myocardial tissue engineering with autologous myoblast implantation." J Thorac Cardiovasc Surg **116**(5): 744-751.

Dubois, N. C., A. M. Craft, P. Sharma, D. A. Elliott, E. G. Stanley, A. G. Elefanty, A. Gramolini and G. Keller (2011). "SIRPA is a specific cell-surface marker for isolating cardiomyocytes derived from human pluripotent stem cells." Nat Biotechnol **29**(11): 1011-1018.

Dumont, K., J. Yperman, E. Verbeken, P. Segers, B. Meuris, S. Vandenberghe, W. Flameng and P. R. Verdonck (2002). "Design of a new pulsatile bioreactor for tissue engineered aortic heart valve formation." Artif Organs **26**(8): 710-714.

Durand DM. "Electrical stimulation of excitable tissue", in: Joseph D Bronzino (ed). The Biomedical Engineering Handbook. 2nd edition. CRC Press. 2000. Chapter 17

Durrani, S., M. Konoplyannikov, M. Ashraf and K. H. Haider (2010). "Skeletal myoblasts for cardiac repair." Regen Med **5**(6): 919-932.

Dvorak, P., D. Dvorakova, S. Koskova, M. Vodinska, M. Najvirtova, D. Krekac and A. Hampl (2005). "Expression and potential role of fibroblast growth factor 2 and its receptors in human embryonic stem cells." Stem Cells **23**(8): 1200-1211.

Dvorak, P. and A. Hampl (2005). "Basic fibroblast growth factor and its receptors in human embryonic stem cells." Folia Histochem Cytobiol **43**(4): 203-208.

Ebert, A. D., J. Yu, F. F. Rose, Jr., V. B. Mattis, C. L. Lorson, J. A. Thomson and C. N. Svendsen (2009). "Induced pluripotent stem cells from a spinal muscular atrophy patient." Nature **457**(7227): 277-280.

Edwards, Y. H., Putt, W., Lekoape, K. M., Stott, D., Fox, M., Hopkinson, D. A., & Sowden, J. (1996). "The human homolog T of the mouse T(Brachyury) gene; gene structure, cDNA sequence, and assignment to chromosome 6q27". Genome Res **6**(3), 226-233.

Egli, R. J. and R. Luginbuehl (2012). "Tissue engineering - nanomaterials in the musculoskeletal system." Swiss Med Wkly **142**: w13647.

Eisenberg, L. M. and C. A. Eisenberg (2006). "Embryonic myocardium shows increased longevity as a functional tissue when cultured in the presence of a noncardiac tissue layer." Tissue Eng **12**(4): 853-865.

Elliott, N. T. and F. Yuan (2011). "A review of three-dimensional in vitro tissue models for drug discovery and transport studies." J Pharm Sci **100**(1): 59-74.

Eminli, S., J. Utikal, K. Arnold, R. Jaenisch and K. Hochedlinger (2008). "Reprogramming of neural progenitor cells into induced pluripotent stem cells in the absence of exogenous Sox2 expression." Stem Cells **26**(10): 2467-2474.

Engelmayr, G. C., Jr., M. Cheng, C. J. Bettinger, J. T. Borenstein, R. Langer and L. E. Freed (2008). "Accordion-like honeycombs for tissue engineering of cardiac anisotropy." Nat Mater **7**(12): 1003-1010.

Eschenhagen, T., M. Didie, J. Heubach, U. Ravens and W. H. Zimmermann (2002). "Cardiac tissue engineering." Transpl Immunol **9**(2-4): 315-321.

Eschenhagen, T., M. Didie, F. Munzel, P. Schubert, K. Schneiderbanger and W. H. Zimmermann (2002). "3D engineered heart tissue for replacement therapy." Basic Res Cardiol **97 Suppl 1**: I146-152.

Eschenhagen, T., C. Fink, U. Remmers, H. Scholz, J. Wattchow, J. Weil, W. Zimmermann, H. H. Dohmen, H. Schafer, N. Bishopric, T. Wakatsuki and E. L. Elson (1997). "Three-dimensional reconstitution of embryonic cardiomyocytes in a collagen matrix: a new heart muscle model system." FASEB J **11**(8): 683-694.

Eschenhagen, T. and W. H. Zimmermann (2005). "Engineering myocardial tissue." Circ Res **97**(12): 1220-1231.

Espira, L. and M. P. Czubryt (2009). "Emerging concepts in cardiac matrix biology." Can J Physiol Pharmacol **87**(12): 996-1008.

Evans, M. J. and M. H. Kaufman (1981). "Establishment in culture of pluripotential cells from mouse embryos." Nature **292**(5819): 154-156.

Evseenko, D., Y. Zhu, K. Schenke-Layland, J. Kuo, B. Latour, S. Ge, J. Scholes, G. Dravid, X. Li, W. R. MacLellan and G. M. Crooks (2010). "Mapping the first stages of mesoderm commitment during differentiation of human embryonic stem cells." Proc Natl Acad Sci U S A **107**(31): 13742-13747.

Farah, C. S. and F. C. Reinach (1995). "The troponin complex and regulation of muscle contraction." FASEB J **9**(9): 755-767.

Feinberg, A. W., A. Feigel, S. S. Shevkoplyas, S. Sheehy, G. M. Whitesides and K. K. Parker (2007). "Muscular thin films for building actuators and powering devices." Science **317**(5843): 1366-1370.

Feng, Z., T. Matsumoto and T. Nakamura (2003). "Measurements of the mechanical properties of contracted collagen gels populated with rat fibroblasts or cardiomyocytes." J Artif Organs **6**(3): 192-196.

Field, L. J. (2004). "Modulation of the cardiomyocyte cell cycle in genetically altered animals." Ann N Y Acad Sci **1015**: 160-170.

Fink, C., S. Ergun, D. Kralisch, U. Remmers, J. Weil and T. Eschenhagen (2000). "Chronic stretch of engineered heart tissue induces hypertrophy and functional improvement." FASEB J **14**(5): 669-679.

Finlayson, K., H. J. Witchel, J. McCulloch and J. Sharkey (2004). "Acquired QT interval prolongation and HERG: implications for drug discovery and development." Eur J Pharmacol **500**(1-3): 129-142.

Food and H. H. S. Drug Administration (2005). "International Conference on Harmonisation; guidance on E14 Clinical Evaluation of QT/QTc Interval Prolongation and Proarrhythmic Potential for Non-Antiarrhythmic Drugs; availability. Notice." Fed Regist **70**(202): 61134-61135.

Food and H. H. S. Drug Administration (2005). "International Conference on Harmonisation; guidance on S7B Nonclinical Evaluation of the Potential for Delayed Ventricular Repolarization (QT Interval Prolongation) by Human Pharmaceuticals; availability. Notice." Fed Regist **70**(202): 61133-61134.

Fortuin, N. J., W. P. Hood, Jr. and E. Craige (1972). "Evaluation of left ventricular function by echocardiography." Circulation **46**(1): 26-35.

Freund, C., R. P. Davis, K. Gkatzis, D. Ward-van Oostwaard and C. L. Mummery (2010). "The first reported generation of human induced pluripotent stem cells (iPS cells) and iPS cell-derived cardiomyocytes in the Netherlands." Neth Heart J **18**(1): 51-54.

Freund, C. and C. L. Mummery (2009). "Prospects for pluripotent stem cell-derived cardiomyocytes in cardiac cell therapy and as disease models." J Cell Biochem **107**(4): 592-599.

Fu, J. D., N. R. Stone, L. Liu, C. I. Spencer, L. Qian, Y. Hayashi, P. Delgado-Olguin, S. Ding, B. G. Bruneau and D. Srivastava (2013). "Direct reprogramming of human fibroblasts toward a cardiomyocyte-like state." Stem Cell Reports **1**(3): 235-247.

Gaborit, N., S. Le Bouter, V. Szuts, A. Varro, D. Escande, S. Nattel and S. Demolombe (2007). "Regional and tissue specific transcript signatures of ion channel genes in the non-diseased human heart." J Physiol **582**(Pt 2): 675-693.

Garlanda, C. and E. Dejana (1997). "Heterogeneity of endothelial cells. Specific markers." Arterioscler Thromb Vasc Biol **17**(7): 1193-1202.

Gepstein, L. (2002). "Derivation and potential applications of human embryonic stem cells." Circ Res **91**(10): 866-876.

Giudice, A. and A. Trounson (2008). "Genetic modification of human embryonic stem cells for derivation of target cells." Cell Stem Cell **2**(5): 422-433.

Goldstein, R. S., M. Drukker, B. E. Reubinoff and N. Benvenisty (2002). "Integration and differentiation of human embryonic stem cells transplanted to the chick embryo." Dev Dyn **225**(1): 80-86.

Gonen-Wadmany, M., L. Gepstein and D. Seliktar (2004). "Controlling the cellular organization of tissue-engineered cardiac constructs." Ann N Y Acad Sci **1015**: 299-311.

Graichen, R., X. Xu, S. R. Braam, T. Balakrishnan, S. Norfiza, S. Sieh, S. Y. Soo, S. C. Tham, C. Mummery, A. Colman, R. Zweigerdt and B. P. Davidson (2008). "Enhanced cardiomyogenesis of human embryonic stem cells by a small molecular inhibitor of p38 MAPK." Differentiation **76**(4): 357-370.

Grayson, W. L., T. P. Martens, G. M. Eng, M. Radisic and G. Vunjak-Novakovic (2009). "Biomimetic approach to tissue engineering." Semin Cell Dev Biol **20**(6): 665-673.

Guo, Y., Zhang, X. Z., Wei, Y., Guo, C., Li, R. X., Zeng, Q. C., & Zhang, Y. J. (2009). "Culturing of ventricle cells at high density and construction of engineered cardiac cell sheets without scaffold." Int Heart J, **50**(5), 653-662.

Guo, X. M., Y. S. Zhao, H. X. Chang, C. Y. Wang, L. L. E, X. A. Zhang, C. M. Duan, L. Z. Dong, H. Jiang, J. Li, Y. Song and X. J. Yang (2006). "Creation of engineered cardiac tissue in vitro from mouse embryonic stem cells." Circulation **113**(18): 2229-2237.

Habeler, W., S. Pouillot, A. Plancheron, M. Puceat, M. Peschanski and C. Monville (2009). "An in vitro beating heart model for long-term assessment of experimental therapeutics." Cardiovasc Res **81**(2): 253-259.

Hagege, A. A. and P. Menasche (2000). "Cellular cardiomyoplasty: a new hope in heart failure?" Heart **84**(5): 465-466.

Hancox, J. C., M. J. McPate, A. El Harchi and Y. H. Zhang (2008). "The hERG potassium channel and hERG screening for drug-induced torsades de pointes." Pharmacol Ther **119**(2): 118-132.

Hanley, J., G. Rastegarlari and A. C. Nathwani (2010). "An introduction to induced pluripotent stem cells." Br J Haematol **151**(1): 16-24.

Hanna, J., S. Markoulaki, P. Schorderet, B. W. Carey, C. Beard, M. Wernig, M. P. Creyghton, E. J. Steine, J. P. Cassady, R. Foreman, C. J. Lengner, J. A. Dausman and R. Jaenisch (2008). "Direct reprogramming of terminally differentiated mature B lymphocytes to pluripotency." Cell **133**(2): 250-264.

Hansen, A., A. Eder, M. Bonstrup, M. Flato, M. Mewe, S. Schaaf, B. Aksehirlioglu, A. P. Schwoerer, J. Uebeler and T. Eschenhagen (2010). "Development of a drug screening platform based on engineered heart tissue." Circ Res **107**(1): 35-44.

Hao, J., J. N. Ho, J. A. Lewis, K. A. Karim, R. N. Daniels, P. R. Gentry, C. R. Hopkins, C. W. Lindsley and C. C. Hong (2010). "In vivo structure-activity relationship study of dorsomorphin analogues identifies selective VEGF and BMP inhibitors." ACS Chem Biol **5**(2): 245-253.

Harkness, R. D. (1966). "Collagen." Sci Prog **54**(214): 257-274.

Hassink, R. J., A. Brutel de la Riviere, C. L. Mummery and P. A. Doevendans (2003). "Transplantation of cells for cardiac repair." J Am Coll Cardiol **41**(5): 711-717.

Hassink, R. J., J. D. Dowell, A. Brutel de la Riviere, P. A. Doevendans and L. J. Field (2003). "Stem cell therapy for ischemic heart disease." Trends Mol Med **9**(10): 436-441.

Hassink, R. J., K. B. Pasumarthi, H. Nakajima, M. Rubart, M. H. Soonpaa, A. B. de la Riviere, P. A. Doevendans and L. J. Field (2008). "Cardiomyocyte cell cycle activation improves cardiac function after myocardial infarction." Cardiovasc Res **78**(1): 18-25.

Hata, H., A. Bar, S. Dorfman, Z. Vukadinovic, Y. Sawa, A. Haverich and A. Hilfiker (2010). "Engineering a novel three-dimensional contractile myocardial patch with cell sheets and decellularised matrix." Eur J Cardiothorac Surg **38**(4): 450-455.

Hattori, F., H. Chen, H. Yamashita, S. Tohyama, Y. S. Satoh, S. Yuasa, W. Li, H. Yamakawa, T. Tanaka, T. Onitsuka, K. Shimoji, Y. Ohno, T. Egashira, R. Kaneda, M. Murata, K. Hidaka, T. Morisaki, E. Sasaki, T. Suzuki, M. Sano, S. Makino, S. Oikawa and K. Fukuda (2010). "Nongenetic method for purifying stem cell-derived cardiomyocytes." Nat Methods **7**(1): 61-66.

Haufe, V., J. A. Camacho, R. Dumaine, B. Gunther, C. Bollensdorff, G. S. von Banchet, K. Benndorf and T. Zimmer (2005). "Expression pattern of neuronal and skeletal muscle voltage-gated Na+ channels in the developing mouse heart." J Physiol **564**(Pt 3): 683-696.

He, J. Q., Y. Ma, Y. Lee, J. A. Thomson and T. J. Kamp (2003). "Human embryonic stem cells develop into multiple types of cardiac myocytes: action potential characterization." Circ Res **93**(1): 32-39.

He, Q., J. Li, E. Bettiol and M. E. Jaconi (2003). "Embryonic stem cells: new possible therapy for degenerative diseases that affect elderly people." J Gerontol A Biol Sci Med Sci **58**(3): 279-287.

Hemmati-Brivanlou, A. and D. A. Melton (1992). "A truncated activin receptor inhibits mesoderm induction and formation of axial structures in Xenopus embryos." Nature **359**(6396): 609-614.

Herrmann, B. G. (1992). "Action of the Brachyury gene in mouse embryogenesis." Ciba Found Symp, **165**, 78-86; discussion 86-91.

Hescheler, J., M. Halbach, U. Egert, Z. J. Lu, H. Bohlen, B. K. Fleischmann and M. Reppel (2004). "Determination of electrical properties of ES cell-derived cardiomyocytes using MEAs." J Electrocardiol **37 Suppl**: 110-116.

Hinek, A. and M. Rabinovitch (1994). "67-kD elastin-binding protein is a protective "companion" of extracellular insoluble elastin and intracellular tropoelastin." J Cell Biol **126**(2): 563-574.

Hirt, M. N., N. A. Sorensen, L. M. Bartholdt, J. Boeddinghaus, S. Schaaf, A. Eder, I. Vollert, A. Stohr, T. Schulze, A. Witten, M. Stoll, A. Hansen and T. Eschenhagen (2012). "Increased afterload induces pathological cardiac hypertrophy: a new in vitro model." Basic Res Cardiol **107**(6): 307.

Hochedlinger, K. and R. Jaenisch (2006). "Nuclear reprogramming and pluripotency." Nature **441**(7097): 1061-1067.

Honda, M., T. S. Hamazaki, S. Komazaki, H. Kagechika, K. Shudo and M. Asashima (2005). "RXR agonist enhances the differentiation of cardiomyocytes derived from embryonic stem cells in serum-free conditions." Biochem Biophys Res Commun **333**(4): 1334-1340.

Hou, P., Y. Li, X. Zhang, C. Liu, J. Guan, H. Li, T. Zhao, J. Ye, W. Yang, K. Liu, J. Ge, J. Xu, Q. Zhang, Y. Zhao and H. Deng (2013). "Pluripotent stem cells induced from mouse somatic cells by small-molecule compounds." Science **341**(6146): 651-654.

Hovatta, O., M. Mikkola, K. Gertow, A. M. Stromberg, J. Inzunza, J. Hreinsson, B. Rozell, E. Blennow, M. Andang and L. Ahrlund-Richter (2003). "A culture system using human foreskin fibroblasts as feeder cells allows production of human embryonic stem cells." Hum Reprod **18**(7): 1404-1409.

Hsueh, W. A., R. E. Law and Y. S. Do (1998). "Integrins, adhesion, and cardiac remodeling." Hypertension **31**(1 Pt 2): 176-180.

Hu, B. Y., J. P. Weick, J. Yu, L. X. Ma, X. Q. Zhang, J. A. Thomson and S. C. Zhang (2010). "Neural differentiation of human induced pluripotent stem cells follows developmental principles but with variable potency." Proc Natl Acad Sci U S A **107**(9): 4335-4340.

Huang, Y. C., L. Khait and R. K. Birla (2007). "Contractile three-dimensional bioengineered heart muscle for myocardial regeneration." J Biomed Mater Res A **80**(3): 719-731.

Huber, I., I. Itzhaki, O. Caspi, G. Arbel, M. Tzukerman, A. Gepstein, M. Habib, L. Yankelson, I. Kehat and L. Gepstein (2007). "Identification and selection of cardiomyocytes during human embryonic stem cell differentiation." FASEB J **21**(10): 2551-2563.

Hutchings, H., N. Ortega and J. Plouet (2003). "Extracellular matrix-bound vascular endothelial growth factor promotes endothelial cell adhesion, migration, and survival through integrin ligation." FASEB J **17**(11): 1520-1522.

Hwang, P. M. and B. D. Sykes (2015). "Targeting the sarcomere to correct muscle function." Nat Rev Drug Discov **14**(5): 313-328

Ichii, T., H. Koyama, S. Tanaka, S. Kim, A. Shioi, Y. Okuno, E. W. Raines, H. Iwao, S. Otani and Y. Nishizawa (2001). "Fibrillar collagen specifically regulates human vascular smooth muscle cell genes involved in cellular responses and the pericellular matrix environment." Circ Res **88**(5): 460-467.

Iijima, Y., T. Nagai, M. Mizukami, K. Matsuura, T. Ogura, H. Wada, H. Toko, H. Akazawa, H. Takano, H. Nakaya and I. Komuro (2003). "Beating is necessary for transdifferentiation of skeletal muscle-derived cells into cardiomyocytes." FASEB J **17**(10): 1361-1363.

Inman, G. J., F. J. Nicolas, J. F. Callahan, J. D. Harling, L. M. Gaster, A. D. Reith, N. J. Laping and C. S. Hill (2002). "SB-431542 is a potent and specific inhibitor of transforming growth factor-beta superfamily type I activin receptor-like kinase (ALK) receptors ALK4, ALK5, and ALK7." Mol Pharmacol **62**(1): 65-74.

International Stem Cell Initiative, C., V. Akopian, P. W. Andrews, S. Beil, N. Benvenisty, J. Brehm, M. Christie, A. Ford, V. Fox, P. J. Gokhale, L. Healy, F. Holm, O. Hovatta, B. B. Knowles, T. E. Ludwig, R. D. McKay, T. Miyazaki, N. Nakatsuji, S. K. Oh, M. F. Pera, J. Rossant, G. N. Stacey and H. Suemori (2010). "Comparison of defined culture systems for feeder cell free propagation of human embryonic stem cells." In Vitro Cell Dev Biol Anim **46**(3-4): 247-258.

Inzunza, J., K. Gertow, M. A. Stromberg, E. Matilainen, E. Blennow, H. Skottman, S. Wolbank, L. Ahrlund-Richter and O. Hovatta (2005). "Derivation of human embryonic stem cell lines in serum replacement medium using postnatal human fibroblasts as feeder cells." Stem Cells **23**(4): 544-549.

Ishii, O., M. Shin, T. Sueda and J. P. Vacanti (2005). "In vitro tissue engineering of a cardiac graft using a degradable scaffold with an extracellular matrix-like topography." J Thorac Cardiovasc Surg **130**(5): 1358-1363.

Islas, J. F., Y. Liu, K. C. Weng, M. J. Robertson, S. Zhang, A. Prejusa, J. Harger, D. Tikhomirova, M. Chopra, D. Iyer, M. Mercola, R. G. Oshima, J. T. Willerson, V. N. Potaman and R. J. Schwartz (2012). "Transcription factors ETS2 and MESP1 transdifferentiate human dermal fibroblasts into cardiac progenitors." Proc Natl Acad Sci U S A **109**(32): 13016-13021.

Jawad, H., N. N. Ali, A. R. Lyon, Q. Z. Chen, S. E. Harding and A. R. Boccaccini (2007). "Myocardial tissue engineering: a review." J Tissue Eng Regen Med **1**(5): 327-342.

Kaji, K., K. Norrby, A. Paca, M. Mileikovsky, P. Mohseni and K. Woltjen (2009). "Virus-free induction of pluripotency and subsequent excision of reprogramming factors." Nature **458**(7239): 771-775.

Kakkar, R. and R. T. Lee (2010). "Intramyocardial fibroblast myocyte communication." Circ Res **106**(1): 47-57.

Kattman, S. J., A. D. Witty, M. Gagliardi, N. C. Dubois, M. Niapour, A. Hotta, J. Ellis and G. Keller (2011). "Stage-specific optimization of activin/nodal and BMP signaling promotes cardiac differentiation of mouse and human pluripotent stem cell lines." Cell Stem Cell **8**(2): 228-240.

Keeley, F. W., C. M. Bellingham and K. A. Woodhouse (2002). "Elastin as a self-organizing biomaterial: use of recombinantly expressed human elastin polypeptides as a model for investigations of structure and self-assembly of elastin." Philos Trans R Soc Lond B Biol Sci **357**(1418): 185-189.

Kehat, I., D. Kenyagin-Karsenti, M. Snir, H. Segev, M. Amit, A. Gepstein, E. Livne, O. Binah, J. Itskovitz-Eldor and L. Gepstein (2001). "Human embryonic stem cells can differentiate into myocytes with structural and functional properties of cardiomyocytes." J Clin Invest **108**(3): 407-414.

Kensah, G., I. Gruh, J. Viering, H. Schumann, J. Dahlmann, H. Meyer, D. Skvorc, A. Bar, P. Akhyari, A. Heisterkamp, A. Haverich and U. Martin (2011). "A novel miniaturized multimodal bioreactor for continuous in situ assessment of bioartificial cardiac tissue during stimulation and maturation." Tissue Eng Part C Methods **17**(4): 463-473.

Kensah, G., A. Roa Lara, J. Dahlmann, R. Zweigerdt, K. Schwanke, J. Hegermann, D. Skvorc, A. Gawol, A. Azizian, S. Wagner, L. S. Maier, A. Krause, G. Drager, M. Ochs, A. Haverich, I. Gruh and U. Martin (2013). "Murine and human pluripotent stem cell-derived cardiac bodies form contractile myocardial tissue in vitro." Eur Heart J **34**(15): 1134-1146.

Khademhosseini, A., G. Eng, J. Yeh, P. A. Kucharczyk, R. Langer, G. Vunjak-Novakovic and M. Radisic (2007). "Microfluidic patterning for fabrication of contractile cardiac organoids." Biomed Microdevices **9**(2): 149-157.

Kikuchi, K., J. E. Holdway, A. A. Werdich, R. M. Anderson, Y. Fang, G. F. Egnaczyk, T. Evans, C. A. Macrae, D. Y. Stainier and K. D. Poss (2010). "Primary contribution to zebrafish heart regeneration by gata4(+) cardiomyocytes." Nature **464**(7288): 601-605.

Kim, D., C. H. Kim, J. I. Moon, Y. G. Chung, M. Y. Chang, B. S. Han, S. Ko, E. Yang, K. Y. Cha, R. Lanza and K. S. Kim (2009). "Generation of human induced pluripotent stem cells by direct delivery of reprogramming proteins." Cell Stem Cell **4**(6): 472-476.

Kim, D. H., E. A. Lipke, P. Kim, R. Cheong, S. Thompson, M. Delannoy, K. Y. Suh, L. Tung and A. Levchenko (2010). "Nanoscale cues regulate the structure and function of macroscopic cardiac tissue constructs." Proc Natl Acad Sci U S A **107**(2): 565-570.

Kispert, A. and B. G. Herrmann (1994). "Immunohistochemical analysis of the Brachyury protein in wild-type and mutant mouse embryos." Dev Biol **161**(1): 179-193.

Kispert, A., B. Koschorz and B. G. Herrmann (1995). "The T protein encoded by Brachyury is a tissue-specific transcription factor." EMBO J **14**(19): 4763-4772.

Kita-Matsuo, H., M. Barcova, N. Prigozhina, N. Salomonis, K. Wei, J. G. Jacot, B. Nelson, S. Spiering, R. Haverslag, C. Kim, M. Talantova, R. Bajpai, D. Calzolari, A. Terskikh, A. D. McCulloch, J. H. Price, B. R. Conklin, H. S. Chen and M. Mercola (2009). "Lentiviral vectors and protocols for creation of stable hESC lines for fluorescent tracking and drug resistance selection of cardiomyocytes." PLoS One **4**(4): e5046.

Kitajima, S., A. Takagi, T. Inoue and Y. Saga (2000). "MesP1 and MesP2 are essential for the development of cardiac mesoderm." Development **127**(15): 3215-3226.

Kitisin, K., T. Saha, T. Blake, N. Golestaneh, M. Deng, C. Kim, Y. Tang, K. Shetty, B. Mishra and L. Mishra (2007). "Tgf-Beta signaling in development." Sci STKE **2007**(399): cm1.

Klug, M. G., M. H. Soonpaa, G. Y. Koh and L. J. Field (1996). "Genetically selected cardiomyocytes from differentiating embronic stem cells form stable intracardiac grafts." J Clin Invest **98**(1): 216-224.

Kofidis, T., P. Akhyari, J. Boublik, P. Theodorou, U. Martin, A. Ruhparwar, S. Fischer, T. Eschenhagen, H. P. Kubis, T. Kraft, R. Leyh and A. Haverich (2002). "In vitro engineering of heart muscle: artificial myocardial tissue." J Thorac Cardiovasc Surg **124**(1): 63-69.

Kofidis, T., P. Akhyari, B. Wachsmann, K. Mueller-Stahl, J. Boublik, A. Ruhparwar, H. Mertsching, L. Balsam, R. Robbins and A. Haverich (2003). "Clinically established hemostatic scaffold (tissue fleece) as biomatrix in tissue- and organ-engineering research." Tissue Eng **9**(3): 517-523.

Kohl, P. (2003). "Heterogeneous cell coupling in the heart: an electrophysiological role for fibroblasts." Circ Res **93**(5): 381-383.

Koivisto, H., M. Hyvarinen, A. M. Stromberg, J. Inzunza, E. Matilainen, M. Mikkola, O. Hovatta and H. Teerijoki (2004). "Cultures of human embryonic stem cells: serum replacement medium or serum-containing media and the effect of basic fibroblast growth factor." Reprod Biomed Online **9**(3): 330-337.

Kolossov, E., Z. Lu, I. Drobinskaya, N. Gassanov, Y. Duan, H. Sauer, O. Manzke, W. Bloch, H. Bohlen, J. Hescheler and B. K. Fleischmann (2005). "Identification and characterization of embryonic stem cell-derived pacemaker and atrial cardiomyocytes." FASEB J **19**(6): 577-579.

Kontrogianni-Konstantopoulos, A., M. A. Ackermann, A. L. Bowman, S. V. Yap and R. J. Bloch (2009). "Muscle giants: molecular scaffolds in sarcomerogenesis." Physiol Rev **89**(4): 1217-1267.

Kuznetsova, T., L. Herbots, T. Richart, J. D'Hooge, L. Thijs, R. H. Fagard, M. C. Herregods and J. A. Staessen (2008). "Left ventricular strain and strain rate in a general population." Eur Heart J **29**(16): 2014-2023.

Laflamme, M. A., K. Y. Chen, A. V. Naumova, V. Muskheli, J. A. Fugate, S. K. Dupras, H. Reinecke, C. Xu, M. Hassanipour, S. Police, C. O'Sullivan, L. Collins, Y. Chen, E. Minami, E. A. Gill, S. Ueno, C. Yuan, J. Gold and C. E. Murry (2007).

"Cardiomyocytes derived from human embryonic stem cells in pro-survival factors enhance function of infarcted rat hearts." Nat Biotechnol **25**(9): 1015-1024.

Laflamme, M. A., J. Gold, C. Xu, M. Hassanipour, E. Rosler, S. Police, V. Muskheli and C. E. Murry (2005). "Formation of human myocardium in the rat heart from human embryonic stem cells." Am J Pathol **167**(3): 663-671.

Lanier, M., D. Schade, E. Willems, M. Tsuda, S. Spiering, J. Kalisiak, M. Mercola and J. R. Cashman (2012). "Wnt inhibition correlates with human embryonic stem cell cardiomyogenesis: a structure-activity relationship study based on inhibitors for the Wnt response." J Med Chem **55**(2): 697-708.

Lee, C. H., A. Singla and Y. Lee (2001). "Biomedical applications of collagen." Int J Pharm **221**(1-2): 1-22.

Lee, E. J., E. Kim do, E. U. Azeloglu and K. D. Costa (2008). "Engineered cardiac organoid chambers: toward a functional biological model ventricle." Tissue Eng Part A **14**(2): 215-225.

LeGrice, I. J., B. H. Smaill, L. Z. Chai, S. G. Edgar, J. B. Gavin and P. J. Hunter (1995). "Laminar structure of the heart: ventricular myocyte arrangement and connective tissue architecture in the dog." Am J Physiol **269**(2 Pt 2): H571-582.

Leor, J., S. Aboulafia-Etzion, A. Dar, L. Shapiro, I. M. Barbash, A. Battler, Y. Granot and S. Cohen (2000). "Bioengineered cardiac grafts: A new approach to repair the infarcted myocardium?" Circulation **102**(19 Suppl 3): III56-61.

Leor, J. and S. Cohen (2004). "Myocardial tissue engineering: creating a muscle patch for a wounded heart." Ann N Y Acad Sci **1015**: 312-319.

Li, B. and V. Daggett (2002). "Molecular basis for the extensibility of elastin." J Muscle Res Cell Motil **23**(5-6): 561-573.

Li, R. K., Z. Q. Jia, R. D. Weisel, D. A. Mickle, A. Choi and T. M. Yau (1999). "Survival and function of bioengineered cardiac grafts." Circulation **100**(19 Suppl): II63-69.

Li, W., W. Wei, S. Zhu, J. Zhu, Y. Shi, T. Lin, E. Hao, A. Hayek, H. Deng and S. Ding (2009). "Generation of rat and human induced pluripotent stem cells by combining genetic reprogramming and chemical inhibitors." Cell Stem Cell **4**(1): 16-19.

Lian, X., C. Hsiao, G. Wilson, K. Zhu, L. B. Hazeltine, S. M. Azarin, K. K. Raval, J. Zhang, T. J. Kamp and S. P. Palecek (2012). "Robust cardiomyocyte differentiation from human pluripotent stem cells via temporal modulation of canonical Wnt signaling." Proc Natl Acad Sci U S A **109**(27): E1848-1857.

Lian, X., J. Zhang, K. Zhu, T. J. Kamp and S. P. Palecek (2013). "Insulin inhibits cardiac mesoderm, not mesendoderm, formation during cardiac differentiation of human pluripotent stem cells and modulation of canonical Wnt signaling can rescue this inhibition." Stem Cells **31**(3): 447-457.

Lian, X., J. Zhang, S. M. Azarin, K. Zhu, L. B. Hazeltine, X. Bao, C. Hsiao, T. J. Kamp and S. P. Palecek (2013). "Directed cardiomyocyte differentiation from human pluripotent stem cells by modulating Wnt/beta-catenin signaling under fully defined conditions." Nat Protoc **8**(1): 162-175.

Lien, C. L., C. Wu, B. Mercer, R. Webb, J. A. Richardson and E. N. Olson (1999). "Control of early cardiac-specific transcription of Nkx2-5 by a GATA-dependent enhancer." Development **126**(1): 75-84.

Lister, R., M. Pelizzola, Y. S. Kida, R. D. Hawkins, J. R. Nery, G. Hon, J. Antosiewicz-Bourget, R. O'Malley, R. Castanon, S. Klugman, M. Downes, R. Yu, R. Stewart, B. Ren, J. A. Thomson, R. M. Evans and J. R. Ecker (2011). "Hotspots of aberrant epigenomic reprogramming in human induced pluripotent stem cells." Nature **471**(7336): 68-73.

Liu, H., F. Zhu, J. Yong, P. Zhang, P. Hou, H. Li, W. Jiang, J. Cai, M. Liu, K. Cui, X. Qu, T. Xiang, D. Lu, X. Chi, G. Gao, W. Ji, M. Ding and H. Deng (2008). "Generation of induced pluripotent stem cells from adult rhesus monkey fibroblasts." Cell Stem Cell **3**(6): 587-590.

Liu, J., J. D. Fu, C. W. Siu and R. A. Li (2007). "Functional sarcoplasmic reticulum for calcium handling of human embryonic stem cell-derived cardiomyocytes: insights for driven maturation." Stem Cells **25**(12): 3038-3044.

Losordo, D. W., P. R. Vale, J. F. Symes, C. H. Dunnington, D. D. Esakof, M. Maysky, A. B. Ashare, K. Lathi and J. M. Isner (1998). "Gene therapy for myocardial angiogenesis: initial clinical results with direct myocardial injection of phVEGF165 as sole therapy for myocardial ischemia." Circulation **98**(25): 2800-2804.

Louault, C., N. Benamer, J. F. Faivre, D. Potreau and J. Bescond (2008). "Implication of connexins 40 and 43 in functional coupling between mouse cardiac fibroblasts in primary culture." Biochim Biophys Acta **1778**(10): 2097-2104.

Lough, J. and Y. Sugi (2000). "Endoderm and heart development." Dev Dyn **217**(4): 327-342.

Lu, H. R., E. Vlaminckx, A. N. Hermans, J. Rohrbacher, K. Van Ammel, R. Towart, M. Pugsley and D. J. Gallacher (2008). "Predicting drug-induced changes in QT interval and arrhythmias: QT-shortening drugs point to gaps in the ICHS7B Guidelines." Br J Pharmacol **154**(7): 1427-1438.

Ludwig, T. E., V. Bergendahl, M. E. Levenstein, J. Yu, M. D. Probasco and J. A. Thomson (2006). "Feeder-independent culture of human embryonic stem cells." Nat Methods **3**(8): 637-646.

Lyons, F., S. Partap and F. J. O'Brien (2008). "Part 1: scaffolds and surfaces." Technol Health Care **16**(4): 305-317.

Mahdavi, V., A. P. Chambers and B. Nadal-Ginard (1984). "Cardiac alpha- and beta-myosin heavy chain genes are organized in tandem." Proc Natl Acad Sci U S A **81**(9): 2626-2630.

Maherali, N. and K. Hochedlinger (2008). "Guidelines and techniques for the generation of induced pluripotent stem cells." Cell Stem Cell **3**(6): 595-605.

Mahoney, L. T., W. Smith, M. P. Noel, M. Florentine, D. J. Skorton and S. M. Collins (1987). "Measurement of right ventricular volume using cine computed tomography." Invest Radiol **22**(6): 451-455.

Malliaras, K. and E. Marban (2014). "Moving beyond surrogate endpoints in cell therapy trials for heart disease." Stem Cells Transl Med **3**(1): 2-6.

Mann, M. J. and V. J. Dzau (2000). "Therapeutic applications of transcription factor decoy oligonucleotides." J Clin Invest **106**(9): 1071-1075.

Martin, R. L., J. S. McDermott, H. J. Salmen, J. Palmatier, B. F. Cox and G. A. Gintant (2004). "The utility of hERG and repolarization assays in evaluating delayed cardiac repolarization: influence of multi-channel block." J Cardiovasc Pharmacol **43**(3): 369-379.

Martinez-Fernandez, A., T. J. Nelson, S. Yamada, S. Reyes, A. E. Alekseev, C. Perez-Terzic, Y. Ikeda and A. Terzic (2009). "iPS programmed without c-MYC yield proficient cardiogenesis for functional heart chimerism." Circ Res **105**(7): 648-656.

Massai, D., G. Cerino, D. Gallo, F. Pennella, M. A. Deriu, A. Rodriguez, F. M. Montevecchi, C. Bignardi, A. Audenino and U. Morbiducci (2013). "Bioreactors as engineering support to treat cardiac muscle and vascular disease." J Healthc Eng **4**(3): 329-370.

Mathers, C. D. and D. Loncar (2006). "Projections of global mortality and burden of disease from 2002 to 2030." PLoS Med **3**(11): e442.

Mauritz, C., K. Schwanke, M. Reppel, S. Neef, K. Katsirntaki, L. S. Maier, F. Nguemo, S. Menke, M. Haustein, J. Hescheler, G. Hasenfuss and U. Martin (2008). "Generation of functional murine cardiac myocytes from induced pluripotent stem cells." Circulation **118**(5): 507-517.

McDevitt, T. C., J. C. Angello, M. L. Whitney, H. Reinecke, S. D. Hauschka, C. E. Murry and P. S. Stayton (2002). "In vitro generation of differentiated cardiac myofibers on micropatterned laminin surfaces." J Biomed Mater Res **60**(3): 472-479.

McDevitt, T. C., K. A. Woodhouse, S. D. Hauschka, C. E. Murry and P. S. Stayton (2003). "Spatially organized layers of cardiomyocytes on biodegradable polyurethane films for myocardial repair." J Biomed Mater Res A **66**(3): 586-595.

Melo, L. G., A. S. Pachori, D. Kong, M. Gnecchi, K. Wang, R. E. Pratt and V. J. Dzau (2004). "Molecular and cell-based therapies for protection, rescue, and repair of ischemic myocardium: reasons for cautious optimism." Circulation **109**(20): 2386-2393.

Menasche, P. (2004). "Skeletal myoblast transplantation for cardiac repair." Expert Rev Cardiovasc Ther **2**(1): 21-28.

Menasche, P. (2008). "Skeletal myoblasts and cardiac repair." J Mol Cell Cardiol **45**(4): 545-553.

Menasche, P., O. Alfieri, S. Janssens, W. McKenna, H. Reichenspurner, L. Trinquart, J. T. Vilquin, J. P. Marolleau, B. Seymour, J. Larghero, S. Lake, G. Chatellier, S. Solomon, M. Desnos and A. A. Hagege (2008). "The Myoblast Autologous Grafting in Ischemic Cardiomyopathy (MAGIC) trial: first randomized placebo-controlled study of myoblast transplantation." Circulation **117**(9): 1189-1200.

Menasche, P., A. A. Hagege, J. T. Vilquin, M. Desnos, E. Abergel, B. Pouzet, A. Bel, S. Sarateanu, M. Scorsin, K. Schwartz, P. Bruneval, M. Benbunan, J. P. Marolleau and D. Duboc (2003). "Autologous skeletal myoblast transplantation for severe postinfarction left ventricular dysfunction." J Am Coll Cardiol **41**(7): 1078-1083.

Messina, E., L. De Angelis, G. Frati, S. Morrone, S. Chimenti, F. Fiordaliso, M. Salio, M. Battaglia, M. V. Latronico, M. Coletta, E. Vivarelli, L. Frati, G. Cossu and A. Giacomello (2004). "Isolation and expansion of adult cardiac stem cells from human and murine heart." Circ Res **95**(9): 911-921.

Miao, W., Z. Luo, R. N. Kitsis and K. Walsh (2000). "Intracoronary, adenovirus-mediated Akt gene transfer in heart limits infarct size following ischemia-reperfusion injury in vivo." J Mol Cell Cardiol **32**(12): 2397-2402.

Millman, J. R., J. H. Tan and C. K. Colton (2009). "The effects of low oxygen on self-renewal and differentiation of embryonic stem cells." Curr Opin Organ Transplant **14**(6): 694-700.

Miyazaki, H., H. Watanabe, T. Kitayama, M. Nishida, Y. Nishi, K. Sekiya, H. Suganami and K. Yamamoto (2005). "QT PRODACT: sensitivity and specificity of the canine telemetry assay for detecting drug-induced QT interval prolongation." J Pharmacol Sci **99**(5): 523-529.

Miyazono, K., Y. Kamiya and M. Morikawa (2010). "Bone morphogenetic protein receptors and signal transduction." J Biochem **147**(1): 35-51.

Mulieri, L. A., G. Hasenfuss, B. Leavitt, P. D. Allen and N. R. Alpert (1992). "Altered myocardial force-frequency relation in human heart failure." Circulation **85**(5): 1743-1750.

Muller-Ehmsen, J., K. L. Peterson, L. Kedes, P. Whittaker, J. S. Dow, T. I. Long, P. W. Laird and R. A. Kloner (2002). "Rebuilding a damaged heart: long-term survival of transplanted neonatal rat cardiomyocytes after myocardial infarction and effect on cardiac function." Circulation **105**(14): 1720-1726.

Muller-Ehmsen, J., P. Whittaker, R. A. Kloner, J. S. Dow, T. Sakoda, T. I. Long, P. W. Laird and L. Kedes (2002). "Survival and development of neonatal rat cardiomyocytes transplanted into adult myocardium." J Mol Cell Cardiol **34**(2): 107-116.

Mohr, J. C., J. Zhang, S. M. Azarin, A. G. Soerens, J. J. de Pablo, J. A. Thomson, G. E. Lyons, S. P. Palecek and T. J. Kamp (2010). "The microwell control of embryoid body size in order to regulate cardiac differentiation of human embryonic stem cells." Biomaterials **31**(7): 1885-1893.

Mummery, C. (2010). "Sorting cardiomyocytes: a simple solution after all?" Nat Methods **7**(1): 40-42.

Mummery, C., D. Ward, C. E. van den Brink, S. D. Bird, P. A. Doevendans, T. Opthof, A. Brutel de la Riviere, L. Tertoolen, M. van der Heyden and M. Pera (2002). "Cardiomyocyte differentiation of mouse and human embryonic stem cells." J Anat **200**(Pt 3): 233-242.

Mummery, C., D. Ward-van Oostwaard, P. Doevendans, R. Spijker, S. van den Brink, R. Hassink, M. van der Heyden, T. Opthof, M. Pera, A. B. de la Riviere, R. Passier and L. Tertoolen (2003). "Differentiation of human embryonic stem cells to cardiomyocytes: role of coculture with visceral endoderm-like cells." Circulation **107**(21): 2733-2740.

Murry, C. E. and G. Keller (2008). "Differentiation of embryonic stem cells to clinically relevant populations: lessons from embryonic development." Cell **132**(4): 661-680.

Nag, A. C. (1980). "Study of non-muscle cells of the adult mammalian heart: a fine structural analysis and distribution." Cytobios **28**(109): 41-61.

Naito, H., I. Melnychenko, M. Didie, K. Schneiderbanger, P. Schubert, S. Rosenkranz, T. Eschenhagen and W. H. Zimmermann (2006). "Optimizing engineered heart tissue for therapeutic applications as surrogate heart muscle." Circulation **114**(1 Suppl): I72-78.

Nam, Y. J., K. Song, X. Luo, E. Daniel, K. Lambeth, K. West, J. A. Hill, J. M. DiMaio, L. A. Baker, R. Bassel-Duby and E. N. Olson (2013). "Reprogramming of human fibroblasts toward a cardiac fate." Proc Natl Acad Sci U S A **110**(14): 5588-5593.

Narazaki, G., H. Uosaki, M. Teranishi, K. Okita, B. Kim, S. Matsuoka, S. Yamanaka and J. K. Yamashita (2008). "Directed and systematic differentiation of cardiovascular cells from mouse induced pluripotent stem cells." Circulation **118**(5): 498-506.

Narmoneva, D. A., R. Vukmirovic, M. E. Davis, R. D. Kamm and R. T. Lee (2004). "Endothelial cells promote cardiac myocyte survival and spatial reorganization: implications for cardiac regeneration." Circulation **110**(8): 962-968.

Narsinh, K. H., N. Sun, V. Sanchez-Freire, A. S. Lee, P. Almeida, S. Hu, T. Jan, K. D. Wilson, D. Leong, J. Rosenberg, M. Yao, R. C. Robbins and J. C. Wu (2011). "Single cell transcriptional profiling reveals heterogeneity of human induced pluripotent stem cells." J Clin Invest **121**(3): 1217-1221.

Nielsen, P. M., I. J. Le Grice, B. H. Smaill and P. J. Hunter (1991). "Mathematical model of geometry and fibrous structure of the heart." Am J Physiol **260**(4 Pt 2): H1365-1378.

Noseda, M., T. Peterkin, F. C. Simoes, R. Patient and M. D. Schneider (2011). "Cardiopoietic factors: extracellular signals for cardiac lineage commitment." Circ Res **108**(1): 129-152.

Nuccitelli, R. (1992). "Endogenous ionic currents and DC electric fields in multicellular animal tissues." Bioelectromagnetics **Suppl 1**: 147-157.

Nusse, R., A. Brown, J. Papkoff, P. Scambler, G. Shackleford, A. McMahon, R. Moon and H. Varmus (1991). "A new nomenclature for int-1 and related genes: the Wnt gene family." Cell **64**(2): 231.

Odedra D, Chiu L, Reis L, Rask F, Chiang K, Radisic M. Cardiac Tissue Engineering, in: Burdick JA, Mauck RL (eds). Biomaterials for Tissue Engineering Applications. A Review of the Past and Future Trends. 2011. Chapter 15).

Okita, K., H. Hong, K. Takahashi and S. Yamanaka (2010). "Generation of mouse-induced pluripotent stem cells with plasmid vectors." Nat Protoc **5**(3): 418-428.

Olmer, R., A. Lange, S. Selzer, C. Kasper, A. Haverich, U. Martin and R. Zweigerdt (2012). "Suspension culture of human pluripotent stem cells in controlled, stirred bioreactors." Tissue Eng Part C Methods **18**(10): 772-784.

Olson, E. N. and M. D. Schneider (2003). "Sizing up the heart: development redux in disease." Genes Dev **17**(16): 1937-1956.

Orecchia, A., P. M. Lacal, C. Schietroma, V. Morea, G. Zambruno and C. M. Failla (2003). "Vascular endothelial growth factor receptor-1 is deposited in the extracellular matrix by endothelial cells and is a ligand for the alpha 5 beta 1 integrin." J Cell Sci **116**(Pt 17): 3479-3489.

Orlic, D., J. Kajstura, S. Chimenti, I. Jakoniuk, S. M. Anderson, B. Li, J. Pickel, R. McKay, B. Nadal-Ginard, D. M. Bodine, A. Leri and P. Anversa (2001). "Bone marrow cells regenerate infarcted myocardium." Nature **410**(6829): 701-705.

Orlic, D., J. Kajstura, S. Chimenti, F. Limana, I. Jakoniuk, F. Quaini, B. Nadal-Ginard, D. M. Bodine, A. Leri and P. Anversa (2001). "Mobilized bone marrow cells repair the infarcted heart, improving function and survival." Proc Natl Acad Sci U S A **98**(18): 10344-10349.

Osafune, K., L. Caron, M. Borowiak, R. J. Martinez, C. S. Fitz-Gerald, Y. Sato, C. A. Cowan, K. R. Chien and D. A. Melton (2008). "Marked differences in differentiation propensity among human embryonic stem cell lines." Nat Biotechnol **26**(3): 313-315.

Ott, H. C., T. S. Matthiesen, S. K. Goh, L. D. Black, S. M. Kren, T. I. Netoff and D. A. Taylor (2008). "Perfusion-decellularized matrix: using nature's platform to engineer a bioartificial heart." Nat Med **14**(2): 213-221.

Paige, S. L., T. Osugi, O. K. Afanasiev, L. Pabon, H. Reinecke and C. E. Murry (2010). "Endogenous Wnt/beta-catenin signaling is required for cardiac differentiation in human embryonic stem cells." PLoS One **5**(6): e11134.

Pandya, N., D. Santani and S. Jain (2005). "Role of mitogen-activated protein (MAP) kinases in cardiovascular diseases." Cardiovasc Drug Rev **23**(3): 247-254.

Papadaki, M., N. Bursac, R. Langer, J. Merok, G. Vunjak-Novakovic and L. E. Freed (2001). "Tissue engineering of functional cardiac muscle: molecular, structural, and electrophysiological studies." Am J Physiol Heart Circ Physiol **280**(1): H168-178.

Park, I. H., N. Arora, H. Huo, N. Maherali, T. Ahfeldt, A. Shimamura, M. W. Lensch, C. Cowan, K. Hochedlinger and G. Q. Daley (2008). "Disease-specific induced pluripotent stem cells." Cell **134**(5): 877-886.

Passier, R., D. W. Oostwaard, J. Snapper, J. Kloots, R. J. Hassink, E. Kuijk, B. Roelen, A. B. de la Riviere and C. Mummery (2005). "Increased cardiomyocyte differentiation from human embryonic stem cells in serum-free cultures." Stem Cells **23**(6): 772-780.

Passier, R., L. W. van Laake and C. L. Mummery (2008). "Stem-cell-based therapy and lessons from the heart." Nature **453**(7193): 322-329.

Pasumarthi, K. B. and L. J. Field (2002). "Cardiomyocyte cell cycle regulation." Circ Res **90**(10): 1044-1054.

Pera, M. F., J. Andrade, S. Houssami, B. Reubinoff, A. Trounson, E. G. Stanley, D. Ward-van Oostwaard and C. Mummery (2004). "Regulation of human embryonic stem cell differentiation by BMP-2 and its antagonist noggin." J Cell Sci **117**(Pt 7): 1269-1280.

Piper, H. M., S. L. Jacobson and P. Schwartz (1988). "Determinants of cardiomyocyte development in long-term primary culture." J Mol Cell Cardiol **20**(9): 825-835.

Planat-Benard, V., C. Menard, M. Andre, M. Puceat, A. Perez, J. M. Garcia-Verdugo, L. Penicaud and L. Casteilla (2004). "Spontaneous cardiomyocyte differentiation from adipose tissue stroma cells." Circ Res **94**(2): 223-229.

Pok, S. and J. G. Jacot (2011). "Biomaterials advances in patches for congenital heart defect repair." J Cardiovasc Transl Res **4**(5): 646-654.

Pollard, C. E., J. P. Valentin and T. G. Hammond (2008). "Strategies to reduce the risk of drug-induced QT interval prolongation: a pharmaceutical company perspective." Br J Pharmacol **154**(7): 1538-1543.

Polo, J. M., S. Liu, M. E. Figueroa, W. Kulalert, S. Eminli, K. Y. Tan, E. Apostolou, M. Stadtfeld, Y. Li, T. Shioda, S. Natesan, A. J. Wagers, A. Melnick, T. Evans and K. Hochedlinger (2010). "Cell type of origin influences the molecular and functional properties of mouse induced pluripotent stem cells." Nat Biotechnol **28**(8): 848-855.

Pope, A. J., G. B. Sands, B. H. Smaill and I. J. LeGrice (2008). "Three-dimensional transmural organization of perimysial collagen in the heart." Am J Physiol Heart Circ Physiol **295**(3): H1243-H1252.

Porrello, E. R., A. I. Mahmoud, E. Simpson, J. A. Hill, J. A. Richardson, E. N. Olson and H. A. Sadek (2011). "Transient regenerative potential of the neonatal mouse heart." Science **331**(6020): 1078-1080.

Portner, R., S. Nagel-Heyer, C. Goepfert, P. Adamietz and N. M. Meenen (2005). "Bioreactor design for tissue engineering." J Biosci Bioeng **100**(3): 235-245.

Prockop, D. J. and K. I. Kivirikko (1995). "Collagens: molecular biology, diseases, and potentials for therapy." Annu Rev Biochem **64**: 403-434.

Ptaszek, L. M., M. Mansour, J. N. Ruskin and K. R. Chien (2012). "Towards regenerative therapy for cardiac disease." Lancet **379**(9819): 933-942.

Qian, L., Y. Huang, C. I. Spencer, A. Foley, V. Vedantham, L. Liu, S. J. Conway, J. D. Fu and D. Srivastava (2012). "In vivo reprogramming of murine cardiac fibroblasts into induced cardiomyocytes." Nature **485**(7400): 593-598.

Radisic, M., M. Euloth, L. Yang, R. Langer, L. E. Freed and G. Vunjak-Novakovic (2003). "High-density seeding of myocyte cells for cardiac tissue engineering." Biotechnol Bioeng **82**(4): 403-414.

Radisic, M., A. Marsano, R. Maidhof, Y. Wang and G. Vunjak-Novakovic (2008). "Cardiac tissue engineering using perfusion bioreactor systems." Nat Protoc **3**(4): 719-738.

Radisic, M., H. Park, F. Chen, J. E. Salazar-Lazzaro, Y. Wang, R. Dennis, R. Langer, L. E. Freed and G. Vunjak-Novakovic (2006). "Biomimetic approach to cardiac tissue engineering: oxygen carriers and channeled scaffolds." Tissue Eng **12**(8): 2077-2091.

Radisic, M., H. Park, H. Shing, T. Consi, F. J. Schoen, R. Langer, L. E. Freed and G. Vunjak-Novakovic (2004). "Functional assembly of engineered myocardium by electrical stimulation of cardiac myocytes cultured on scaffolds." Proc Natl Acad Sci U S A **101**(52): 18129-18134.

Radisic M, Sefton MV. Cardiac Tissue, in: Atala A, Lanza R, Thomson JA, Nerem R (eds). Principles Of Regenerative Medicine Second Edition. Academic Press. 2011. Chapter 48.

Raines, E. W. (2000). "The extracellular matrix can regulate vascular cell migration, proliferation, and survival: relationships to vascular disease." Int J Exp Pathol **81**(3): 173-182.

Rais, Y., A. Zviran, S. Geula, O. Gafni, E. Chomsky, S. Viukov, A. A. Mansour, I. Caspi, V. Krupalnik, M. Zerbib, I. Maza, N. Mor, D. Baran, L. Weinberger, D. A. Jaitin, D. Lara-Astiaso, R. Blecher-Gonen, Z. Shipony, Z. Mukamel, T. Hagai, S. Gilad, D. Amann-Zalcenstein, A. Tanay, I. Amit, N. Novershtern and J. H. Hanna (2013). "Deterministic direct reprogramming of somatic cells to pluripotency." Nature **502**(7469): 65-70.

Rajala, K., Pekkanen-Mattila, M., & Aalto-Setala, K. (2011). "Cardiac differentiation of pluripotent stem cells." Stem Cells Int, 2011, 383709. doi: 10.4061/2011/383709

Ravichandran, R., J. R. Venugopal, S. Sundarrajan, S. Mukherjee, R. Sridhar and S. Ramakrishna (2013). "Expression of cardiac proteins in neonatal cardiomyocytes on PGS/fibrinogen core/shell substrate for Cardiac tissue engineering." Int J Cardiol **167**(4): 1461-1468.

Raya, A., I. Rodriguez-Piza, B. Aran, A. Consiglio, P. N. Barri, A. Veiga and J. C. Izpisua Belmonte (2008). "Generation of cardiomyocytes from new human embryonic stem cell lines derived from poor-quality blastocysts." Cold Spring Harb Symp Quant Biol **73**: 127-135.

Raya, A., I. Rodriguez-Piza, G. Guenechea, R. Vassena, S. Navarro, M. J. Barrero, A. Consiglio, M. Castella, P. Rio, E. Sleep, F. Gonzalez, G. Tiscornia, E. Garreta, T. Aasen, A. Veiga, I. M. Verma, J. Surralles, J. Bueren and J. C. Izpisua Belmonte (2009). "Disease-corrected haematopoietic progenitors from Fanconi anaemia induced pluripotent stem cells." Nature **460**(7251): 53-59.

Redfern, W. S., L. Carlsson, A. S. Davis, W. G. Lynch, I. MacKenzie, S. Palethorpe, P. K. Siegl, I. Strang, A. T. Sullivan, R. Wallis, A. J. Camm and T. G. Hammond (2003). "Relationships between preclinical cardiac electrophysiology, clinical QT interval prolongation and torsade de pointes for a broad range of drugs: evidence for a provisional safety margin in drug development." Cardiovasc Res **58**(1): 32-45.

Reffelmann, T. and R. A. Kloner (2003). "Cellular cardiomyoplasty--cardiomyocytes, skeletal myoblasts, or stem cells for regenerating myocardium and treatment of heart failure?" Cardiovasc Res **58**(2): 358-368.

Reifers, F., E. C. Walsh, S. Leger, D. Y. Stainier and M. Brand (2000). "Induction and differentiation of the zebrafish heart requires fibroblast growth factor 8 (fgf8/acerebellar)." Development **127**(2): 225-235.

Reppel, M., F. Pillekamp, Z. J. Lu, M. Halbach, K. Brockmeier, B. K. Fleischmann and J. Hescheler (2004). "Microelectrode arrays: a new tool to measure embryonic heart activity." J Electrocardiol **37 Suppl**: 104-109.

Reubinoff, B. E., M. F. Pera, C. Y. Fong, A. Trounson and A. Bongso (2000). "Embryonic stem cell lines from human blastocysts: somatic differentiation in vitro." Nat Biotechnol **18**(4): 399-404.

Roden, D. M. (2004). "Drug-induced prolongation of the QT interval." N Engl J Med **350**(10): 1013-1022.

Roger, V. L., A. S. Go, D. M. Lloyd-Jones, E. J. Benjamin, J. D. Berry, W. B. Borden, D. M. Bravata, S. Dai, E. S. Ford, C. S. Fox, H. J. Fullerton, C. Gillespie, S. M. Hailpern, J. A. Heit, V. J. Howard, B. M. Kissela, S. J. Kittner, D. T. Lackland, J. H. Lichtman, L. D. Lisabeth, D. M. Makuc, G. M. Marcus, A. Marelli, D. B. Matchar, C. S. Moy, D. Mozaffarian, M. E. Mussolino, G. Nichol, N. P. Paynter, E. Z. Soliman, P. D. Sorlie, N. Sotoodehnia, T. N. Turan, S. S. Virani, N. D. Wong, D. Woo, M. B. Turner, C. American Heart Association Statistics and S. Stroke Statistics (2012). "Executive summary: heart disease and stroke statistics--2012 update: a report from the American Heart Association." Circulation **125**(1): 188-197.

Rosler, E. S., G. J. Fisk, X. Ares, J. Irving, T. Miura, M. S. Rao and M. K. Carpenter (2004). "Long-term culture of human embryonic stem cells in feeder-free conditions." Dev Dyn **229**(2): 259-274.

Rudy-Reil, D. and J. Lough (2004). "Avian precardiac endoderm/mesoderm induces cardiac myocyte differentiation in murine embryonic stem cells." Circ Res **94**(12): e107-116.

Rust, W., T. Balakrishnan and R. Zweigerdt (2009). "Cardiomyocyte enrichment from human embryonic stem cell cultures by selection of ALCAM surface expression." Regen Med **4**(2): 225-237.

Rybin, V. O. and S. F. Steinberg (1994). "Protein kinase C isoform expression and regulation in the developing rat heart." Circ Res **74**(2): 299-309.

Sachinidis, A., B. K. Fleischmann, E. Kolossov, M. Wartenberg, H. Sauer and J. Hescheler (2003). "Cardiac specific differentiation of mouse embryonic stem cells." Cardiovasc Res **58**(2): 278-291.

Saggin, L., L. Gorza, S. Ausoni and S. Schiaffino (1989). "Troponin I switching in the developing heart." J Biol Chem **264**(27): 16299-16302.

Sanchez-Danes, A., Y. Richaud-Patin, I. Carballo-Carbajal, S. Jimenez-Delgado, C. Caig, S. Mora, C. Di Guglielmo, M. Ezquerra, B. Patel, A. Giralt, J. M. Canals, M. Memo, J. Alberch, J. Lopez-Barneo, M. Vila, A. M. Cuervo, E. Tolosa, A. Consiglio and A. Raya (2012). "Disease-specific phenotypes in dopamine neurons from human iPS-based models of genetic and sporadic Parkinson's disease." EMBO Mol Med **4**(5): 380-395.

Saric, T., L. P. Frenzel and J. Hescheler (2008). "Immunological barriers to embryonic stem cell-derived therapies." Cells Tissues Organs **188**(1-2): 78-90.

Sartiani, L., E. Bettiol, F. Stillitano, A. Mugelli, E. Cerbai and M. E. Jaconi (2007). "Developmental changes in cardiomyocytes differentiated from human embryonic stem cells: a molecular and electrophysiological approach." Stem Cells **25**(5): 1136-1144.

Satin, J., I. Itzhaki, S. Rapoport, E. A. Schroder, L. Izu, G. Arbel, R. Beyar, C. W. Balke, J. Schiller and L. Gepstein (2008). "Calcium handling in human embryonic stem cell-derived cardiomyocytes." Stem Cells **26**(8): 1961-1972.

Schaaf, S., A. Shibamiya, M. Mewe, A. Eder, A. Stohr, M. N. Hirt, T. Rau, W. H. Zimmermann, L. Conradi, T. Eschenhagen and A. Hansen (2011). "Human engineered heart tissue as a versatile tool in basic research and preclinical toxicology." PLoS One **6**(10): e26397.

Schaffer, W. and R. S. Williams (1986). "Age-dependent changes in expression of alpha 1-adrenergic receptors in rat myocardium." Biochem Biophys Res Commun **138**(1): 387-391.

Schneck D. An outline of cardiovascular structure and function, in: Bernhard Palsson, Jeffrey A. Hubbell, Robert Plonsey, Joseph D. Bronzino (eds). Tissue Engineering. CRC Press. 2003. I-1–I-12).

Schneck D. An outline of cardiovascular structure and function, in: Bernhard Palsson, Jeffrey A. Hubbell, Robert Plonsey, Joseph D. Bronzino (eds). Tissue Engineering. CRC Press. 2003. I-1–I-12) Klingensmith ME, Ern Chen L, Glasgow SC, Goers TA, Melby SJ. The Washington Manual of Surgery. Wolters Kluwer Health/Lippincott Williams & Wilkins. 2008

Schwarzbauer, J. E. (1991). "Fibronectin: from gene to protein." Curr Opin Cell Biol **3**(5): 786-791.

Schwarzkopf, R., M. Shachar, T. Dvir, Y. Dayan, R. Holbova, J. Leor and S. Cohen (2006). "Autospecies and post-myocardial infarction sera enhance the viability, proliferation, and maturation of 3D cardiac cell culture." Tissue Eng **12**(12): 3467-3475.

Segers, V. F. and R. T. Lee (2008). "Stem-cell therapy for cardiac disease." Nature **451**(7181): 937-942.

Semechkin, R. A., T. V. Abramihina and D. A. Isaev (2011). "Activin A suppresses induced formation of neuroectoderm in colonies of parthenogenetic stem cells in vitro." Bull Exp Biol Med **151**(4): 502-505.

Severs, N. J. (2000). "The cardiac muscle cell." Bioessays **22**(2): 188-199.

Shah, R. R. and L. M. Hondeghem (2005). "Refining detection of drug-induced proarrhythmia: QT interval and TRIaD." Heart Rhythm **2**(7): 758-772.

Shi, Y. and J. Massague (2003). "Mechanisms of TGF-beta signaling from cell membrane to the nucleus." Cell **113**(6): 685-700.

Shimizu, T., H. Sekine, J. Yang, Y. Isoi, M. Yamato, A. Kikuchi, E. Kobayashi and T. Okano (2006). "Polysurgery of cell sheet grafts overcomes diffusion limits to produce thick, vascularized myocardial tissues." FASEB J **20**(6): 708-710.

Shimizu, T., M. Yamato, Y. Isoi, T. Akutsu, T. Setomaru, K. Abe, A. Kikuchi, M. Umezu and T. Okano (2002). "Fabrication of pulsatile cardiac tissue grafts using a novel 3-dimensional cell sheet manipulation technique and temperature-responsive cell culture surfaces." Circ Res **90**(3): e40.

Showell, C., O. Binder and F. L. Conlon (2004). "T-box genes in early embryogenesis." Dev Dyn **229**(1): 201-218.

Si-Tayeb, K., F. K. Noto, A. Sepac, F. Sedlic, Z. J. Bosnjak, J. W. Lough and S. A. Duncan (2010). "Generation of human induced pluripotent stem cells by simple transient transfection of plasmid DNA encoding reprogramming factors." BMC Dev Biol **10**: 81.

Skottman, H. and O. Hovatta (2006). "Culture conditions for human embryonic stem cells." Reproduction **132**(5): 691-698.

Smith, R. R., L. Barile, E. Messina and E. Marban (2008). "Stem cells in the heart: what's the buzz all about?--Part 1: preclinical considerations." Heart Rhythm **5**(5): 749-757.

Smits, A. M., P. van Vliet, C. H. Metz, T. Korfage, J. P. Sluijter, P. A. Doevendans and M. J. Goumans (2009). "Human cardiomyocyte progenitor cells differentiate into functional mature cardiomyocytes: an in vitro model for studying human cardiac physiology and pathophysiology." Nat Protoc **4**(2): 232-243.

Snider, P., K. N. Standley, J. Wang, M. Azhar, T. Doetschman and S. J. Conway (2009). "Origin of cardiac fibroblasts and the role of periostin." Circ Res **105**(10): 934-947.

Snir, M., I. Kehat, A. Gepstein, R. Coleman, J. Itskovitz-Eldor, E. Livne and L. Gepstein (2003). "Assessment of the ultrastructural and proliferative properties of human embryonic stem cell-derived cardiomyocytes." Am J Physiol Heart Circ Physiol **285**(6): H2355-2363.

Soldner, F., D. Hockemeyer, C. Beard, Q. Gao, G. W. Bell, E. G. Cook, G. Hargus, A. Blak, O. Cooper, M. Mitalipova, O. Isacson and R. Jaenisch (2009). "Parkinson's disease patient-derived induced pluripotent stem cells free of viral reprogramming factors." Cell **136**(5): 964-977.

Sommer, C. A., A. G. Sommer, T. A. Longmire, C. Christodoulou, D. D. Thomas, M. Gostissa, F. W. Alt, G. J. Murphy, D. N. Kotton and G. Mostoslavsky (2010). "Excision of reprogramming transgenes improves the differentiation potential of iPS cells generated with a single excisable vector." Stem Cells **28**(1): 64-74.

Sommer, C. A., M. Stadtfeld, G. J. Murphy, K. Hochedlinger, D. N. Kotton and G. Mostoslavsky (2009). "Induced pluripotent stem cell generation using a single lentiviral stem cell cassette." Stem Cells **27**(3): 543-549.

Sosnik, A. and M. V. Sefton (2005). "Semi-synthetic collagen/poloxamine matrices for tissue engineering." Biomaterials **26**(35): 7425-7435.

Souders, C. A., S. L. Bowers and T. A. Baudino (2009). "Cardiac fibroblast: the renaissance cell." Circ Res **105**(12): 1164-1176.

Stadtfeld, M., M. Nagaya, J. Utikal, G. Weir and K. Hochedlinger (2008). "Induced pluripotent stem cells generated without viral integration." Science **322**(5903): 945-949.

Steinberg, M. S. (1963). "Reconstruction of tissues by dissociated cells. Some morphogenetic tissue movements and the sorting out of embryonic cells may have a common explanation." Science **141**(3579): 401-408.

Stevens, K. R., L. Pabon, V. Muskheli and C. E. Murry (2009). "Scaffold-free human cardiac tissue patch created from embryonic stem cells." Tissue Eng Part A **15**(6): 1211-1222.

Sugi, Y. and J. Lough (1995). "Activin-A and FGF-2 mimic the inductive effects of anterior endoderm on terminal cardiac myogenesis in vitro." Dev Biol **168**(2): 567-574.

Synnergren, J., K. Akesson, K. Dahlenborg, H. Vidarsson, C. Ameen, D. Steel, A. Lindahl, B. Olsson and P. Sartipy (2008). "Molecular signature of cardiomyocyte clusters derived from human embryonic stem cells." Stem Cells **26**(7): 1831-1840.

Szabo, E., S. Rampalli, R. M. Risueno, A. Schnerch, R. Mitchell, A. Fiebig-Comyn, M. Levadoux-Martin and M. Bhatia (2010). "Direct conversion of human fibroblasts to multilineage blood progenitors." Nature **468**(7323): 521-526.

Tada, M., E. S. Casey, L. Fairclough and J. C. Smith (1998). "Bix1, a direct target of Xenopus T-box genes, causes formation of ventral mesoderm and endoderm." Development **125**(20): 3997-4006.

Tada, M. and J. C. Smith (2000). "Xwnt11 is a target of Xenopus Brachyury: regulation of gastrulation movements via Dishevelled, but not through the canonical Wnt pathway." Development **127**(10): 2227-2238.

Taghavi, S., T. E. Sharp, 3rd, J. M. Duran, C. A. Makarewich, R. M. Berretta, T. Starosta, H. Kubo, M. Barbe and S. R. Houser (2015). "Autologous c-Kit+ Mesenchymal Stem Cell Injections Provide Superior Therapeutic Benefit as Compared to c-Kit+ Cardiac-Derived Stem Cells in a Feline Model of Isoproterenol-Induced Cardiomyopathy." Clin Transl Sci.

Takahashi, K., K. Tanabe, M. Ohnuki, M. Narita, T. Ichisaka, K. Tomoda and S. Yamanaka (2007). "Induction of pluripotent stem cells from adult human fibroblasts by defined factors." Cell **131**(5): 861-872.

Takahashi, K. and S. Yamanaka (2006). "Induction of pluripotent stem cells from mouse embryonic and adult fibroblast cultures by defined factors." Cell **126**(4): 663-676.

Takahashi, T., B. Lord, P. C. Schulze, R. M. Fryer, S. S. Sarang, S. R. Gullans and R. T. Lee (2003). "Ascorbic acid enhances differentiation of embryonic stem cells into cardiac myocytes." Circulation **107**(14): 1912-1916.

Tandon, N., C. Cannizzaro, P. H. Chao, R. Maidhof, A. Marsano, H. T. Au, M. Radisic and G. Vunjak-Novakovic (2009). "Electrical stimulation systems for cardiac tissue engineering." Nat Protoc **4**(2): 155-173.

ten Dijke, P. and C. S. Hill (2004). "New insights into TGF-beta-Smad signalling." Trends Biochem Sci **29**(5): 265-273.

Tenhunen, O., J. Rysa, M. Ilves, Y. Soini, H. Ruskoaho and H. Leskinen (2006). "Identification of cell cycle regulatory and inflammatory genes as predominant targets of p38 mitogen-activated protein kinase in the heart." Circ Res **99**(5): 485-493.

Thierfelder, L., H. Watkins, C. MacRae, R. Lamas, W. McKenna, H. P. Vosberg, J. G. Seidman and C. E. Seidman (1994). "Alpha-tropomyosin and cardiac troponin T mutations cause familial hypertrophic cardiomyopathy: a disease of the sarcomere." Cell **77**(5): 701-712.

Thomas, R. J., D. Anderson, A. Chandra, N. M. Smith, L. E. Young, D. Williams and C. Denning (2009). "Automated, scalable culture of human embryonic stem cells in feeder-free conditions." Biotechnol Bioeng **102**(6): 1636-1644.

Thomson, J. A., J. Itskovitz-Eldor, S. S. Shapiro, M. A. Waknitz, J. J. Swiergiel, V. S. Marshall and J. M. Jones (1998). "Embryonic stem cell lines derived from human blastocysts." Science **282**(5391): 1145-1147.

Tobacman, L. S. (1996). "Thin filament-mediated regulation of cardiac contraction." Annu Rev Physiol **58**: 447-481.

Tobita, K., L. J. Liu, A. M. Janczewski, J. P. Tinney, J. M. Nonemaker, S. Augustine, D. B. Stolz, S. G. Shroff and B. B. Keller (2006). "Engineered early embryonic cardiac tissue retains proliferative and contractile properties of developing embryonic myocardium." Am J Physiol Heart Circ Physiol **291**(4): H1829-1837.

Toma, C., M. F. Pittenger, K. S. Cahill, B. J. Byrne and P. D. Kessler (2002). "Human mesenchymal stem cells differentiate to a cardiomyocyte phenotype in the adult murine heart." Circulation **105**(1): 93-98.

Tomasek, J. J., G. Gabbiani, B. Hinz, C. Chaponnier and R. A. Brown (2002). "Myofibroblasts and mechano-regulation of connective tissue remodelling." Nat Rev Mol Cell Biol **3**(5): 349-363.

Tulloch, N. L. and C. E. Murry (2013). "Trends in cardiovascular engineering: organizing the human heart." Trends Cardiovasc Med **23**(8): 282-286.

Ungrin, M. D., C. Joshi, A. Nica, C. Bauwens and P. W. Zandstra (2008). "Reproducible, ultra high-throughput formation of multicellular organization from single cell suspension-derived human embryonic stem cell aggregates." PLoS One **3**(2): e1565.

Utikal, J., N. Maherali, W. Kulalert and K. Hochedlinger (2009). "Sox2 is dispensable for the reprogramming of melanocytes and melanoma cells into induced pluripotent stem cells." J Cell Sci **122**(Pt 19): 3502-3510.

Vallier, L., M. Alexander and R. A. Pedersen (2005). "Activin/Nodal and FGF pathways cooperate to maintain pluripotency of human embryonic stem cells." J Cell Sci **118**(Pt 19): 4495-4509.

van den Borne, S. W., J. Diez, W. M. Blankesteijn, J. Verjans, L. Hofstra and J. Narula (2010). "Myocardial remodeling after infarction: the role of myofibroblasts." Nat Rev Cardiol **7**(1): 30-37.

van den Eijnden-van Raaij, A. J., T. A. van Achterberg, C. M. van der Kruijssen, A. H. Piersma, D. Huylebroeck, S. W. de Laat and C. L. Mummery (1991). "Differentiation of aggregated murine P19 embryonal carcinoma cells is induced by a novel visceral endoderm-specific FGF-like factor and inhibited by activin A." Mech Dev **33**(2): 157-165.

Van der Flier, L. G., J. Sabates-Bellver, I. Oving, A. Haegebarth, M. De Palo, M. Anti, M. E. Van Gijn, S. Suijkerbuijk, M. Van de Wetering, G. Marra and H. Clevers (2007). "The Intestinal Wnt/TCF Signature." Gastroenterology **132**(2): 628-632.

van Laake, L. W., R. Hassink, P. A. Doevendans and C. Mummery (2006). "Heart repair and stem cells." J Physiol **577**(Pt 2): 467-478.

van Laake, L. W., R. Passier, K. den Ouden, C. Schreurs, J. Monshouwer-Kloots, D. Ward-van Oostwaard, C. J. van Echteld, P. A. Doevendans and C. L. Mummery (2009). "Improvement of mouse cardiac function by hESC-derived cardiomyocytes correlates with vascularity but not graft size." Stem Cell Res **3**(2-3): 106-112.

van Laake, L. W., R. Passier, P. A. Doevendans and C. L. Mummery (2008). "Human embryonic stem cell-derived cardiomyocytes and cardiac repair in rodents." Circ Res **102**(9): 1008-1010.

van Laake, L. W., R. Passier, J. Monshouwer-Kloots, A. J. Verkleij, D. J. Lips, C. Freund, K. den Ouden, D. Ward-van Oostwaard, J. Korving, L. G. Tertoolen, C. J. van Echteld, P. A. Doevendans and C. L. Mummery (2007). "Human embryonic stem cell-derived cardiomyocytes survive and mature in the mouse heart and transiently improve function after myocardial infarction." Stem Cell Res **1**(1): 9-24.

Vandenberg, J. I., B. D. Walker and T. J. Campbell (2001). "HERG K+ channels: friend and foe." Trends Pharmacol Sci **22**(5): 240-246.

Venugopal, J. R., M. P. Prabhakaran, S. Mukherjee, R. Ravichandran, K. Dan and S. Ramakrishna (2012). "Biomaterial strategies for alleviation of myocardial infarction." J R Soc Interface **9**(66): 1-19.

Vidarsson, H., J. Hyllner and P. Sartipy (2010). "Differentiation of human embryonic stem cells to cardiomyocytes for in vitro and in vivo applications." Stem Cell Rev **6**(1): 108-120.

Vunjak-Novakovic, G., N. Tandon, A. Godier, R. Maidhof, A. Marsano, T. P. Martens and M. Radisic (2010). "Challenges in cardiac tissue engineering." Tissue Eng Part B Rev **16**(2): 169-187.

Wada, R., N. Muraoka, K. Inagawa, H. Yamakawa, K. Miyamoto, T. Sadahiro, T. Umei, R. Kaneda, T. Suzuki, K. Kamiya, S. Tohyama, S. Yuasa, K. Kokaji, R. Aeba, R. Yozu, H. Yamagishi, T. Kitamura, K. Fukuda and M. Ieda (2013). "Induction of human cardiomyocyte-like cells from fibroblasts by defined factors." Proc Natl Acad Sci U S A **110**(31): 12667-12672.

Wang, Y., G. A. Ameer, B. J. Sheppard and R. Langer (2002). "A tough biodegradable elastomer." Nat Biotechnol **20**(6): 602-606.

Warren, L., P. D. Manos, T. Ahfeldt, Y. H. Loh, H. Li, F. Lau, W. Ebina, P. K. Mandal, Z. D. Smith, A. Meissner, G. Q. Daley, A. S. Brack, J. J. Collins, C. Cowan, T. M. Schlaeger and D. J. Rossi (2010). "Highly efficient reprogramming to pluripotency and directed differentiation of human cells with synthetic modified mRNA." Cell Stem Cell **7**(5): 618-630.

Watzka, S. B., J. Lucien, M. Shimada, V. Edwards, H. Yeger, G. Hannigan and J. G. Coles (2000). "Selection of viable cardiomyocytes for cell transplantation using three-dimensional tissue culture." Transplantation **70**(9): 1310-1317.

Weinhaus AJ, Roberts KP. Anatomy of the Human Heart, in: Iazzo PA (ed). Handbook of Cardiac Anatomy, Physiology, and Devices. 2nd Edition. 2009.

Wernig, M., C. J. Lengner, J. Hanna, M. A. Lodato, E. Steine, R. Foreman, J. Staerk, S. Markoulaki and R. Jaenisch (2008). "A drug-inducible transgenic system for direct reprogramming of multiple somatic cell types." Nat Biotechnol **26**(8): 916-924.

Wernig, M., A. Meissner, R. Foreman, T. Brambrink, M. Ku, K. Hochedlinger, B. E. Bernstein and R. Jaenisch (2007). "In vitro reprogramming of fibroblasts into a pluripotent ES-cell-like state." Nature **448**(7151): 318-324.

Wobus, A. M., G. Kaomei, J. Shan, M. C. Wellner, J. Rohwedel, G. Ji, B. Fleischmann, H. A. Katus, J. Hescheler and W. M. Franz (1997). "Retinoic acid accelerates embryonic stem cell-derived cardiac differentiation and enhances development of ventricular cardiomyocytes." J Mol Cell Cardiol **29**(6): 1525-1539.

Woltjen, K., I. P. Michael, P. Mohseni, R. Desai, M. Mileikovsky, R. Hamalainen, R. Cowling, W. Wang, P. Liu, M. Gertsenstein, K. Kaji, H. K. Sung and A. Nagy (2009). "piggyBac transposition reprograms fibroblasts to induced pluripotent stem cells." Nature **458**(7239): 766-770.

Wu, S. M., K. R. Chien and C. Mummery (2008). "Origins and fates of cardiovascular progenitor cells." Cell **132**(4): 537-543.

Wu, S. M., Y. Fujiwara, S. M. Cibulsky, D. E. Clapham, C. L. Lien, T. M. Schultheiss and S. H. Orkin (2006). "Developmental origin of a bipotential myocardial and smooth muscle cell precursor in the mammalian heart." Cell **127**(6): 1137-1150.

Wu, Z., J. Chen, J. Ren, L. Bao, J. Liao, C. Cui, L. Rao, H. Li, Y. Gu, H. Dai, H. Zhu, X. Teng, L. Cheng and L. Xiao (2009). "Generation of pig induced pluripotent stem cells with a drug-inducible system." J Mol Cell Biol **1**(1): 46-54.

Xu, C., S. Police, M. Hassanipour and J. D. Gold (2006). "Cardiac bodies: a novel culture method for enrichment of cardiomyocytes derived from human embryonic stem cells." Stem Cells Dev **15**(5): 631-639.

Xu, R. H., X. Chen, D. S. Li, R. Li, G. C. Addicks, C. Glennon, T. P. Zwaka and J. A. Thomson (2002). "BMP4 initiates human embryonic stem cell differentiation to trophoblast." Nat Biotechnol **20**(12): 1261-1264.

Xu, X. Q., R. Graichen, S. Y. Soo, T. Balakrishnan, S. N. Rahmat, S. Sieh, S. C. Tham, C. Freund, J. Moore, C. Mummery, A. Colman, R. Zweigerdt and B. P. Davidson (2008). "Chemically defined medium supporting cardiomyocyte differentiation of human embryonic stem cells." Differentiation **76**(9): 958-970.

Xu, X. Q., S. Y. Soo, W. Sun and R. Zweigerdt (2009). "Global expression profile of highly enriched cardiomyocytes derived from human embryonic stem cells." Stem Cells **27**(9): 2163-2174.

Xu, X. Q., R. Zweigerdt, S. Y. Soo, Z. X. Ngoh, S. C. Tham, S. T. Wang, R. Graichen, B. Davidson, A. Colman and W. Sun (2008). "Highly enriched cardiomyocytes from human embryonic stem cells." Cytotherapy **10**(4): 376-389.

Yang, L., M. H. Soonpaa, E. D. Adler, T. K. Roepke, S. J. Kattman, M. Kennedy, E. Henckaerts, K. Bonham, G. W. Abbott, R. M. Linden, L. J. Field and G. M. Keller (2008). "Human cardiovascular progenitor cells develop from a KDR+ embryonic-stem-cell-derived population." Nature **453**(7194): 524-528.

Yildirim, Y., H. Naito, M. Didie, B. C. Karikkineth, D. Biermann, T. Eschenhagen and W. H. Zimmermann (2007). "Development of a biological ventricular assist device: preliminary data from a small animal model." Circulation **116**(11 Suppl): I16-23.

Yook, J. Y., M. J. Kim, M. J. Son, S. Lee, Y. Nam, Y. M. Han and Y. S. Cho (2011). "Combinatorial activin receptor-like kinase/Smad and basic fibroblast growth factor signals stimulate the differentiation of human embryonic stem cells into the cardiac lineage." Stem Cells Dev **20**(9): 1479-1490.

Yu, J., K. Hu, K. Smuga-Otto, S. Tian, R. Stewart, Slukvin, II and J. A. Thomson (2009). "Human induced pluripotent stem cells free of vector and transgene sequences." Science **324**(5928): 797-801.

Yu, J., M. A. Vodyanik, K. Smuga-Otto, J. Antosiewicz-Bourget, J. L. Frane, S. Tian, J. Nie, G. A. Jonsdottir, V. Ruotti, R. Stewart, Slukvin, II and J. A. Thomson (2007). "Induced pluripotent stem cell lines derived from human somatic cells." Science **318**(5858): 1917-1920.

Yu, P., G. Pan, J. Yu and J. A. Thomson (2011). "FGF2 sustains NANOG and switches the outcome of BMP4-induced human embryonic stem cell differentiation." Cell Stem Cell **8**(3): 326-334.

Yuasa, S., Y. Itabashi, U. Koshimizu, T. Tanaka, K. Sugimura, M. Kinoshita, F. Hattori, S. Fukami, T. Shimazaki, S. Ogawa, H. Okano and K. Fukuda (2005). "Transient inhibition of BMP signaling by Noggin induces cardiomyocyte differentiation of mouse embryonic stem cells." Nat Biotechnol **23**(5): 607-611.

Yusa, K., R. Rad, J. Takeda and A. Bradley (2009). "Generation of transgene-free induced pluripotent mouse stem cells by the piggyBac transposon." Nat Methods **6**(5): 363-369.

Yutzey, K. E., J. T. Rhee and D. Bader (1994). "Expression of the atrial-specific myosin heavy chain AMHC1 and the establishment of anteroposterior polarity in the developing chicken heart." Development **120**(4): 871-883.

Zareba, W. and I. Cygankiewicz (2008). "Long QT syndrome and short QT syndrome." Prog Cardiovasc Dis **51**(3): 264-278.

Zhang, J., G. F. Wilson, A. G. Soerens, C. H. Koonce, J. Yu, S. P. Palecek, J. A. Thomson and T. J. Kamp (2009). "Functional cardiomyocytes derived from human induced pluripotent stem cells." Circ Res **104**(4): e30-41.

Zhang, M., D. Methot, V. Poppa, Y. Fujio, K. Walsh and C. E. Murry (2001). "Cardiomyocyte grafting for cardiac repair: graft cell death and anti-death strategies." J Mol Cell Cardiol **33**(5): 907-921.

Zhang, P., J. Li, Z. Tan, C. Wang, T. Liu, L. Chen, J. Yong, W. Jiang, X. Sun, L. Du, M. Ding and H. Deng (2008). "Short-term BMP-4 treatment initiates mesoderm induction in human embryonic stem cells." Blood **111**(4): 1933-1941.

Zhou, H., S. Wu, J. Y. Joo, S. Zhu, D. W. Han, T. Lin, S. Trauger, G. Bien, S. Yao, Y. Zhu, G. Siuzdak, H. R. Scholer, L. Duan and S. Ding (2009). "Generation of induced pluripotent stem cells using recombinant proteins." Cell Stem Cell **4**(5): 381-384.

Zimmermann, W. H., M. Didie, G. H. Wasmeier, U. Nixdorff, A. Hess, I. Melnychenko, O. Boy, W. L. Neuhuber, M. Weyand and T. Eschenhagen (2002). "Cardiac grafting of engineered heart tissue in syngenic rats." Circulation **106**(12 Suppl 1): I151-157.

Zimmermann, W. H. and T. Eschenhagen (2007). "Embryonic stem cells for cardiac muscle engineering." Trends Cardiovasc Med **17**(4): 134-140.

Zimmermann, W. H., C. Fink, D. Kralisch, U. Remmers, J. Weil and T. Eschenhagen (2000). "Three-dimensional engineered heart tissue from neonatal rat cardiac myocytes." Biotechnol Bioeng **68**(1): 106-114.

Zimmermann, W. H., I. Melnychenko and T. Eschenhagen (2004). "Engineered heart tissue for regeneration of diseased hearts." Biomaterials **25**(9): 1639-1647.

Zimmermann, W. H., I. Melnychenko, G. Wasmeier, M. Didie, H. Naito, U. Nixdorff, A. Hess, L. Budinsky, K. Brune, B. Michaelis, S. Dhein, A. Schwoerer, H. Ehmke and T. Eschenhagen (2006). "Engineered heart tissue grafts improve systolic and diastolic function in infarcted rat hearts." Nat Med **12**(4): 452-458.

Zimmermann, W. H., K. Schneiderbanger, P. Schubert, M. Didie, F. Munzel, J. F. Heubach, S. Kostin, W. L. Neuhuber and T. Eschenhagen (2002). "Tissue engineering of a differentiated cardiac muscle construct." Circ Res **90**(2): 223-230.

Zong, X., H. Bien, C. Y. Chung, L. Yin, D. Fang, B. S. Hsiao, B. Chu and E. Entcheva (2005). "Electrospun fine-textured scaffolds for heart tissue constructs." Biomaterials **26**(26): 5330-5338.

Zwaka, T. P. and J. A. Thomson (2003). "Homologous recombination in human embryonic stem cells." Nat Biotechnol **21**(3): 319-321.

Zwi-Dantsis, L., I. Mizrahi, G. Arbel, A. Gepstein and L. Gepstein (2011). "Scalable production of cardiomyocytes derived from c-Myc free induced pluripotent stem cells." Tissue Eng Part A **17**(7-8): 1027-1037.

NAMASTE

Reconozco la presencia de la esencia divina en ti. Reconozco la presencia de la esencia divina en mí. En un acto de humildad, nuestras esencias divinas se saludan, y se reconocen.

Riconosco la presenza dell'essenza divina in te. Riconosco la presenza dell'essenza divina in me. In un atto di umiltà, le nostre essenze divine si salutano e si riconoscono.

A los quien sin ellos este trabajo no hubiera sido posible:

Ángel, gracias por haberme acogido en tu grupo de investigación y hacerme ser parte de este proyecto tan importante. Gracias de corazón por todo lo que he podido aprender en estos años. Gracias a los miembros de la comisión de seguimiento del doctorado por sus consejos: profesores **Manuel Galiñanes**, **Antonio Del Rio**, **Ramon Farré**. **Elena Martinez**, por tu imprescindible y preciosa colaboración. **Antonella**, grazie per la disponibilità e il sostegno in questi anni. **Maria Valls**, ets el meu àngel. Infinites gràcies per haver sempre hi estat, per no haver-me mai dit que no. Per les ajudes, pels ànims. Gràcies per les converses, científiques i no. Pels moments de pura bogeria! Per haver-me portat a la teva família. Has estat la meva Germana i has estat la BOOOOOOOOOMBAAAAAA!! mai ho oblidaré. **Yvonne**, gracias por ser un modelo y una inspiración increíbles. Gracias por estar siempre para todos, por sacar tantas ideas, tantas bromas y compartirlas con los demás! Reconozco en ti un corazón especial: me has ayudado a sentir mas cerca mi abuela lejana, y para esto un "gracias" no basta. Gracias también por los dibujos de las celulitas, que utilicé en las figuras de esta tesis! **Juanlu**, gracias por poder contar siempre sobre ti. Por todos tus cambios de medio, por la escucha y los ánimos continuos, hasta el final! Franki tiene a un muy buen tío! **Olalla**, por haber acogido este proyecto en su tramo final y haberlo cuidado y nutrido: que sus frutos crezcan ricos en tus manos! Gracias!

Mis amados compañeros del barco!!

Gracias a todos por la colaboración y la simpatía (en el sentido etimológico de "syn - pathos")!! Me siento inmensamente agradecida de haberos encontrado! De cada uno he aprendido y me llevaré algo: **Sendi**, tu espontaneidad y el mar de tus ojos; **Isil**, tu ilusión para el amor y poder sacar tu carácter firme, que lo tienes! **Juan**, tu desorden ordenado; **Raquel**, tu dedicación; **Cris**, tu acogedora sonrisa; **Anna**, tu meticulosidad; **Juanlu** otra vez, tu contentamiento. **Isacco**! Gracias por engancharme con tu voz, enamorarme con tu humor, y alegrarme las horas en el cuarto de cultivo! **Sergiiiii**!! Gracias por haberme asistido en mi primeros meses en el labo y ayudarme con el castellano, por introducirme a los genes de la pluripotencia con tanta pasión, por las bromas locas y descuidadas que nos hemos tirado…y por aguantarme cuando tenia los nervios de la regla!!! **Alberto**, por las horas en el confocal y por alegrar la atmosfera en el labo! **Adriana** (la del pelo rizado), por tu dedicación, por tus gracias, por hacerme de mama cuando estaba enferma y la mía estaba lejos.
Los "Antos": **Charli**, gracias por tu interés y ideas para el proyecto y por tus ayudas. Por ser un ejemplo en el labo y fuera: como dijo Isacco eres un "nano cojonudo" y eres especial!!! **Irene**, gracias de las ayudas con las immunos y por tu

confianza; **Rochi**, por tu paciencia y hilaridad; **Armi** la praticità che quando ce vò ce vò!! **Angi**, thanks for your advices with English grammar and for sharing your yogini passion! **Giulia**, il sorriso con la ragazza intorno!! **Neus**, por tus risas y dedicación. **Adriana** (la del pelo liso), por haber sido literalmente nuestro Sol! Gracias por todo el tiempo que me has dedicado explicándome técnicas y truquillos, fuera la hora que fuera. **Carla**, por tu amistad y por aliviar las horas en el cuarto de cultivo. **Francesca**, per le idee e per los ánimos.

Gracias también a todos los estudiantes que habéis pasado en los años, dejando lindas memorias: **Bahaaaa**, **Mario**, **Alice**, **Kike**, **Jonathan**, **Vero**, **Carola**, **Sara**, **Ana**, **Catarina**, **Patty**, **Annarita**, **Jannis**, **Carles**, **Floriana**, **Marta**.

Gracias a **Patricia** y **Laia**, por todo lo que aprendí yo de vosotras.

Gracias a todos los que habéis colaborado conmigo en los años de la tesis por vuestra disponibilidad, paciencia y enseñanzas: **Leif**, **Pilar Sepulveda** y **Delia**, **Benjamin**, **Maria Bulwan, Maria Lopez** y **Annahita**. A los miembros de la plataforma de citometria del Parc Cientific: **Jaume**, **Sonia**, **Ricard**, **Chary**. Gracias a el formidable equipo de la plataforma de histología del CMRB: **Mercé**, **Lola**, **Cristina** y **Cristina**. Gracias también a **Vaquero** y **Laia**. Los que habeis tramitado la burocracia: **Anna Alsina**, **Ricard**, **Pilar** y **Esther**, **Maria**, gracias por la paciencia en contestar a todas mis preguntas!

Gracias de corazón a todos aquellos que han compartido conmigo los años de la tesis fuera del laboratorio por ser compañeros de vida impagables y hacerme crecer:

Christian, stella gemella. Grazie per percorrere questa vita sulla retta parallela alla mia e rispondere sempre, volendo o no, quando tiro quel filo che ci unisce. Grazie per avermi risollevato nei momenti duri e fatto tanto ridere!! Grazie al tuo sorriso e grazie alla tua voce… "Se c'è una cosa che mi fa impazzireeee… É il sorriso di Christiaaaaan!!!". Il resto della famiglia poliamorosa! **Amó**, **Paola** e **Roberto**!! Grazie per mantenere viva la nostra famiglia (ed espanderla :D) e per fermare il tempo con le nostre assurde risate!
Franci, saggia amica. Grazie per credere nella scienza e per essere una Donna scienziata. **Patato**, il più grande spettacolo dopo il Big Bang siamo noi, io e te! Grazie per esserci stato sempre, dal primo giorno in cui ci siamo incontrati. Per i tuoi buongiorno solidali alle sei e mezzo del mattino, per gli abbracci, per capire il mio bisogno di raccontare tutto e ascoltare sempre, per la costante presenza da vicino e da lontano. Grazie per avermi sopportato in questi ultimi mesi e per avermi ricordato che potevo farcela con questa tesi. Grazie per credere in me e nel mio "cammino di luce", come lo chiami tu, sin dall'inizio: è stato bello percorrerlo in insieme a te il tuo, me ne hai dato la forza! **Marti**! Amica e compagna di avventura barcellonese! Ti ho sempre sentito presente, grazie per esserlo stata quando davvero ne avevo bisogno! **Ariel**, Grande Ariel! grande amigo, grande corazón, grandes palabras, siempre. Gracias por mantenerme atada a la realidad. **Carol**, por aquel 2011 inimitable y por haberme inspirado, súper mujer! **Luis**, por aguantar mis historias y transformarlas en sit-com!! **Cor Trobada** y **Ramones Gospel Choir**! Per haver amenitzat moltes tardes després del laboratori. Las Patatas, **Andrea** y **Adela**, preciosas almas detrás de hermosas sonrisas. **Mao**, compañero de piso y de reflexiones… ah la vida y sus vicisitudes!

Blanca, gracias por enseñarme a escucharme, conocerme, quererme, cuidarme… y a disfrutar de los días de lluvia.

Namaste a mis Maestros, por entregarse y compartir la practica con tanto respeto y humildad. **Aleix**, por tu sensibilidad, tu paciencia y tu comprensión. Por haberme dado la posibilidad de asistirte y por enseñarme. Por todo aquello que he podido descubrir a través de tus enseñanzas: tesoro inestimable como la deuda que tengo contigo. **Lucas y Maria**, educadores y ejemplos de educación excelsos. **Leticia**, tu esencia brilla! Gracias por haber plantado la semilla del acroyoga en mi y por seguir jugando con el mundo. **César**, por darme herramientas para transmitir "Metta" y por compartir el valor del poder de la voluntad en tus clases! **Clara** y **Alessa** por haber guiado mis primeras practicas de "asanas", que han hecho de mi cuerpo mi hogar.

Acrodream Team y el **Parc de la Ciutadela**, mi escape! **Llatzer, Elis**, **Irune**, **Luis**, **Joan**, **Isa**, **Cristina**, **Sonia**, **Carla**, **Danny**, **Ade**, **Maxim**, **Leticia**... Pura magia! Lo conseguiremos, cambiaremos al mundo haciéndolo volar! Gracias por cada segundo de "aquí y ahora"! Un gracias especial, **Pilar**, por la pureza y la coherencia de tu alma. Y **Alex**, gracias por haberme guiado y animado siempre, gracias por creer en mi y por dejarme realizar mi deseo de compartir la practica en Yogacrobatic.

Mágica **Barcelona**… donde todo lo inesperado pasa! Mágicos los números, mágicos los músicos e magica la **musica**, fiel compañera de noche y de día!

La mia famiglia:

Pali, ennaino ennaino pitu pitu pitu!! Patatina, per la More Sorellineo che a parole non si puó! Mesplodilcuore se si tratta di te. Grazie per avermi cuidado da lontano. Grazie **Ugi** per essere verde e renderla felice!! I miei **nonni**, che semplicemente siete il mio perché. Spero di non avervi deluso e di non deludervi mai, ovunque voi siate e sarete. Mamma e papà, per avermi donato la Vita attraverso l'Amore. **Mamma**, ogni volta che al microscopio osservavo le mie cellule iniziare a battere pensavo alla magia del pulsare del cuore; il primo battito del mio è avvenuto dentro di te. Grazie per averlo accolto e protetto, grazie per il tuo sangue quando ancora non avevo il mio; per essere stata la mia prima casa, e farmela ritrovare sempre ogni volta che torno e ti abbraccio. **Papà**, per essere diventato un grande amico, restando sempre il mio papà… Anche se non ti telefono mai! Questa tesi è per voi, che mi avete sostenuto durante questo periodo di studi, soprattutto quando non sarebbe spettato a voi. Grazie.

Fondamentale sostegno, grazie per avermi accompagnato, aiutato e motivato come non pensavo fosse possibile. Per condividere la Vita, per insegnarmi, per stupirmi sempre e non deludermi mai. **Andrea**, grata sempre ti sarò, per regalarmi in ogni momento la Felicitò.

Lokah samastah sukhino bhavantu.

Que todo ser en todo lugar pueda ser feliz y libre. Y puedan los pensamientos, las palabras y las acciones de mi vida contribuir de alguna manera a esa felicidad y libertad para todos.

Che tutti gli esseri, in ogni luogo, possano essere felici e liberi, e che i miei pensieri, parole e azioni possano contribuire in qualche modo a ciò.

Namaste.

Namaste